Complex yet Coordinated: Regulation of transcriptional factors and cell signaling pathways to endure anoxia in *Rana sylvatica*

Aakriti Gupta
B.Sc. Panjab University, 2007
M.Sc. Panjab University, 2009

A thesis submitted to the Faculty of Graduate Studies and Research in partial fulfilment of the requirements for the degree of

Doctor of Philosophy
Department of Biology

Carleton University,
Ottawa, Ontario, Canada

Abstract

Wood frogs *(Rana sylvatica*) are a well-studied vertebrate model of natural freeze tolerance, surviving several months of winter subzero temperatures with 65-70% of total body water frozen as extracellular ice. Freezing halts blood circulation, heartbeat and breathing, restricting oxygen availability throughout the body and requiring a switch to anaerobic glycolysis for energy production, with its much lower ATP yield. To survive, wood frogs suppress their metabolic rate by about 90% to match ATP availability from glycolysis alone. Multiple cellular processes are regulated and suppressed, sustaining only pro-survival pathways until thawing occurs. Episodes of anoxia/reoxygenation also elevate reactive oxygen species (ROS) production that can surpass the antioxidant capacity of cells causing oxidative stress and tissue damage. This thesis examined a network of stress-responsive transcription factors (NRF2, OCT1, OCT4, YAP/TEAD, and RBPJ) and their associated pathways to determine their response and regulation over the anoxia/reoxygenation cycle. Decreased binding of transcriptional complexes to the promoter regions of target genes indicated a global reduction in transcription/translation processes. The data show also "functional switching" of OCT1, OCT4, and MAML while selectively upregulating antioxidants in a stress/organ specific manner. The present studies also shed new light on tissue repair mechanisms by demonstrating upregulation of selected pathway proteins. An increase in AHCY levels in liver also suggests maintenance of redox control, and elevated JMJD2C, TAZ, and MAML in skeletal and cardiac muscles indicates a potential increase in the expression of MyoD for muscle regeneration. Overall, the findings of this thesis document a complex yet coordinated network of transcriptional

factors that support metabolic rate depression during freezing, combat oxidative stress, and initiate tissue repair mechanisms to endure prolonged anoxia and maintain cellular homeostasis in frozen wood frogs.

Statement of contribution

I designed and performed all experiments outlined in this thesis, analyzed the data, generated the figures, and wrote all chapters. Dr. Kenneth B. Storey provided funding, materials and reagents, editorial review, and has approved all chapters. Janet M. Storey assisted in animal sampling and provided editorial review of this thesis.

Chapter 2:

This chapter has been published in *Comparative Biochemistry and Physiology, Part B*

Gupta, A., Storey, K.B., Regulation of antioxidant systems in response to anoxia and reoxygenation in *Rana sylvatica*, *Comp. Biochem. Physiol. Part B Biochem. Mol. Biol.* 243–244 (2020) 110436. https://doi.org/10.1016/j.cbpb.2020.110436.

Chapter 3:

This chapter has been published in *Gene*

Gupta, A., Storey, K.B., Coordinated expression of Jumonji and AHCY under OCT transcription factor control to regulate gene methylation in wood frogs during anoxia, Gene 788:145671 (2021). https://doi.org/10.1016/j.gene.2021.145671

Chapter 4:

This chapter has been published in *Life*

Gupta, A., Storey, K.B., Activation of the Hippo Pathway in *Rana sylvatica*: Yapping Stops in Response to Anoxia. Life 11:1422 (2021). https://doi.org/10.3390/life11121422

Chapter 5:

This chapter has been published in Cellular Signaling

Gupta, A., Storey, K.B., A "notch" in the cellular communication network in response to anoxia by wood frog (*Rana sylvatica*). Cellular signaling 93: 110305 (2022). https://doi.org/10.1016/j.cellsig.2022.110305.

Acknowledgement

Well, a lot to write but scarcity of words. I guess this is the hardest part of the thesis. The skype call from India was my first impression of Storey lab, and at that very instance, I felt like I belong here. Based on that one-hour call, I took the leap of faith, packed up everything in India, and moved to Canada, and this was the best decision of my life. I would start by thanking my supervisor Dr. Kenneth Storey for accepting me as a student and providing me with immense opportunities that helped me grow into the person I am today. I always enjoyed those small talks with you, where you mentioned songs and music bands "I had never heard of", and sharing Hudson's picture and videos as rewards for doing something good (and not to forget those chocolates). I have been here for four years, I also understand the difference in culture between India and Canada, but you both would always be "Sir" and "Ma'am" for me.

"Ma'am" Jan Storey, you are the foundation and pillar of this lab. Thank you for your edits and detailed comments that helped me understand the key points essential for manuscript writing. I would miss those long Friday talks from anything to everything. Thank you for the support, for being so approachable, and for your valuable advice. I would now move to 511, where I would thank Rasha, my mentor and friend who had never let me feel alone during my initial days (considering me being away from my family for the first time), and the AAAS office group- Aline, Anchal, Aakriti, and Sarah "+ Stuart". AAAS room was a complete package of our stupid and illogical talks, wall of shame, venting out 2200 report marking, and above all, "our quote list" where every quote has a story behind it. I thank you guys for giving me so many memories- my failed attempt to make you have lunch at 10:30 am, Stuart trying to teach me French in multiple ways (I am sorry Stuart, for not being a good/ supportive student 😟), teasing Anchal on many topics (that would remain between four of us 😉), and my unlimited crisis (even those that no one could even think of) and Maire your spice tolerance will still be a thing to work on.

Even though I mention people who belong to my personal life now, that would never mean that they are less important to me as there is a saying, "it's the feelings that matter, not the sequence". I would first thank my parents and their never-ending support and unshattered faith in me. My answer to your question is still the same - I have not

discovered a cure for any disease, and my findings are just the initial step towards a bigger goal. Your love and patience were my invisible strengths. I would never be able to pay back the sacrifice made by my 9 years old son for being away from me for four years. It is a big deal for a 5-year-old kid to agree to stay with his grandparents without his mother around. I love you baccha and I owe you every second of the time I missed when you were growing up. Now comes my brother Akhil- the pillar of my life. He has always motivated me to go beyond my limits and fulfill my dreams. Akhil this degree belongs to you because it was you who pushed me towards it. You might be four years younger than me but in intelligence and maturity, you are way elder than me. I am still that stupid, careless, and talkative girl with issues we used to laugh about. This acknowledgment and thesis would not be complete if I do not name my best friend Gaurang, who is my support, troubleshooter, and punching bag. All my manuscripts (that would even include this acknowledgment 😜) would go via him before I send them to sir for editing and he would critique it the best based on his understanding- thanks for taking that torture. He is the one who reminded me that there are screens other than laptops, laptops can also be used for many other things than just writing manuscripts and data analysis, and there is a life beyond science.

Lastly, I thank all my friends, relatives, and people who were a part my life to give me lessons that motivated me to get going. Their criticism and appreciation helped me explore my capabilities and challenged me to make a better version of myself. I have a firm belief that God would plan everything well, and I just need to go with the flow. I know this is very long and dramatic… but I am from the land of Bollywood… and drama and emotions are in my blood 😜 😜

Table of Contents

List of abbreviations

ADAM	A Disintegrin and Metalloproteinase Domain-Containing Protein 10
ADP	Adenosine Diphosphate
AHCY	Adenosyl homocysteinase
AKR	Aldo-Keto Reductase
ANOVA	Analysis of Variance
APS	Ammonium Persulfate
ARE	Antioxidant Response Element
ATP	Adenosine Triphosphate
BMP	Bone Morphogenetic Protein
ChIP-Seq	Chromatin Immunoprecipitation with Massive Parallel DNA Sequencing
DEPC	Diethyl Pyrocarbonate
DLL	Delta-Like Ligand
DMSO	Dimethyl Sulfoxide
DNA	Deoxyribonucleic Acid
dNTP	Deoxynucleoside Triphosphate
DPI-ELISA	DNA-Protein Interaction Enzyme Linked Immunosorbent Assay
DTT	Dithiothreitol
ECL	Enhanced Chemiluminescence
EDTA	Ethylene Diamine Tetra acetic Acid
ELISA	Enzyme-Linked Immunosorbent Assay
GLUT	Glucose Transporter
GPox	Glutathione Peroxidase

GST	Glutathione-S-Transferase
H3K9Me	Histone 3 Demethylation on Lysine 9
HCl	Hydrochloric Acid
HEPES	4-(2-Hydroxyethyl)-1-Piperazineethanesulfonic Acid
HES	Hairy And Enhancer of Split-1
HEY	Hairy/Enhancer-Of-Split Related with YRPW Motif Protein
HIF	Hypoxia Inducible Factor
HRP	Horse-Radish Peroxidase
INP	Ice Nucleating Proteins
JAG	Jagged
JMJD	Jumonji Domain Containing Demethylases
KCl	Potassium Chloride
kDa	Kilodalton
KEAP-1	Kelch-Like ECH Associated Protein-1
KH2PO4	Potassium Dihydrogen Phosphate
KLF4	Kruppel-Like Factor 4
LATS1/2	Large Tumor Suppressor 1 And 2 Kinases
MAFG	MAF Beta-ZIP Transcription Factor G
MAML	Mastermind-Like Protein 1
MAT	Methionine Adenosyl Transferase
MgCl2	Magnesium Chloride
miRNA	Microrna
MRD	Metabolic Rate Depression

mRNA	Messenger RNA
MST	Mammalian Ste20-Like Kinases 1/2
Mw	Molecular Weight
Na2HPO4	Disodium Phosphate
Na3VO4	Sodium Orthovanadate
NaCl	Sodium Chloride
NECD	Notch Extracellular Domain
NFκB	Nuclear Factor Kappa-Light-Chain-Enhancer Of Activated B Cells
NICD	Notch Intracellular Domain
NOG	Noggin
NQO-1	NADPH Quinone Oxidoreductase-1
Nrf2	Nuclear Factor Erythroid 2-Related Factor 2
NuRD	Nucleosome Remodeling and the Histone Deacetylation
OCT	Octamer Binding Transcription Factor
PBS	Phosphate Buffered Saline
PMSF	Phenylmethylsulfonylfluoride
POMP	Proteasome Maturation Protein
PTM	Posttranslational Modification
PUFA	Polyunsaturated Fatty Acids
PVA	Polyvinyl Alcohol
PVDF	Polyvinylidene Fluoride
RBPJ	Recombination Signal Binding Protein for Immunoglobulin Kappa J Region
ROS	Reactive Oxygen Species

RT	Room Temperature
RT-qPCR	Reverse Transcription Quantitative Polymerase Chain Reaction
SAH	S-Adenosylhomocysteine
SAHH	S-Adenosylhomocysteine Hydrolase
SAM	S-Adenosylmethionine
SAV	Salvador 1
SDSPAGE	Sodium Dodecyl Sulphate Polyacrylamide Gel Electrophoresis
SEM	Standard Error of Mean
SOD	Superoxide Dismutase
SOX2	SRY (Sex Determining Region Y)-Box 2.
TACE	Tumor Necrosis Factor-Alpha Converting Enzyme
TAZ	Transcriptional Coactivator With PDZ-Binding Motif
TBA	Thiobarbituric Acid
TBS	Tris-Buffered Saline
TBST	Tris-Buffered Saline with Tween-20
TEAD	TEA Domain Family Member
TEMED	N,N,N′,N′-Tetramethylethane-1,2-Diamine
TMB	Tetramethylbenzidine
YAP	Yes Associated Protein

List of Figures

1.General Introduction

1.1 Strategies to survive extremely cold conditions

Exposure to extended periods of extreme winter cold can be lethal for animals that do not have strategies for cold hardiness. Animals face multiple challenges in winter including subzero temperatures, short photoperiods, and limitations of water and food availability that affect their physiology and biochemistry [1]. Many are also subjected to freezing injuries, that can damage cells and the macromolecules within them, often irreversibly. When frozen, vital processes like circulation, heartbeat, muscle movements, and neural conduction come to halt [2]. Not only this, but animals also experience extreme reductions in cell volume due to water exiting to form ice in extracellular and extra organ spaces such as the abdominal cavity, between the skin and muscle layers, or in the eye lens [1]. This results not only in osmotic stress due to increased solute concentrations (as water turns to ice) but also cell dehydration that hinders normal cellular operations. Consequently, cells shrink and can rupture due to ice-induced mechanical stress. In addition to this, the freezing of body fluids disrupts critical physiological processes since freezing stops lung function, heartbeat, and blood circulation leading to additional stresses of anoxia and ischemia [2]. Considering that such damage is commonly irreversible and fatal, an unadapted animal would not be able to survive. Therefore, to endure the winter, many species have developed adaptive responses that allow them to cope with natural episodes of freezing and thawing; these include strategies of anhydrobiosis, vitrification, freeze tolerance, or freeze avoidance [3].

To deal with the dangers of subzero winter temperatures, animals have evolved multiple strategies. Many species, such as the Monarch butterfly (*Danaus plexippus*) or the willow warbler (*Phylloscopus trochilus*), migrate to warmer climates in winter but this kind of

geographical movement is not possible for most species [4]. More commonly, animals must use protective strategies to deal with winter. Many organisms spend the winter in a simple life stage: eggs, embryos, cysts, or seeds, and certain species use strategies such as anhydrobiosis (removal of all free water from the body so that no water is available to freeze) or vitrification (water solidifies in an amorphous "glass" state to prevent osmotic and physical injuries by the alternate formation of ice crystals) [5]. Freeze avoidance is another widely used strategy that involves extreme supercooling of body fluids and ensures maintenance of a liquid state of body fluids even at deep subzero temperatures; this strategy is widely used by arthropods [6] and some reptiles [7]. High levels of carbohydrates solutes (e.g. glycerol, sorbitol, mannitol, glucose, sucrose, trehalose, etc.) are accumulated and lower the freezing point of body fluids and the synthesis of antifreeze proteins (AFPs) further prevents ice nucleation [1]. The goldenrod gall moth (*Epiblema scudderiana*) is a prominent example of freeze avoidance and survives the winter in the galls formed on the stems of the goldenrod plant supported by the accumulation of huge amounts of glycerol as a cryoprotectant that lowers the supercooling point of their body fluids to about -38°C [8].

Freeze tolerance is another strategy of winter survival and involves controlled freezing of body fluids in extracellular spaces while the intracellular space remains liquid (unfrozen) due to the production of high levels of low molecular weight cryoprotectants [4,9]. Ice nucleation begins when skin contacts environmental ice which triggers nucleation of body fluids by one of three methods: inoculating body fluids across the skin, epithelial contact with nonspecific nucleators like bacteria, or synthesis of ice nucleating proteins (INPs) by the body [10–12]. INPs work in two ways: 1. INPs slow down the formation of ice crystals

to prevent recrystallization of small ice crystals to larger ones, thereby minimizing architectural damage to cells/tissues. This provides the animal with the time to execute adaptive strategies without which body fluids would super cool to the point where “flash freezing” can occur in an unorganised way and cause irreversible damage by ice. 2. INPs ensure that ice formation is extracellular and thereby prevent damage that would result from intracellular ice formation that includes rupturing of plasma membranes [4]. In addition to INPs, certain antifreeze activities have also been observed in freeze tolerant species that show low thermal hysteresis activity compared to freeze avoidance. As a result, they do not prevent freezing but regulate the decrease of the site temperature, rate of freezing, and formation of ice crystals in a controlled manner [13]. A study from our lab also investigated the expression of fr10 (freeze responsive protein in insects) and found it to be upregulated during freezing, anoxia, and dehydration in a tissue specific manner [14,15]. Moreover it was observed that FR10 showed a structural homology with DRP10, a dehydration responsive protein found in Xenopus laevis [16]. Both DRP10 and FR10 showed similar roles as AFPs and apolipoproteins. Recent studies on freeze tolerance also elaborated the role of glycolipids as antifreeze in insects, and freeze tolerant frogs that includes Alaskan wood frogs [13]. Antifreeze glycolipids (AFGLs) are mostly the repeating units of βmanpyranoside-βxylpyranoside forming mannose-xylose disaccharides, that binds to the cell membranes and inhibit inoculation of ice crystals from extracellular regions to the cytosol [13].

As ice formation proceeds extracellular fluids get converted to ice crystals and pure water moves out of the cells via osmosis [10]. The outflow of water from cells into extracellular compartments leads to increased intracellular solute concentrations (that helps

to resist freezing) and decreased volume of cells. To prevent extreme shrinkage of cells, animals synthesise high amounts of cryoprotectants like glucose or glycerol that help to maintain a critical minimum cell volume so that membrane and cell functions can be restored easily during thawing [10,17]. Even though freeze tolerant animals have developed INPs that help to prevent mechanical damage by limiting ice crystal sizes and cryoprotectants that counteract water outflow from cells and preserve a minimum cell volume, there are still many physiological challenges that these animals encounter. Freezing of blood plasma causes an interruption of heart and lung function. Neural conductivity is no longer measurable, and basic survival processes like inter-organ distribution of oxygen, fuels, and metabolic wastes via the blood are halted [10,11] resulting in anoxia and ischemia. Freeze tolerant animals face these physiological challenges but have evolved some adaptive mechanisms to survive prolonged freezing without these essential physiological processes.

Oxygen is the terminal electron acceptor in the electron transport chain during respiration and is required for ATP production via oxidative phosphorylation. Oxygen deprivation during freezing necessitates a switch to anaerobic metabolism to synthesize ATP [18]. Although body temperature falls below 0°C, cells still need to generate ATP to sustain pro-survival activities. Another challenge during freezing is the availability of resources. Inter-organ transport of fuels and oxygen is halted by frozen plasma and so energy must be derived anaerobically, primarily via glycolysis. To maintain regular cell/tissue function, the amount of fuel and energy required could be a lot more than the amount available, leading to death. Hence, freeze tolerant animals switch to “survival

mode" where the animal undergoes metabolic rate depression (MRD) for the duration of the freezing period [3,19,20].

Under MRD, animals survive in minimal energy mode by reducing many energy expensive reactions including DNA replication, transcription, translation, cell cycle progression, and suppress or halt the use of ATP for many other functions such as active transport through ion channels. Transcription and translation consume about 36% of the total energy produced by cells [21–23] and hence become key targets for suppression in the hypometabolic state. MRD or hypometabolism is not just an adaptive technique acquired by animals to survive freezing but is used by many other stress tolerant animals. Mammalian hibernators [19,24], estivating animals [25–27], and diving species [19] also suppress their metabolism to ensure survival under harsh conditions. Extended anoxia exposure and later reoxygenation can also present oxidative damage due to increased production of reactive oxygen species (ROS). Enhanced production of ROS is particularly associated with recovery due to rapid reoxygenation of tissues. Increased oxidative stress triggers destructive pathways like apoptosis [28].

The overview presented above shows a complex yet coordinated channeling of multiple pathways that operate to enable the survival of animals for extended periods of time while frozen. These adaptations are in accordance with the limited energy available to support pro-survival biochemical and molecular pathways in a frozen state.

1.2 *Rana sylvatica*: a model freeze-tolerant animal

The wood frog, *Rana sylvatica,* is a well-established freeze tolerant model animal that has been extensively studied. Stretching from Alaska across the boreal forests of Canada and down the Appalachian Mountain range of the eastern USA, wood frogs spend the

winter buried under leaf litter on the forest floor. This gives animals an advantage since even though the air temperature could fall as low as -35 °C, the temperature rarely drops below -5°C under leaf and snow cover [29]. Under these conditions, when the temperature drops below -2°C, freezing is triggered and the wood frogs can survive with ~65% of total body water frozen for about six months. Ice propagates through all extracellular spaces and fills the abdominal cavity [30,31].

Ice nucleation begins as soon as environmental ice touches the outer layer of skin and inoculates extracellular water to trigger ice formation that then propagates throughout the body. Freezing can also be triggered by non-specific bacteria on the skin and in the gut as well as by the synthesis of specific ice nucleating proteins (INPs) in the blood. Previous studies from our lab showed INP activities in cell free blood of wood frog [32]. It further suggested that INPs initiate early freezing that is advantageous in many ways [32]. The use of nucleators helps to control the formation of ice crystals and limit ice formation to extracellular sites [11]. Many physiological and biochemical processes work in a coordinated manner to enable survival during long freezing periods. With the onset of ice nucleation, frogs reaches the supercooling (the temperature at which ice crystallization occurs) point that initiates glycogenolysis (forming glucose from stored glycogen in the liver) triggered by catecholamine signals through adrenergic receptors transmitted to the liver [3,33,34]. Conversion of about 70% of total body water into extracellular ice crystals results in high ion/protein/cryoprotectant concentrations in tissues and organs and severe cell dehydration [10] causing cell shrinkage. To prevent cellular damage frogs synthesize extremely high amounts of glucose from the breakdown of stored liver glycogen. This is

delivered as an osmolyte to all other tissues to help limit the decrease in cell volume and minimize compression stress that might otherwise cause membrane damage [10].

The glucose produced by the liver is used as a cryoprotectant. It is rapidly transported to all body parts via the blood until freezing restricts further blood flow. Glucose in unfrozen tissues is about 2-5 mM but during freezing rises to ~50 mM in peripheral tissues (skin, muscle) that freeze first and to as high as 200-300 mM in internal organs (heart, liver) that freeze later as ice penetrates the abdominal cavity [3,4,31,35]. Glucose metabolism is an excellent example of quantitative and qualitative adaptation since it represents changes in regulatory mechanisms (qualitative) along with increased enzymatic activity (quantitative). A five-fold increase in the number of glucose transporters was also observed in liver cell membranes and other organs and aids rapid export and uptake of glucose [35]. This increase in transporters ensures the timely distribution of large quantities of glucose over a short time frame. Glucose levels in the body are maintained throughout the freezing period until the beginning of thawing, when the process is reversed and glucose is reconverted to glycogen, chiefly in the liver. Upon thawing, the high concentrations of glucose would result in hyperglycemic stress. Therefore, upon thawing, the levels of β2-adrenergic receptors decrease rapidly, suppressing the activity of glycogen phosphorylase and, at the same time, glycogen synthase activity is rapidly increased to restore glucose as glycogen in the liver [4,30].

As described above, the cessation of heartbeat and interrupted functioning of lungs along with the freezing of blood plasma cuts off the oxygen supply to organs; consequently, wood frogs experience anoxia [2,22]. Prolonged anoxia presents many biochemical challenges that need to be managed to ensure survival. These challenges include 1.

requirement for a large quantity of fuel such as glycogen to meet the energy needs via anaerobic metabolism (fermentation or lactic acid cycle), 2. an efficient way to neutralise toxic end products, 3. decreased energy consumption since energy production via anaerobic respiration is much lower compared to aerobic respiration, and 4. regulating antioxidant defence mechanisms in response to increased/potential oxidative damage that results during recovery from anoxia [22].

1.3 Anoxia: a side-stress of freeze tolerance

Wood frogs can survive anoxia as independent stress. Even though glucose acts as the main carbohydrate source, during anoxia (independent of freezing) no hyperglycemic response was observed as compared with the freezing conditions [3]. This is reasonable since anoxic conditions do not affect cell volume or involve the formation of ice crystals. Therefore, the glucose available is used to provide ATP anaerobically as opposed to being "on hold" as a cryoprotectant. A balance between the rate of ATP synthesis and ATP utilization needs to be maintained for the functioning of cellular processes. Oxygen dependent production of ATP via oxidative phosphorylation in mitochondria efficiently uses metabolic fuels and releases CO_2 and H_2O as end products [20] but under oxygen crisis, oxidative phosphorylation shuts down and an alternative gets activated to supply ATP.

There are two immediate problems that a cell encounters if the oxygen supply is cut off. Firstly, fuel sources such as lipids and amino acids cannot be catabolised in an oxygen-independent way, and secondly, increased glycolysis is an immediate but inefficient way to synthesize ATP. Similar to long-term freezing, enduring prolonged anoxia also requires several adaptive mechanisms. 1. Switching from aerobic to anaerobic pathways to provide

ATP for cell survival, 2. Stocking up on fermentable fuels like glycogen to support the low ATP yield via anaerobic metabolism, 3. Neutralizing the by products of fermentation such as lactic acid, 4. Regulation of pathways to meet ATP needs, and 5. Ability to combat reactive oxygen species.

As mentioned above, under anaerobic conditions, lipids cannot be used as a fuel source. Hence, control over glycolysis is essential. Organs of anoxia tolerant animals including wood frogs demonstrate a very well-developed glycolytic capacity. Glycolytic enzymes, specifically in the liver undergo reversible phosphorylation in response to anoxia in many species [34,36–39]. Multiple studies have shown tissue specific regulation of pyruvate dehydrogenase, pyruvate kinase, fructose 1,6-bisphosphatase, lactate dehydrogenase, and phosphofructokinase 2 to facilitate prolonged energy production under anoxia [36,40–42]. Many anoxia tolerant animals (e.g. molluscs and some other invertebrates) also ferment certain amino acids like glutamate, glutamine, aspartate, and asparagine [43,44], whereas turtles and frogs primarily use stored glycogen and rely on anaerobic glycolysis to produce ATP [22,40]. However, glycolysis with lactate as end product has two major limitations: 1. A decrease in the production of ATP from a net 36 ATP per glucose molecule during respiration to a net of just 2 ATP under lactic acid fermentation [20] and 2. Cellular acidification.

The ATP obtained via fermentative pathways is 90% less than the amount obtained from oxidative metabolism and requires strict regulation to maintain the balance between demands and utilization. In the short term, this could be attained by increasing the rate of glycolysis to generate more ATP but generally fails for the long term [20] since it would quickly deplete the fuel reserves. Therefore, in the long term, multicellular organisms rely

on MRD which allows net ATP utilization to be reduced to about 10% under anoxic conditions. This solves two purposes, 1. the 10% of the ATP generated during anoxia compared to respiration meets the ATP needs during metabolic suppression, and 2. Reduced ATP turnover reduces the amount of acidification and net building up of end products. Among other modifications, MRD includes well-developed anaerobic metabolism, regulatory modifications to enzymes, production of protective chaperone proteins, and preventing/repairing tissue damage. Two important survival strategies that need to be adopted are global metabolic rate depression to minimize ATP demands and enhanced antioxidant defenses [4,10].

1.3.1 Oxidative stress and Antioxidant defence mechanisms

Protective responses such as DNA damage repair, up-regulation of chaperones to stabilize proteins, antioxidant defence systems, and control over energy-expensive pathways like protein synthesis and degradation [3] need to be channeled. Activation of regulatory pathways to control oxidative stress involves an enhanced antioxidant defence system [10]. Under aerobic conditions, water is the end product formed by the reduction of oxygen but anoxia halts oxidative phosphorylation. Reducing agents like NADH and $FADH_2$ build up, making electrons more available to reduce O_2 to O_2^- (superoxide) [45]. Elevated superoxide then initiates a chain of reactions producing other types of reactive oxygen species (ROS) including hydrogen peroxide and hydroxyl radical [46]. The three primary free radicals, that are, superoxides, hydrogen peroxide, and hydroxyl radical are commonly called ROS since they contain oxygen with reactive properties [46].

ROS are highly reactive yet short-lived ions that are formed in low amounts during aerobic metabolism, but levels increase significantly under hypoxia/anoxia and later during

reoxygenation [47]. At low concentrations, ROS plays important role in physiological functioning by acting as a second messenger. However, overproduction of ROS can cause disastrous effects and irreversible damage to cells [48,49]. Upon reoxygenation with a rush of oxygen in the system, controlling ROS production can become challenging [47]. Since accumulated electrons and reducing equivalents in the cytochrome chain could react with oxygen entering cells, ROS could be generated at a very high rate. Even though ROS are very short-lived, their rate of production is very high during reoxygenation and this could cause damage to macromolecules (including nucleic acids, lipids, and proteins), leading to their dysfunction and/or degradation, even potentially leading to cell death [49].

Oxidative stress is a condition where the rate of ROS generation exceeds the antioxidant capacity of the cells. Severe consequences of oxidative stress include protein oxidation, DNA damage, and lipid peroxidation. Lipid peroxidation is a chain reaction catalysed by transition metals and causes the breakdown of polyunsaturated fatty acids (PUFA) contained in phospholipids present in membranes [50]. This has the potential to damage all types of cell and subcellular membranes, for example, damage to the sarcoplasmic reticulum of muscles could lead to the release of Ca^{+} ions into the cytoplasm causing uncontrolled activation of Ca^{+2} dependent proteases or phospholipases [20,50].

Antioxidant defence mechanisms help minimize oxidative stress. The antioxidant defense system can be categorised into four classes 1. Primary antioxidant defenses that deal with oxygen and ROS, e.g. SOD, catalase, 2. Auxiliary enzyme systems that support the function of primary antioxidants, e.g. glutathione reductase, 3. Metal-forming complexes with enzymes, e.g. ferritin, transferrin, metallothionein, etc., and 4. Repair biomolecules to fix damage caused by ROS; e.g. DNA repair enzymes [50]. Studies from

our lab have evaluated changes in the activity and enzymatic properties of antioxidant enzymes in multiple tissues over stress/recovery cycles of wood frogs [51–54]. An increase of 20-150% in enzyme activity of glutathione peroxidase (GPox) was observed in different organs during 24 H freezing [53]. Another study showed that total protein levels of GSTT1 increased by 2.3 fold and 3.1 fold during anoxia in the liver and muscles of wood frogs, respectively [54]. In a similar study, the total protein levels of AKR1A3 showed an increase of 1.72 fold in the liver during anoxia [54]. This suggests the probable role of antioxidant defence mechanisms in combating oxidative stress and promoting survival under prolonged anoxic conditions.

1.3.2 Metabolic Rate Depression (MRD) during anoxia

Metabolic rate depression (MRD) is the most important adaptation that aims to regulate available fuel reserves to allow animals to sustain homeostasis and survive over long periods under adverse environmental conditions. MRD could be referred to as the conservation-based solution to limited availability of fuel/energy where animals lower their metabolic rate to match ATP output via fermentation (anaerobic metabolism) [20]. Metabolic suppression is not implemented in all the organs and cellular processes uniformly. Therefore, cells need to reprioritise their processes and metabolic needs. For example, in anoxic turtles, total ATP turnover dropped by 94% compared to aerobic conditions but ATP consuming processes were differentially affected. For example, the activity of the Na^+/K^+ pump decreased by 75% whereas the protein synthesis dropped by 93% [55]. Reprioritisation of processes also occurs between organs. For example, in hibernating ground squirrels, brain showed a 66% decrease in protein synthesis as well as an 85% reduction in kidneys but rates remained unchanged in brown adipose tissue [56].

Hence it can be said that MRD is based on three principles 1. involvement of both intrinsic and extrinsic mechanisms, 2. coordinated suppression of energy production and consumption rates to ensure longer sustainability based on new lower ATP turnover, and 3. reprioritisation of pro-survival pathways and suppression of less essential ones like translation.

Review articles from our lab have presented the concept of "Preparation for oxidative stress" [47,57] that discuss the idea of elevated levels of antioxidant defenses put in place in advance of predictable cycles of seasonal variation. This concept is essential for stress tolerant animals during hypometabolic states (frozen, anoxic, dehydrated, etc.) with limited time and energy to react to environmental stress. The response is mediated by transcriptional and translational arrest, metabolic rate depression, rerouting of metabolic pathways from oxidative to fermentative, and activation of mechanisms that are involved in the repair and detoxification of cellular derived oxidants [25]. Cells respond to elevated rates of ROS production by activating antioxidant defence systems. This suggests that redox regulation of transcription factors determines the expression profile of various genes in response to stress.

1.4 Regulation of transcriptional pathways in response to MRD and oxidative stress

Management of MRD involves a complicated network of many cellular signaling pathways that work in a coordinated manner. MRD is regulated at multiple levels: transcriptional, post-transcriptional, translational, and post-translational [23,27]. MRD is not associated with the loss of metabolic capacity but with the flexible application of reversible controls that can quickly suppress the metabolic rate of cells while maintaining

the capacity to rapidly return to normal during recovery. Reversible epigenetic mechanisms play a significant role in this process by mediating changes in DNA accessibility to transcription factors and thereby altering the expression of selected genes without altering the genome itself [58]. Such epigenetic controls can effectively alter gene expression in response to altered environmental conditions and can work on a short time scale. These mechanisms include DNA methylation, posttranslational modifications of histones, and microRNA regulation.

1.4.1. Role of Jumonji demethylases (JMJD) in regulating antioxidants under MRD

The hypoxia inducible factor 1 (HIF-1) is an important transcription factor with respect to MRD, specifically in situations where oxygen availability is highly restricted (e.g. exposure to complete anoxic conditions). HIF-1 is induced/stabilized under low oxygen conditions and is responsible for upregulating a range of genes whose protein products support survival under hypoxia or anoxia conditions [59]. Active HIF-1 is a dimer composed of an active short-lived HIF-1 alpha subunit that targets specific genes and a beta subunit (also called ARNT) that aids in binding to genes.

Of particular interest in the present thesis is the role of HIF-1 in the upregulation of the expression of the Jumonji domain containing demethylases (JMJDs) [60]. JMJDs are lysine demethylases that have been explored recently for their role in regulating stress specific gene expression [61–63] to survive stress with limited availability of energy. The Octamer binding transcription factor (OCT) family also mediates the recruitment of JMJD1A and JMJD2C to demethylate target genes like adenosylhomocysteinase (*ahcy*) and DNA-directed RNA polymerase II subunit RPB1 (*polr2a*) in response to oxidative stress [64]. The AHCY protein prevents the accumulation of S-adenosylhomocysteine (SAH) by

hydrolysing it to adenosine and homocysteine [65] and hence suppresses the inhibition of methyltransferases. This regulates SAH to SAM ratio which determines the cellular methylation capacity [66] and acts as a deciding factor in DNA and RNA methylation.

JMJD1A and JMJD2C catalyse oxidative demethylation of H3K9 and H3K36 residues on histone 3, respectively [67,68]. In addition to regulation at the transcriptional level by demethylating histones and activating genes encoding proteins involved in the methylation cycle, JMJDs are also associated with genes related to free radical quenchers such as glutathione, an antioxidant that protects against free radicals [61–64]. A 20-150% increase in enzymatic levels of glutathione peroxidase (GPox) occurred in different organs of wood frogs after 24 H frozen but no change was observed in other antioxidant enzymes [53] showing the activity of glutathione to elevated rates of ROS.

1.4.2. NRF2 mediated response to oxidative stress

Another transcription factor that is extensively studied with respect to oxidative stress is the Nuclear Factor Erythroid 2-Related Factor 2 transcription factor (NRF2) [26,69–71]. NRF2 regulates the expression of genes having an antioxidant response element (ARE) sequence in their promoter region. In general, NRF2 is present in association with the Kelch-like ECH associated protein-1 (KEAP-1) in the cytoplasm and undergoes ubiquitination. When oxidative stress rises in the cell, the bond between NRF2 and KEAP-1 dissociates and NRF2 translocates into the nucleus where it binds with MAFG. The heterodimer complex then binds to the ARE sequence present in the promoter region of the genes associated with antioxidant enzymes. Some of the enzymes regulated by NRF2 are glutathione S-transferases (GSTs), NADPH quinone oxidoreductase-1 (NQO-1), and aldo-keto reductases (AKRs) [71,72]. Previous studies showed increases in transcript and

protein levels of NRF2 in response to 5 H freezing in tissues of hatchling painted turtles (*Chrysemys picta marginata*) [73]. Turtles also showed a significant increase in the total protein levels of GSTs in a tissue specific manner. African clawed frogs, *Xenopus laevis,* also showed a stress-responsive increase in NRF2 total protein and its downstream factors in a tissue specific manner [74]. For example, dehydration exposure of *X. laevis* led to a 2-fold increase in the transcript levels of *nrf2* in the liver, 2-4 fold increases in total NRF2 protein levels in lungs, heart, skin, liver, and a 4.3 fold increase in skeletal muscle [74]. The examples represent the antioxidant role of NRF2 in the cells in varied stresses.

NRF2 also binds to the promoter regions of OCT4 and regulates its expression [75]. OCT1 and OCT4 are ubiquitously expressed transcription factors that act either directly or as coregulators to control the expression of genes in a stress specific manner [76–80]. They play a major role in oxidative stress and genotoxicity. The transcriptional regulation by OCTs work via three processes, 1. gene activation, 2. transcriptionally silent gene targets, and 3. transcriptionally repressed targets or gene repression. However, OCT1 is essential for post-stress transcriptional responses and OCT4 induces responses during stress exposure of cells [78,79]. In response to increased oxidative stress, metabolic suppression, and DNA damage, OCT1 halts the expression of genes like *bbc3, daf1* [81,82] and downregulates H2B and U2RNA to promote cell survival [77]. In addition to transcriptional repression and activation, another mode of regulation is gene poising. Gene poising is a chromatin free repressive modification where the genes are kept on standby in a readily inducible configuration [83]. Different modes of regulation including transcription repression, transcription activation, or gene poising (binding to JMJDs) can be switched on/off by regulatory inputs upstream of binding sites [82,83]. The OCT4 in

association with SOX2 and KLF4 forms Yamanaka factors to regulate cellular reprogramming, cell cycle, apoptosis, etc. [84]. In response to stress signals, OCT4 alters its affinity for complex binding sites [78] to play a key role in tissue homeostasis, cell renewal, and tissue repair [80]. Furthermore, the expression of OCT4 is regulated by many other stress responsive transcription factors/ signaling pathways like yes associated protein (YAP) [85], recombination signal binding protein for immunoglobulin kappa J region (RBPJ) [86,87], via hippo pathway and notch signaling, respectively.

1.4.3. Hippo pathway in response to oxidative and energy stress

The hippo signaling pathway regulates organ size and a variety of cellular processes related to cell proliferation and differentiation [88,89]. Many factors including ROS, DNA damage, mechanical stress, energy crisis, and oxygen stress can stimulate the pathway that is initiated by phosphorylation of the first component of the pathway, the Ste20-like kinases 1/2 (MST1/2) at Thr183 and Thr180 followed by a cascade of reactions in a stress specific manner [89]. Studies showed that under anoxic conditions, activation of the Hippo pathway phosphorylates YAP/TAZ sequestering it in the cytoplasm [90,91]. This prevents binding of YAP/TAZ/TEAD to promoter regions and restricts apoptosis and activation of energy expensive processes to promote survival under energy crisis. Studies showed that during the metabolic depression, AMPK directly phosphorylates YAP and prevents YAP/TAZ/TEAD mediated transcription [92]. It has been shown that AMPK activity increased during anoxia in wood frog liver [93] suggesting activation of the pathway. The Hippo pathway cross-talks with other pathways such as Notch, Hedgehog, Wnt, and transcription factors such as bone morphogenic proteins (BMPs) that affect the functioning of YAP/TAZ [92,94].

1.4.4. Establishing cellular communication via a notch signaling pathway

Effective inter-cellular communication is essential to regulate pro-survival pathways under stress [95]. Notch signaling is one such pathway and is initiated when the ligands Delta-like (DLL) and Jagged (JAG) on the plasma membrane of one cell interact with the Notch receptors on a neighbouring cell to transmit the signal and activate the signaling pathway. Upon encountering oxidative stress, Notch receptors undergo O-linked glycosylation and multiple cleavages to release the Notch intracellular domain (NICD) protein in the cytoplasm. NICD can either be sequestered in the cytoplasm or translocate to the nucleus to bind with mastermind-like protein 1 (MAML) and recombination signal binding protein for immunoglobulin kappa J region (RBP-Jk) [96] to form the notch transcriptional complex. This complex binds to promoter regions in the DNA fragment and initiates gene expression [97]. Under hypoxic conditions, HIF1α also activates notch signaling to initiate transcription of genes in other signaling pathways in a stress specific manner [97]. Indeed, Notch signaling plays a crucial role not only in inducing angiogenesis but also triggers repair mechanisms for myocardial regeneration [98]. The regenerative role of notch signaling has been studied in mammals and suggests its importance during tissue injuries and damage in a stress specific manner [86,87,99,100].

1.5 General hypothesis and objectives

Taken together, to allow long term survival during anoxic conditions, many stress responsive transcription factors including hypoxia inducible factors (HIF) [54,96], nuclear factor erythroid 2–related factor 2 (Nrf2) [65,66,68,69], octamer binding transcription factor (OCT) [73], yes associated protein (YAP) [80], Recombination Signal Binding Protein For Immunoglobulin Kappa J Region (RBPJ) [81,82], and others mediate and re-

organise cellular processes to combat oxidative stress. This is particularly important under environmental stress conditions that trigger MRD as a survival strategy (Figure 1.1). To gather novel information about responses to oxygen deprivation by freeze tolerant wood frogs, the research presented in this thesis addresses the following hypothesis.

General hypothesis: In wood frogs, a well communicated and coordinated network of transcription factors regulate pro-survival pathways and mediate gene responses involved in antioxidant defense mechanisms and tissue repair systems to maintain cellular homeostasis in accordance with metabolic rate depression as a strategy for enduring prolonged anoxia.

Objective 1. Regulation of antioxidant system responses to anoxia in the wood frog, *Rana sylvatica*.

It is proposed that OCT4, along with its coregulators, KLF4 and SOX2 works in coordination with the NRF2 antioxidant pathway to prevent/ minimise oxidative stress. Two stress responsive transcription factors, NRF2 and OCT4, and their roles in antioxidant defense systems are investigated in Chapter 2. Relative total levels of proteins involved in regulating NRF2 and OCT4 and their relative DNA binding ability to gene promoter regions are analyzed in liver and skeletal muscle under 24 H anoxia and 4 H reoxygenation compared to control. Relative changes in total protein levels of selected key antioxidants (GSTs and AKRs) under the control of these transcription factors are also assessed.

Objective 2. Regulation of gene methylation by Jumonji and AHCY under OCT control.

JMJDs exert epigenetic controls on various genes by mediating histone 3 demethylation on lysine 9 (H3K9). Given that JMJDs are oxygen sensitive demethylases and regulate the

gene expression for enzymes involved in the methylation cycle and antioxidants, the study of JMJDs would provide better insights into animal's responses to anoxia. Therefore, chapter 3 examines the differential regulation of JMJDs by OCT1 and OCT4 in response to low oxygen by analysing their relative total protein and transcript levels in response to anoxia and recovery compared with controls in the liver and skeletal muscles. JMJD1A and JMJD2C, two enzymes of the methylation cycle are analyzed as well as AHCY and MAT protein levels.

Objective 3. Regulation of the hippo signaling pathway

The hippo signaling pathway is a signaling network that controls a variety of pro-survival pathways upon stimulation by low oxygen concentration and energy crisis. The pathway on activation sequesters an important transcription factor, YAP, in the cytoplasm and prevents the formation of the YAP transcription complex to initiate gene expression. Chapter 4 analyses major components of the pathway at transcript and protein levels and relative binding of TEAD to the promoter regions of downstream targets in liver and heart during 24 H anoxia and 4 H recovery.

Objective 4. Study of the Notch communication network.

Notch signaling provides an effective communication channel between cells to regulate tissue repair resulting due to oxidative stress. In chapter 5, the major components of the notch signaling pathway were analysed at transcript and protein levels in liver and heart upon encountering 24 H anoxia and 4 H of reoxygenation compared to control conditions. Structural analysis of protein sequences was also used for a better comprehension of the receptor, ligands, and transcriptional complex.

1.6 Crosstalk between proposed pathways

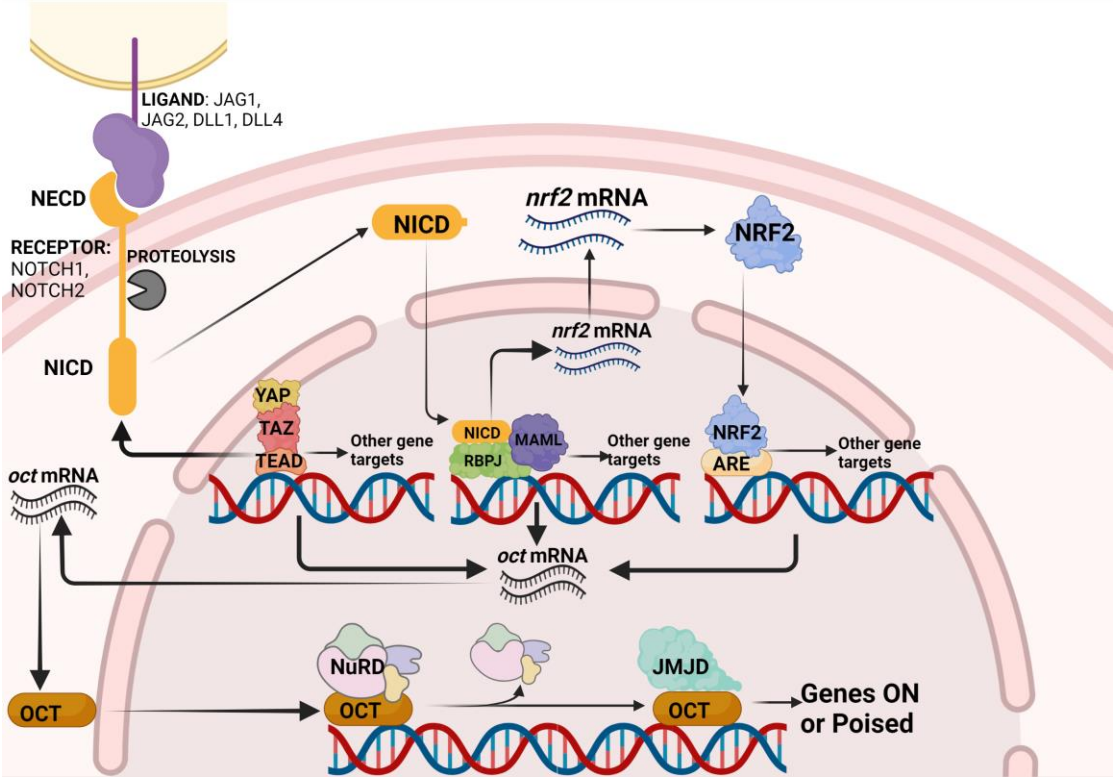

Figure 1.1: The schematic diagram demonstrating crosstalk between the proposed pathways. Abbreviations: DLL: Delta-like, JAG: Jagged, NECD: Notch extracellular domain, NICD: Notch intracellular domain, MAML: Mastermind-like protein, RBPJ: Recombination Signal Binding Protein for Immunoglobulin Kappa J Region,YAP: yes-associated protein, TAZ: transcriptional coactivator with PDZ-binding motif, TEAD: TEA domain family member, NRF2: Nuclear factor (erythroid-derived 2)-like 2 transcription factor, ARE: antioxidant response element, OCT: Octamer Binding Transcription factor , NuRD: nucleosome remodeling and the histone deacetylation, JMJD: jumonji domain-containing proteins.

1.7 References:

[1] K.B. Storey, Strategies for exploration of freeze responsive gene expression: advances in vertebrate freeze tolerance, Cryobiology. 48 (2004) 134–145. https://doi.org/10.1016/j.cryobiol.2003.10.008.

[2] K.B. Storey, Survival under stress: molecular mechanisms of metabolic rate depression in animals, South African J. Zool. l33 (1998) 55–64. https://doi.org/10.1080/02541858.1998.11448454.

[3] K.B. Storey, J.M. Storey, Molecular biology of freezing tolerance, Compr. Physiol. 3 (2013) 1283–1308. https://doi.org/10.1002/cphy.c130007.

[4] K.B. Storey, J.M. Storey, Freeze tolerance in animals, Physiol. Rev. 68 (1988) 27–84. https://doi.org/10.1152/physrev.1988.68.1.27.

[5] J.M. Storey, K.B. Storey, Cold Hardiness and Freeze Tolerance, in: Funct. Metab., John Wiley & Sons, Inc., Hoboken, NJ, USA, 2005: pp. 473–503. https://doi.org/10.1002/047167558X.ch17.

[6] L. Sømme, Supercooling and winter survival in terrestrial arthropods, Comp. Biochem. Physiol. Part A Physiol. 73 (1982) 519–543. https://doi.org/10.1016/0300-9629(82)90260-2.

[7] C.H. Lowe, P.J. Lardner, E.A. Halpern, Supercooling in reptiles and other vertebrates, Comp. Biochem. Physiol. Part A Physiol. 39 (1971) 125–135. https://doi.org/10.1016/0300-9629(71)90352-5.

[8] M.J. Kelleher, J. Rickards, K.B. Storey, Strategies of freeze avoidance in larvae of the goldenrod gall moth, *Epiblema scudderiana*: Laboratory investigations of temperature cues in the regulation of cold hardiness, J. Insect Physiol. 33 (1987) 581–586. https://doi.org/10.1016/0022-1910(87)90073-4.

[9] K.B. Storey, Reptile freeze tolerance: Metabolism and gene expression, Cryobiology. 52 (2006) 1–16. https://doi.org/10.1016/j.cryobiol.2005.09.005.

[10] K.B. Storey, J.M. Storey, Molecular physiology of freeze tolerance in vertebrates, Physiol. Rev. 97 (2017) 623–665. https://doi.org/10.1152/physrev.00016.2016.

[11] J.M. Storey, K.B. Storey, Triggering of cryoprotectant synthesis by the initiation of ice nucleation in the freeze tolerant frog , *Rana sylvatica*, J. Comp. Physiol. B. 156 (1985) 191–195. https://doi.org/10.1007/BF00695773.

[12] K.E. Zachariassen, E. Kristiansen, Ice Nucleation and Antinucleation in Nature, Cryobiology. 41 (2000) 257–279. https://doi.org/10.1006/cryo.2000.2289.

[13] J.G. Duman, Animal ice-binding (antifreeze) proteins and glycolipids: an overview with emphasis on physiological function, J. Exp. Biol. 218 (2015) 1846–1855. https://doi.org/10.1242/jeb.116905.

[14] K.J. Sullivan, K.K. Biggar, K.B. Storey, Transcript expression of the freeze responsive gene fr10 in *Rana sylvatica* during freezing, anoxia, dehydration, and development, Mol. Cell. Biochem. 399 (2015) 17–25. https://doi.org/10.1007/s11010-014-2226-9.

[15] Q. Cai, K. B. Storey, Upregulation of a novel gene by freezing exposure in the freeze-tolerant wood frog (*Rana sylvatica*), Gene. 198 (1997) 305–312. https://doi.org/10.1016/S0378-1119(97)00332-6.

[16] K.K. Biggar, Y. Biggar, K.B. Storey, Identification of a novel dehydration responsive gene, drp10 , from the African clawed frog, *Xenopus laevis*, J. Exp. Zool. Part A Ecol. Genet. Physiol. 323 (2015) 375–381. https://doi.org/10.1002/jez.1930.

[17] W.D. Schmid, Survival of Frogs in Low Temperature, Science. 215 (1982) 697–698. https://doi.org/10.1126/science.7058335.

[18] K.B. Storey, J.M. Storey, Freeze tolerant frogs: cryoprotectants and tissue metabolism during freeze–thaw cycles, Can. J. Zool. 64 (1986) 49–56. https://doi.org/10.1139/z86-008.

[19] K.B. Storey, J.M. Storey, Tribute to P. L. Lutz: putting life on `pause' - molecular regulation of hypometabolism, J. Exp. Biol. 210 (2007) 1700–1714. https://doi.org/10.1242/jeb.02716.

[20] K.B. Storey, J.M. Storey, Oxygen Limitation and Metabolic Rate Depression, in: K.B. Storey (Ed.), Funct. Metab., John Wiley & Sons, Inc., Hoboken, NJ, USA, 2005: pp. 415–442. https://doi.org/10.1002/047167558X.ch15.

[21] D.F.S. Rolfe, G.C. Brown, Cellular energy utilization and molecular origin of standard metabolic

rate in mammals, Physiol. Rev. 77 (1997) 731–758. https://doi.org/10.1152/physrev.1997.77.3.731.
[22] K.B. Storey, Molecular mechanisms of anoxia tolerance, Int. Congr. Ser. 1275 (2004) 47–54. https://doi.org/10.1016/j.ics.2004.08.072.
[23] K.B. Storey, J.M. Storey, Metabolic rate depression in animals: transcriptional and translational controls, Biol. Rev. 79 (2004) 207–233. https://doi.org/10.1017/S1464793103006195.
[24] S. Wijenayake, B.E. Luu, J. Zhang, S.N. Tessier, J.F. Quintero-Galvis, J.D. Gaitán-Espitia, R.F. Nespolo, K.B. Storey, Strategies of biochemical adaptation for hibernation in a South American marsupial *Dromiciops gliroides*: 1. Mitogen-activated protein kinases and the cell stress response, Comp. Biochem. Physiol. Part B Biochem. Mol. Biol. 224 (2018) 12–18. https://doi.org/10.1016/j.cbpb.2017.12.007.
[25] M.F. Oliveira, M.A. Geihs, T.F.A. França, D.C. Moreira, M. Hermes-Lima, Is "Preparation for Oxidative Stress" a Case of Physiological Conditioning Hormesis?, Front. Physiol. 9 (2018) 945. https://doi.org/10.3389/fphys.2018.00945.
[26] M. Hermes-Lima, D.C. Moreira, G.A. Rivera-Ingraham, M. Giraud-Billoud, T.C. Genaro-Mattos, É.G. Campos, Preparation for oxidative stress under hypoxia and metabolic depression: Revisiting the proposal two decades later, Free Radic. Biol. Med. 89 (2015) 1122–1143. https://doi.org/10.1016/j.freeradbiomed.2015.07.156.
[27] K.B. Storey, J.M. Storey, Metabolic Rate Depression and Biochemical Adaptation in Anaerobiosis, Hibernation and Estivation, Q. Rev. Biol. 65 (1990) 145–174. https://doi.org/10.1086/416717.
[28] K.B. Storey, Oxidative stress: Animal adaptations in nature, Brazilian J. Med. Biol. Res. 29 (1996) 1715–1733.
[29] R.E. Lee, J.P. Costanzo, Biological ice nucleation and ice distribution in cold-hardy ectothermic animals, Annu. Rev. Physiol. 60 (1998) 55–72. https://doi.org/10.1146/annurev.physiol.60.1.55.
[30] K.B. Storey, J.M. Storey, Signal transduction and gene expression in the regulation of natural freezing survival, in: J.M. Storey, K.B. and Storey (Ed.), Cell Mol. Response to Stress, Vol. 2: Pr, Elsevier Press, Amsterdam, 2001: pp. 1–19. https://doi.org/10.1016/S1568-1254(01)80003-6.
[31] K.B. Storey, J.M. Storey, Frozen and Alive, Sci. Am. 263 (1990) 92–97. https://doi.org/10.1038/scientificamerican1290-92.
[32] J.P. Wolanczyk, K.B. Storey, J.G. Baust, Ice nucleating activity in the blood of the freeze-tolerant frog, *Rana sylvatica*, Cryobiology. 27 (1990) 328–335. https://doi.org/10.1016/0011-2240(90)90032-Y.
[33] K.B. Storey, J.M. Storey, Biochemical adaption for freezing tolerance in the wood frog, *Rana sylvatica*, J. Comp. Physiol. B. 155 (1984) 29–36. https://doi.org/10.1007/BF00688788.
[34] K.B. Storey, Regulation of liver metabolism by enzyme phosphorylation during mammalian hibernation., J. Biol. Chem. 262 (1987) 1670–1673. https://doi.org/10.1016/S0021-9258(19)75689-0.
[35] K.J. Cowan, K.B. Storey, Freeze-Thaw Effects on Metabolic Enzymes in Wood Frog Organs, Cryobiology. 43 (2001) 32–45. https://doi.org/10.1006/cryo.2001.2338.
[36] L.J. Hawkins, M. Wang, B. Zhang, Q. Xiao, H. Wang, K.B. Storey, Glucose and urea metabolic enzymes are differentially phosphorylated during freezing, anoxia, and dehydration exposures in a freeze tolerant frog, Comp. Biochem. Physiol. Part D Genomics Proteomics. 30 (2019) 1–13. https://doi.org/10.1016/j.cbd.2019.01.009.
[37] T.J. Park, J. Reznick, B.L. Peterson, G. Blass, D. Omerbašić, N.C. Bennett, P.H.J.L. Kuich, C. Zasada, B.M. Browe, W. Hamann, D.T. Applegate, M.H. Radke, T. Kosten, H. Lutermann, V. Gavaghan, O. Eigenbrod, V. Bégay, V.G. Amoroso, V. Govind, R.D. Minshall, E.S.J. Smith, J. Larson, M. Gotthardt, S. Kempa, G.R. Lewin, Fructose-driven glycolysis supports anoxia resistance in the naked mole-rat, Science. 356 (2017) 307–311.
[38] W.G. Willmore, K.J. Cowan, K.B. Storey, Effects of anoxia exposure and aerobic recovery on metabolic enzyme activities in the freshwater turtle *Trachemys scripta elegans*, Can. J. Zool. 79

(2001) 1822–1828. https://doi.org/10.1139/z01-149.

[39] K.B. Storey, S.P.J. Brooks, Chapter 6 The basis of enzymatic adaptation, in: Princ. Med. Biol., 1995: pp. 147–169. https://doi.org/10.1016/S1569-2582(06)80008-5.

[40] A. Gupta, A. Varma, K.B. Storey, New Insights to Regulation of Fructose-1,6-bisphosphatase during Anoxia in Red-Eared Slider, *Trachemys scripta elegans*, Biomolecules. 11 (2021) 1548. https://doi.org/10.3390/biom11101548.

[41] R. Al-attar, S. Wijenayake, K.B. Storey, Metabolic reorganization in winter: Regulation of pyruvate dehydrogenase (PDH) during long-term freezing and anoxia, Cryobiology. 86 (2019) 10–18. https://doi.org/10.1016/j.cryobiol.2019.01.006.

[42] Z.J. Xiong, K.B. Storey, Regulation of liver lactate dehydrogenase by reversible phosphorylation in response to anoxia in a freshwater turtle, Comp. Biochem. Physiol. Part B Biochem. Mol. Biol. 163 (2012) 221–228. https://doi.org/10.1016/j.cbpb.2012.06.001.

[43] K. Larade, K. Storey, Living without Oxygen: Anoxia-Responsive Gene Expression and Regulation, Curr. Genomics. 10 (2009) 76–85. https://doi.org/10.2174/138920209787847032.

[44] A. de Zwaan, P. Cortesi, G. van den Thillart, J. Roos, K.B. Storey, Differential sensitivities to hypoxia by two anoxia-tolerant marine molluscs: A biochemical analysis, Mar. Biol. 111 (1991) 343–351. https://doi.org/10.1007/BF01319405.

[45] T. McGarry, M. Biniecka, D.J. Veale, U. Fearon, Hypoxia, oxidative stress and inflammation, Free Radic. Biol. Med. 125 (2018) 15–24. https://doi.org/10.1016/j.freeradbiomed.2018.03.042.

[46] K.B. Storey, Metabolic adaptations supporting anoxia tolerance in reptiles: Recent advances, Comp. Biochem. Physiol. Part B Biochem. Mol. Biol. 113 (1996) 23–35. https://doi.org/10.1016/0305-0491(95)02043-8.

[47] M. Giraud-Billoud, G.A. Rivera-Ingraham, D.C. Moreira, T. Burmester, A. Castro-Vazquez, J.M. Carvajalino-Fernández, A. Dafre, C. Niu, N. Tremblay, B. Paital, R. Rosa, J.M. Storey, I.A. Vega, W. Zhang, G. Yepiz-Plascencia, T. Zenteno-Savin, K.B. Storey, M. Hermes-Lima, Twenty years of the 'Preparation for Oxidative Stress' (POS) theory: Ecophysiological advantages and molecular strategies, Comp. Biochem. Physiol. Part A Mol. Integr. Physiol. 234 (2019) 36–49. https://doi.org/10.1016/j.cbpa.2019.04.004.

[48] M. Redza-Dutordoir, D.A. Averill-Bates, Activation of apoptosis signalling pathways by reactive oxygen species, Biochim. Biophys. Acta - Mol. Cell Res. 1863 (2016) 2977–2992. https://doi.org/10.1016/j.bbamcr.2016.09.012.

[49] S.W. Ryter, H.P. Kim, A. Hoetzel, J.W. Park, K. Nakahira, X. Wang, A.M.K. Choi, Mechanisms of Cell Death in Oxidative Stress, Antioxid. Redox Signal. 9 (2007) 49–89. https://doi.org/10.1089/ars.2007.9.49.

[50] M. Hermes-Lima, Oxygen in Biology and Biochemistry: Role of Free Radicals, in: Funct. Metab., John Wiley & Sons, Inc., Hoboken, NJ, USA, 2005: pp. 319–368. https://doi.org/10.1002/047167558X.ch12.

[51] N.J. Dawson, B.A. Katzenback, K.B. Storey, Free-radical first responders: The characterization of CuZnSOD and MnSOD regulation during freezing of the freeze-tolerant North American wood frog, *Rana sylvatica*, Biochim. Biophys. Acta - Gen. Subj. 1850 (2015) 97–106. https://doi.org/10.1016/j.bbagen.2014.10.003.

[52] N.J. Dawson, K.B. Storey, A hydrogen peroxide safety valve: The reversible phosphorylation of catalase from the freeze-tolerant North American wood frog, *Rana sylvatica*, Biochim. Biophys. Acta - Gen. Subj. 1860 (2016) 476–485. https://doi.org/10.1016/j.bbagen.2015.12.007.

[53] D.R. Joanisse, K.B. Storey, Oxidative damage and antioxidants in *Rana sylvatica*, the freeze-tolerant wood frog., Am. J. Physiol. 271 (1996) R545-53. https://doi.org/10.1152/ajpregu.1996.271.3.R545.

[54] A. Gupta, K.B. Storey, Regulation of antioxidant systems in response to anoxia and reoxygenation in *Rana sylvatica*, Comp. Biochem. Physiol. Part B Biochem. Mol. Biol. 243–244 (2020) 110436. https://doi.org/10.1016/j.cbpb.2020.110436.

[55] P.W. Hochachka, L.T. Buck, C.J. Dollt, S.C. Landt, Unifying theory of hypoxia tolerance: Molecular/metabolic defense and rescue mechanisms for surviving oxygen lack (oxygen sensing/hypoxia defense/turtle hepatocytes/turtle brain), Biochemistry. 93 (1996) 9493–9498.

[56] D. Hittel, K.B. Storey, The translation state of differentially expressed mRNAs in the hibernating 13-lined ground squirrel (*Spermophilus tridecemlineatus*), Arch. Biochem. Biophys. 401 (2002) 244–254. https://doi.org/10.1016/S0003-9861(02)00048-6.

[57] M. Hermes-Lima, J.M. Storey, K.B. Storey, Antioxidant defenses and metabolic depression. The hypothesis of preparation for oxidative stress in land snails, Comp. Biochem. Physiol. Part B Biochem. Mol. Biol. 120 (1998) 437–448. https://doi.org/10.1016/S0305-0491(98)10053-6.

[58] A.P. Wolffe, M.A. Matzke, Epigenetics: Regulation Through Repression, Science (80-.). 286 (1999) 481–486. https://doi.org/10.1126/science.286.5439.481.

[59] G.L. Semenza, Oxygen Sensing, Hypoxia-Inducible Factors, and Disease Pathophysiology, Annu. Rev. Pathol. Mech. Dis. 9 (2014) 47–71. https://doi.org/10.1146/annurev-pathol-012513-104720.

[60] X. Xia, M.E. Lemieux, W. Li, J.S. Carroll, M. Brown, X.S. Liu, A.L. Kung, Integrative analysis of HIF binding and transactivation reveals its role in maintaining histone methylation homeostasis, Proc. Natl. Acad. Sci. 106 (2009) 4260–4265. https://doi.org/10.1073/pnas.0810067106.

[61] M. Batie, L. del Peso, S. Rocha, Hypoxia and Chromatin: A Focus on Transcriptional Repression Mechanisms, Biomedicines. 6 (2018) 47. https://doi.org/10.3390/biomedicines6020047.

[62] P.J. Pollard, C. Loenarz, D.R. Mole, M.A. McDonough, J.M. Gleadle, C.J. Schofield, P.J. Ratcliffe, Regulation of Jumonji-domain-containing histone demethylases by hypoxia-inducible factor (HIF)-1α, Biochem. J. 416 (2008) 387–394. https://doi.org/10.1042/BJ20081238.

[63] X. Qian, X. Li, Z. Shi, X. Bai, Y. Xia, Y. Zheng, D. Xu, F. Chen, Y. You, J. Fang, Z. Hu, Q. Zhou, Z. Lu, KDM3A Senses Oxygen Availability to Regulate PGC-1α-Mediated Mitochondrial Biogenesis, Mol. Cell. 76 (2019) 885-895.e7. https://doi.org/10.1016/j.molcel.2019.09.019.

[64] A. Shakya, J. Kang, J. Chumley, M.A. Williams, D. Tantin, Oct1 Is a Switchable, Bipotential Stabilizer of Repressed and Inducible Transcriptional States, J. Biol. Chem. 286 (2011) 450–459. https://doi.org/10.1074/jbc.M110.174045.

[65] R. Abeles, The Mechanism of Action of S-Adenosylhomocysteinase, in: H. Eggerer, R. Huber (Eds.), Struct. Funct. Asp. Enzym. Catal., Springer, Berlin, Heidelberg, 1981: pp. 192–195. https://doi.org/10.1007/978-3-642-81738-0_17.

[66] M.A. Caudill, J.C. Wang, S. Melnyk, I.P. Pogribny, S. Jernigan, M.D. Collins, J. Santos-Guzman, M.E. Swendseid, E.A. Cogger, S.J. James, Intracellular S-Adenosylhomocysteine Concentrations Predict Global DNA Hypomethylation in Tissues of Methyl-Deficient Cystathionine β-Synthase Heterozygous Mice, J. Nutr. 131 (2001) 2811–2818. https://doi.org/10.1093/jn/131.11.2811.

[67] R.J. Klose, K. Yamane, Y. Bae, D. Zhang, H. Erdjument-Bromage, P. Tempst, J. Wong, Y. Zhang, The transcriptional repressor JHDM3A demethylates trimethyl histone H3 lysine 9 and lysine 36, Nature. 442 (2006) 312–316. https://doi.org/10.1038/nature04853.

[68] K. Yamane, C. Toumazou, Y. Tsukada, H. Erdjument-Bromage, P. Tempst, J. Wong, Y. Zhang, JHDM2A, a JmjC-Containing H3K9 Demethylase, Facilitates Transcription Activation by Androgen Receptor, Cell. 125 (2006) 483–495. https://doi.org/10.1016/j.cell.2006.03.027.

[69] J. Zhang, A. Gupta, K.B. Storey, Freezing stress adaptations: Critical elements to activate Nrf2 related antioxidant defense in liver and skeletal muscle of the freeze tolerant wood frogs, Comp. Biochem. Physiol. Part B Biochem. Mol. Biol. 254 (2021) 110573. https://doi.org/10.1016/j.cbpb.2021.110573.

[70] R. Li, Z. Jia, H. Zhu, Regulation of Nrf2 Signaling., React. Oxyg. Species (Apex, N.C.). 8 (2019) 312–322. http://www.ncbi.nlm.nih.gov/pubmed/31692987.

[71] J.D. Hayes, A.T. Dinkova-Kostova, The Nrf2 regulatory network provides an interface between redox and intermediary metabolism, Trends Biochem. Sci. 39 (2014) 199–218. https://doi.org/10.1016/j.tibs.2014.02.002.

[72] D. Hyndman, D.R. Bauman, V. V. Heredia, T.M. Penning, The aldo-keto reductase superfamily homepage, Chem. Biol. Interact. 143–144 (2003) 621–631. https://doi.org/10.1016/S0009-2797(02)00193-X.

[73] A. Krivoruchko, K.B. Storey, Activation of antioxidant defenses in response to freezing in freeze-tolerant painted turtle hatchlings, Biochim. Biophys. Acta - Gen. Subj. 1800 (2010) 662–668. https://doi.org/10.1016/j.bbagen.2010.03.015.

[74] A.I. Malik, K.B. Storey, Activation of antioxidant defense during dehydration stress in the African clawed frog, Gene. 442 (2009) 99–107. https://doi.org/10.1016/j.gene.2009.04.007.

[75] X. Dai, X. Yan, K.A. Wintergerst, L. Cai, B.B. Keller, Y. Tan, Nrf2: Redox and Metabolic Regulator of Stem Cell State and Function, Trends Mol. Med. 26 (2020) 185–200. https://doi.org/10.1016/j.molmed.2019.09.007.

[76] D. Tantin, OCT transcription factors in development and stem cells: insights and mechanisms, Development. 140 (2013) 2857–2866. https://doi.org/10.1242/dev.095927.

[77] F.-Q. Zhao, Octamer-binding transcription factors: genomics and functions, Front. Biosci. 18 (2013) 1051. https://doi.org/10.2741/4162.

[78] J. Kang, M. Gemberling, M. Nakamura, F.G. Whitby, H. Handa, W.G. Fairbrother, D. Tantin, A general mechanism for transcription regulation by Oct1 and Oct4 in response to genotoxic and oxidative stress, Genes Dev. 23 (2009) 208–222. https://doi.org/10.1101/gad.1750709.

[79] J. Kang, A. Shakya, D. Tantin, Stem cells, stress, metabolism and cancer: a drama in two Octs, Trends Biochem. Sci. 34 (2009) 491–499. https://doi.org/10.1016/j.tibs.2009.06.003.

[80] I.R. Lemischka, Hooking Up with Oct4, Cell Stem Cell. 6 (2010) 291–292. https://doi.org/10.1016/j.stem.2010.03.011.

[81] J. Kang, B. Goodman, Y. Zheng, D. Tantin, Dynamic Regulation of Oct1 during Mitosis by Phosphorylation and Ubiquitination, PLoS One. 6 (2011) e23872. https://doi.org/10.1371/journal.pone.0023872.

[82] D. Tantin, C. Schild-Poulter, V. Wang, R.J.G. Haché, P.A. Sharp, The Octamer Binding Transcription Factor Oct-1 Is a Stress Sensor, Cancer Res. 65 (2005) 10750–10758. https://doi.org/10.1158/0008-5472.CAN-05-2399.

[83] K. Vázquez-Arreguín, D. Tantin, The Oct1 transcription factor and epithelial malignancies: Old protein learns new tricks, Biochim. Biophys. Acta - Gene Regul. Mech. 1859 (2016) 792–804. https://doi.org/10.1016/j.bbagrm.2016.02.007.

[84] X. Liu, J. Huang, T. Chen, Y. Wang, S. Xin, J. Li, G. Pei, J. Kang, Yamanaka factors critically regulate the developmental signaling network in mouse embryonic stem cells, Cell Res. 18 (2008) 1177–1189. https://doi.org/10.1038/cr.2008.309.

[85] B. Mao, Y. Gao, Y. Bai, Z. Yuan, Hippo signaling in stress response and homeostasis maintenance, Acta Biochim. Biophys. Sin. (Shanghai). 47 (2015) 2–9. https://doi.org/10.1093/abbs/gmu109.

[86] A. V. Boopathy, K.D. Pendergrass, P.L. Che, Y.-S. Yoon, M.E. Davis, Oxidative stress-induced Notch1 signaling promotes cardiogenic gene expression in mesenchymal stem cells, Stem Cell Res. Ther. 4 (2013) 43. https://doi.org/10.1186/scrt190.

[87] X. Zhou, L. Wan, Q. Xu, Y. Zhao, J. Liu, Notch signaling activation contributes to cardioprotection provided by ischemic preconditioning and postconditioning, J. Transl. Med. 11 (2013) 251. https://doi.org/10.1186/1479-5876-11-251.

[88] D. Shao, P. Zhai, D.P. Del Re, S. Sciarretta, N. Yabuta, H. Nojima, D.-S. Lim, D. Pan, J. Sadoshima, A functional interaction between Hippo-YAP signalling and FoxO1 mediates the oxidative stress response, Nat. Commun. 5 (2014) 3315. https://doi.org/10.1038/ncomms4315.

[89] H. Song, K.K. Mak, L. Topol, K. Yun, J. Hu, L. Garrett, Y. Chen, O. Park, J. Chang, R.M. Simpson, C.-Y. Wang, B. Gao, J. Jiang, Y. Yang, Mammalian Mst1 and Mst2 kinases play essential roles in organ size control and tumor suppression, Proc. Natl. Acad. Sci. 107 (2010) 1431–1436. https://doi.org/10.1073/pnas.0911409107.

[90] W. Kim, Y.S. Cho, X. Wang, O. Park, X. Ma, H. Kim, W. Gan, E. Jho, B. Cha, Y. Jeung, L. Zhang, B. Gao, W. Wei, J. Jiang, K.-S. Chung, Y. Yang, Hippo signaling is intrinsically regulated during cell cycle progression by APC/C Cdh1, Proc. Natl. Acad. Sci. 116 (2019) 9423–9432. https://doi.org/10.1073/pnas.1821370116.

[91] J.R. Misra, K.D. Irvine, The Hippo Signaling Network and Its Biological Functions, Annu. Rev. Genet. 52 (2018) 65–87. https://doi.org/10.1146/annurev-genet-120417-031621.

[92] Z. Meng, T. Moroishi, K.-L. Guan, Mechanisms of Hippo pathway regulation, Genes Dev. 30 (2016) 1–17. https://doi.org/10.1101/gad.274027.115.

[93] M.H. Rider, N. Hussain, S. Horman, S.M. Dilworth, K.B. Storey, Stress-induced activation of the AMP-activated protein kinase in the freeze-tolerant frog *Rana sylvatica*, Cryobiology. 53 (2006) 297–309. https://doi.org/10.1016/j.cryobiol.2006.08.001.

[94] B. Zhao, L. Li, K.-L. Guan, Hippo signaling at a glance, J. Cell Sci. 123 (2010) 4001–4006. https://doi.org/10.1242/jcs.069070.

[95] R. Schwanbeck, S. Martini, K. Bernoth, U. Just, The Notch signaling pathway: Molecular basis of cell context dependency, Eur. J. Cell Biol. 90 (2011) 572–581. https://doi.org/10.1016/j.ejcb.2010.10.004.

[96] B. Keith, M.C. Simon, Hypoxia-Inducible Factors, stem cells, and cancer, Cell. 129 (2007) 465–472. https://doi.org/10.1016/j.cell.2007.04.019.

[97] M. V. Gustafsson, X. Zheng, T. Pereira, K. Gradin, S. Jin, J. Lundkvist, J.L. Ruas, L. Poellinger, U. Lendahl, M. Bondesson, Hypoxia requires Notch signaling to maintain the undifferentiated cell state, Dev. Cell. 9 (2005) 617–628. https://doi.org/10.1016/j.devcel.2005.09.010.

[98] X.L. Zhou, J.C. Liu, Role of Notch signaling in the mammalian heart, Brazilian J. Med. Biol. Res. 47 (2013) 1–10. https://doi.org/10.1590/1414-431X20133177.

[99] G. Chen, Y. Qiu, L. Sun, M. Yu, W. Wang, W. Xiao, Y. Yang, Y. Liu, S. Yang, D.H. Teitelbaum, Y. Ma, D. Lu, H. Yang, The Jagged-2/Notch-1/Hes-1 pathway is involved in intestinal epithelium regeneration after intestinal ischemia-reperfusion injury, PLoS One. 8 (2013) e76274. https://doi.org/10.1371/journal.pone.0076274.

[100] S. Gupta, S. Li, M.J. Abedin, L. Wang, E. Schneider, B. Najafian, M. Rosenberg, Effect of Notch activation on the regenerative response to acute renal failure, Am. J. Physiol. Physiol. 298 (2010) F209–F215. https://doi.org/10.1152/ajprenal.00451.2009.

[101] P. Morin, D.C. McMullen, K.B. Storey, HIF-1α involvement in low temperature and anoxia survival by a freeze tolerant insect, Mol. Cell. Biochem. 280 (2005) 99–106. https://doi.org/10.1007/s11010-005-8236-x.

2.Regulation of antioxidant system

Regulation of antioxidant systems in response to anoxia and reoxygenation in *Rana sylvatica*

Aakriti Gupta and Kenneth B. Storey

Department of Biology, Carleton University, Ottawa, Canada K1S 5B6

***Correspondence to:**

Dr. Kenneth B. Storey

Department of Biology, Carleton University,

1125 Colonel By Drive, Ottawa, ON, K1S 5B6

Tel: (613) 520-2600, ext. 3678

E-mail: kenstorey@cunet.carleton.ca

Highlights

- Antioxidant defense response gets activated in response to anoxia in wood frogs.
- Upregulation of Glutathione S Transferases (GST) T1 and GSTP1 were observed in anoxia.
- Aldo Keto Reductases show a tissue specific regulation in response to oxidative stress.

Abbreviations

Nrf-2: Nuclear factor (erythroid-derived 2)-like 2 transcription factor, OCT: Octamer binding transcription factor, ROS: Reactive oxygen species, AKR: aldo-keto reductase, ARE: antioxidant response element, BMP: Bone morphogenetic protein, GST: glutathione-S-transferase, HIF: hypoxia inducible factor, KEAP: Kelch-like ECH-associated protein, KLF4: Kruppel-like factor 4, MAFG: MAF beta-ZIP transcription factor G, NOG: noggin, NQO: NAD(P)H quinone acceptor oxidoreductase, POMP: proteasome maturation protein, SOX2: SRY (sex determining region Y)-box 2.

Keywords

Oxidative stress, wood frog, amphibian, Nrf2, Oct4, reactive oxygen species, anti-oxidative genes

2.1 Abstract

The wood frog (*Rana sylvatica*) is a remarkable species. These frogs can endure prolonged oxygen deprivation as well as dehydration to ~60% of total body water lost and, combining these two abilities, they survive whole body freezing for weeks at a time during the winter. Episodes of anoxia/reoxygenation or freeze/thaw can trigger elevated production of reactive oxygen species (ROS) causing cellular damage, especially when oxygen is reintroduced during reoxygenation or thawing. To mitigate ROS damage, stress-responsive transcription factors such as the Octamer Binding Transcription factor (OCT4) and Nuclear factor (erythroid-derived 2)-like 2 transcription factor (Nrf2) were postulated to be involved in enhancing pro-survival pathways and antioxidant defenses. The present study used immunoblotting to analyze OCT4 and Nrf2 responses (and downstream factors under their control) to 24 h anoxia and 4 h reoxygenation in liver and skeletal muscle of wood frogs, with an emphasis on antioxidant systems. Surprisingly, no change was observed in relative total protein expression of either of the two transcription factors in liver. Furthermore, a significant decrease in total protein levels of OCT4 and Nrf2 occurred in skeletal muscle after 4 h recovery. However, essential cofactors of OCT4 and Nrf2 were significantly upregulated during anoxia and/or recovery. Downstream targets of the Nrf2-ARE pathway were evaluated, including glutathione-S-transferases (GSTs) and aldo-keto reductases (AKRs). Significant increases in GSTT1 and GSTP1 were observed in liver and muscle whereas AKRs showed a tissue specific response to both anoxia and recovery from anoxia. This study demonstrates activation of antioxidants as a cell protective mechanism against generation of reactive oxygen species during anoxia in wood frogs.

2.2 Introduction

Wood frogs (*Rana sylvatica*) are one of just a few frog species with the remarkable ability to survive whole body freezing during the winter months, enduring the conversion of about 65–70% of their body water into extracellular ice and surviving frozen for weeks or months (Larson and Barnes, 2016; Storey and Storey, 1988, Storey and Storey, 2017). During freezing, controlled ice formation occurs within extracellular spaces and this leads to elevated osmolality of extracellular fluids, that then draws water out of cells, reducing their volume (Storey and Storey, 2017). The liver is one of the last organs to freeze and it is also the first to thaw due to its important role in synthesizing cryoprotective osmolytes such as glucose and urea that provide colligative resistance against further water loss by cells to help maintain their structural integrity (Storey, 1987; Storey and Storey, 2017, Storey and Storey, 1986). By contrast, skeletal muscle is one of the first organs to freeze. Freezing of striated and smooth muscles inhibits essential physiological processes including movement, respiration, heartbeat, and blood circulation, leading to cellular anoxia/hypoxia for up to months without relief (Storey and Storey, 1984).

Episodes of freeze/thaw require frog cells to cope with transitions between anoxia/reoxygenation and dehydration/rehydration, which can interrupt many of the essential functions of life with multiple damaging consequences. One possible consequence of anoxia/reoxygenation is the enhanced production of reactive oxygen species (ROS) that can damage cellular macromolecules; elevated ROS are particularly associated with the recovery period after ischemia when there is a rapid reoxygenation of tissues (Storey and Storey, 2004). Increased oxidative stress also triggers destructive pathways such as apoptosis. Generation of ROS needs to be suppressed to prevent

oxidative damage and apoptosis (La Rosa et al., 2011; Sánchez-de-Diego et al., 2019; Tian et al., 2012). To survive extended bouts of freezing, the cells and tissues of wood frogs implement a variety of preservation strategies and minimize their use of endogenous fuel reserves. Among other things, they utilize well-developed anaerobic metabolism, regulatory modifications of enzymes, global metabolic rate depression to minimize ATP demands, production of protective chaperone proteins, control over apoptosis, and enhanced antioxidant defenses (Storey and Storey, 2019, Storey and Storey, 2017, Storey and Storey, 1988).

The role of antioxidant defenses in freezing survival by wood frogs has received some attention, primarily evaluating changes in antioxidant enzyme activities in tissues over the course of freeze/thaw (Joanisse and Storey, 1996) and analyzing enzymatic properties of major antioxidant enzymes (superoxide dismutase, catalase) (Dawson et al., 2015; Dawson and Storey, 2016). To further probe the role and regulation of antioxidant defenses in the stress tolerance of wood frogs, it is also necessary to understand how environmental stress, and specifically low-oxygen stress, triggers the gene expression of antioxidant enzymes. The present study takes a first look at this by exploring a prominent signal transduction pathway involving the Octamer Binding Transcription factor 4 (OCT4) and Nuclear factor (erythroid-derived 2)-like 2 transcription factor (Nrf2) and multiple proteins/enzymes under their control that are involved in antioxidant defense. Because freeze tolerance has many components, we chose to first analyze the responses of this signaling pathway to anoxia exposure, one of the component stresses of freezing, since hypoxia/anoxia is well-known to trigger antioxidant defenses in multiple systems (Giraud-Billoud et al., 2019; Hermes-Lima et al., 2015).

OCT4 is important in the context of wood frog anoxia tolerance due to its role as a potent stress-responsive transcription factor regulating the expression of many antioxidant defense and pro-survival pathway genes (Tantin, 2013). OCT4, SOX2 (SRY [sex determining region Y]-box 2), KLF4 (Kruppel-like factor 4) and c-Myc form a complex called OSKM that plays a major role in regulating cellular gene expression during stress (Fig. 2.1). Under hypoxic conditions, the Hypoxia-Inducible Factor 2 (HIF-2) induces the expression of antioxidant enzymes, various regulatory proteins of intermediary metabolism, apoptosis and cell differentiation, as well as the OSKM complex proteins OCT4 and SOX2 (Covello, 2006; Fatrai et al., 2011; Lee et al., 2018; Majmundar et al., 2010). Hypoxia and reoxygenation can induce ROS formation, leading to the activation of Bone Morphogenic Protein 4 (BMP4) (Sánchez-de-Diego et al., 2019). BMP4 can further stimulate the production of ROS by induction of NADPH oxidase 4 (Nox), but OCT4 can decrease ROS production by inducing the expression of noggin protein (NOG), a potent inhibitor of BMP4 (Teo et al., 2012). In addition to its role in controlling ROS production, BMP4 can also activate Nrf2 (Fig. 2.1) (Jang et al., 2014).

The Nrf2 transcription factor regulates the expression of genes containing the antioxidant response element (ARE) in their promoter region. Nrf2 also binds to the promoter regions of OCT4 and affects its expression. The expression levels of OCT4 are finely balanced by proteasomal ubiquitination and degradation by a protein called proteosomal maturation protein (POMP) under Nrf2 regulation (Dai et al., 2019). Under normal conditions, Nrf2 is held in the cytoplasm in association with Kelch-like ECH associated protein-1 (KEAP-1) that forms a complex with Cullin 3 (Cul3) and Ring box protein 1 (Rbx1) which together act as a ubiquitin ligase complex (**Fig. 2.1**) (Kaspar and

Jaiswal, 2010). Therefore, even though Nrf2 is constitutively present in the cytoplasm, it has a very short life of about fifteen minutes since it gets ubiquitinated and targeted for proteolysis. Under oxidative stress conditions, the cytoplasmic complex of Nrf2-KEAP1 dissociates and Nrf2 translocates to the nucleus. There, Nrf2 forms a heterodimer with MafG and activates antioxidant enzyme genes by binding to AREs in their promoters (**Fig. 2.1**) (Chen and Maltagliati, 2018). Some of the Nrf2-regulated enzymes include NADPH quinone oxidoreductase-1 (NQO-1), glutathione S-transferases (GSTs) and aldo-keto reductases (AKRs) (Jang et al., 2014; Ma, 2013; Malik and Storey, 2009). NQO-1 catalyzes the reduction of quinones (two electron reduction) to convert them into hydroquinone. Hydroquinone acts as superoxide scavenger to minimize superoxide conversion to hydrogen peroxide. GSTs are a large family of enzymes with multiple subclasses, the major ones being alpha, theta, pi, and mu. They catalyze detoxification reactions to deal with both exogenous xenobiotics and endogenous products such as aldehydes formed from lipid peroxidation reactions (Storey and Storey, 2017). AKRs perform oxidoreductase reactions on foreign and natural substrates and are divided into fourteen families. For example, AKR7 (or AFAR) is an alpha toxin aldehyde reductase that reduces dicarbonyl containing substrates (Ellis and Hayes, 1995; Hyndman et al., 2003)

The present study analyzes the responses by wood frog liver and skeletal muscle to anoxia stress and reoxygenation. It was proposed that the actions of OCT4 and co-regulators like SOX2 and KLF4 would decrease oxidative stress by suppressing BMP4 (a potent inducer of ROS) through NOG. Downstream of BMP4, another antioxidant pathway including Nrf2, POMP, MafG and the Nrf2 repressor KEAP1 and their downstream targets (members of the GST and AKR families) were also analyzed to better understand how

wood frog tissues may use antioxidant pathways to prevent or minimize oxidative damage during low oxygen stress and recovery.

2.3 Methods

2.3.1. Animal treatment

In early spring, male wood frogs were collected from breeding ponds in the Limerick forest near Ottawa and transported on ice to Carleton University. Frogs were washed in a tetracycline bath, placed in plastic containers lined with damp sphagnum moss, and then acclimated in an incubator at 5 °C for two weeks. Control frogs were sampled from this condition and others were treated to anoxia exposure. In all cases, animals were euthanized by pithing and tissues were immediately dissected, flash frozen in liquid nitrogen and then stored at −80 °C until use. Animal care, holding, euthanasia and experimental procedures received the prior approval of the Carleton University animal care committee (protocol #106 935) in accordance with the guidelines issued by the Canadian Council on Animal Care.

2.3.2. Anoxia treatment

For anoxia exposure, frogs were placed in plastic chambers that had two ports in the lid, one to flush the chamber with nitrogen gas and the other to vent gas. A damp paper towel (previously wetted with distilled water that had been bubbled with 100% nitrogen gas for ~20 min) was placed on the bottom of the chamber to maintain frog hydration. Each container was then flushed with nitrogen gas for ~20 min (while sitting in crushed ice) and then frogs were placed in the container (4–5 frogs per jar). The lid was closed tightly and sealed with parafilm. Nitrogen gas was again flushed through the inlet port for ~30 min and then containers were returned to an incubator at 5 °C for 24 h. Subsequently, frogs in

half of the chambers were sampled while still under anoxic conditions. To do this, containers were reconnected to the nitrogen gas lines (while held in crushed ice) and frogs were quickly sampled. Frogs in the other anoxic chambers were rapidly transferred into fresh containers with normal air and were allowed to recover for 4 h at 5 °C, prior to sampling.

2.3.3. Total protein extraction for immunoblots

Total soluble protein was extracted from liver and skeletal muscle samples of control, 24 h anoxic and 4 h aerobic recovered frogs ($n = 4$ biological replicates in all cases). Samples of frozen tissues were quickly weighed and homogenized 1:2 w:v in buffer (20 mM Hepes, pH 7.4, 100 mM NaCl, 0.1 mM EDTA, 10 mM NaF, 1 mM Na_3VO_4, 10 mM β-glycerophosphate) with a few crystals of phenylmethylsulfonyl fluoride (PMSF) and 1% of Protease inhibitor cocktail (Bioshop, Burlington, ON, Canada, catalog no. PIC001.1) (reconstituted in 100 ml of deionized water) added immediately before tissue disruption using a Polytron homogenizer for ~15–20 s. Homogenates were centrifuged at 12,000*g* at 4 °C for 15 min and supernatant was collected.

Protein concentrations in supernatant samples were measured using the Bio-Rad protein assay (Bio-Rad, Mississauga, ON, Canada, catalog no. 500.006). Concentrations of samples were then standardized to a final 10 μg/μl by the calculated addition of small volumes of homogenization buffer. Equal volumes of standardized total protein extracts and 2× SDS-PAGE (sodium dodecyl sulphate polyacrylamide gel electrophoresis) buffer (100 mM Tris-HCl, 20% *v*/v glycerol, 4% *w*/*v* SDS, 0.2% w/v bromophenol blue and 10% v/v 2-mercaptoethanol) were then mixed and boiled for 5 min in a water bath followed by

immediate cooling on ice for 5–10 min. Samples were then aliquoted in 100 µl portions and stored at −80 °C until further use.

2.3.4. SDS-PAGE and Western blotting

Total protein extracts were run on 12% or 15% SDS-PAGE gels (depending on the subunit M.W. of the protein of interest). Resolving gel composition was: 12% or 15% *v*/v acrylamide, 0.4 M Tris pH 8.8, 10% SDS (*w*/*v*), 10% ammonium persulfate (APS) (w/v) and N,N,N′,N′-tetramethylethane-1,2-diamine (TEMED). Stacking gels were 5% acrylamide, 0.13 M Tris pH 6.8, 10% SDS (*w*/*v*), 10% APS (w/v) and TEMED (w/v).

Equal amounts of protein (25 µg) for all three experimental conditions for both liver and muscle were loaded into wells on SDS-PAGE gels along with a low molecular weight ladder (Pink Plus Prestained Protein Ladder, Frogga Bio, Toronto, ON, catalog no. PM005–0500) in one lane. Gels were run on a Bio-Rad mini-gel apparatus with running buffer (25 mM Tris-base, 190 mM glycine, 0.1% w:v SDS, pH 7.6) at 180 V until the migration of the ladder proteins indicated a good separation for the protein of interest.

Proteins were then transferred to PVDF membranes by either electroblotting at 160 mA constant current for ~80–90 min using transfer buffer (25 mM Tris, pH 8.5, 192 mM glycine and 10% *v*/v methanol) or using a trans-blot turbo transfer system (BioRad, Mississauga, ON, Canada). Membranes were washed three times for 5 min each using TBST (Tris-buffered saline with Tween-20): 20 mM Tris base pH 7.6, 150 mM NaCl, 0.05% v/v Tween-20. Membranes were later blocked with 3–5% w/v milk in TBST or 2 mg/ml polyvinyl alcohol (PVA) in TBST (Sigma-Aldrich, Oakville, ON, catalog no. P8136-250G) for 30 min. Membranes were again washed for 3 × 5 min in TBST and then

probed with 1:1000 v:v primary antibody diluted in TBST. Membranes were incubated overnight at 4 °C on the rocker.

Antibodies for OCT4 (catalog no. GTX100468), SOX2 (catalog no. GTX101507), and KLF4 (catalog no. GTX101508) were purchased from Genetex and antibodies for KEAP1 (catalog no. SC-15246) and Nrf2 (catalog no. SC-722P) were from Santa Cruz Biotechnology. Antibodies for downstream of NRF-ARE pathway targets (GSTs, AKRs, AFAR) were gifted from Dr. John Hayes (Biomedical Research Centre, University of Dundee) and were raised in rabbit.

After incubation, membranes were washed for 3 × 5 min in TBST at room temperature (RT) and then incubated with 1:5000 v:v with an anti-rabbit IgG secondary antibody conjugated with horseradish peroxidase (catalog no. APA007P.2, Bioshop, Burlington, ON, Canada) for all targets except KEAP which was incubated with anti-goat IgG secondary antibody conjugated with horseradish peroxidase (catalog no. APA002P.2, Bioshop, Burlington, ON, Canada), in TBST for 30 min at RT. Membranes were then washed for 3 × 5 min using TBST and visualized using a Chemi-Genius Bioimager (Syngene, Frederick, MD) with 700 µl each of hydrogen peroxide and Luminol. Subsequently, the membranes were stained with Coomassie blue (0.25% *w*/*v* Coomassie brilliant blue, 7.5% *v*/v acetic acid, and 50% methanol) and then membranes were re-imaged. Both immunoblot and Coomassie stained band intensities were quantified using GeneTools software (Syngene, Frederick, MD) and then immunoblot band intensities were standardized against the corresponding intensity of a group of Coomassie-stained bands in the same lane that remained constant across all the samples (Eaton et al., 2013).

2.3.5. Total protein extraction for TF ELISA

Total soluble proteins were extracted from frozen samples of liver and muscle for all three conditions (control, 24 h anoxia, 4 h recovery) ($n = 4$ biological replicates). Approximately 50 mg of each was homogenized 1:5 w:v in pre-chilled Lysis Buffer (Millipore, Etobicoke, ON, catalog no. 43–040), with the further addition of 1 mM Na_3VO_4, 10 mM NaF, 10 mM β-glycerophosphate and 1% protease inhibitor cocktail (BioShop, Burlington, ON, Canada, catalog no. PIC001) using a Dounce homogenizer. Homogenates were incubated on ice for 30 min with intermittent vortexing followed by centrifugation at 14,000*g* for 20 min at 4 °C. The supernatant was collected and soluble protein concentration was measured using the Bio-Rad protein assay. Samples were aliquoted in 50 µl amounts and stored at −80 °C until further use. To confirm the integrity of the proteins in the samples, 10 µl amounts of each sample were mixed with 10 µl of 2× SDS-PAGE sample buffer and run on SDS-PAGE as described previously and stained with Coomassie blue. Bands were visualized using Chemi-Genius Bioimager.

2.3.6. DNA binding activity using TF-ELISA

Biotin-labeled DNA oligonucleotides containing the OCT or Nrf2 consensus sequences were used to assess the binding capacity of these transcription factors:

OCT (5′Biotin GGTTGTCGAATGCAAATCACTTAAGAA 3′).

OCT complementary (5′ TTCTTAAGTGATTTGCATTCGACAACC 3′).

Nrf2 (5′ Biotin CTCCAGTGACTCAGCACAGGTTCCCCA 3′.

Nrf 2 complementary (5′ TGGGGAACCTGTGCTGAGTCACTGGAG).

All four probes (biotinylated and complementary probes) were reconstituted to final concentrations of 500 pmol/µl with autoclaved double distilled water (ddH_2O). The

forward and its respective reverse probe were mixed in a 1:1 v:v ratio and heated in a thermocycler at 95 °C for 10 min, then cooled at RT for 10 min. The double stranded probe was further diluted to 50 pmol/µl using 1× PBS (Phosphate Buffered Saline) (137 mM NaCl, 2.7 mM KCl, 10 mM Na_2HPO_4, 2 mM KH_2PO_4, pH 7.4). A 50 µl aliquot of the diluted probe (containing 40 pmol) was added to each well of a streptavidin coated microplate (R&D Systems, Minneapolis, MB, Canada, catalog no. CA73521–134). The plate was incubated at RT for 1 h. Unbound probe was removed with two rinses of 100 µl wash buffer (1× PBS, 0.1% Tween-20) and then once with 1× PBS buffer.

A test strip of all the pooled samples was run at different protein concentrations to determine the efficiency of the probe and optimise the protein concentrations using (a) no probe (wells coated with streptavidin that were not probed with the double stranded probe), (b) no protein (lysis buffer alone), (c) no primary antibody, and (d) the complete reaction mix.

Based on test strip optimization, 25 µg of TF-ELISA protein extracts were used (diluted in water) for OCT4 and 35 µg for Nrf2 for all three conditions (control, 24 h anoxia, 4 h recovery) of both liver and muscle. The reaction contained transcription factor binding buffer (10 mM HEPES, 50 mM KCl, 0.5 mM EDTA, 3 mM $MgCl_2$, 10% *v*/v glycerol, 0.5 mg/ml BSA, 0.05% NP-40; pH 7.9) with 10 mM DTT and 1 µg salmon sperm DNA added. The contents were vortexed and then spun down. A 50 µl aliquot of the reaction mix was added to each well. For the negative control, lysis buffer replaced the protein sample in the reaction mix. Two technical replicates of each biological replicate were run and three negative controls per transcription factor were used. The samples were incubated at RT for 1 h on a plate shaker (Denville Scientific, Holliston, MA). Unbound transcription

factors were discarded by inverting the plate on paper towels and the plate was washed with 3 × 200 µl of wash buffer per well. A 60 µl aliquot of antibody (OCT-4 or Nrf2) (used in western blotting; diluted 1:1000 in PBST) was then added to each well and incubated at RT for 1 h. The unbound antibodies were discarded by inverting the plate and then washing with 3 × 200 µl of wash buffer per well.

HRP conjugated anti-rabbit IgG (Bio-Shop, Burlington, ON, catalog no. APA007P.2) was used as the secondary antibody (diluted 1:2000 in PBST) and 60 µl was added to each well. The plate was incubated at RT for 1 h and then unbound antibodies were discarded by inverting the plate and then washing with 3 × 200 µl of wash buffer per well. Then 60 µl TMB (tetramethylbenzidine) (BioShop, Burlington, ON, catalog no. TMB333.100) was added to each well. After the blue colour was well-developed, the reaction was terminated by addition of 1 M HCl Stop solution (60 µ/well). Absorbance was measured at 450 nm (using 655 nm as a reference) using a Multiskan spectrophotometer (Thermo Electron Corporation, Waltham, ME). The signal from technical replicates was averaged for each biological replicate (n = 4) before data were standardized for stress and recovery against control samples (set to one).

2.3.7. Quantification and statistics

Band intensities for all chemiluminescent blots and Coomassie-stained membranes were imaged using the Chemi-Genius Bioimager (Syngene, Frederick, MD) and the associated Gene Tools software was used to carry out densitometric analysis. Immunoblot band density in each lane was standardized against a group of Coomassie stained bands in the same lane that was distant from the immune band (the same group of bands was used in all lanes) to correct for minor sample loading variations. Fold changes for 24 h anoxia

and 4 h recovery conditions were calculated relative to their corresponding controls that were set to 1. Data analysis used one-way ANOVA followed by Tukey's post hoc test using RBioplot (Zhang and Storey, 2016), with $P < .05$ accepted as a significant difference between groups. Data for ELISA was also analyzed in the same way. In all cases, data are reported as mean ± SEM for n = 4 biological replicates.

2.4 Results

2.4.1. Total protein expression of Nrf2 and its co-factors

Nrf2 protein was detected in both liver and muscle of wood frogs with immunoblotting showing a single band at the expected subunit molecular weight of 61 kDa. Total Nrf2 protein levels (assessed by immunoblotting) did not change significantly in the liver between control, anoxic and recovery conditions (**Fig. 2.2a**). However, in skeletal muscle, Nrf2 expression was unchanged after 24 h anoxia but decreased significantly during aerobic recovery to ~60% ± 5% of the control value (**Fig. 2.2b**).

Expression of the Nrf2 repressor protein, KEAP1, increased significantly under 24 h anoxia conditions in wood frog liver, rising by 2.0 ± 0.08 fold and remaining high at 1.7 ± 0.07 fold over controls after 4 h reoxygenation (**Fig. 2.2a**). In muscle, however, KEAP1 levels were unchanged over anoxia-recovery (**Fig. 2.2b**). The expression of POMP increased by 1.45 ± 0.04 under anoxia in liver (**Fig. 2.2a**) and stayed high at 1.32 ± 0.09 fold over controls under reoxygenated conditions. In skeletal muscle, POMP did not change under anoxia but increased strongly during aerobic recovery, rising significantly to 5.25 ± 0.6 fold over controls (**Fig. 2.2b**). Total protein levels of MafG increased by 2.5 ± 0.06 and 2 ± 0.06 fold in liver during anoxia/recovery but rose by nearly 6 ± 0.53

fold in anoxic muscle and remained at 4.7 ± 0.32 fold higher than controls after 4 h reoxygenation (**Fig. 2.2a and b**).

2.4.2. Protein expression of OCT4 and its co-factors

Total protein levels of OCT4 were assessed using western blotting for both liver (**Fig. 2.3a**) and skeletal muscle (**Fig. 2.3b**), comparing control, 24 h anoxic, and 4 h aerobic recovery conditions. In both tissues, a single band for OCT4 was detected at the expected molecular mass of ~48 kDa. No significant change in OCT4 was seen in liver over the three conditions (**Fig. 2.3a**), whereas in muscle, OCT4 expression remained constant during anoxia but decreased significantly by 50% ± 6% during recovery (**Fig. 2.3b**).

Total protein levels of the OCT4 co-factors, SOX2 and KLF4, were also assessed via immunoblotting for liver and muscle under anoxia and recovery conditions, with respect to controls. SOX2 levels showed a significant increase in liver by 1.6 ± 0.04 fold in anoxia and 2.23 ± 0.13 fold during recovery from anoxia (**Fig. 2.3a**). On the other hand, SOX2 levels in anoxic muscle showed a downward trend by 20% ± 9% as compared to controls and expression decreased more during aerobic recovery, a significant decrease of 40% ± 5% compared with controls (**Fig. 2.3b**). The protein expression of KLF4 increased strongly in anoxic liver by 2.65 ± 0.07 fold compared to controls and rose further to 3.46 ± 0.54 fold over controls during aerobic recovery (**Fig. 2.3a**). A very strong increase in KLF4 expression also occurred in anoxic skeletal muscle, an increase of 8.1 ± 0.30 fold that remained high (8.0 ± 0.21 fold over control) after 4 h of aerobic recovery (**Fig. 2.3b**).

2.4.3. Total protein levels of downstream targets of OCT4

OCT4 activates NOG that acts as an antagonist to BMP4. In the present study, total protein levels of NOG rose significantly in liver under anoxia and increased further during

aerobic recovery to 2.04 ± 0.11 fold over control levels (**Fig. 2.4a**). However, an opposite response was seen in skeletal muscle where NOG expression decreased in muscle by 50% ± 5% in anoxia and remained low in recovery (**Fig. 2.4b**). NOG is said to be an antagonist of BMP4 but increased NOG expression in liver during aerobic recovery did not lead to any change in the level of BMP4. However, BMP4 levels decreased significantly in muscle to 78% ± 10% in anoxia and 34% ± 4% in recovery rather than responding oppositely, as predicted.

2.4.4. Total protein levels of antioxidants

Among the GST family of enzymes, GSTA3, GSTP1, GSTM3, GSTK1, and GSTT1 were assessed in liver and muscle extracts via immunoblotting to evaluate the effects of anoxia/recovery on their protein expression. In liver, the levels of GSTA3 did not change significantly from control values after 24 h anoxia exposure but decreased to 74% ± 3% of control after 4 h reoxygenation; similarly, in muscle, no significant change was observed under anoxia but levels decreased by 60% ± 3% during aerobic recovery (**Fig. 2.5a and5b**). GSTP1 levels in liver increased significantly to 1.58 ± 0.2 fold over controls during aerobic recovery (**Fig. 2.5a**). A similar effect was seen in anoxic muscle with a significant increase of 1.45 ± 0.12 fold over controls during aerobic recovery (**Fig. 2.5b**). GSTM3 and GSTK1 did not show any significant change under anoxia or reoxygenation in either tissue. Levels of GSTT1 increased strongly in both liver and muscle, rising by 2.3 ± 0.15 fold and 3.1 ± 0.17 fold, under anoxia and reoxygenated conditions in liver and by 1.5 ± 0.10 and 1.3 ± 0.10 fold in muscle as compared to controls (**Fig. 2.5a and b**).

Another group of Nrf2 targets is the aldo-keto reductase family of enzymes. Three members of AKR family were studied: AKR1A3, AKR1B4 and AFAR1 (aflatoxin

aldehyde reductase, also known as AKR7A2). A significant decrease in AFAR1 levels was observed in liver under anoxia and recovery conditions, values decreasing to just 23% ± 13% and 11% ± 3% of control, respectively (**Fig. 2.6a**). The situation differed in muscle with an apparent decrease during anoxia but a significant rise over the anoxia value during recovery to reach a final 1.19 ± 0.11 fold over controls (**Fig. 2.6b**). AKR1A3 levels increased in anoxic liver by 1.72 ± 0.16 fold but returned to control levels during recovery. On the other hand, AKR1A3 did not change significantly in muscle. AKR1B4 protein levels were unchanged anoxic and recovery in both tissues (**Fig. 2.6a and b**).

Protein levels of NQO-1 were also assessed but remained unchanged in liver under both anoxia and aerobic recovery (**Fig. 2.6a**). However, in muscle NQO-1 decreased significantly during anoxia to 38% ± 13% of the control value but subsequently returned to a value that was 81 ± 15% of the control during recovery (**Fig. 2.6b**).

2.4.5. DNA binding activity of OCT4

The binding ability of OCT4 to its consensus DNA binding sequence was assessed using a transcription factor ELISA. DNA binding activity by OCT4 in extracts of liver and muscle from anoxic frogs was significantly reduced to 30% ± 3% and 40% ± 7%, respectively, of the corresponding control levels (**Fig. 2.7**). Binding activity remained low during aerobic recovery for liver extracts (28% ± 5% compared with control) but increased substantially in reoxygenated muscles to 70% ± 7%.

2.4.6. DNA binding activity of Nrf2

The DNA binding affinity of Nrf2 was also assessed using a TF ELISA. The binding activity of Nrf2 in extracts of liver from anoxic conditions decreased by approximately 42% ± 8% as compared with controls and remained low at 33% ± 3% of controls under

reoxygenated conditions (**Fig. 2.8**). Nrf2 binding activity in muscle was similarly affected by anoxia with binding activity decreased by 53% ± 4%. However, in contrast to liver, DNA binding activity in muscle extracts rose again during aerobic recovery to 85 ± 9% of control values (**Fig. 2.8**).

2.5 Discussion

Wood frogs (*R. sylvatica*) are an ideal study system for learning about animal adaptation to extreme environmental conditions for they can endure long term anoxia, extensive dehydration, and whole body freezing. How these extreme amphibians regulate their antioxidant systems in the face of anoxia and reoxygenation was explored in this study through the analysis of OCT4 and Nrf2 pathways. These transcription factors are of great interest because both can be upregulated by the oxygen-sensitive transcription factor HIF-2, and they are able to regulate each other's activities through the upregulation of downstream genes such as NOG and POMP (Chaturvedi et al., 2009; Dai et al., 2019; Keith and Simon, 2007).

Nrf2, a transcription factor involved in upregulating the expression of several antioxidant enzymes, showed no change in total protein levels in liver over anoxia/recovery, but Nrf2 expression decreased in muscle during recovery (**Fig. 2.2**). Tissue-specific trends for Nrf2 protein levels were also observed in freeze-tolerant painted turtles (*Chrysemys picta marginata),* where no changes were observed in Nrf2 protein levels of in liver during freezing, but a 1.5-fold increase was seen in muscle compared to normoxic controls (Krivoruchko and Storey, 2010b). Total protein levels of Nrf2 also decreased in muscle during dehydration stress in *Xenopus laevis* but increased by four-fold in liver (Malik and Storey, 2009). Overall, these results imply that muscle does not increase

Nrf2 protein levels in amphibians or reptiles during low-oxygen stress, but the response to low-oxygen stress in liver is more variable across species. In this study, the lack of change in *R. sylvatica* Nrf2 protein levels in liver was consistent with decreasing Nrf2 DNA binding levels during anoxia and recovery (**Fig. 2.7a**). Wood frog muscle Nrf2 DNA binding activity decreased in anoxia but began to rise in recovery towards control levels (**Fig. 2.7**). The enhanced DNA binding ability (relative to anoxia) of Nrf2 in muscle suggests activation of a response to oxidative stress during recovery since re-exposure to oxygen can cause a rapid increase in ROS generation. The expression of KEAP1, a negative regulator of Nrf2, significantly increased in anoxia and remained high in liver during recovery but no change was observed in muscle (**Fig. 2.2a and b**). These results suggest that KEAP1 could promote the ubiquitinylation of Nrf2, resulting in its destabilization and proteasomal degradation (Ma, 2013). The results seem to indicate that low oxygen stress and recovery conditions induced more changes in liver than muscle, suggesting that the threshold of ROS required to induce the antioxidant pathways may be high in liver but low in muscle. For this reason, high levels of KEAP1 in liver could cause *R. sylvatica* liver to limit Nrf2 expression during anoxia and recovery, that, in turn, may limit its translocation to the nucleus and DNA binding activity. Maintained Nrf2 levels during anoxia/recovery with respect to the control could result from a balance between low-oxygen stress-induced Nrf2 expression and KEAP1-mediated Nrf2 ubiquitinylation. Notably, the results of the DNA binding ELISA using total protein extracts also suggest that Nrf2 affinity for DNA is also decreased in the liver of wood frogs sampled during anoxia and recovery. By contrast, muscle Nrf2 may be slightly reduced during recovery

because its expression, just like that of KEAP1, OCT4, and SOX2, was not induced by cell stress.

Nrf2 was expected to increase POMP levels by blocking the downregulation of its expression (Pickering et al., 2012). However, low Nrf2 total protein and DNA binding levels suggest that another protein is responsible for the increased total protein levels of POMP that were observed in anoxic and recovery liver (relative to the control), and the increased POMP levels that were observed during recovery from anoxia in skeletal muscle (**Fig. 2.2a and b**). Studies have demonstrated that as an adaptive immune response during low oxygen, interferon γ accelerates the expression of POMP that plays an essential role in i20S biogenesis (a catalytic complex of 26S proteasome present in cytotoxic T lymphocytes) (Heink et al., 2005; Poli et al., 2018; Roman et al., 2010). Nrf2 regulates the expression of OCT4 by POMP mediated ubiquitination and degradation (Dai et al., 2019; Jang et al., 2014). Therefore, a decrease in muscle OCT4 levels during recovery when POMP is strongly increased (>5-fold) suggests a role for POMP in regulation of OCT4 upon reoxygenation. The lack of a decrease in OCT4 protein levels in liver when POMP levels are only 1.5-fold increased relative to the control could suggest that the increase in POMP is not sufficient to reduce the levels of OCT4 during anoxia or recovery in this tissue. However, further studies are required to determine the mechanism of these finely tuned regulation actions.

To study the effects of OCT4 in regulating responses to anoxia in wood frogs, total protein levels of OCT4 were first analyzed. As previously mentioned, these did not change significantly in liver (**Fig. 2.3a**) but decreased in muscle during aerobic recovery with respect to levels in control and anoxic muscles (**Fig. 2.3b**). However, DNA binding activity

by OCT4 in anoxic and reoxygenated liver and muscle showed a decrease when compared to controls (**Fig. 2.8**). Cells under anoxic conditions frequently undergo metabolic rate depression to minimize energy utilization. This includes reducing the activity and expression of transcription factors such as OCT4, such that less cellular energy is used in transcript synthesis and later, protein translation.

Despite unchanged levels of OCT4, the current study showed a significant increase in the total protein levels of SOX2 in anoxic and recovered liver. By contrast, SOX2 levels decreased significantly in recovered muscle when compared with control and anoxia conditions. OCT4 is a transcription factor that is upregulated along with its co-regulator SOX in response to low oxygen stress and is responsible for regulating the survival and maintenance of cells under hypoxia (Covello, 2006; Lee et al., 2018). SOX2 is an OCT4 co-factor but it can also regulate gene expression on its own. Upregulation of SOX2 activates sonic hedgehog, Wnt and notch signaling pathways that maintain cellular homeostasis and tissue repair (Bani-Yaghoub et al., 2006). Hence, it is possible that SOX2 may play an important role in repair and regeneration in response to stress incurred during anoxia and recovery in *R. sylvatica* liver.

KLF4, another OCT4 co-factor, showed very strong increases in both liver and muscle of wood frogs during anoxia and recovery with respect to controls (**Fig. 2.3a and b**). KLF4 is also involved in pro-survival actions; it inhibits TP53 and BAX expression, thereby suppressing the p53-dependent apoptotic pathway (Ghaleb et al., 2007; Rowland et al., 2005). A previous study from our lab showed that anoxia triggered tissue-specific anti-apoptotic pathway regulation in liver and muscle of wood frogs that would aid cell survival (Gerber et al., 2016). Specifically, significant changes in Bax and p53 proteins in liver and

a significant decrease in p53 expression in skeletal muscles were identified (Gerber et al., 2016). Interestingly, KLF4 is activated by p53 in response to DNA damage caused by oxidative stress, which leads to p21 (an inhibitor of cyclin dependent kinases) upregulation and subsequently, cell cycle arrest at G1/S phase (Liu et al., 2015; Yoon et al., 2003). Overall, KLF4 activation in response to oxidative stress leads to increased genomic stability (Liu et al., 2015; Yoon et al., 2003). The increase in KLF4 protein level seen in this study correlate well with previous reports of anoxia-triggered anti-apoptotic responses in wood frog liver and muscle.

The OCT4 target NOG can suppress BMP4 expression, where BMP4 is known to increase intracellular ROS levels (Kang et al., 2009; Murgai et al., 2018). SOX2 and KLF4 may regulate protective genes on their own in anoxic and recovered liver and muscle from wood frogs or they may work in a complex with OCT4 to respond to low-oxygen stress, as they do when they are regulating cellular reprogramming (Wei et al., 2009). In liver, it is possible that maintained OCT4 levels are sufficient to facilitate the increased expression of downstream genes such as NOG (**Fig. 2.4a**), since the expression of the OKSM proteins SOX2 and KLF4 were increased in liver during anoxia and recovery, relative to the control (**Fig. 2.3**). It is also possible that SOX2 or KLF4 were able to increase NOG expression since they all exhibit extreme similarities in the promoter sequences that they can bind (Wei et al., 2009). An increase in liver NOG protein levels could help maintain BMP4 at control levels throughout anoxia exposures and upon reoxygenation. Since NOG is capable of reducing BMP4 activity in conditions of oxidative stress (Wong et al., 2010), increased NOG may be important to reduce ROS accumulation in wood frog liver. By contrast, wood frog muscle only increased KLF4 protein levels during anoxia and recovery compared to

the control (**Fig. 2.3**). If NOG is regulated by the OKSM complex in response to oxidative stress, it is important to note that it may be dependent on sufficiently high levels of OCT4 and SOX2, but perhaps not KLF4, since high KLF4 levels in muscle did not induce an increase in NOG during anoxia or recovery (**Fig. 2.4b**). A decrease in muscle BMP4 levels during recovery, despite significant decreases in the BMP inhibitor NOG during anoxia and recovery, can be explained by a lack of sensed ROS, thus preventing BMP4 expression in the first place. A lack of sensed ROS is also consistent with maintained or decreased OCT4, SOX2, NOG, and Nrf2 protein levels and decreased OCT4 or Nrf2 DNA binding in wood frog muscle. Importantly, BMP4 only stimulates the production of ROS in a positive loop following its upregulation in response to ROS (Sánchez-de-Diego et al., 2019).

Downstream of BMP4, NRF2 can heterodimerize with MAFG or MAFG can homodimerize in the nucleus to bind to the ARE and activate antioxidant genes (Hirotsu et al., 2012; Kimura et al., 2007). MAFG showed a 2.6-fold increase in protein expression in anoxic liver and ~ 6-fold increase in anoxic muscle (**Fig. 2.2a and b**). In both cases, protein levels decreased somewhat after 4 h recovery but remained approximately 2- and 4.5-fold higher than control values. Overexpression of MAFG has been shown to affect the expression of NQO-1 negatively (Dhakshinamoorthy and Jaiswal, 2000). In our study, we found no change in the levels of NQO-1 in anoxia or recovery in liver but, in anoxic muscles, a significant decrease was observed that was reversed during recovery (**Fig. 2.6a and b**). Since MAFG can inhibit NQO-1, the overexpression of MafG may have influenced the response of NQO-1 to anoxia and recovery in both liver and muscle of wood frogs. In muscle, for example, MAFG protein levels rose under anoxia (**Fig. 2.3b**) whereas NQO-1

levels decreased (**Fig. 2.6b**). Furthermore, MAFG can homodimerize and may be able to upregulate many of the same genes that NRF2-MAFG heterodimers upregulate (Kimura et al., 2007). Since MAFG protein levels increased in both liver and muscle of anoxic and reoxygenated wood frogs, and we observed an increase in NRF-2 mediated genes such as POMP, GSTs, and AKRs, future experiments should focus on exploring the role of MAFG homodimers in the regulation of antioxidant pathways.

Downstream of NRF-ARE pathway are GSTs and AKRs. GSTs showed a similar pattern in liver and muscle (**Fig. 2.5a and b**). Tissue-specific changes in total GST activity were also observed over the freeze-thaw cycle in wood frogs with antioxidants being significantly upregulated in liver of frozen and thawed wood frogs compared with controls but unchanged in skeletal muscle (Joanisse and Storey, 1996). GSTs are detoxifying enzymes that regulate various signal transduction pathways like JNK/SAPK, MEK/ERK, etc. (Pajaud et al., 2012) and are regulated by transcription factors like NRF2, c-Jun and c-Fos (Satoh et al., 2002). However, although the total activity of GSTs can change, effects on specific GST isozymes can be variable. For example, *nrf* gene disruption reduced GSTP1 to 60% activity of the basal level whereas only 8% was observed for GSTM1 (Satoh et al., 2002). The current study shows no significant changes in GSTM3 but the total protein levels of GSTP1 showed a significant increase under stress and recovery with respect to control in both the tissues. Similarly, under oxidative stress, GSTT1 is also upregulated through p38 MAPK pathways (Ito et al., 2011) suggesting a role for p38 MAPK in an anoxia-induced GSTT1 response. Previous studies have confirmed the role of MAPKs in stress survival (Cowan, 2003; Greenway and Storey, 2000; Pajaud et al.,

2012)therefore, it is reasonable to assume that the MAPK/c-Jun pathway is involved in regulating GSTs even at constant levels of NRF2.

AKRs also showed a tissue-specific response in their relative total protein levels (**Fig. 2.6a and b**). Total protein levels of AFAR1 decreased in both anoxic liver and muscle, remaining low in liver but rebounding in reoxygenated muscle. AFAR1 detoxifies alfatoxins and is involved in biodetoxification of cytotoxic compounds and mutagens (Ahmed et al., 2011). Decreased protein levels in both tissues suggests an absence or negligible xenobiotic toxicity in frogs under anoxic conditions. No change in levels of AKR1A3 and AKR1B4 in skeletal muscle and AKR1B4 in liver also correlates with no changes in the levels of NRF2. However, AKR1A3 increased significantly in anoxic liver compared to control and recovery. The AKR1A group of the AKR1 family are aldehyde reductases that use NADPH as a hydrogen donor and reduce aldehyde carbonyl groups. AKR1A is a major enzyme in liver that detoxifies 3-deoxyglucosone (Koh et al., 2000). Under anoxia/reoxygenation conditions lipid peroxidation increases, generating malondialdehyde (MDA) and 4-hydroxynonenal (4-HNE). Upregulation of aldose reductases is directly related to generation of MDA and 4-HNE (Koh et al., 2000). Hence, the increase in AKR1A3 seen in the present study may be responding to a detected increase in lipid peroxidation in frog tissues or could be an adaptive response that is triggered and put in place to deal with one of the major injurious consequences of reoxygenation – peroxidation damage to macromolecules (particularly lipids). Previous studies found tissue specific responses of AFAR1, AKR1A3 and AKR1B4 during dehydration in liver and skeletal muscle of *X. laevis* (Malik and Storey, 2009) and during freezing in liver and muscle of freeze tolerant turtle hatchlings (Krivoruchko and Storey, 2010b). Hence, the

present study concurs with other work on frogs and turtles in showing that AKRs have significant responses to environmental stress in multiple species that must deal with oxidative stress.

In summary, significant increases in the co-factors of NRF2 and OCT4 such as SOX2, KLF4, and MafG suggest that under anoxic conditions, selected transcription factors may activate antioxidant genes in a tissue-specific manner to combat low oxygen stress. Selected GSTs and AKRs were upregulated in liver and muscle of wood frogs. Future directions should include an analysis of subcellular localization of downstream targets of the Nrf2 pathway since antioxidant activity at specific loci in the cell may provide information regarding the source of ROS. It would also be interesting to investigate roles of individual organelles in protecting cells from reactive oxygen species. Finally, large increases in the levels of KLF4 and MAFG require further investigation, since they may play important roles in promoting cell survival under anoxic stress in wood frogs.

2.6 References

Ahmed, M.M.E., Wang, T., Luo, Y., Ye, S., Wu, Q., Guo, Z., Roebuck, B.D., Sutter, T.R., Yang, J.Y., 2011. Aldo-keto reductase-7A protects liver cells and tissues from acetaminophen-induced oxidative stress and hepatotoxicity. Hepatology 54, 1322–1332. https://doi.org/10.1002/hep.24493

Bani-Yaghoub, M., Tremblay, R.G., Lei, J.X., Zhang, D., Zurakowski, B., Sandhu, J.K., Smith, B., Ribecco-Lutkiewicz, M., Kennedy, J., Walker, P.R., Sikorska, M., 2006. Role of Sox2 in the development of the mouse neocortex. Dev. Biol. 295, 52–66. https://doi.org/10.1016/j.ydbio.2006.03.007

Chaturvedi, G., Simone, P.D., Ain, R., Soares, M.J., Wolfe, M.W., 2009. Noggin maintains pluripotency of human embryonic stem cells grown on Matrigel. Cell Prolif. 42, 425–433. https://doi.org/10.1111/j.1365-2184.2009.00616.x

Chen, Q.M., Maltagliati, A.J., 2018. Nrf2 at the heart of oxidative stress and cardiac protection. Physiol. Genomics 50, 77–97. https://doi.org/10.1152/physiolgenomics.00041.2017

Covello, K.L., 2006. HIF-2 regulates Oct-4: effects of hypoxia on stem cell function, embryonic development, and tumor growth. Genes Dev. 20, 557–570. https://doi.org/10.1101/gad.1399906

Cowan, K.J., 2003. Mitogen-activated protein kinases: new signaling pathways functioning in cellular responses to environmental stress. J. Exp. Biol. 206, 1107–1115. https://doi.org/10.1242/jeb.00220

Dai, X., Yan, X., Wintergerst, K.A., Cai, L., Keller, B.B., Tan, Y., 2019. Nrf2: Redox and Metabolic Regulator of Stem Cell State and Function. Trends Mol. Med. https://doi.org/10.1016/j.molmed.2019.09.007

Dawson, N.J., Katzenback, B.A., Storey, K.B., 2015. Free-radical first responders: The characterization of CuZnSOD and MnSOD regulation during freezing of the freeze-tolerant North American wood frog, *Rana sylvatica*. Biochim. Biophys. Acta - Gen. Subj. 1850, 97–106. https://doi.org/10.1016/j.bbagen.2014.10.003

Dawson, N.J., Storey, K.B., 2016. A hydrogen peroxide safety valve: The reversible phosphorylation of catalase from the freeze-tolerant North American wood frog, *Rana sylvatica*. Biochim. Biophys. Acta - Gen. Subj. 1860, 476–485. https://doi.org/10.1016/j.bbagen.2015.12.007

Dhakshinamoorthy, S., Jaiswal, A.K., 2000. Small Maf (MafG and MafK) proteins negatively regulate antioxidant response element-mediated expression and antioxidant induction of the NAD(P)H:Quinone oxidoreductase1 gene. J. Biol. Chem. 275, 40134–40141. https://doi.org/10.1074/jbc.M003531200

Eaton, S.L., Roche, S.L., Llavero Hurtado, M., Oldknow, K.J., Farquharson, C., Gillingwater, T.H., Wishart, T.M., 2013. Total protein analysis as a reliable loading control for quantitative fluorescent western blotting. PLoS One 8, e72457. https://doi.org/10.1371/journal.pone.0072457

Ellis, E.M., Hayes, J.D., 1995. Substrate specificity of an aflatoxin-metabolizing aldehyde reductase. Biochem. J. 312, 535–541. https://doi.org/10.1042/bj3120535

Fatrai, S., Wierenga, A.T.J., Daenen, S.M.G.J., Vellenga, E., Schuringa, J.J., 2011. Identification of HIF2 as an important STAT5 target gene in human hematopoietic stem cells. Blood 117, 3320–3330. https://doi.org/10.1182/blood-2010-08-303669

Gerber, V.E.M., Wijenayake, S., Storey, K.B., 2016. Anti-apoptotic response during anoxia and recovery in a freeze-tolerant wood frog (*Rana sylvatica*). PeerJ 4, e1834. https://doi.org/10.7717/peerj.1834

Ghaleb, A.M., Katz, J.P., Kaestner, K.H., Du, J.X., Yang, V.W., 2007. Krüppel-like factor 4 exhibits antiapoptotic activity following γ-radiation-induced DNA damage. Oncogene 26, 2365–2373. https://doi.org/10.1038/sj.onc.1210022

Giraud-Billoud, M., Rivera-Ingraham, G.A., Moreira, D.C., Burmester, T., Castro-Vazquez, A., Carvajalino-Fernández, J.M., Dafre, A., Niu, C., Tremblay, N., Paital, B., Rosa, R., Storey, J.M., Vega, I.A., Zhang, W., Yepiz-Plascencia, G., Zenteno-Savin, T., Storey, K.B., Hermes-Lima, M., 2019. Twenty years of the 'Preparation for Oxidative Stress' (POS) theory: Ecophysiological advantages and molecular strategies. Comp. Biochem. Physiol. Part A Mol. Integr. Physiol. 234, 36–49. https://doi.org/10.1016/j.cbpa.2019.04.004

Greenway, S.C., Storey, K.B., 2000. Activation of mitogen-activated protein kinases during natural freezing and thawing in the wood frog. Mol. Cell. Biochem. 209, 29–37. https://doi.org/10.1023/a:1007077522680

Heink, S., Ludwig, D., Kloetzel, P.-M., Kruger, E., 2005. From The Cover: IFN- -induced immune adaptation of the proteasome system is an accelerated and transient response. Proc. Natl. Acad. Sci. 102, 9241–9246. https://doi.org/10.1073/pnas.0501711102

Hermes-Lima, M., Moreira, D.C., Rivera-Ingraham, G.A., Giraud-Billoud, M., Genaro-Mattos, T.C., Campos, É.G., 2015. Preparation for oxidative stress under hypoxia and metabolic depression: Revisiting the proposal two decades later. Free Radic. Biol. Med. 89, 1122–1143. https://doi.org/10.1016/j.freeradbiomed.2015.07.156

Hirotsu, Y., Katsuoka, F., Funayama, R., Nagashima, T., Nishida, Y., Nakayama, K., Douglas Engel, J., Yamamoto, M., 2012. Nrf2–MafG heterodimers contribute globally to antioxidant and metabolic networks. Nucleic Acids Res. 40, 10228–10239. https://doi.org/10.1093/nar/gks827

Hyndman, D., Bauman, D.R., Heredia, V. V., Penning, T.M., 2003. The aldo-keto reductase superfamily homepage. Chem. Biol. Interact. 143–144, 621–631. https://doi.org/10.1016/S0009-2797(02)00193-X

Ito, M., Imai, M., Muraki, M., Miyado, K., Qin, J., Kyuwa, S., Yoshikawa, Y., Hosoi, Y., Saito, H., Takahashi, Y., 2011. GSTT1 is upregulated by oxidative stress through p38-MK2 signaling pathway in human granulosa cells: possible association with mitochondrial activity. Aging (Albany. NY). 3, 1213–1223. https://doi.org/10.18632/aging.100418

Jang, J., Wang, Y., Kim, H.-S., Lalli, M.A., Kosik, K.S., 2014. Nrf2, a regulator of the proteasome, controls self-renewal and pluripotency in human embryonic stem cells. Stem Cells 32, 2616–2625. https://doi.org/10.1002/stem.1764

Joanisse, D.R., Storey, K.B., 1996. Oxidative damage and antioxidants in *Rana sylvatica*, the freeze-tolerant wood frog. Am. J. Physiol. 271, R545-53. https://doi.org/10.1152/ajpregu.1996.271.3.R545

Kang, J., Gemberling, M., Nakamura, M., Whitby, F.G., Handa, H., Fairbrother, W.G., Tantin, D., 2009. A general mechanism for transcription regulation by Oct1 and Oct4 in response to genotoxic and oxidative stress. Genes Dev. 23, 208–222. https://doi.org/10.1101/gad.1750709

Kaspar, J.W., Jaiswal, A.K., 2010. An Autoregulatory loop between Nrf2 and Cul3-Rbx1 controls their cellular abundance. J. Biol. Chem. 285, 21349–21358. https://doi.org/10.1074/jbc.M110.121863

Keith, B., Simon, M.C., 2007. Hypoxia-Inducible Factors, stem cells, and cancer. Cell 129, 465–472. https://doi.org/10.1016/j.cell.2007.04.019

Kimura, M., Yamamoto, T., Zhang, J., Itoh, K., Kyo, M., Kamiya, T., Aburatani, H., Katsuoka, F., Kurokawa, H., Tanaka, T., Motohashi, H., Yamamoto, M., 2007. Molecular Basis Distinguishing the DNA Binding Profile of Nrf2-Maf Heterodimer from That of Maf Homodimer. J. Biol. Chem. 282, 33681–33690. https://doi.org/10.1074/jbc.M706863200

Koh, Y.H., Park, Y.S., Takahashi, M., Suzuki, K., Taniguchi, N., 2000. Aldehyde reductase gene expression by lipid peroxidation end products, MDA and HNE. Free Radic. Res. 33, 739–746. https://doi.org/10.1080/10715760000301261

Krivoruchko, A., Storey, K.B., 2015. Turtle anoxia tolerance: Biochemistry and gene regulation. Biochim. Biophys. Acta - Gen. Subj. 1850, 1188–1196. https://doi.org/10.1016/j.bbagen.2015.02.001

Krivoruchko, A., Storey, K.B., 2010a. Regulation of the heat shock response under anoxia in the turtle, *Trachemys scripta elegans*. J. Comp. Physiol. B 180, 403–414. https://doi.org/10.1007/s00360-009-0414-9

Krivoruchko, A., Storey, K.B., 2010b. Activation of antioxidant defenses in response to freezing in freeze-tolerant painted turtle hatchlings. Biochim. Biophys. Acta - Gen. Subj. 1800, 662–668. https://doi.org/10.1016/j.bbagen.2010.03.015

La Rosa, I., Camargo, L.S.A., Pereira, M.M., Fernandez-Martin, R., Paz, D.A., Salamone, D.F., 2011. Effects of bone morphogenic protein 4 (BMP4) and its inhibitor, Noggin, on in vitro maturation and culture of

bovine preimplantation embryos. Reprod. Biol. Endocrinol. 9, 18. https://doi.org/10.1186/1477-7827-9-18

Larson, D.J., Barnes, B.M., 2016. Cryoprotectant production in freeze-tolerant wood frogs is augmented by multiple freeze-thaw cycles. Physiol. Biochem. Zool. 89, 340–346. https://doi.org/10.1086/687305

Lee, J., Cho, Y.S., Jung, H., Choi, I., 2018. Pharmacological regulation of oxidative stress in stem cells. Oxid. Med. Cell. Longev. 2018, 1–13. https://doi.org/10.1155/2018/4081890

Liu, C., La Rosa, S., Hagos, E.G., 2015. Oxidative DNA damage causes premature senescence in mouse embryonic fibroblasts deficient for Krüppel-like factor 4. Mol. Carcinog. 54, 889–899. https://doi.org/10.1002/mc.22161

Ma, Q., 2013. Role of Nrf2 in oxidative stress and toxicity. Annu. Rev. Pharmacol. Toxicol. 53, 401–426. https://doi.org/10.1146/annurev-pharmtox-011112-140320

Majmundar, A.J., Wong, W.J., Simon, M.C., 2010. Hypoxia-Inducible Factors and the response to hypoxic stress. Mol. Cell 40, 294–309. https://doi.org/10.1016/j.molcel.2010.09.022

Malik, A.I., Storey, K.B., 2009. Activation of extracellular signal-regulated kinases during dehydration in the African clawed frog, *Xenopus laevis*. J. Exp. Biol. 212, 2595–2603. https://doi.org/10.1242/jeb.030627

Murgai, A., Altmeyer, S., Wiegand, S., Tylzanowski, P., Stricker, S., 2018. Cooperation of BMP and IHH signaling in interdigital cell fate determination. PLoS One 13, e0197535. https://doi.org/10.1371/journal.pone.0197535

Pajaud, J., Kumar, S., Rauch, C., Morel, F., Aninat, C., 2012. Regulation of Signal Transduction by Glutathione Transferases. Int. J. Hepatol. 2012, 1–11. https://doi.org/10.1155/2012/137676

Pickering, A.M., Linder, R.A., Zhang, H., Forman, H.J., Davies, K.J.A., 2012. Nrf2-dependent induction of proteasome and Pa28αβ regulator are required for adaptation to oxidative stress. J. Biol. Chem. 287, 10021–10031. https://doi.org/10.1074/jbc.M111.277145

Poli, M.C., Ebstein, F., Nicholas, S.K., de Guzman, M.M., Forbes, L.R., Chinn, I.K., Mace, E.M., Vogel, T.P., Carisey, A.F., Benavides, F., Coban-Akdemir, Z.H., Gibbs, R.A., Jhangiani, S.N., Muzny, D.M., Carvalho, C.M.B., Schady, D.A., Jain, M., Rosenfeld, J.A., Emrick, L., Lewis, R.A., Lee, B., Zieba, B.A., Küry, S., Krüger, E., Lupski, J.R., Bostwick, B.L., Orange, J.S., 2018. Heterozygous Truncating Variants in POMP Escape Nonsense-Mediated Decay and Cause a Unique Immune Dysregulatory Syndrome. Am. J. Hum. Genet. 102, 1126–1142. https://doi.org/10.1016/j.ajhg.2018.04.010

Roman, J., Rangasamy, T., Guo, J., Sugunan, S., Meednu, N., Packirisamy, G., Shimoda, L.A., Golding, A., Semenza, G., Georas, S.N., 2010. T-Cell Activation under Hypoxic Conditions Enhances IFN-γ Secretion. Am. J. Respir. Cell Mol. Biol. 42, 123–128. https://doi.org/10.1165/rcmb.2008-0139OC

Rowland, B.D., Bernards, R., Peeper, D.S., 2005. The KLF4 tumour suppressor is a transcriptional repressor of p53 that acts as a context-dependent oncogene. Nat. Cell Biol. 7, 1074–1082. https://doi.org/10.1038/ncb1314

Sánchez-de-Diego, C., Valer, J.A., Pimenta-Lopes, C., Rosa, J.L., Ventura, F., 2019. Interplay between BMPs and Reactive Oxygen Species in Cell Signaling and Pathology. Biomolecules 9, 534. https://doi.org/10.3390/biom9100534

Satoh, K., Itoh, K., Yamamoto, M., Tanaka, M., Hayakari, M., Ookawa, K., Yamazaki, T., Sato, T., Tsuchida, S., Hatayama, I., 2002. Nrf2 transactivator-independent GSTP1-1 expression in `GSTP1-1 positive' single cells inducible in female mouse liver by DEN: a preneoplastic character of possible initiated cells. Carcinogenesis 23, 457–462. https://doi.org/10.1093/carcin/23.3.457

Storey, J.M., Storey, K.B., 2019. In defense of proteins: Chaperones respond to freezing, anoxia, or dehydration stress in tissues of freeze tolerant wood frogs. J. Exp. Zool. Part A Ecol. Integr. Physiol. 331, 392–402. https://doi.org/10.1002/jez.2306

Storey, K.B., 1987. Organ-specific metabolism during freezing and thawing in a freeze-tolerant frog. Am. J. Physiol. 253, 292–297.

Storey, K.B., Storey, J.M., 2017. Molecular physiology of freeze tolerance in vertebrates. Physiol. Rev. 97, 623–665. https://doi.org/10.1152/physrev.00016.2016

Storey, K.B., Storey, J.M., 2004. Metabolic rate depression in animals: transcriptional and translational controls. Biol. Rev. 79, 207–233. https://doi.org/10.1017/S1464793103006195

Storey, K.B., Storey, J.M., 1988. Freeze tolerance in animals. Physiol. Rev. 68, 27–84. https://doi.org/10.1152/physrev.1988.68.1.27

Storey, K.B., Storey, J.M., 1986. Freeze tolerant frogs: cryoprotectants and tissue metabolism during freeze–thaw cycles. Can. J. Zool. 64, 49–56. https://doi.org/10.1139/z86-008

Storey, K.B., Storey, J.M., 1984. Biochemical adaption for freezing tolerance in the wood frog, *Rana sylvatica*. J. Comp. Physiol. B 155, 29–36. https://doi.org/10.1007/BF00688788

Tantin, D., 2013. OCT transcription factors in development and stem cells: insights and mechanisms. Development 140, 2857–2866. https://doi.org/10.1242/dev.095927

Teo, A.K.K., Ali, Y., Wong, K.Y., Chipperfield, H., Sadasivam, A., Poobalan, Y., Tan, E.K., Wang, S.T., Abraham, S., Tsuneyoshi, N., Stanton, L.W., Dunn, N.R., 2012. Activin and BMP4 Synergistically Promote Formation of Definitive Endoderm in Human Embryonic Stem Cells. Stem Cells 30, 631–642. https://doi.org/10.1002/stem.1022

Tian, X.Y., Yung, L.H., Wong, W.T., Liu, J., Leung, F.P., Liu, L., Chen, Y., Kong, S.K., Kwan, K.M., Ng, S.M., Lai, P.B.S., Yung, L.M., Yao, X., Huang, Y., 2012. Bone morphogenic protein-4 induces endothelial cell apoptosis through oxidative stress-dependent p38MAPK and JNK pathway. J. Mol. Cell. Cardiol. 52, 237–244. https://doi.org/10.1016/j.yjmcc.2011.10.013

Wei, Z., Yang, Y., Zhang, P., Andrianakos, R., Hasegawa, K., Lyu, J., Chen, X., Bai, G., Liu, C., Pera, M., Lu, W., 2009. Klf4 Directly Interacts with Oct4 and Sox2 to Promote Reprogramming. Stem Cells 27, 2969–2978. https://doi.org/10.1002/stem.231

Wong, W.T., Tian, X.Y., Chen, Y., Leung, F.P., Liu, L., Lee, H.K., Ng, C.F., Xu, A., Yao, X., Vanhoutte, P.M., Tipoe, G.L., Huang, Y., 2010. Bone Morphogenic Protein-4 impairs endothelial function through oxidative stress–dependent cyclooxygenase-2 upregulation. Circ. Res. 107, 984–991. https://doi.org/10.1161/CIRCRESAHA.110.222794

Yoon, H.S., Chen, X., Yang, V.W., 2003. Krüppel-like Factor 4 Mediates p53-dependent G 1 /S Cell Cycle Arrest in Response to DNA Damage. J. Biol. Chem. 278, 2101–2105. https://doi.org/10.1074/jbc.M211027200

Zhang, J., Storey, K.B., 2016. RBioplot: an easy-to-use R pipeline for automated statistical analysis and data visualization in molecular biology and biochemistry. PeerJ 4, e2436. https://doi.org/10.7717/peerj.2436

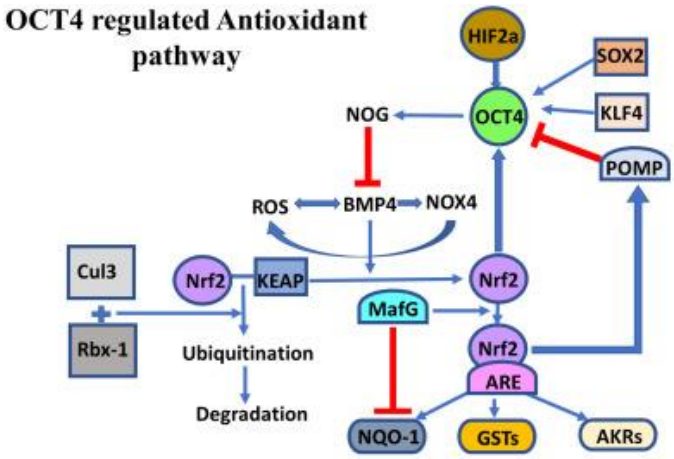

Fig. 2.1. Schematic representation of the NRF2-OCT4 pathway showing the inter-relationship between OCT4 and Nrf2 and regulation of antioxidant system. The proteins shown in circles are the transcription factors actively involved in the pathway. The proteins shown in squares are co-factors associated with the transcription factors. The proteins shown in semi-circles are proteins associated with transcription factors, and proteins shown in ovals are antioxidants activated by Nrf2. AKR: aldo-keto reductase, ARE: antioxidant response element, BMP: bone morphogenetic protein, Cul3: Cullin 3, GST: glutathione-S-transferase, HIF: hypoxia inducible factor, KEAP: Kelch-like ECH-associated protein, KLF4: Kruppel-like factor 4, MAFG: MAF beta-ZIP transcription factor G, NOG: noggin, NOX4: NADPH oxidase 4, NQO1: NAD(P)H quinone acceptor oxidoreductase1, Nrf2: nuclear factor (erythroid-derived 2)-like 2, OCT4: octamer binding transcription factor 4, POMP: proteasome maturation protein, Rbx-1: RING-box protein 1, SOX2: SRY (sex determining region Y)-box 2.

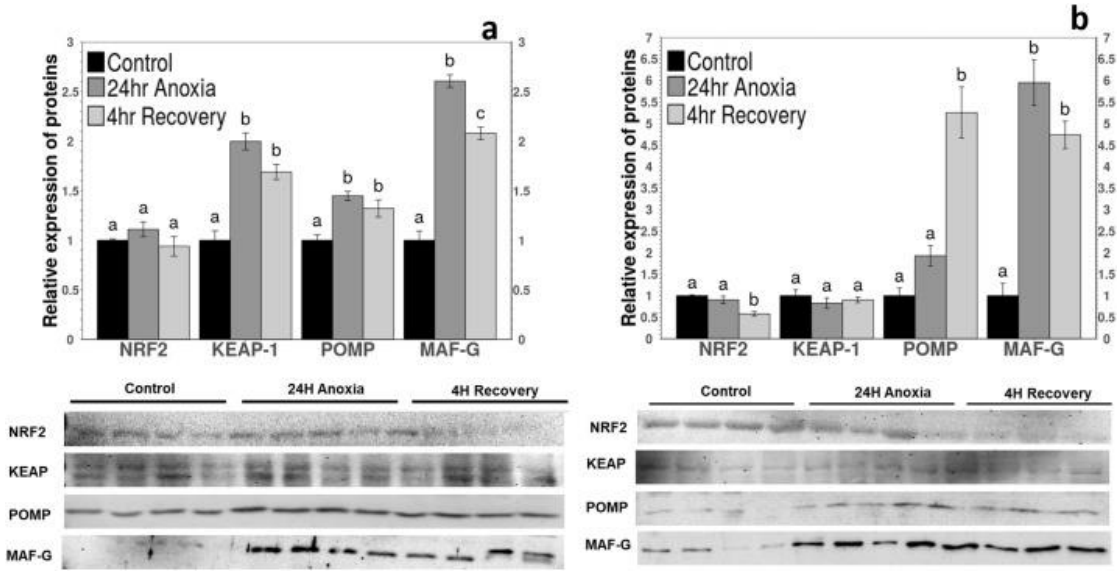

Fig. 2.2. Relative protein expression levels of Nrf2 and its co-factors KEAP-1, POMP, and MAF-G in (A) liver and (B) skeletal muscle of *R. sylvatica* under control, 24 h anoxia exposure or 4 h aerobic recovery from anoxia conditions as determined by western immunoblotting. Corresponding western immunoblot bands are shown below histograms. Data are mean ± SEM, $n = 4$ independent trials on samples from different animals. Data were analyzed using analysis of variance with a post hoc Tukey test; different letters denote values that are significantly different from each other ($p < .05$).

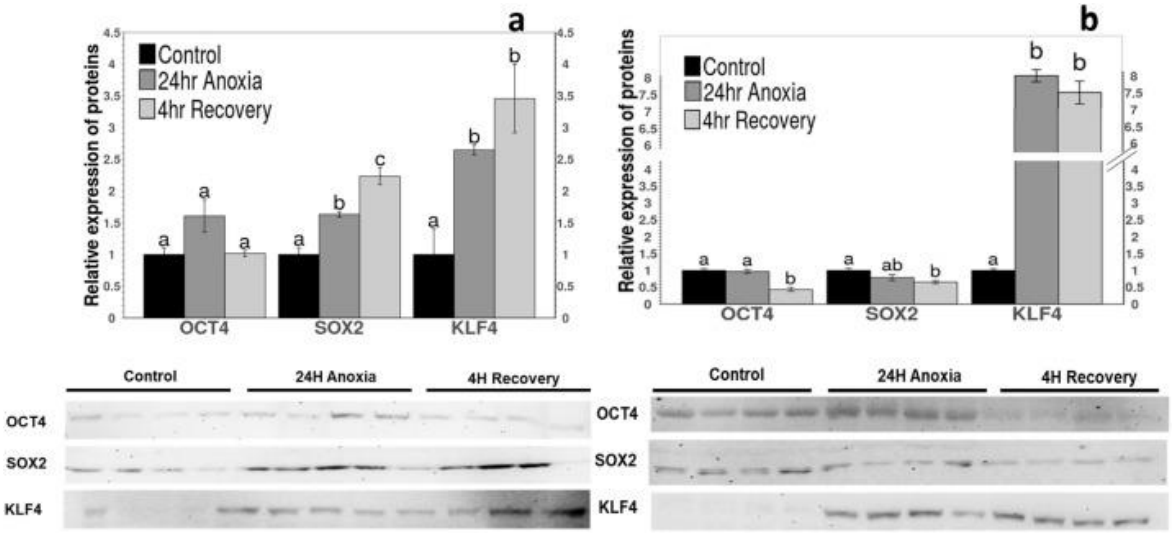

Fig. 2.3. Relative protein expression levels of OCT4 and its co-factors SOX2 and KLF4 in (A) liver and (B) skeletal muscle of *R. sylvatica* under control, 24 h anoxia exposure or 4 h aerobic recovery from anoxia conditions as determined by western immunoblotting. Other information as in Fig. 2.2.

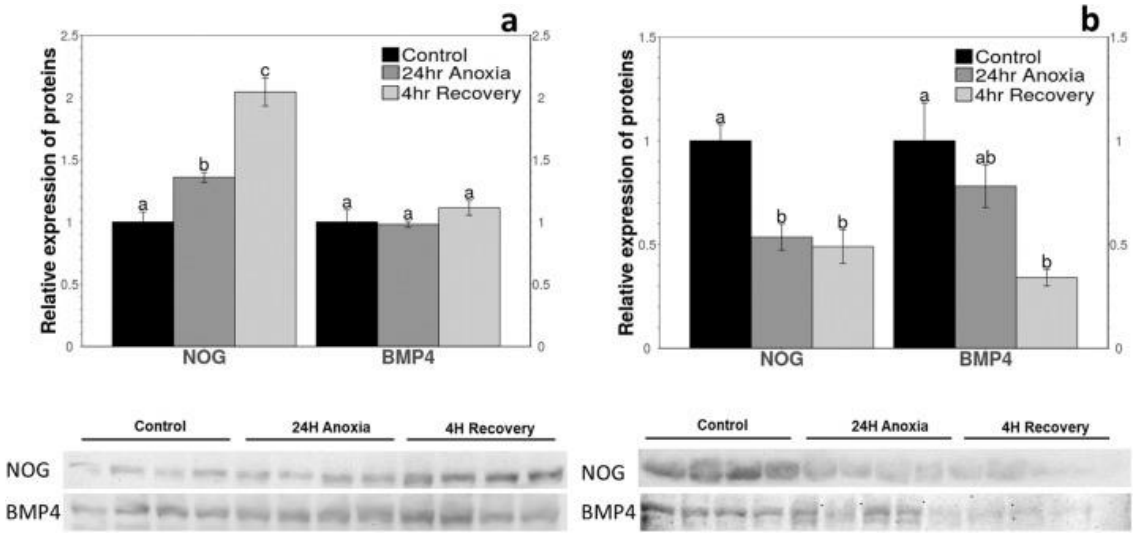

Fig. 2.4. Relative protein expression levels of NOG and BMP4 in (A) liver and (B) muscle of R. sylvatica under control, 24 h anoxia or 4 h recovery from anoxia as determined by western immunoblotting. Other information as in Fig. 2.2.

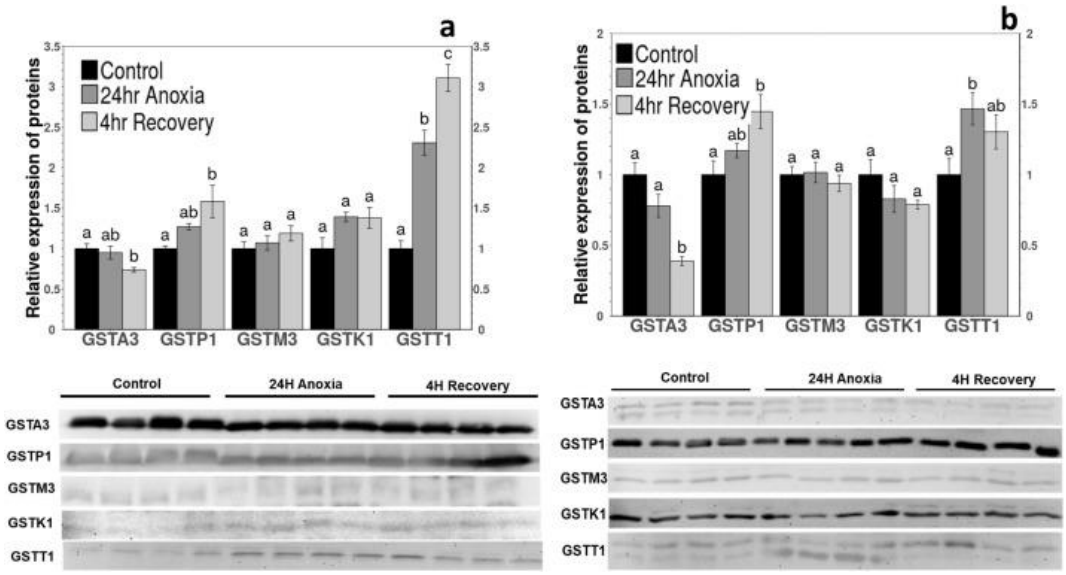

Fig. 2.5. Relative protein expression levels of five subclasses of GSTs (GSTA3, GSTP1, GSTM3, GSTK1 and GSTT1) in (A) liver (B) skeletal muscle of R. sylvatica under control, 24 h anoxia or 4 h recovery from anoxia as determined by western immunoblotting. Other information as in Fig. 2.2.

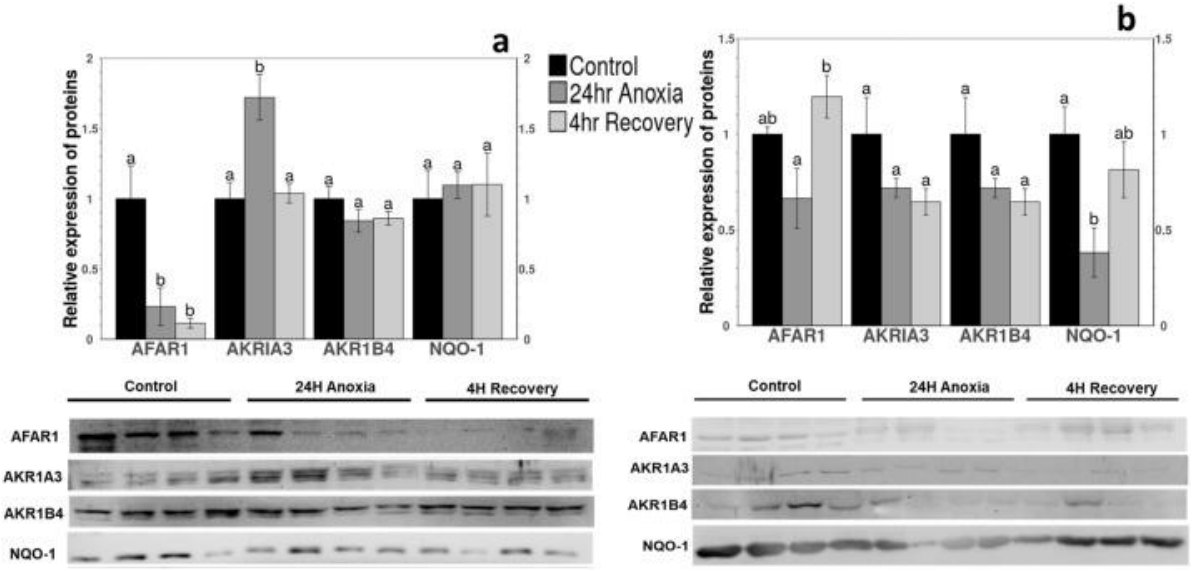

Fig. 2.6. Relative protein expression levels of AFAR1 (AKR7A2), AKR1A3, AKR1B4 and NQO1 in (A) liver and (B) skeletal muscle of R. sylvatica under control, 24 h anoxia or 4 h recovery from anoxia as determined by western immunoblotting. Other information as in Fig. 2.2.

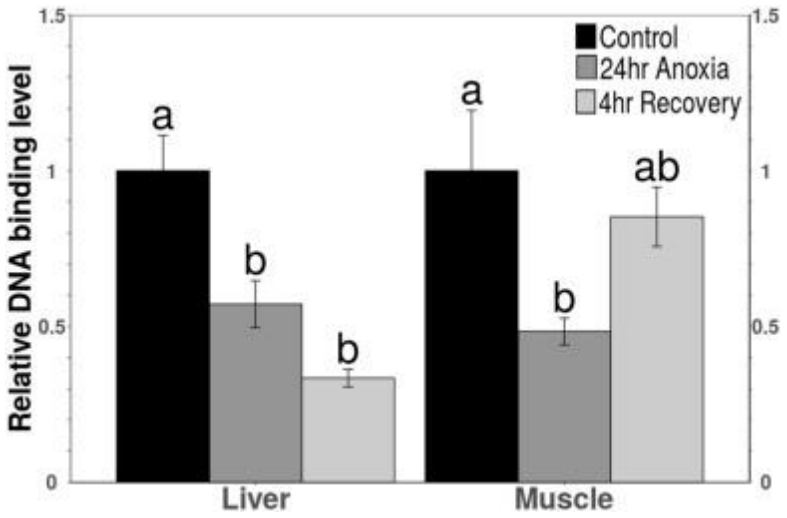

Fig. 2.7. Relative DNA binding levels of Nrf2 under control, 24 h anoxia or 4 h recovery from anoxia in extracts of R. sylvatica liver and skeletal muscle as determined by Transcription Factor ELISA (TF-ELISA) analysis. Data are mean ± SEM, n = 4 (in two technical duplicates) independent trials on samples from different animals. Data were analyzed using analysis of variance with a post hoc Tukey test; different letters denote values that are significantly different from each other ($p < .05$).

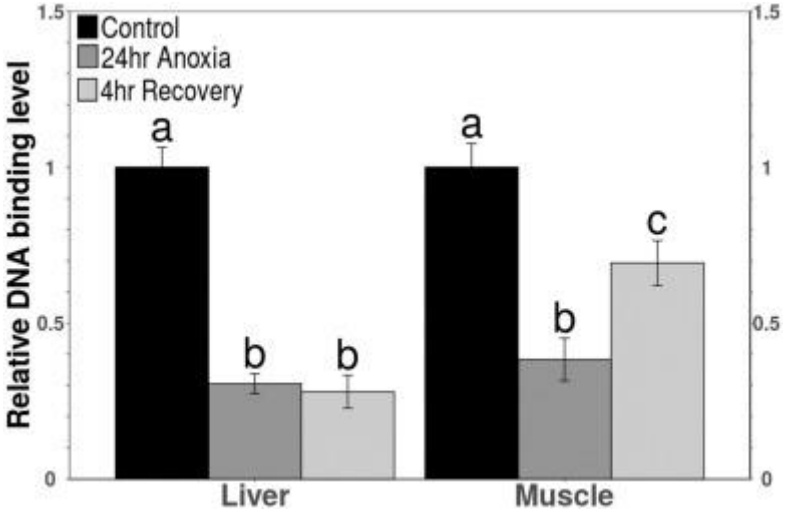

Fig. 2.8. Relative DNA binding levels of OCT4 under control, 24 h anoxia or 4 h recovery from anoxia in extracts of R. sylvatica liver and skeletal muscle as determined by TF-ELISA. Other information as in Fig. 2.7.

3.Coordinated expression of demethylases

Coordinated expression of Jumonji and AHCY under OCT transcription factor control to regulate gene methylation in wood frogs during anoxia

Aakriti Gupta and Kenneth B. Storey

Department of Biology, Carleton University, Ottawa, Canada K1S 5B6

***Correspondence to:**

Dr. Kenneth B. Storey

Department of Biology, Carleton University,

1125 Colonel By Drive, Ottawa, ON, K1S 5B6

Tel: (613) 520-2600, ext. 3678

E-mail: kenstorey@cunet.carleton.ca

3.1 Abstract

Wood frogs (*Rana sylvatica*) can survive extended periods of whole body freezing. Freezing imparts multiple stresses on cells that include anoxia and dehydration, but these can also be experienced as independent stresses. Under anoxia stress, energy metabolism is suppressed, and pro-survival pathways are prioritized to differentially regulate some transcription factors including OCT1 and OCT4. Jumonji C domain proteins (JMJD1A and JMJD2C) are hypoxia responsive demethylases whose expression is accelerated by OCT1 and OCT4 which act to demethylate genes related to the methionine cycle. The responses by these factors to 24 h anoxia exposure and 4 h aerobic recovery was analyzed in liver and skeletal muscle of wood frogs to assess their involvement in metabolic adaptation to oxygen limitation. Immunoblot results showed a decrease in JMJD1A levels under anoxia in liver and muscle, but an increase was observed in JMJD2C demethylase protein in anoxic skeletal muscle. Protein levels of adenosylhomocysteinase (AHCY) and methionine adenosyl transferase (MAT), enzymes of the methionine cycle, also showed an increase in the reoxygenated liver, whereas the levels decreased in muscle. A transcription factor ELISA showed a decrease in DNA binding by OCT1 in the reoxygenated liver and anoxic skeletal muscle, and transcript levels also showed tissue specific gene expression. The present study provides the first analysis of the role of the OCT1 transcription factor, associated proteins, and lysine demethylases in mediating responses to anoxia by wood frog tissues.

Highlights

- JMJDs regulate gene transcription to reprioritize pro-survival pathways.
- JMJD targets include antioxidation and cellular repair genes under MRD.
- Changes in total protein levels of AHCY and MAT maintain cellular SAM/SAH ratio.
- Increased GSH concentration provide antioxidant protection during anoxia in liver.
- Regulation of *myod* with increased levels of JMJD2C and H3K9Me2 in anoxic muscle.

Abbreviations

OCT: Octamer binding transcription factor, JMJD: Jumonji C domain proteins, AHCY: adenosylhomocysteinase, MAT: methionine adenosyl transferase, NuRD: nucleosome remodeling and the histone deacetylation, SAH: *S*-adenosylhomocysteine, SAHH: *S*-adenosylhomocysteine hydrolase, SAM: S-adenosylmethionine

Keywords

Jumonji C domain proteins, metabolic rate depression, Octamer binding transcription factor (OCT), Ahcy, methylation cycle, demethylation, histone (H3K9)

3.2 Introduction

The wood frog (*Rana sylvatica*) is one of the few ectothermic vertebrates that can survive long term whole body freezing during the winter. As much as 65–70% of the body water freezes in extracellular spaces, halting vital functions that include circulation, heartbeat, breathing, waste removal, muscle movement, and neuronal activity (Storey and Storey, 2017, Storey and Storey, 2013). Hence, anoxia is one major side stress of freezing. Wood frogs also have ability to survive anoxia as an independent stress. Anoxia limits the capacity for ATP generation which causes a switch to oxygen-independent metabolism, and suppress energy expensive cell processes when oxygen is limited (e.g. transmembrane ion pumping, protein synthesis, and cell cycle) (Storey and Storey, 2004). Therefore, a combination of three events would greatly aid wood frog survival under freeze-induced anoxic conditions: 1) increased glycolysis for the generation of ATP, 2) inhibition of various energy expensive processes to allocate ATP to essential cell functions only, and 3) activation of stress specific genes.

Transcription and translation are among the most energy expensive processes in cells; for example, the formation of one peptide bond needs 5 ATP equivalents (Storey and Storey, 2004). Hence, these processes require regulation under energy-restricted situations (Storey and Storey, 1999, Willmore and Storey, 2005). However, cell stress conditions also require the upregulation of specific genes and synthesis of specific proteins to provide protective actions including antioxidant defenses, anti-apoptosis, and chaperone functions (Storey and Storey, 2019, Storey and Storey, 2017, Wu et al., 2018). Therefore, the suppression of transcription and translation needs to be regulated selectively. To have stringent control over the activation vs. suppression of selected genes, a variety of

regulatory mechanisms can be applied including epigenetic controls on DNA (e.g. methylation and histone modifications) as well as altered synthesis of selected transcription factors (Hawkins and Storey, 2018).

Epigenetic controls, such as enhanced histone methylation under oxygen limiting conditions, have been well studied in selected systems. Di- or tri-methylation (Me) of lysine 9 (K9) on histone 3 (H3K9Me2, H3K9Me3) is associated with transcriptional repression (Batie et al., 2018). Recently, studies have also explored the role of lysine demethylase (KDM) action mediated by jumonji domain-containing proteins (JMJDs) in regulating gene expression responses to cellular stress. For example, the lysine demethylases; KDM3A (JMJD1A) and KDM4C (JMJD2C) are targets of hypoxia-inducible transcription factors-1 (HIF-1) that regulate cellular responses to low oxygen (Batie et al., 2018, Pollard et al., 2008, Qian et al., 2019). Recruitment of JMJD1A and JMJD2C is further mediated by OCT1 and OCT4 transcription factors, respectively (Shakya et al., 2011).

OCT1 and OCT4 are POU (Pit-1, Oct1/2, Unc-86) domain containing transcription factors that under oxidative stress, regulate the binding with JMJD1A and JMJD2C to target genes that encode adenosylhomocysteinase (ahcy) and (DNA-directed RNA polymerase II subunit RPB1) (polr2a) (Loh et al., 2007, Shakya et al., 2011) (**Fig. 3.1a**). JMJD1A and JMJD2C proteins catalyse oxidative demethylation, where JMJD1A can demethylate H3K9 mono- and dimethylation and JMJD2C is specific for the conversion of trimethylation to dimethylation on H3K9 and H3K36 (Yamane et al., 2006). Being hypoxia responsive, both JMJDs are associated with gene activation under oxygen deficient conditions with major targets including genes encoding free radical quenchers and the

methylation cycle (Batie et al., 2018, Pollard et al., 2008, Qian et al., 2019, Shakya et al., 2011).

OCT1 and OCT4 are also associated with nucleosome remodeling and the histone deacetylation (NuRD) chromatin complex to mediate gene repression via DNA methylation and histone deacetylation (**Fig. 3.1a**) (Liang et al., 2008, Shakya et al., 2011). Upon sensing stress, OCT switches its interaction from NuRD to JMJD to regulate the expression of target genes (Loh et al., 2007, Shakya et al., 2011) (**Fig. 3.1a**). Overexpression of JMJD demethylates the target genes at their respective H3K9Me to activate gene expression. AHCY is a cytoplasmic enzyme that is involved in multiple cellular processes including cell proliferation, cell cycle arrest, and DNA damage (Baric et al., 2004, Schubert et al., 2003). AHCY (also known as *S*-adenosylhomocysteine hydrolase, SAHH) catalyzes the hydrolysis of S-adenosylhomocysteine (SAH) to adenosine and homocysteine (Abeles, 1981) (**Fig. 3.1b**). This process prevents the inhibition of methyltransferases by restricting the accumulation of SAH. Homocysteine can either be methylated to methionine or removed via cystathionine β-synthase to create cysteine and glutathione (Panayiotidis et al., 2009). Methionine can also be metabolized by methionine adenosyl transferase (MAT) to S-adenosylmethionine (SAM) which is then converted to SAH to continue the cycle (**Fig. 3.1b**). SAM is used in all biological reactions that require a methyl donor and is essential to determining the methylation capacity of cells (Caudill et al., 2001) as measured by the SAH to SAM ratio. SAM is crucial for histone, DNA, and RNA methylation.

Given that the Jumonji C domain (JMJC) or KDM proteins are oxygen sensitive lysine demethylases, we chose to study histone methylation (H3K9Me2) modifications

under anoxia and recovery in wood frog tissues along with enzymes involved in the methylation pathway (e.g. AHCY and MAT) that act in histone methylation control. The present study investigates the responses of JMJ demethylases and their regulatory elements as well as the downstream target AHCY in the liver and skeletal muscle of wood frogs exposed to 24 h anoxia and 4 h aerobic recovery.

3.3 Methods

3.3.1. Animal treatment

Male wood frogs were collected from spring breeding ponds near Ottawa, Ontario, Canada. In the laboratory, frogs were briefly washed in a tetracycline bath and then transferred into a plastic box containing damp sphagnum moss for two weeks at 5 °C to acclimate. Control frogs were sampled from this condition. Other frogs were exposed to 24 h anoxia treatment at 5 °C, following the procedure described by Gerber *et al.* (Gerber et al., 2016). Briefly, the animals were placed on dampened paper towels (pre-wetted with distilled water previously bubbled with 100% nitrogen gas) in plastic jars that were previously flushed via a nitrogen gas line for 20 min. After adding frogs (4–5 per jar), the jars were again flushed with nitrogen gas 20 min and then both input and output vents in the lids were sealed. The jars were returned to 5 °C for 24 h. After anoxia exposure, half of the jars were reconnected to the nitrogen gas lines and then frogs were sampled quickly as the 24 h anoxic group. Frogs in the remaining jars were transferred to fresh jars with normal air and held at 5 °C for a 4 h aerobic recovery period before sampling. All frogs were euthanized by pithing and tissues (liver and hind leg skeletal muscle) were rapidly dissected from control, 24 h anoxia, and 4 h aerobic recovery conditions, flash frozen in

liquid nitrogen, and then stored at −80 °C until use. All animal experimental procedures had the prior approval of the Carleton University Animal Care Committee (protocol no. 106935) and followed the guidelines of the Canadian Council on Animal Care.

3.3.2. Total protein extraction for immunoblots

Total protein extracts from liver and skeletal muscle were prepared following procedures previously described by Gerber *et al.* (Gerber et al., 2016). Briefly, frozen tissue samples were weighed and then mixed with 1:2 w:v with prechilled homogenization buffer (20 mM Hepes, pH 7.4, 100 mM NaCl, 0.1 mM EDTA, 10 mM NaF, 1 mM Na_3VO_4, and 10 mM β-glycerophosphate) with the immediate addition of 1 mM phenylmethylsulfonyl fluoride and 1 µl/ml protease inhibitor cocktail (Bioshop, Burlington, ON, Canada, catalog no. PIC001.1) (reconstituted in 100 ml of deionized water). Samples were immediately homogenized using a Polytron PT10 homogenizer for ~ 20 sec followed by centrifugation for 15 min at 12,000 g at 4 °C. Supernatants were collected and protein concentrations were determined by the Coomassie blue dye-binding method using the Bio-Rad prepared reagent (BioRad Laboratories, Hercules, CA; Cat # 500–0006). The samples were then standardized to 10 µg/µl by the calculated addition of a small volume of homogenization buffer. Equal volumes of standardized total protein extracts and 2X SDS (sodium dodecyl sulphate) buffer (100 mM Tris-HCl, 20% v/v glycerol, 4% w/v SDS, 0.2% w/v bromophenol blue, and 10% v/v 2-mercaptoethanol) were then mixed and samples were boiled for 5 min in a water bath followed by immediate cooling on ice for 5–10 min. Samples were then aliquoted in 100 µl portions and stored at −80 °C until further use.

3.3.3. SDS PAGE and Western Blotting

Samples were run following procedures described previously by Gerber et al., 2016 (Gerber et al., 2016). Briefly 5% upper stacking gels were used with 10%, 12%, or 15% SDS PAGE resolving gels, depending on the molecular weight of the protein of interest. PiNK Plus Prestained Protein Ladder (Froggabio: PM005-0500) was loaded in the first lane and 20 µg of the protein in samples for all three conditions (aerobic control, 24 h anoxia, 4 h aerobic recovery) were loaded in the other lanes. Gels were run at 180 V. Proteins were transferred to PVDF membrane by electroblotting in 1X transfer buffer (25 mM Tris pH 8.5, 192 mM glycine, 20% methanol) at 160 mA 4 °C for 90 min. The membranes were blocked using 3% milk in TBST (20 mM Tris base, pH 7.6, 140 mM NaCl, 0.05% v: v Tween-20). After washing, the membranes were incubated with a specific primary antibody (diluted 1:1000 v:v in TBST) overnight at 4 °C. Later membranes were washed with TBST for 3 × 5 min and then incubated for 30 min with HRP linked secondary antibody and visualised using hydrogen peroxide and luminol.

The antibody for OCT1 (Catalog no. GTX100468) was purchased from GeneTex (Irvine, CA, USA). Antibodies for OCA (Catalog no. A6696), JMJD1A (Catalog no. A2322), JMJD2C (Catalog no. A8485), AHCY (Catalog no. A5300), MAT (Catalog no. A8436), and H3K9Me2 (Catalog no. A2359) were purchased from Abclonal (Woburn, MA, USA). All antibodies were incubated with an anti-rabbit IgG secondary antibody conjugated with horseradish peroxidase (catalog no. APA007P.2, Bioshop, Burlington, ON, Canada).

3.3.4. Total protein extractions for TF ELISA

Total protein was extracted from frozen samples of liver and skeletal muscle for all conditions (control, 24 h anoxia, and 4 h recovery) as described previously in Gupta and Storey, 2020 (Gupta and Storey, 2020). Briefly, samples were homogenized in a pre-chilled lysis buffer cocktail and protease inhibitor (Bioshop, Burlington, ON, Canada, Catalog No. PIC001) using a homogenizer. After incubation on ice for 30 min, samples were centrifuged at 14,000g for 20 min at 4 °C and the supernatant was collected. Protein concentrations were measured using the Bio-Rad protein assay and sample integrity was checked by running samples on SDS-PAGE.

3.3.5. DNA binding activity using TF ELISA

Biotin labeled DNA oligonucleotides were used for OCT (Gupta and Storey, 2020) to determine the binding capacity of the transcription factor to DNA. A standardized protocol from previous work was followed (Gupta and Storey, 2020). The primary antibody for OCT1 (described above) was used in a 1:1000 v:v dilution in phosphate buffer saline (137 mM NaCl, 2.7 mM KCl, 10 mM Na_2HPO_4, 2 mM KH_2PO_4, pH 7.4) containing 0.1% Tween-20 (PBST).

3.3.6. RNA isolation and cDNA synthesis

Samples of tissue (50 mg, n = 4, per condition) were homogenized in 1 ml of Trizol (BioShop, TRI118.100) using a Polytron PT10 homogenizer. Samples were incubated for 5 min at room temperature and then mixed with 200 µl of chloroform. Samples were then vortexed, incubated for 5 min and centrifuged at 10,000 rpm for 15 min at 4 °C. The upper aqueous layer containing total RNA was collected. RNA was precipitated by adding 500 µl of isopropanol and incubated at room temperature for 15 min

followed by centrifugation at 12,000 rpm for 15 min at 4 °C. The supernatant was discarded and the pellets were washed with 70% ethanol. Pellets were then dissolved in autoclaved ddH_2O. The purity of RNA was checked using the 260/280 ratio and concentration was standardized to 1 µg/µl. The integrity of the samples was checked using agarose gel electrophoresis (Al-attar et al., 2020).

A 5 µl aliquot of the sample (5 µg RNA) was mixed with 1 µl of 200 ng/µl oligo dT and incubated at 65 °C for 5 min using a thermocycler (iCycler, BioRad). Samples were removed and held on ice for 2 min followed by the addition of 4 µl of first-strand buffer (Invitrogen), 1 µl of 25 mM dNTPs, 2 µl of 100 mM DTT, and 1 µl of MMLV reverse transcriptase to each sample. Samples were incubated at 42 °C for 60 min in a thermocycler and then cDNA was diluted and stored at −20 °C.

3.3.7. Primer design and qPCR

Forward and reverse primers were designed for *oct1*, *jmjd2c*, and *ahcy*. Wood frogs are not genome sequenced so consensus sequences were identified from alignments of gene sequences from multiple vertebrates and conserved regions were used to design primers using Primer Blast on the NCBI. The list of primers used is:

oct1: Forward 5′ AGGAGGAAGAAACGCACCAG 3′

Reverse 5′ CCTCCGAGGTAGGCTTTTGG 3′

jmjd2c: Forward 5′ GTTGCGATGCTTTTCTGAGG 3′

Reverse 5′ CATGGTTTCAACTGTGCCGA 3′

ahcy: Forward 5′ CCATCGTCTGCAACATTGGC 3′

	Reverse 5′ CGATCCACCTGGGGTTTGAT 3′	
β-actin	Forward 5′-AGAAGTCGTGCCAGGCATCA-3′	
	Reverse 5′-AGGAGGAAGCTATCCGTGTT-3′	

Reagents for qPCR were prepared and the reaction was performed as described in previously (Pellissier et al., 2006, Zhang and Storey, 2013) using a CFX-96 Real-Time PCR detection system (Bio-Rad, Hercules, CA, USA). The PCR reaction cycles were as follows:

β-actin: 95 °C 3 min and then 40 cycles of (95 °C 20 sec, 53.8 °C 30 sec and 72 °C 20 sec)

oct1: 95 °C 3 min and then 40 cycles of (95 °C 20 sec, 57.3 °C 30 sec and 72 °C 20 sec)

jmjd2c: 95 °C 3 min and then 40 cycles of (95 °C 10 sec, 45.5 °C 30 sec and 72 °C 20 sec)

ahcy: 95 °C 3 min and then 40 cycles of (95 °C 10 sec, 57.8 °C 30 sec and 72 °C 20 sec)

PCR runs were followed by melt curve analysis to ensure a single peak during amplification and later a final hold at 4 °C was applied. A two-fold serial dilution curve testing was also performed to ensure the non-amplification of primer dimers following MIQE guidelines (Bustin et al., 2009). Beta-actin was used as the reference gene for standardization as its expression did not change significantly between control, anoxia, and recovery treatments (Schmittgen and Zakrajsek, 2000). Considering that wood frog is not a sequenced animal, sequence analysis of the amplicons would have benefitted and further supported our study, this was not possible in our current study due

to COVID-19 limitations and as such future work could expand on this study with sequence analysis and performing miRNA study.

3.3.8. Statistical analysis

Immunoblots were imaged using a Chemi-Genius Bioimager (Syngene, Frederick, MD) and Gene Tools software was used to quantify band intensities. Proteins bands were standardized against the summed intensity of a group of Coomassie stained protein bands in the same lane account for minor differences in sample loading (Eaton et al., 2013). This group of bands was present in all lanes and was well separated from the band of interest. qPCR data analysis used the $\Delta\ \Delta$ Ct method (Bustin et al., 2009, Taylor et al., 2019). Fold changes for 24 h anoxia and 4 h recovery from anoxia were calculated relative to controls that were set to 1. The values obtained were analyzed using one-way ANOVA followed by a Tukey post hoc test ($n = 4$) using RBioplot (Zhang and Storey, 2016) with $p < 0.05$ accepted as a significant difference between groups.

3.4. Results

3.4.1. Total protein levels of upstream of lysine demethylases

OCT1 protein was detected in the liver and muscle of wood frogs using immunoblotting and showed a single band at the expected size of 75 kDa. Total OCT1 protein levels in the liver did not change significantly compared to controls during anoxia exposure or aerobic recovery (**Fig. 3.2a**). However, a significant increase in liver OCT1 content was seen between anoxia and aerobic recovery, a 1.37 ± 0.07 fold change (**Fig. 3.2a**). In skeletal muscle, no significant change was observed in OCT1 expression between control, anoxic or recovery conditions (**Fig. 3.2b**).

OCA, a coactivator of OCT1 for a select group of genes, showed a significant decrease to 60% ± 9% of the control value during recovery from anoxia in liver (**Fig. 3.2a**). In muscle, OCA expression decreased to 40% ± 5% of the control under anoxia and dropped further to just 12% ± 1.5% of the control value during aerobic recovery (**Fig. 3.2b**).

3.4.2. Total protein levels of lysine demethylases

Relative total protein levels of the jumonji domain demethylases, JMJD1A and JMJD2C (expected sizes 147 kDa and 100 kDa, respectively) were also assessed using western blotting for both liver (**Fig. 3.2a**) and skeletal muscle (**Fig. 3.2b**) comparing control, 24 h anoxia and 4 h aerobic recovery after anoxia conditions. The relative protein levels of JMJD1A decreased during anoxia to 51.6% ± 8.5% of control values in liver and to 26.5% ± 3% of controls in skeletal muscle. Protein levels of JMJD1A decreased further to only 27% ± 5% of control in liver during aerobic recovery, whereas in skeletal muscle, expression remained low during aerobic recovery (16% ± 3%) but this value was not significantly different from the anoxia condition (**Fig. 3.2a and b**).

No significant change was seen in the expression of JMJD2C in liver over the three conditions (Fig. 2a). However, a very strong significant increase was observed in the level of JMJD2C in skeletal muscle by 3.16 ± 0.03 fold relative to control during anoxia with a further increase to 3.71 ± 0.06 fold over controls during recovery (**Fig. 3.2b**).

3.4.3. Total protein levels of major proteins involved in the SAM/SAH pathway and histones

AHCY, the enzyme responsible for the hydrolysis of SAH to homocysteine, is involved in the methyl transfer reaction (Lee et al., 2018). The relative total protein level of AHCY in anoxic liver rose significantly by 1.53 ± 0.08 fold relative to control conditions

and remained high at 1.52 ± 0.04 fold of control during aerobic recovery (**Fig. 3.3a**). However, in skeletal muscle, AHCY levels did not change under anoxia but decreased significantly to 34% ± 0.5% of controls during recovery (**Fig. 3.3b**).

The levels of MAT protein, the only known SAM synthesizing enzyme (Shafqat et al., 2013), in anoxic liver were similar to controls but levels increased significantly during aerobic recovery to 2.77 ± 0.25 fold over controls (**Fig. 3.3a**). However, in skeletal muscle, a decreasing trend in MAT was observed to levels that were 80% ± 6% and 67.7% ± 10% of controls during anoxia and recovery, respectively, but values were not significantly different from controls (**Fig. 3.3b**).

No significant change was observed in H3K9Me2 protein levels in liver over the three conditions whereas in muscle an increase of 2.54 ± 0.19 fold relative to control was observed during anoxia and levels remained high (1.88 ± 0.27 fold) after 4 h of aerobic recovery (**Fig. 3.3a and b**).

3.4.4. DNA binding activity of OCT1

The binding ability of OCT1 to its consensus DNA sequence was examined using a transcription factor ELISA, also known as DNA-protein binding ELISA. No change was observed in DNA binding levels by OCT1 under anoxia in liver versus control values, but binding decreased significantly to 51.7% ± 2.6% of the control during aerobic recovery (**Fig. 3.4**). By contrast, DNA binding levels in anoxic skeletal muscle were reduced to 51.3% ± 7.5% of the control value but raised again to control levels after aerobic recovery (**Fig. 3.4**).

3.4.5. Transcript levels of *oct1*, *jmjd2c*, and *ahcy*

Transcript levels of three key genes were also assessed in liver and muscle. Transcript levels of oct1 decreased significantly in anoxic liver to 44% ± 7.5% of the aerobic control value and remained low during aerobic recovery at 61% ± 6.3% of control (**Fig. 3.5a**). By contrast, *oct1* transcript levels increased significantly in anoxic muscles by 1.98 ± 0.34 fold over controls but decreased again during recovery to a level (1.26 ± 0.20 fold over control) that was not significantly different from either the control or anoxic values (**Fig. 3.5b**). No change was observed in transcript levels of jmjd1a in anoxic liver, but levels increased significantly by 1.49 ± 0.10 fold upon reoxygenation (**Fig. 3.5a**). However, skeletal muscle showed an opposite response with a significant increase of 3.76 ± 0.22 fold over control during anoxia exposure, but values dropped again to just 1.35 ± 0.26 fold higher than controls after 4 h aerobic recovery (**Fig. 3.5b**). Transcript levels of ahcy in liver decreased significantly to just 37.7% ± 4.8% of the control values under anoxia but rose strongly to 1.60 ± 0.11 fold over controls during aerobic recovery (**Fig. 3.5a**). However, no significant change in *ahcy* transcripts occurred in skeletal muscle under either of the two experimental conditions, compared to controls (**Fig. 3.5b**).

3.5. Discussion

Wood frogs have the remarkable ability to survive prolonged whole body freezing over the winter months. Upon freezing, vital activities cease (Storey and Storey, 2017, Storey and Storey, 2013) and because of this, frozen frogs experience weeks or months of anoxia and ischemia. Not surprisingly, these frogs exhibit well developed anoxia tolerance. Anoxia stress triggers the initiation and regulation of multiple cellular responses that include changes in gene expression (both upregulation of crucial genes and global

suppression of most transcriptional activity) to cope with the stress efficiently (Kenneth and Rocha, 2008). Histone modifications play an essential role in regulating gene expression by modifying chromatin structure. Modifications such as acetylation on key histone residues (chiefly on histone 3) produce an open conformation (euchromatin) that allows transcription factors to bind and initiate gene transcription whereas methylation leads to a closed conformation (heterochromatin) that transcription factors cannot penetrate (Batie et al., 2018, Saksouk et al., 2015). The major lysine methylation sites on histone 3 are H3K4, H3K9, H3K27, and H3K36. Demethylation at H3K9 is regulated by a JMJD histone demethylase that is an oxygen sensitive enzyme (Kenneth and Rocha, 2008, Perez-Perri et al., 2011). ChIP assays further confirmed that OCT1 and OCT4 regulate the expression of JMJD1A and JMJD2C to remove methyl residues from histones (& other proteins) (Loh et al., 2007).

The total protein levels of OCT1 showed a significant increase during recovery from anoxia in liver (**Fig. 3.2a**). OCT1 has proven to act as a regulatory switch between oxidative and glycolytic metabolism (Shakya et al., 2009). A study by Xu *et al.* showed that the activity of OCT1 is regulated by the Akt signaling pathway (Xu et al., 2015) and a previous study from our lab showed increased Akt protein levels in reoxygenated liver of wood frogs (Zhang and Storey, 2013). OCT1 also responds to signals of metabolic as well as oxidative stress occurring in cells and initiates responses by regulating the expression of RNA polymerases and snRNA genes (Ford et al., 1998, Murphy et al., 1992, Tanaka et al., 1992). Therefore, OCT1 being an oxidative stress sensor (Tantin et al., 2005), could be expected to be upregulated in wood frog cells during recovery from freeze-induced ischemia, as observed in the current study.

However, DNA binding capacity of OCT1 decreased significantly in the reoxygenated liver and in anoxic skeletal muscle (**Fig. 3.4**). Transcript levels of *oct1* also decreased in the liver during anoxia and recovery and this might be linked with reduced DNA binding by OCT1 during recovery. Cells under anoxic conditions undergo metabolic rate depression to minimize ATP consumption by reprioritising energy expenditures (mainly reducing anabolic activities) and suppressing energy expensive processes that include transcription, translation, cell cycle, and transmembrane ion pumping (Storey and Storey, 2004). Therefore, a reduction in the activity of transcription factors like OCT may be expected during anoxia and initial recovery. The probable reason for low DNA binding even with high total protein levels could be post translational modifications. However, we lack information on multiple OCT1 post-translational modifications with respect to wood frog that can affect its action such as p-Ser-385, ubiquitination, and GlcNAcylation. In response to anoxia these could aid in regulating the expression of its target genes without necessarily needing altered OCT1 protein levels. Analysis of PTMs is beyond the scope of the current study but further research in this area is warranted as this could make a key difference in assessing the activity of OCT1. Studies of OCT4 showed similar changes in total protein levels and DNA binding ability in both liver and skeletal muscle of wood frogs during anoxia (Gupta and Storey, 2020).

High rates of ROS production during recovery from anoxia exposure can lead to DNA damage and studies suggest that the binding activity of OCT1 increases in response to DNA damage (Schieber and Chandel, 2014, Zhao et al., 2000). Increased binding activity without any changes in protein levels also suggest post-translational modification that could increased movement of OCT1 into the nucleus. Previous studies from our lab

have described tissue specific responses of several transcription factors with different patterns of response in muscle and liver during anoxia stress in wood frogs (Gerber et al., 2016, Gupta and Storey, 2020, Storey and Storey, 2019). To further understand the role of OCT1 the expression of downstream factors was studied.

OCT1 associates with its cofactors to activate the expression of genes. For example, in the ERK signaling pathway, OCA enhances the activity of the promoter region of JMJD1A to replace NuRD (a repressive cofactor) in the transcriptional complex (Shakya et al., 2015, 2011). Despite varying changes in the levels of OCT1, OCA showed a continuous decrease in protein levels in both liver and skeletal muscle of wood frogs during anoxia and recovery (**Fig. 3.2**). A decrease in this cofactor could contribute to the reduced expression of the downstream protein JMJD1A. Indeed, a continuous and significant decrease in total protein levels of JMJD1A was observed in anoxia and reoxygenation in both frog tissues. A study with mice showed that JMJD1A was not expressed in OCT1 deficient T cells resulting in a significant increase in H3K9Me2 content (Shakya et al., 2011). Hence, both OCT1 and OCA appear to be essential for the recruitment of JMJD1A. A decrease in JMJD1A in both wood frog tissues during anoxia suggests a reduction in the demethylation of genes and, hence, suppression of gene expression; this correlates with anoxia-induced metabolic rate depression.

Surprisingly, a strong increase was observed in total protein levels of JMJD2C in anoxic muscles (>3-fold) and levels increased further during recovery whereas no significant changes occurred in liver (**Fig. 3.2**). Transcript levels of *jmjd2c* in muscle also increased strongly (>3.5-fold) under anoxia but dropped again during recovery (**Fig. 3.5**). By contrast, liver showed only a small increase in *jmjd2c* transcripts during aerobic

recovery but no change in protein levels (**Fig. 3.2a**). Hence, anoxia exposure triggered *jmjd2c* transcription in skeletal muscle and this translated into an increase in JMJD2C protein levels that were sustained through anoxia and into at least the early hours of aerobic recovery. This indicates an important role for this demethylase in muscle. JMJD2C is a direct target of HIF-1α (Xia et al., 2009); HIF-1α binds to the hypoxia response element in the promoter region of the *jmjd2c* gene and significantly upregulates its expression under hypoxic conditions (Xia et al., 2009). This suggests that HIF-1α is the likely trigger for JMJD2C production in wood frog muscles under hypoxia/anoxia. Furthermore, in a positive feedback loop, JMJD2C protein acts as a cofactor that interacts with HIF-1α to enhance its binding to the promoter regions of genes that encode proteins involved in metabolic reprogramming and survival (Liu et al., 2015, Luo et al., 2012).

In liver, overexpression of JMJD2C is known to increase the expression of Cul4A (a ubiquitin ligase protein) that targets p53 and initiates its degradation (Li and Jiang, 2017). The p53 protein is an important transcription factor that is involved in cell cycle regulation, energy metabolism, DNA repair, and apoptosis (Haupt, 2003, Yogosawa and Yoshida, 2018). The lack of changes in JMJD2C levels in liver in the current study suggests that Cul4A and p53 may remain unaltered under anoxia, allowing continued p53 function in the organ. However, an increase in transcript levels of *jmjd2c* during reoxygenation in the liver suggests preparation to return to normal conditions by reactivating global gene transcription including those genes that are required to combat oxidative stress. In skeletal muscle, JMJD2C increases the transcriptional activity of MyoD (Jin et al., 2016, Jung et al., 2015), a protein required for muscle regeneration/repair (Hernández-Hernández et al., 2017, Le Grand and Rudnicki, 2007). Oxygen deprivation could have detrimental effects

on skeletal muscle contractile proteins that, if prolonged, could lead to atrophy (Chaillou et al., 2014, Chaillou1 and Lanner, 2016, Favier et al., 2015). Thus, it may be possible that a demethylation of MyoD by JMJD2C could facilitate skeletal muscle maintenance and/or repair during anoxia and recovery.

JMJD2C has also been identified as an H3K9Me2/3 demethylase that converts H3K9Me3 to H3K9Me2 (Chen et al., 2006, Trojer and Reinberg, 2006, Whetstine et al., 2006, Zhang et al., 2006). Hence, it was not unexpected that the increase in JMJD2C expression led to increased levels of H3K9Me2 in wood frog skeletal muscle (**Fig. 3.2 and Fig. 3.3**). However, neither JMJD2C nor H3K9Me2 changed significantly under anoxia/recovery in liver, and since JMJD1A levels did not increase in liver, H3K9Me2 conversion to H3K9Me1 would remain low, thereby restricting gene activation in the liver. Since H3K9Me2 is the intermediate methylated form between Me3 and Me1, it is called a chromatin free repressive modification where genes are maintained in a silent but readily inducible position that could be activated immediately upon receiving a stress signal (e.g. a rush of oxygen or oxygen free radicals during reoxygenation) (Vázquez-Arreguín and Tantin, 2016).

One of the targets of jumonji demethylases is *ahcy* (Kang et al., 2009, Shakya et al., 2011, Vázquez-Arreguín and Tantin, 2016), the gene that encodes AHCY (also known as *S*-adenosylhomocysteine hydrolase or SAHH), that catalyses the breakdown of *S*-adenosylhomocysteine (SAH) to adenosine and homocysteine (Parkhitko et al., 2019, Turner et al., 2000). Relative protein levels of AHCY increased significantly in the liver under anoxia and remained elevated during recovery (**Fig. 3.3a**). AHCY inhibits methyltransferases and maintains the cellular methylation capacity indicated by

the SAM/SAH ratio. SAM is the principal methyl donor for cellular methylation reactions that include DNA, RNA, and proteins as methyl acceptors. Protein levels of MAT also increased significantly during aerobic recovery in liver (**Fig. 3.3a**) and this could lead to increased levels of SAM. An increase in hepatic glutathione, an important antioxidant in liver, has been positively correlated with SAM (Guo et al., 2015). Enhanced transcript levels of *ahcy* during recovery from anoxia (**Fig. 3.5a**) suggest a probable increase in enzyme activity during reoxygenation. This would increase the hydrolysis of SAH resulting in two outcomes: 1) Increase in SAM/SAH ratio to promote DNA methyltransferase activity (DNMT) that methylates and protects DNA from free radical damage (James et al., 2002) and 2) prevent SAH toxicity that could result in apoptosis (Sipkens et al., 2012).

In skeletal muscle, no significant change occurred in total protein levels of AHCY (or *ahcy* transcript levels,) under anoxia but AHCY protein decreased significantly during aerobic recovery (**Fig. 3.3b and Fig. 3.5b**). Protein levels of MAT were also unchanged in skeletal muscle over anoxia/recovery (**Fig. 3.3b**). Hence, these results suggest that the levels of SAM would increase in skeletal muscle. As discussed above, elevated SAM could lead to increased production of GSH to protect against oxidative damage.

3.5. Conclusion

In summary, a decrease in the protein levels of OCA and the binding activity of OCT1 is consistent with reduced protein levels of JMJD1A, suggesting that OCT controls the recruitment of this demethylase to regulate gene methylation under anoxic conditions. Changes in the levels of AHCY and MAT can help maintain the SAM/SAH ratio and increase GSH concentration to provide antioxidant protection during low oxygen stress in

the liver. Increased levels of JMJD2C and H3K9Me2 in anoxic muscle suggest that genes such as MyoD, which are essential for muscle repair and regeneration, are maintained in a poised state that can be immediately activated during aerobic recovery but further investigation is required. Finally, it is proposed that a coordinated regulation between Jumonji-domain containing histone demethylases and AHCY (a crucial enzyme in the methionine cycle) is maintained in a tissue specific manner to help protect cells under anoxia stress.

3.6 References

Abeles, R., 1981. The Mechanism of Action of S-Adenosylhomocysteinase, in: Eggerer, H., Huber, R. (Eds.), Structural and Functional Aspects of Enzyme Catalysis. Springer, Berlin, Heidelberg, pp. 192–195. https://doi.org/10.1007/978-3-642-81738-0_17

Al-attar, R., Wu, C.-W., Biggar, K.K., Storey, K.B., 2020. Carb-Loading: Freeze-Induced Activation of the Glucose-Responsive ChREBP Transcriptional Network in Wood Frogs. Physiol. Biochem. Zool. 93, 49–61. https://doi.org/10.1086/706463

Baric, I., Fumic, K., Glenn, B., Cuk, M., Schulze, A., Finkelstein, J.D., James, S.J., Mejaski-Bosnjak, V., Pazanin, L., Pogribny, I.P., Rados, M., Sarnavka, V., Scukanec-Spoljar, M., Allen, R.H., Stabler, S., Uzelac, L., Vugrek, O., Wagner, C., Zeisel, S., Mudd, S.H., 2004. S-adenosylhomocysteine hydrolase deficiency in a human: A genetic disorder of methionine metabolism. Proc. Natl. Acad. Sci. 101, 4234–4239. https://doi.org/10.1073/pnas.0400658101

Batie, M., del Peso, L., Rocha, S., 2018. Hypoxia and Chromatin: A Focus on Transcriptional Repression Mechanisms. Biomedicines 6, 47. https://doi.org/10.3390/biomedicines6020047

Bustin, S.A., Benes, V., Garson, J.A., Hellemans, J., Huggett, J., Kubista, M., Mueller, R., Nolan, T., Pfaffl, M.W., Shipley, G.L., Vandesompele, J., Wittwer, C.T., 2009. The MIQE Guidelines: Minimum Information for Publication of Quantitative Real-Time PCR Experiments. Clin. Chem. 55, 611–622. https://doi.org/10.1373/clinchem.2008.112797

Caudill, M.A., Wang, J.C., Melnyk, S., Pogribny, I.P., Jernigan, S., Collins, M.D., Santos-Guzman, J., Swendseid, M.E., Cogger, E.A., James, S.J., 2001. Intracellular S-Adenosylhomocysteine Concentrations Predict Global DNA Hypomethylation in Tissues of Methyl-Deficient Cystathionine β-Synthase Heterozygous Mice. J. Nutr. 131, 2811–2818. https://doi.org/10.1093/jn/131.11.2811

Chaillou, T., Koulmann, N., Meunier, A., Chapot, R., Serrurier, B., Beaudry, M., Bigard, X., 2014. Effect of hypoxia exposure on the recovery of skeletal muscle phenotype during regeneration. Mol. Cell. Biochem. 390, 31–40. https://doi.org/10.1007/s11010-013-1952-8

Chaillou1, T., Lanner, J.T., 2016. Regulation of myogenesis and skeletal muscle regeneration: effects of oxygen levels on satellite cell activity. FASEB J. 30, 3929–3941. https://doi.org/10.1096/fj.201600757R

Chen, Z., Zang, J., Whetstine, J., Hong, X., Davrazou, F., Kutateladze, T.G., Simpson, M., Mao, Q., Pan, C.-H., Dai, S., Hagman, J., Hansen, K., Shi, Y., Zhang, G., 2006. Structural Insights into Histone Demethylation by JMJD2 Family Members. Cell 125, 691–702. https://doi.org/10.1016/j.cell.2006.04.024

Eaton, S.L., Roche, S.L., Llavero Hurtado, M., Oldknow, K.J., Farquharson, C., Gillingwater, T.H., Wishart, T.M., 2013. Total protein analysis as a reliable loading control for quantitative fluorescent western blotting. PLoS One 8, e72457. https://doi.org/10.1371/journal.pone.0072457

Favier, F.B., Britto, F.A., Freyssenet, D.G., Bigard, X.A., Benoit, H., 2015. HIF-1-driven skeletal muscle adaptations to chronic hypoxia: Molecular insights into muscle physiology. Cell. Mol. Life Sci. https://doi.org/10.1007/s00018-015-2025-9

Ford, E., Strubin, M., Hernandez, N., 1998. The Oct-1 POU domain activates snRNA gene transcription by contacting a region in the SNAPc largest subunit that bears sequence similarities to the Oct-1 coactivator OBF-1. Genes Dev. 12, 3528–3540. https://doi.org/10.1101/gad.12.22.3528

Gerber, V.E.M., Wijenayake, S., Storey, K.B., 2016. Anti-apoptotic response during anoxia and recovery in a freeze-tolerant wood frog (*Rana sylvatica*). PeerJ 4, e1834. https://doi.org/10.7717/peerj.1834

Guo, T., Chang, L., Xiao, Y., Liu, Q., 2015. S-Adenosyl-L-Methionine for the Treatment of Chronic Liver Disease: A Systematic Review and Meta-Analysis. PLoS One 10, e0122124. https://doi.org/10.1371/journal.pone.0122124

Gupta, A., Storey, K.B., 2020. Regulation of antioxidant systems in response to anoxia and reoxygenation in *Rana sylvatica*. Comp. Biochem. Physiol. Part B Biochem. Mol. Biol. 243–244, 110436.

https://doi.org/10.1016/j.cbpb.2020.110436
Haupt, S., 2003. Apoptosis - the p53 network. J. Cell Sci. 116, 4077–4085. https://doi.org/10.1242/jcs.00739
Hawkins, L.J., Storey, K.B., 2018. Histone methylation in the freeze-tolerant wood frog (*Rana sylvatica*). J. Comp. Physiol. B 188, 113–125. https://doi.org/10.1007/s00360-017-1112-7
Hernández-Hernández, J.M., García-González, E.G., Brun, C.E., Rudnicki, M.A., 2017. The myogenic regulatory factors, determinants of muscle development, cell identity and regeneration. Semin. Cell Dev. Biol. 72, 10–18. https://doi.org/10.1016/j.semcdb.2017.11.010
James, S.J., Melnyk, S., Pogribna, M., Pogribny, I.P., Caudill, M.A., 2002. Elevation in S-Adenosylhomocysteine and DNA Hypomethylation: Potential Epigenetic Mechanism for Homocysteine-Related Pathology. J. Nutr. 132, 2361S-2366S. https://doi.org/10.1093/jn/132.8.2361S
Jin, W., Peng, J., Jiang, S., 2016. The epigenetic regulation of embryonic myogenesis and adult muscle regeneration by histone methylation modification. Biochem. Biophys. Reports 6, 209–219. https://doi.org/10.1016/j.bbrep.2016.04.009
Jung, E.-S., Sim, Y.-J., Jeong, H.-S., Kim, S.-J., Yun, Y.-J., Song, J.-H., Jeon, S.-H., Choe, C., Park, K.-T., Kim, C.-H., Kim, K.-S., 2015. Jmjd2C increases MyoD transcriptional activity through inhibiting G9a-dependent MyoD degradation. Biochim. Biophys. Acta - Gene Regul. Mech. 1849, 1081–1094. https://doi.org/10.1016/j.bbagrm.2015.07.001
Kang, J., Gemberling, M., Nakamura, M., Whitby, F.G., Handa, H., Fairbrother, W.G., Tantin, D., 2009. A general mechanism for transcription regulation by Oct1 and Oct4 in response to genotoxic and oxidative stress. Genes Dev. 23, 208–222. https://doi.org/10.1101/gad.1750709
Kenneth, N.S., Rocha, S., 2008. Regulation of gene expression by hypoxia. Biochem. J. 414, 19–29. https://doi.org/10.1042/BJ20081055
Le Grand, F., Rudnicki, M.A., 2007. Skeletal muscle satellite cells and adult myogenesis. Curr. Opin. Cell Biol. 19, 628–633. https://doi.org/10.1016/j.ceb.2007.09.012
Lee, H.-O., Wang, L., Kuo, Y.-M., Andrews, A.J., Gupta, S., Kruger, W.D., 2018. S-adenosylhomocysteine hydrolase over-expression does not alter S-adenosylmethionine or S-adenosylhomocysteine levels in CBS deficient mice. Mol. Genet. Metab. Reports 15, 15–21. https://doi.org/10.1016/j.ymgmr.2018.01.002
Li, N., Jiang, D., 2017. Jumonji domain containing 2C promotes cell migration and invasion through modulating CUL4A expression in lung cancer. Biomed. Pharmacother. 89, 305–315. https://doi.org/10.1016/j.biopha.2017.02.014
Liang, J., Wan, M., Zhang, Y., Gu, P., Xin, H., Jung, S.Y., Qin, J., Wong, J., Cooney, A.J., Liu, D., Songyang, Z., 2008. Nanog and Oct4 associate with unique transcriptional repression complexes in embryonic stem cells. Nat. Cell Biol. 10, 731–739. https://doi.org/10.1038/ncb1736
Liu, Q., Geng, H., Xue, C., Beer, T.M., Qian, D.Z., 2015. Functional regulation of hypoxia inducible factor-1α by SET9 lysine methyltransferase. Biochim. Biophys. Acta - Mol. Cell Res. 1853, 881–891. https://doi.org/10.1016/j.bbamcr.2015.01.011
Loh, Y.-H., Zhang, W., Chen, X., George, J., Ng, H.-H., 2007. Jmjd1a and Jmjd2c histone H3 Lys 9 demethylases regulate self-renewal in embryonic stem cells. Genes Dev. 21, 2545–2557. https://doi.org/10.1101/gad.1588207
Luo, W., Chang, R., Zhong, J., Pandey, A., Semenza, G.L., 2012. Histone demethylase JMJD2C is a coactivator for hypoxia-inducible factor 1 that is required for breast cancer progression. Proc. Natl. Acad. Sci. 109, E3367–E3376. https://doi.org/10.1073/pnas.1217394109
Murphy, S., Yoon, J.B., Gerster, T., Roeder, R.G., 1992. Oct-1 and Oct-2 potentiate functional interactions of a transcription factor with the proximal sequence element of small nuclear RNA genes. Mol. Cell. Biol. 12, 3247–3261. https://doi.org/10.1128/MCB.12.7.3247
Panayiotidis, M.I., Stabler, S.P., Allen, R.H., Pappa, A., White, C.W., 2009. Oxidative stress-induced regulation of the methionine metabolic pathway in human lung epithelial-like (A549) cells. Mutat. Res. Toxicol. Environ. Mutagen. 674, 23–30. https://doi.org/10.1016/j.mrgentox.2008.10.006

Parkhitko, A.A., Jouandin, P., Mohr, S.E., Perrimon, N., 2019. Methionine metabolism and methyltransferases in the regulation of aging and lifespan extension across species. Aging Cell 18. https://doi.org/10.1111/acel.13034

Pellissier, F., Glogowski, C.M., Heinemann, S.F., Ballivet, M., Ossipow, V., 2006. Lab assembly of a low-cost, robust SYBR green buffer system for quantitative real-time polymerase chain reaction. Anal. Biochem. 350, 310–312. https://doi.org/10.1016/j.ab.2005.12.002

Perez-Perri, J.I., Acevedo, J.M., Wappner, P., 2011. Epigenetics: New Questions on the Response to Hypoxia. Int. J. Mol. Sci. 12, 4705–4721. https://doi.org/10.3390/ijms12074705

Pollard, P.J., Loenarz, C., Mole, D.R., McDonough, M.A., Gleadle, J.M., Schofield, C.J., Ratcliffe, P.J., 2008. Regulation of Jumonji-domain-containing histone demethylases by hypoxia-inducible factor (HIF)-1α. Biochem. J. 416, 387–394. https://doi.org/10.1042/BJ20081238

Qian, X., Li, X., Shi, Z., Bai, X., Xia, Y., Zheng, Y., Xu, D., Chen, F., You, Y., Fang, J., Hu, Z., Zhou, Q., Lu, Z., 2019. KDM3A Senses Oxygen Availability to Regulate PGC-1α-Mediated Mitochondrial Biogenesis. Mol. Cell 76, 885-895.e7. https://doi.org/10.1016/j.molcel.2019.09.019

Saksouk, N., Simboeck, E., Déjardin, J., 2015. Constitutive heterochromatin formation and transcription in mammals. Epigenetics Chromatin 8, 3. https://doi.org/10.1186/1756-8935-8-3

Schieber, M., Chandel, N.S., 2014. ROS Function in Redox Signaling and Oxidative Stress. Curr. Biol. 24, R453–R462. https://doi.org/10.1016/j.cub.2014.03.034

Schmittgen, T.D., Zakrajsek, B.A., 2000. Effect of experimental treatment on housekeeping gene expression: validation by real-time, quantitative RT-PCR. J. Biochem. Biophys. Methods 46, 69–81. https://doi.org/10.1016/S0165-022X(00)00129-9

Schubert, H.L., Blumenthal, R.M., Cheng, X., 2003. Many paths to methyltransfer: a chronicle of convergence. Trends Biochem. Sci. 28, 329–335. https://doi.org/10.1016/S0968-0004(03)00090-2

Shafqat, N., Muniz, J.R.C., Pilka, E.S., Papagrigoriou, E., von Delft, F., Oppermann, U., Yue, W.W., 2013. Insight into S-adenosylmethionine biosynthesis from the crystal structures of the human methionine adenosyltransferase catalytic and regulatory subunits. Biochem. J. 452, 27–36. https://doi.org/10.1042/BJ20121580

Shakya, A., Cooksey, R., Cox, J.E., Wang, V., McClain, D.A., Tantin, D., 2009. Oct1 loss of function induces a coordinate metabolic shift that opposes tumorigenicity. Nat. Cell Biol. 11, 320–327. https://doi.org/10.1038/ncb1840

Shakya, A., Goren, A., Shalek, A., German, C.N., Snook, J., Kuchroo, V.K., Yosef, N., Chan, R.C., Regev, A., Williams, M.A., Tantin, D., 2015. Oct1 and OCA-B are selectively required for CD4 memory T cell function. J. Exp. Med. 212, 2115–2131. https://doi.org/10.1084/jem.20150363

Shakya, A., Kang, J., Chumley, J., Williams, M.A., Tantin, D., 2011. Oct1 Is a Switchable, Bipotential Stabilizer of Repressed and Inducible Transcriptional States. J. Biol. Chem. 286, 450–459. https://doi.org/10.1074/jbc.M110.174045

Sipkens, J.A., Hahn, N.E., Blom, H.J., Lougheed, S.M., Stehouwer, C.D.A., Rauwerda, J.A., Krijnen, P.A.J., van Hinsbergh, V.W.M., Niessen, H.W.M., 2012. S-Adenosylhomocysteine induces apoptosis and phosphatidylserine exposure in endothelial cells independent of homocysteine. Atherosclerosis 221, 48–54. https://doi.org/10.1016/j.atherosclerosis.2011.11.032

Storey, J.M., Storey, K.B., 2019. In defense of proteins: Chaperones respond to freezing, anoxia, or dehydration stress in tissues of freeze tolerant wood frogs. J. Exp. Zool. Part A Ecol. Integr. Physiol. 331, 392–402. https://doi.org/10.1002/jez.2306

Storey, K.B., Storey, J.M., 2017. Molecular physiology of freeze tolerance in vertebrates. Physiol. Rev. 97, 623–665. https://doi.org/10.1152/physrev.00016.2016

Storey, K.B., Storey, J.M., 2013. Molecular biology of freezing tolerance. Compr. Physiol. 3, 1283–1308. https://doi.org/10.1002/cphy.c130007

Storey, K.B., Storey, J.M., 2004. Metabolic rate depression in animals: transcriptional and translational controls. Biol. Rev. 79, 207–233. https://doi.org/10.1017/S1464793103006195

Tanaka, M., Lai, J.-S., Herr, W., 1992. Promoter-selective activation domains in Oct-1 and Oct-2 direct differential activation of an snRNA and mRNA promoter. Cell 68, 755–767. https://doi.org/10.1016/0092-8674(92)90150-B

Tantin, D., Schild-Poulter, C., Wang, V., Haché, R.J.G., Sharp, P.A., 2005. The Octamer Binding Transcription Factor Oct-1 Is a Stress Sensor. Cancer Res. 65, 10750–10758. https://doi.org/10.1158/0008-5472.CAN-05-2399

Taylor, S.C., Nadeau, K., Abbasi, M., Lachance, C., Nguyen, M., Fenrich, J., 2019. The Ultimate qPCR Experiment: Producing Publication Quality, Reproducible Data the First Time. Trends Biotechnol. 37, 761–774. https://doi.org/10.1016/j.tibtech.2018.12.002

Trojer, P., Reinberg, D., 2006. Histone Lysine Demethylases and Their Impact on Epigenetics. Cell 125, 213–217. https://doi.org/10.1016/j.cell.2006.04.003

Turner, M.A., Yang, X., Yin, D., Kuczera, K., Borchardt, R.T., Howell, P.L., 2000. Structure and Function of S-Adenosylhomocysteine Hydrolase. Cell Biochem. Biophys. 33, 101–125. https://doi.org/10.1385/CBB:33:2:101

Vázquez-Arreguín, K., Tantin, D., 2016. The Oct1 transcription factor and epithelial malignancies: Old protein learns new tricks. Biochim. Biophys. Acta - Gene Regul. Mech. 1859, 792–804. https://doi.org/10.1016/j.bbagrm.2016.02.007

Whetstine, J.R., Nottke, A., Lan, F., Huarte, M., Smolikov, S., Chen, Z., Spooner, E., Li, E., Zhang, G., Colaiacovo, M., Shi, Y., 2006. Reversal of Histone Lysine Trimethylation by the JMJD2 Family of Histone Demethylases. Cell 125, 467–481. https://doi.org/10.1016/j.cell.2006.03.028

Willmore, W.G., Storey, K.B., 2005. Purification and properties of the glutathione S-transferases from the anoxia-tolerant turtle, *Trachemys scripta elegans*. FEBS J. 272, 3602–3614. https://doi.org/10.1111/j.1742-4658.2005.04783.x

Wu, C.-W., Tessier, S.N., Storey, K.B., 2018. Stress-induced antioxidant defense and protein chaperone response in the freeze-tolerant wood frog *Rana sylvatica*. Cell Stress Chaperones 23, 1205–1217. https://doi.org/10.1007/s12192-018-0926-x

Xia, X., Lemieux, M.E., Li, W., Carroll, J.S., Brown, M., Liu, X.S., Kung, A.L., 2009. Integrative analysis of HIF binding and transactivation reveals its role in maintaining histone methylation homeostasis. Proc. Natl. Acad. Sci. 106, 4260–4265. https://doi.org/10.1073/pnas.0810067106

Xu, S.-H., Huang, J.-Z., Xu, M.-L., Yu, G., Yin, X.-F., Chen, D., Yan, G.-R., 2015. ACK1 promotes gastric cancer epithelial-mesenchymal transition and metastasis through AKT-POU2F1-ECD signalling. J. Pathol. 236, 175–185. https://doi.org/10.1002/path.4515

Yamane, K., Toumazou, C., Tsukada, Y., Erdjument-Bromage, H., Tempst, P., Wong, J., Zhang, Y., 2006. JHDM2A, a JmjC-Containing H3K9 Demethylase, Facilitates Transcription Activation by Androgen Receptor. Cell 125, 483–495. https://doi.org/10.1016/j.cell.2006.03.027

Yogosawa, S., Yoshida, K., 2018. Tumor suppressive role for kinases phosphorylating p53 in DNA damage-induced apoptosis. Cancer Sci. 109, 3376–3382. https://doi.org/10.1111/cas.13792

Zhang, D., Klose, R.J., Tempst, P., Bae, Y., Yamane, K., Wong, J., Erdjument-Bromage, H., Zhang, Y., 2006. The transcriptional repressor JHDM3A demethylates trimethyl histone H3 lysine 9 and lysine 36. Nature.

Zhang, J., Storey, K.B., 2016. RBioplot: an easy-to-use R pipeline for automated statistical analysis and data visualization in molecular biology and biochemistry. PeerJ 4, e2436. https://doi.org/10.7717/peerj.2436

Zhang, J., Storey, K.B., 2013. Akt signaling and freezing survival in the wood frog, *Rana sylvatica*. Biochim. Biophys. Acta - Gen. Subj. 1830, 4828–4837. https://doi.org/10.1016/j.bbagen.2013.06.020

Zhao, H., Jin, S., Fan, F., Fan, W., Tong, T., Zhan, Q., 2000. Activation of the transcription factor Oct-1 in response to DNA damage. Cancer Res. 60, 6276–6280.

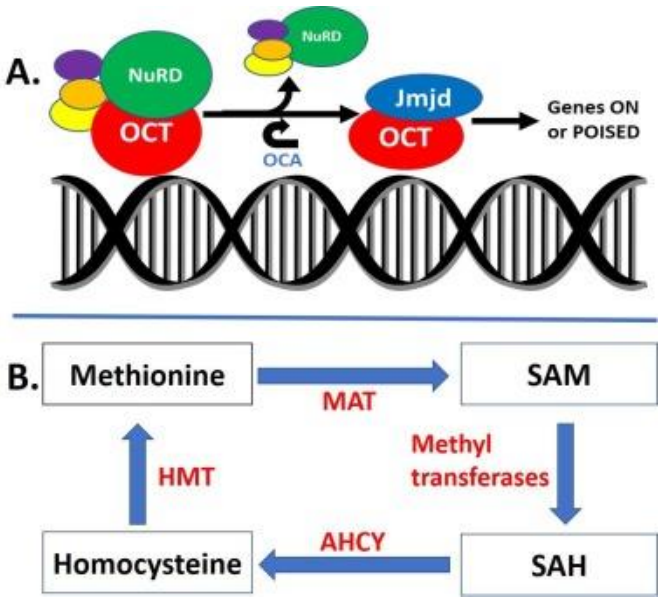

Fig. 3.1. (A) Schematic representation of the recruitment of Jmjd by OCT to initiate demethylation and regulate gene activation or gene poising. On methylated histones, NuRD is recruited by OCT. Once triggered, in association with OCA, OCT dissociates from NuRD and recruits Jmjd that demethylates H3K9Me3 to either activate genes by complete demethylation or keep them in a poised form by partial demethylation. OCT: Octamer binding transcription factor, NuRD: Nucleosome remodeling and histone deacetylation protein, OCA: OCT coactivator, Jmjd: Jumonji C-domain containing protein**. (B)** Pictorial representation of the methionine cycle. MAT: Methionine adenosyl transferase, AHCY: Adeno-homocysteine hydrolase, HMT: homocysteine methyltransferase, SAM: S-adenosyl methionine, SAH: S-adenosyl homocysteine.

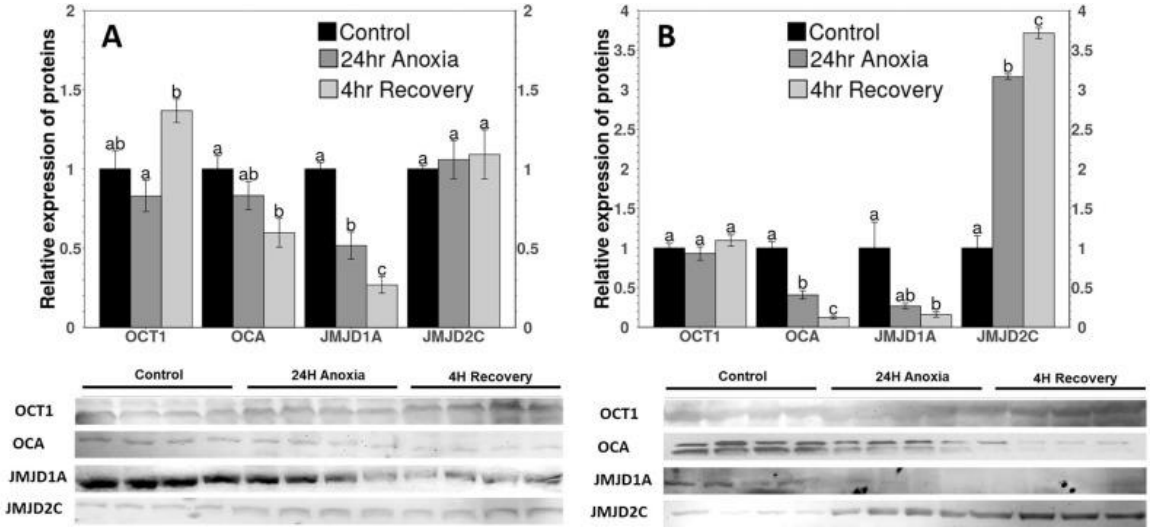

Fig. 3.2. Relative protein expression levels of OCT1, OCA, JMJD1A and JMJD2C in (A) liver and (B) skeletal muscle of *R. sylvatica* under control, 24 h anoxia exposure or 4 h aerobic recovery from anoxia conditions as determined by western immunoblotting. Corresponding Western immunoblot bands are shown below histograms. Data are mean ± SEM, n = 4 independent trials on samples from different animals. Data were analyzed using analysis of variance with a post hoc Tukey test; different letters denote values that are significantly different from each other ($p < 0.05$).

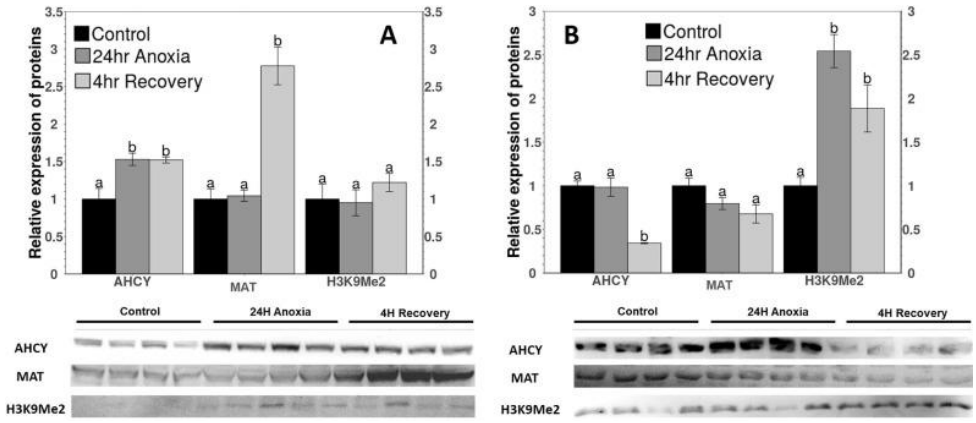

Fig. 3.3. Relative protein expression levels of factors in methylation cycle in (A) liver and (B) skeletal muscle of *R. sylvatica* under control, 24 h anoxia exposure or 4 h aerobic recovery from anoxia conditions as determined by western immunoblotting. Other information similar to Fig. 3.2.

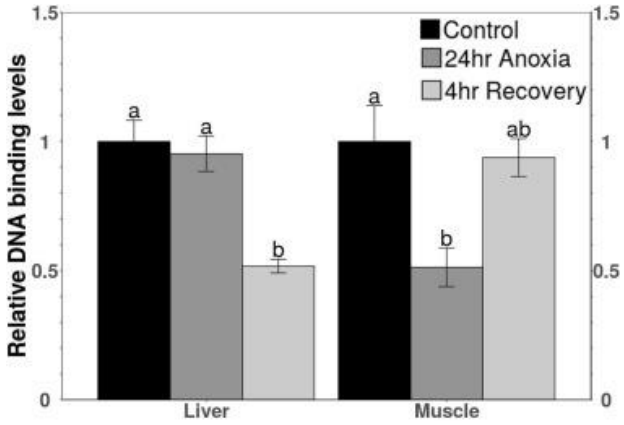

Fig. 3.4. Relative DNA binding levels of OCT1 in total protein extracts in liver and skeletal muscle of *R. sylvatica* under control, 24 h anoxia or 4 h recovery conditions as determined by TF-ELISA or DPI-ELISA. Other information similar to Fig. 3.2.

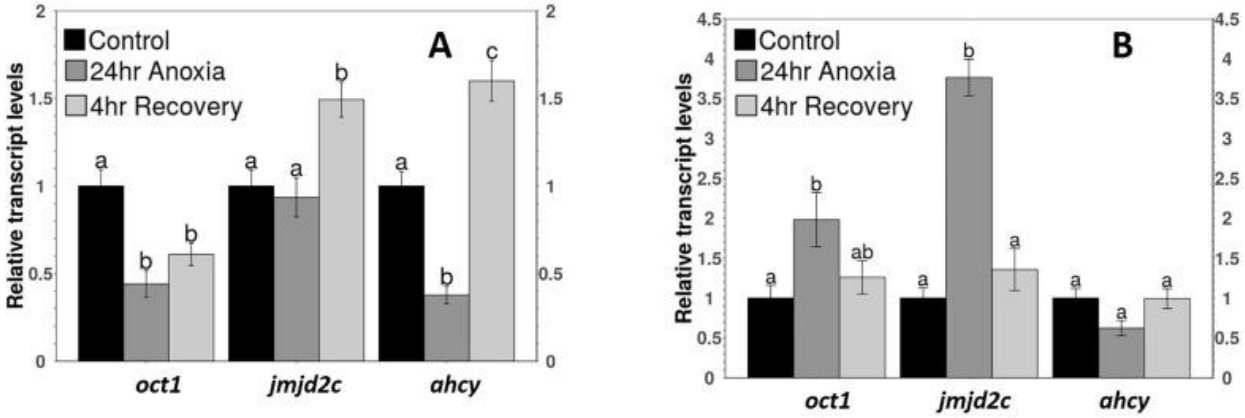

Fig. 3.5. Relative expression of *oct1*, *jmjd2c* and *ahcy* gene transcripts in (A) liver and (B) skeletal muscle of *R. sylvatic*a in control, 24 h anoxia, and 4 h recovery from anoxia as determined by qPCR. Other information similar to Fig.3.2.

4.Hippo Pathway

Activation of Hippo pathway in *Rana sylvatica:* yapping stops in response to anoxia

Aakriti Gupta and Kenneth B. Storey

Department of Biology, Carleton University, Ottawa, Canada K1S 5B6

***Correspondence to:**

Dr. Kenneth B. Storey

Department of Biology, Carleton University,

1125 Colonel By Drive, Ottawa, ON, K1S 5B6

Tel: (613) 520-2600, ext. 3678

E-mail: kenstorey@cunet.carleton.ca

4.1 Abstract

Wood frogs (*Rana sylvatica*) display well-developed anoxia tolerance as one component of their capacity to endure prolonged whole-body freezing during the winter months. Under anoxic conditions, multiple cellular responses are triggered to efficiently cope with stress by suppressing gene transcription and promoting activation of mechanisms that support cell survival. Activation of the Hippo signaling pathway initiates a cascade of protein kinase reactions that end with phosphorylation of YAP protein. Multiple pathway components of the Hippo pathway were analyzed via immunoblotting, qPCR or DNA-binding ELISAs to assess the effects of 24 h anoxia and 4 h aerobic recovery, compared with controls, on liver and heart metabolism of wood frogs. Immunoblot results showed significant increases in the relative levels of multiple proteins of the Hippo pathway representing an overall activation of the pathway in both organs under anoxia stress. Upregulation of transcript levels further confirmed this. A decrease in YAP and TEAD protein levels in the nuclear fraction also indicated reduced translocation of these proteins. Decreased DNA-binding activity of TEAD at the promoter region also suggested repression of gene transcription of its downstream targets such as SOX2 and OCT4. Furthermore, changes in the protein levels of two downstream targets of TEAD, OCT4 and SOX2, established regulated transcriptional activity and could possibly be associated with the activation of the Hippo pathway. Increased levels of TAZ in anoxic hearts also suggested its involvement in the repair mechanism for damage caused to cardiac muscles during anoxia. In summary, this study provides the first insights into the role of the Hippo pathway in maintaining cellular homeostasis in response to anoxia in amphibians.

Highlights

- Hippo pathway activates in response to anoxia in wood frogs.
- Decreased levels of YAP/TAZ/TEAD transcription complex suggests transcriptional repression under MRD.
- Increased levels of TAZ in anoxic heart indicates repair mechanism for cardiac muscles.

Abbreviations

MST: mammalian Ste20-like kinases 1/2, SAV: salvador 1, LATS1/2: large tumor suppressor 1 and 2 kinases, MOB: Mps one Binder, YAP: Yes-associated protein, TAZ: transcriptional coactivator with PDZ-binding motif, TEAD: TEA domain family member, OCT4: Octamer-binding transcription factor 4 and SOX2: SRY (sex determining region Y)-box 2.

Keywords

Hippo pathway, MST, SAV, LATS1/2, MOB, YAP, TAZ, TEAD, OCT4 and SOX2, anoxia, metabolic rate depression, energy stress

4.2 Introduction

The freeze-tolerant wood frog (*Rana sylvatica*) displays an incredible survival strategy to endure the seasonal cold of winter. These frogs can survive the freezing of 65–70% of total body water that accumulates as ice in extracellular spaces. In the frozen state, frogs do not show any vital signs: no breathing, heartbeat, blood circulation, or measurable neural conductivity [1,2]. Loss of water into extracellular ice leads to a strong reduction in cell volume while also increasing cellular osmolality. High quantities of glucose are produced and packed into cells to act as a cryoprotectant to protect cells from damage. Glucose is produced from glycogen stored in the liver and is distributed to all other tissues when triggered by ice nucleation on the skin. As a result, tissue and plasma glucose concentrations increase from 1–5 mM (when unfrozen) to as high as 200–300 mM as frogs freeze [2,3]. Because freezing halts blood circulation, tissues rapidly become ischemic and anoxic [4,5]. Hence, wood frog survival of freezing also depends on a well-developed anoxia tolerance. Prolonged exposure to anoxia typically causes an imbalance in ATP production vs. utilization. ATP production decreases steadily when mitochondrial oxygen-based ATP synthesis is impaired since the ATP yield from anaerobic glycolysis is only a small fraction of that produced from aerobic respiration [6]. When oxygen-restricted by freezing, frogs switch to “survival mode” [7] which includes a transition to the use of fermentation fuels, activation of cell survival pathways, and suppression of ATP-expensive nonessential cellular processes [8]. One pathway that may be involved in regulating the transition into anaerobiosis in cells of anoxia-tolerant species is the Hippo or YAP signaling pathway. However, the potential involvement of this pathway in freeze tolerance has never before been considered.

The Hippo pathway is a signaling network that controls a variety of cell processes involved in cell proliferation, differentiation, and cell death. It is also known to regulate organ size by controlling both apoptosis and cell proliferation [9]. The pathway can be stimulated by multiple cellular stresses which include energy crisis, oxygen stress, reactive oxygen species, mechanical stress, and DNA damage [10]. Most of the pathway components are highly conserved, including in amphibians [11,12,13,14], and the mode of pathway activation depends on the stress signal involved. The pathway is activated when stress-specific signals lead to phosphorylation of mammalian Ste20-like kinases 1/2 (MST1/2) (Thr183 and Thr180), and MST1/2 binds to its regulatory subunit, salvador 1 (SAV1), to form an active protein that can phosphorylate large tumor suppressor 1 and 2 kinases (LATS1/2) on T1079 for LATS1 or T1041 for LATS2 [15]. Active LATS1/2 phosphorylates yes-associated protein (YAP) and the transcriptional coactivator with PDZ-binding motif (TAZ) at S127 and S381, respectively. This stabilizes a YAP/TAZ complex. Phosphorylation of YAP/TAZ sequesters the complex in the cytoplasm and leads to ubiquitination. By contrast, nonphosphorylated YAP/TAZ translocates to the nucleus and binds to the TEA domain family member (TEAD) protein to activate stress-dependent transcription factors. Amongst others, transcription factors activated by this pathway are OCT4 and SOX2 (**Figure 4.1**) [16,17]. In fact, YAP/TAZ is a part of the TSO (TEAD–SMAD–OCT4) complex and acts as a repressor by recruiting NuRD (a multicomponent chromatin remodeling complex that regulates gene transcription) [18], whereas when released from TSO, OCT4 acts as a stress-responsive transcription factor to regulate expression of genes involved in antioxidant defense [19,20,21].

Anoxic conditions can lead to cell quiescence (or even cell death), activating the Hippo pathway to result in phosphorylation of YAP/TAZ and inhibiting its nuclear localization [22,23,24,25]. This prevents activation of genes that might lead to apoptosis or other energy expensive processes [26]. The Hippo pathway also promotes cell survival. Stress responsive regulation of the Hippo pathway can lead either to activation of cell survival genes by translocation of unphosphorylated YAP/TAZ into the nucleus, or other stresses (e.g., low energy, membrane shear stress) can trigger phosphorylation of YAP to halt gene transcription [10,27,28]. Since anoxia tolerance is a crucial component of freezing survival for wood frogs, it is important to analyze the potential role played by the Hippo pathway with respect to winter cryopreservation in this amazing freeze-tolerant species.

4.3 Methods

4.3.1. Animal Treatment

Male wood frogs (weighing 5–7 g) were collected from breeding ponds near Ottawa, Ontario, Canada in early spring. Frogs were briefly washed in a tetracycline bath and then transferred to plastic containers lined with damp sphagnum moss, followed by acclimation at 4 °C for ~2 weeks. Control frogs were sampled from this condition. For anoxia exposure, frogs were treated as described by Gerber et al. [29]. Briefly, animals (4–5 per jar) were placed into plastic jars (sitting in ice) that were pre-flushed with nitrogen gas for 20 min and contained a pad of pre-wetted paper towels on the bottom (wetted with water previously bubbled with 100% nitrogen gas). Jars were again flushed with nitrogen gas before sealing both input and output vents present on the lids. The jars were returned to 5 °C for 24 h. After the anoxia treatment, frogs in half of the jars were sampled as the 24 h anoxic group, whereas the remaining frogs were transferred to other jars with normal air.

These jars were returned to 5 °C for 4 h as an aerobic recovery period and then sampled. Frogs were euthanized by pithing and tissues were dissected rapidly for all three conditions (control, 24 h anoxia, 4 h recovery), immediately frozen in liquid nitrogen, and stored at −80 °C until use. All animal experiments followed the guidelines of the Canadian Council on Animal Care and had prior approval from the Carleton University Animal Care Committee (protocol no. 106935).

4.3.2. Total Protein Extractions for Immunoblots

Total protein was extracted from frozen heart and liver samples as described by Gerber et al. [29]. Briefly, frozen tissue samples (previously stored at −80 °C) were weighed and mixed 1:2 w/v with homogenization buffer (20 mM Hepes, pH 7.4, 100 mM NaCl, 0.1 mM EDTA, 10 mM NaF, 1 mM Na3VO4, and 10 mM β-glycerophosphate) with the immediate addition of 1 mM phenylmethylsulfonyl fluoride and 1 µL/mL protease inhibitor cocktail (BioShop, Burlington, ON, Canada, catalog no. PIC001.1) (reconstituted in 100 mL of deionized water). Samples were then immediately homogenized using a Polytron PT10 homogenizer and then stored on ice for ~15 min. Samples were centrifuged at 12,000× g for 15 min at 4 °C. The supernatant was collected, and the protein concentrations were determined using the Coomassie blue dye-binding method using the Bio-Rad prepared reagent (Bio-Rad Laboratories, Hercules, CA, USA; Cat # 500-0006). The concentrations of the samples were then standardized to 10 µg/µL by the addition of calculated small volumes of homogenization buffer. Standardized total protein extracts were then mixed 1:1 v/v with 2X SDS (sodium dodecyl sulphate) buffer (100 mM Tris-HCl, 20% v/v glycerol, 4% w/v SDS, 0.2% w/v bromophenol blue, and 10% v/v 2-mercaptoethanol) and then

boiled for 5 min in a water bath followed by snap chilling on ice for 10 min and stored at −80 °C until further use.

4.3.3. Nuclear Protein Extractions for Immunoblots

Frozen samples of liver and heart were weighed and homogenized 1:5 w/v in buffer A (10 mM HEPES, pH 7.9; 10 mM KCl; 10 mM EDTA; 20 mM β-glycerophosphate) with addition of 10 µL of 100 mM dithiothreitol (DTT) and 10 µL of protease inhibitor cocktail added per mL. Tissue was disrupted using a Dounce homogenizer with 4–5 strokes. Samples were incubated on ice for 25 min and then centrifuged at 12,000× g for 15 min at 4 °C. Supernatant was transferred to pre-chilled new tubes and stored as the cytoplasmic fraction.

Pellets were re-suspended in 1:5 w/v (based on original sample weights) in homogenization buffer B (100 mM HEPES; 2 M NaCl; 5 mM EDTA; 50% v/v glycerol; 100 mM β-glycerol phosphate pH 7.9; 100 mM DTT and protease inhibitor cocktail at 1:1000). Samples were sonicated using a Polytron PT1000 homogenizer (Brinkmann Instruments, Rexdale, ON, Canada) for 5 s and then incubated on ice for 10 min followed by centrifugation at 14,000× g for 15 min at 4 °C. The supernatant was transferred to pre-chilled new tubes and stored as the nuclear fraction.

Protein concentrations in both cytoplasmic and nuclear extracts were measured using the Bio-Rad protein assay. Samples were checked for their integrity and the purity of both fractions by running two SDS-PAGE gels each with cytoplasmic and corresponding nuclear fractions. The membranes were probed with anti-histone H3 (Cell Signaling, Beverly, MA, USA, catalog no. 9715) and alpha-tubulin antibody (Santa Cruz

Biotechnology, Santa Cruz, CA, USA. catalog no. sc-5286). Histone H3 served as the nuclear marker and alpha-tubulin as the cytoplasmic marker.

4.3.4. SDS PAGE and Western Blotting

The procedure described by Gerber et al., 2016 [29] was followed to run the samples on SDS PAGE gels. Briefly, 5% upper stacking gels and 10–15% resolving gels (depending on the molecular weight of the protein of interest) were used with 5 µg PiNK Plus Prestained Protein Ladder (Froggabio: PM005-0500) loaded in the first lane as a MW marker. Samples of 20 µg protein for all three conditions (control, 24 h anoxia, and 4 h recovery after anoxia, all n = 4) were loaded in other lanes. Gels were run at a constant voltage of 180 V until the band in the ladder lane (corresponding closest to the MW of the protein of interest) was well resolved from other bands. Proteins were then transferred from the gels to PVDF (polyvinylidene difluoride) membranes (Millipore, Etobicoke, ON, Canada, catalog no. IPVH07850, 45 µm pore) by electroblotting in 1X transfer buffer (25 mM Tris pH 8.5, 192 mM glycine, 20% methanol) at a constant current of 160 mA at 4 °C for 90 min. Subsequently, blots were blocked with 3% milk in TBST (20 mM Tris base, pH 7.6, 140 mM NaCl, 0.05% v/v Tween-20) for 30 min. Membranes were then washed for 3 × 5 min each followed by incubation with a specific primary antibody (diluted 1:1000 in TBST) overnight at 4 °C. Subsequently, the membranes were washed 3 × 5 min with TBST and incubated with horseradish peroxide-linked secondary antibody specific for the primary antibody for 30 min. Bands on membranes were visualized using hydrogen peroxide and luminol and quantified using a Chemi-Genius Bioimager (Syngene, Frederick, MD, USA).

The antibodies for OCT4 (Catalog no. GTX100468) and SOX2 (Catalog no. GTX101507) were purchased from GeneTex (Irvine, CA, USA). Antibodies for Mst-1 (Catalog no. A12963), Mst-2 (Catalog no. A6992), Sav-1 (Catalog no. A9980), LATS (Catalog no. A16249), p-LATS (Catalog no. AP0880), YAP (Catalog no. A1002), p-YAP (Catalog no. AP0489), TAZ (Catalog no. A12722), and TEAD1 (Catalog no. A6768) were purchased from Abclonal (Woburn, MA, USA). An anti-rabbit IgG conjugated with horseradish peroxidase (catalog no. APA007P.2, BioShop, Burlington, ON, Canada) was used as a secondary antibody.

4.3.5. Total Protein Extractions for TF ELISA

Total protein was extracted for all three conditions (control, 24 h anoxia, 4 h recovery) from frozen samples of heart and liver following the procedure described by Gupta and Storey, 2020 [20]. Briefly, samples were weighed and homogenized in a lysis buffer cocktail that included a protease inhibitor (BioShop, Burlington, ON, Canada, Catalog No. PIC001). Samples were incubated on ice for 30 min and later centrifuged at 14,000× g for 20 min at 4 °C. Supernatants were collected and protein concentrations were measured using Bio-Rad assay. Sample integrity was checked by running aliquots on SDS PAGE as described above.

4.3.6. DNA-Binding Activity Using TF ELISA

Biotin labeled DNA oligonucleotides corresponding to the binding site of TEAD were used to determine the binding capacity of the transcription factor to DNA. The following consensus sequences were used:

TEAD (5′Biotin-TGCCTAAATTTGGAATGTTCTGCT 3′)

TEAD complementary (5′ AGCAGAACATTCCAAATTTAGGCA 3′)

A standard protocol from previous work was followed [20]. The primary antibody for TEAD (described above) was used at 1:1000 v/v dilution in phosphate-buffered saline (PBST) containing 137 mM NaCl, 2.7 mM KCl, 10 mM Na2HPO4, 2 mM KH2PO4, pH 7.4) and 0.1% Tween-20.

4.3.7. RNA Isolation and cDNA Synthesis

RNA was isolated from frozen tissue samples of heart and liver following the method described by Gupta and Storey (2021) [30]. Briefly, samples were homogenized in TRIzol (BioShop, TRI118.100) at 1:20 w/v using a Polytron PT10 homogenizer and incubated at room temperature for 5 min. Subsequently, chloroform was added at 1:4 w/v and vortexed well. Samples were incubated for 5 min and then centrifuged at 10,000 rpm for 15 min at 4 °C. The upper aqueous layer was collected, and RNA was precipitated by incubating with 500 µL isopropanol at room temperature for 15 min. Samples were then centrifuged at 12,000 rpm for 15 min at 4 °C, and the supernatant was discarded. The pellet was washed with 70% ethanol and dissolved in autoclaved distilled water. The purity of RNA was checked by determining the OD 260/280 ratio and integrity was checked using agarose gel electrophoresis. Sample concentrations were standardized to 1 µg/µL. cDNA was synthesized from the RNA samples following the protocol of Gupta and Storey, 2021 [30], and cDNA was stored at −20 °C till further use.

4.3.8. Primer Design and qPCR

Forward and reverse primers were designed for mst1, mst2, sav, taz, tead, and yap. Since the genome of wood frogs is not sequenced, we identified consensus sequences by aligning sequences from several vertebrate species to identify conserved regions. Primer

Blast on the NCBI was used to design primers from the conserved sequences. Primers used were:

mst1:	Forward 5′ GTTGGGGCATGTGAGGGAGACT 3′
	Reverse 5′ CTCTGGCGGGCACAATGACAC 3′
mst2:	Forward 5′ GAAGGGAAGCCGCCGTATGC 3′
	Reverse 5′ TGGGTGGTGGATTTGTGGGGA 3′
sav:	Forward 5′ GAAAGAGACCTCCCCGCTGCT 3′
	Reverse 5′ TGGGCAGATATCAGTCCGTCTCG 3′
taz:	Forward 5′ GGACACGCCGCTCATCACA 3′
	Reverse 5′ GTGCAAGTTCCACAGGTGCTTT 3′
tead:	Forward 5′ CGTTTGGGAAACAAGTCGTGGAG 3′
	Reverse 5′ ACATCGGGGAGCGGTTTATCC 3′
yap:	Forward 5′ TGCCCATGCGGATGAGGAAAC 3′
	Reverse 5′ GCTGATCCCCCATCTGTGCTG 3′
β-actin:	Forward 5′-AGAAGTCGTGCCAGGCATCA-3′
	Reverse 5′-AGGAGGAAGCTATCCGTGTT-3′

The qPCR reaction was performed as described in previously [31,32] using a CFX-96 Real-Time PCR detection system (Bio-Rad, Hercules, CA, USA). The PCR reaction cycles used were as follows:

β-actin: 95 °C for 3 min and then 40 cycles of (95 °C 20 s, 53.8 °C 30 s, and 72 °C 20 s)

mst1, mst2, sav, taz, and tead: 95 °C 3 min and then 40 cycles of (95 °C 20 s, 54.3 °C 30 s, and 72 °C 20 s)

yap: 95 °C 3 min and then 40 cycles of (95 °C 10 s, 52.0 °C 30 s, and 72 °C 20 s)

PCR reaction runs were followed by a melt curve analysis to ensure a single product during amplification, and a final hold at 4 °C was applied. The primers were tested by performing a two-fold serial dilution curve test following MIQE guidelines [33] to ensure non-amplification primer dimers. Beta-actin was used as the reference gene for

standardization since its expression did not change significantly between all three experimental conditions [34].

4.3.9 Statistical Analysis

The Chemi Genius Bioimager was used to image immunoblots, and band intensities were quantified using the associated Gene Tools software. Blots were then Coomassie-stained, and the summed intensity of the group of bands well separated from the band of interest was used to standardized protein band intensities to account for any minor differences that occurred during sample loading [35]. The results for qPCR were analyzed using the ΔΔCt method [33,36]. Control values were set to 1, and the fold change for 24 h anoxia and 4 h recovery was calculated relative to control values to ease data interpretation. One-way ANOVA followed by a Tukey post hoc test ($n = 4$) was used to analyze the standardized values; the program RBioplot [37] was used and $p < 0.05$ was accepted as a significant difference between groups.

4.4 Results

4.4.1. Protein Levels of Cytoplasmic Components of the Hippo Pathway

Relative levels of proteins associated with the Hippo pathway that are known to be cytoplasmic were assessed in total protein extracts of liver and heart tissue from wood frogs and assessed using SDS-PAGE and immunoblotting. A significant increase in MST1 content was observed after 24 h anoxia exposure in both liver and heart, by 1.35 ± 0.05-fold and 2.45 ± 0.1-fold, respectively, compared to controls (**Figure 4.2**). However, during aerobic recovery (4 h back in normal air) the tissues differed in their responses. In liver, MST1 levels had decreased to 76 ± 2.5% of control values (not significantly different from

controls) within 4 h (**Figure 4.2A**), whereas heart MST1 levels remained unchanged compared to anoxic values (**Figure 4.2B**).

The relative protein levels of MST2 increased strongly under anoxia in both liver (2.78 ± 0.18-fold) (**Figure 4.2A**) and heart (2.66 ± 0.16-fold) (**Figure 4.2B**) compared to controls. During recovery, MST2 responses were similar to those of MST1. MST2 levels in liver decreased significantly to a value intermediate between control and anoxic values (1.7 ± 0.14-fold over controls) (**Figure 4.2A**) but, again, MST2 values remained high in heart after 4 h aerobic recovery (**Figure 4.2B**).

The levels of SAV protein in liver decreased to just 32 ± 5% of controls in response to 24 h anoxia and had fallen further to 21.2 ± 4% of controls after 4 h aerobic recovery (**Figure 4.2A**). By contrast, no significant change was observed under either anoxia or recovery as compared to control values in heart (**Figure 4.2B**). No significant changes were observed in LATS protein levels in either tissue in response to anoxia or recovery (**Figure 4.2**). However, when the phosphorylation state of LATS protein was assessed, both tissues showed strong reductions in p-LATS content under anoxia, decreasing to 34.67 ± 3% and 43.14 ± 6% of the control values in liver and heart, respectively (**Figure 4.2**). However, phosphorylation of LATS returned to control values during aerobic recovery. Phosphorylation of YAP protein was also assessed; p-YAP is sequestered in the cytoplasm, preventing its translocation to nucleus to initiate gene expression. The responses by p-YAP differed between the two tissues. In liver, p-YAP content did not change during anoxia, but a significant decrease was observed during aerobic recovery to just 38 ± 8% of control levels (**Figure 4.2A**). In heart, the opposite effect was seen with a significant increase in

p-YAP by 1.7 ± 0.13-fold during anoxia, compared to controls, and levels remaining unchanged after 4 h aerobic recovery (**Figure 4.2B**).

4.4.2. Protein Levels of Nuclear Components of the Hippo Pathway

Relative protein levels of three proteins belonging to the Hippo pathway that have primary functions in the nucleus (YAP, TAZ, TEAD) were evaluated in nuclear extracts of liver and heart tissue (**Figure 4.3**). In liver, YAP protein showed a significant decrease in the nuclear fraction during 24 h anoxia to 66.8 ± 4% of control values and fell further to 33.5 ± 1.5% of controls during aerobic recovery (**Figure 4.3A**). YAP levels in heart also decreased significantly during anoxia to 63.6 ± 4.8% of control values and remained unchanged during the 4 h recovery period (**Figure 4.3B**). The levels of TAZ in nuclear extracts decreased drastically to just 12.4 ± 1% in anoxic liver, as compared with controls, and fell further to just 3.6 ± 0.5% of controls during recovery (**Figure 4.3A**). By contrast, TAZ levels increased by 1.50 ± 0.13-fold over control values in anoxic heart, suggesting an important role for TAZ in anoxia heart (**Figure 4.3B**). However, TAZ levels were reduced again to control levels during aerobic recovery. TEAD protein levels were not significantly affected by 24 h anoxia in liver but had decreased to just 29 ± 2.7% of controls after 4 h aerobic recovery (**Figure 4.3A**). TEAD levels in heart showed little change between the three experimental groups, although a small but significant difference between anoxia and recovery conditions was detected (**Figure 4.3B**).

4.4.3. Protein Levels of OCT4 and SOX2 Downstream Targets

The relative protein levels of OCT4 and SOX2 under control, anoxia, and aerobic recovery conditions in wood frogs were analyzed in liver in a previous study [20]. Figure 4 shows the comparable effects of these conditions on relative total protein levels of OCT4

and SOX2 in heart. Under anoxia, OCT4 levels decreased significantly to 69.5 ± 3.5% of control values and remained low during aerobic recovery (**Figure 4.4**). However, no significant change was observed in the relative levels of SOX2 protein among the three conditions (**Figure 4.4**).

4.4.4. DNA-Binding Activity of TEAD

The binding ability of TEAD to its consensus DNA sequence was examined using a transcription factor ELISA, previously known as DNA-protein binding ELISA (DPI-DNA protein interaction). A significant decrease was observed in DNA-binding levels by TEAD under anoxic conditions in both liver and heart. Binding capacity decreased to 60.8 ± 7% in anoxic liver and to 73.3 ± 2.6% in anoxic heart, as compared with controls. These levels remained unchanged during aerobic recovery in liver, but binding rose again to control levels after 4 h aerobic recovery in heart (**Figure 5**).

4.4.5. Transcript Levels of Key Components of the Pathway

Transcript levels of key genes involved in Hippo signaling were assessed in liver and heart (**Figure 6**). Transcript levels of *mst1* increased significantly by 2.44 ± 0.12-fold under anoxia in liver but returned to control values during aerobic recovery (**Figure 6A**), whereas an increasing trend was observed in heart under anoxia with a significant increase of 1.5 ± 0.15-fold over controls during recovery (**Figure 6B**). Transcript levels of *mst2* increased significantly during anoxia in both organs by 2.01 ± 0.29-fold and 1.72 ± 0.26-fold over controls in liver and heart, respectively (**Figure 6**). During recovery, *mst2* transcripts remained unchanged in liver but increased further to 2.53 ± 0.12-fold over controls in heart.

Transcript levels of *sav* and *taz* decreased significantly during anoxia in liver to 57.4 ± 5% and 58.3 ± 6% of control values, respectively (**Figure 6A**) and remained unchanged during recovery. No significant changes were observed in the transcript levels of sav under all three conditions in heart, but *taz* transcripts increased significantly in heart under anoxia by 2.37 ± 0.23-fold but retuned to control values during recovery (**Figure 6B**). Transcript levels of *tead* showed a decreasing trend with no significant decrease in anoxic liver but a significant reduction during recovery to 15.5 ± 8.3% of controls (**Figure 6A**). In heart, the transcript levels of *tead* decreased significantly to 50.6 ± 7.5% of the control values, and the values remained unchanged during recovery (**Figure 6B**). Transcript levels of *yap* showed a decreasing trend but no significant change under any of the three conditions in liver, whereas *yap* transcript levels decreased significantly in anoxic heart to 39 ± 6% of controls but rose again to 71.4 ± 8.1% of control values during recovery in heart (**Figure 6**).

4.5 Discussion

Wood frogs can survive whole-body freezing over many months in the winter [1,2]. Stresses such as anoxia and ischemia arise because ice formation shuts down all movements, including breathing, blood circulation, and nerve transmission and isolates cells, tissues, and organs so that they must endure with only their own internal reserves and regulatory mechanisms to maintain viability. Under these conditions, tolerance of anoxia is essential. Indeed, frogs initiate and regulate the expression of many genes/proteins involved in multiple cellular processes in an energy-efficient manner to enable long-term survival without oxygen [38]. For example, the hypoxia-inducible factor (HIF-1) is undoubtedly one transcription factor that supports cell/tissue survival during freezing. The

present study shows that the Hippo signaling pathway is involved in metabolic regulation under the limited availability of energy and oxygen to suppress gene transcription of the targets regulated by the YAP/TAZ/TEAD complex by preventing the translocation of YAP to the nucleus [9,15] to initiate stress-specific responses. Recent studies have also linked the Hippo pathway with ROS-mediated cellular responses or oxidative stress, where key components of the pathway act as ROS scavengers [39,40,41]. Taken together, it is evident that this pathway plays an important role in maintenance of overall cellular homeostasis under stress, and regulation study under anoxic conditions is pertinent.

The total protein levels of core components involved in the Hippo pathway were analyzed for liver and heart under control, 24 h anoxia, and 4 h recovery conditions. Protein levels of MST1 and MST2 were significantly elevated in both tissues during anoxia and after 4 h aerobic recovery from anoxia (**Figure 2**), and transcript levels of both *mst1* and *mst2* rose under anoxia (**Figure 6**). This indicates a transcription-factor-initiated process to upregulate genes whose transcribed mRNAs then support enhanced synthesis of selected proteins in response to anoxia. This makes sense given that MST1 and MST2 are the initial proteins of the Hippo pathway, and their elevation represents an activation of the pathway [42]. Further support for the importance of MST1/2 in initiating anoxia-triggered cell processes is supplied by the responses of SAV protein (the binding partner of MST1/2); both *sav* transcript and SAV protein levels were reduced (liver) or unchanged (heart) over anoxia/recovery.

A study by Zhou et al. using mouse hepatocytes showed that MST1 and MST2 negatively regulate the expression of YAP in mammalian liver [24]. The study further showed that MST1/2-deficient liver showed inhibition of the phosphorylation of YAP and

therefore increased the abundance of YAP in the nucleus [24]. These findings are in accordance with the current study since a significant decrease in the protein levels of YAP were observed in nuclear fractions of both liver and heart. Moreover, transcript levels of *yap* were unchanged in the liver under anoxia, whereas levels decreased significantly in heart (**Figure 3 and 6**). During recovery from anoxia, in liver, the protein levels decreased further, and the transcript levels of *yap* showed a decreasing trend with no significant difference, but in heart the YAP protein levels remained unchanged, and transcripts increased significantly during recovery (**Figure 3 and 6**). Increased transcript levels represent preparation of the organ for protein translation in response to the upcoming event. During recovery, cardiomyocytes could experience a rush of oxygen into the blood that could potentially increase ROS levels [43,44]. An increased rate of ROS production during recovery causes oxidative stress and could lead to cardiomyocyte death. Activation of YAP could protect from cell death [41] through myocardial regeneration by promoting the proliferation of cardiomyocytes after myocardial injury, suggesting a protective role of YAP after oxidative stress [9,25].

A tissue-specific response was observed in the expression of SAV and p-YAP under both anoxia and aerobic recovery conditions, as compared to controls (**Figure 2**). Activation of the Hippo pathway initiates a series of kinase activities that would phosphorylate YAP and sequester it in the cytoplasm. YAP is known to be phosphorylated at multiple sites and inhibited by two mechanisms [45]. Phosphorylation at Ser-127 results in binding of 14-3-3 protein which mediates spatial regulation (cytoplasmic-nuclear shuttling) [46], whereas phosphorylation at Ser-381 is required for phosphodegron-induced protein degradation (i.e., primed for ubiquitination-based degradation) [45]. The current

research focused on the analysis of relative levels of p-YAP at Ser-127, but a detailed study on multiple phosphorylation sites on YAP and AMPK levels during anoxia and recovery with respect to control for both the tissues could be used to further validate the findings presented in this paper.

In the current study, expected results with respect to activation of the Hippo pathway were observed in the heart. The levels of p-YAP increased during anoxia and remained unchanged during recovery; however, the levels of SAV and LATS showed no significant change in any condition. Interestingly, liver showed contrasting results for the relative protein expression of SAV and p-YAP. A significant decrease in the levels of SAV, as well as p-YAP, was observed (**Figure 2**). Multiple studies have reported that activation of MST1/2 under stress is sufficient to turn off YAP/TAZ [23,24,47,48] by directly phosphorylating MST1/2. It was also observed that under energy stress, AMPK directly phosphorylates YAP to prevent its interaction with TEAD and inhibiting YAP/TAZ/TEAD-mediated gene transcription [15,49]. Previous studies have described an organ-specific increase in AMPK levels in response to environmental stress in stress-tolerant animals [50,51,52,53,54].

Therefore, multiple possibilities could be inferred: (1) the increased levels of AMPK and MST1/2 could lead to direct phosphorylation of YAP in the heart without other components of the Hippo pathway being involved; (2) in heart, YAP is sequestered in the cytoplasm by phosphorylation at Ser-127 so it can be immediately dephosphorylated and translocated to the nucleus to initiate cytoprotective gene response when oxidative stress is encountered; (3) in liver, YAP is phosphorylated at S-381 to be tagged for immediate degradation, thereby reducing YAP/pYAP levels; (4) posttranslational modifications of

YAP such as GlcNAcylation and ubiquitination could also be responsible for the varied expression of YAP. However, the specific regulation pattern remains elusive and therefore, further research in this context is required.

The DNA-binding levels of TEAD to the promoter regions of gene sequences of its downstream targets during anoxia decreased significantly during 24 h anoxia for both tissues and remained unchanged in liver after aerobic recovery but increased to return the control levels in the heart after 4 h recovery (**Figure 5**). This observation is in accordance with the relative expression of proteins in nuclear fractions of the liver and heart for all the stresses, showing a similar trend (**Figure 3**). The transcript levels of *tead* showed a decreasing trend compared to controls in the anoxic liver that was further reduced during recovery (**Figure 6A**). Decreased transcript and total protein levels during recovery could be linked with reduced binding in the liver. The decreased levels of YAP and TAZ that act as a co-activators of TEAD (to enhance its binding to the promoter region of target genes), further justifies the decreased DNA binding [55,56]. Cells encountering anoxic conditions reduce their metabolic rate to decrease ATP consumption. They reprioritise the expenditure of available energy for cell survival pathways by regulating the expression of selected transcription factors that include OCT4 and SOX2 [16,17]. In previous study from our lab, similar changes in total protein levels and DNA-binding ability of OCT4 were observed under anoxia conditions in wood frog liver [20].

The binding of TEAD increased during recovery in heart for selective activation of genes (**Figure 5**). The increased binding levels coincide with increased total protein levels of TEAD during recovery from anoxia in wood frog heart (**Figure 3B**). Selective gene activation could be assumed since a different trend was observed in the total protein levels

of OCT4 and SOX2, which are amongst the important downstream targets of YAP/TAZ mediated TEAD activation. It was observed that in heart, total protein levels of OCT4 decreased significantly during anoxia and remained low during recovery whereas the levels of SOX2 did not change under any condition compared to control (**Figure 4**). The relative levels of OCT4 and SOX2 during anoxia and recovery were studied in liver previously in our lab [20]. The study showed no significant change in the levels of OCT4 during anoxia as well as recovery but levels of SOX2 increased significantly during anoxia and further during recovery as compared to controls [20]. SOX2 is responsible for the regulation of cell survival pathways in response to low oxygen levels [57,58]. In addition, SOX2 is also involved in tissue repair and maintaining self-renewal capacity [59,60]. Consistent or increased expression levels of SOX2 (in a tissue-specific manner) represent the possibility that it plays an essential role in tissue regeneration and repair in response to increased ROS during recovery from anoxia (or other stresses that restrict oxygen availability such as freezing).

Surprisingly, a significant increase was observed in the protein levels of TAZ in the anoxic heart, but levels returned to control values during aerobic recovery. By contrast, TAZ levels decreased significantly in anoxic liver (**Figure 3**). The transcript levels of *taz* showed a similar pattern for both tissues (**Figure 6**). Reduced levels of TAZ in the nucleus in response to anoxia in the liver is consistent with activation of the Hippo signaling pathway since YAP/TAZ is sequestered via phosphorylation. TAZ has been characterized as a transcriptional coactivator for Runx2, PPARγ, TEAD, T-Box transcription factors, and SMAD complexes [61,62,63,64]. It is suggested to function as a transcriptional modulator and regulator of cellular functions. TAZ is also known to act as

an enhancer to MyoD in response to injuries of adult muscle (skeletal, smooth, and cardiac) [65] by directly interacting with MyoD in the nucleus to accelerate its DNA-binding activity. MyoD is required for the repair and regeneration of muscle fibers [66,67]. Prolonged oxygen deficiency or anoxic conditions could lead to detrimental effects where heart muscle could tend to lose contractility [68,69]. Prolonged exposure to such conditions might cause atrophy [70,71,72]. Therefore, increased TAZ in the heart could potentially activate/enhance the function of MyoD to initiate repair mechanisms during/after anoxia stress.

Hence, it can be deduced that, under anoxic conditions, the small yet significantly increased levels of major cytoplasmic components and decreased levels of nuclear components represent the possibility of activation of the Hippo pathway. Activation of the pathway phosphorylates and sequesters YAP in the cytoplasm. Phosphorylated YAP restrains the translocation of YAP/TAZ in the nucleus, preventing the formation of the YAP-TAZ-TEAD complex that could have bound to the promoter region of selective genes and activated the gene expression. Increased transcript and protein levels of TAZ are essential to protect cardiac muscle during anoxia. The unchanged/increased total protein levels of SOX2 in heart and liver during anoxia and recovery could activate tissue repair under increased oxidative stress. In total, it is proposed that the Hippo pathway is activated to suppress gene expression under anoxic conditions, allowing for energy conservation and increasing the chances of survival under oxygen-restricted conditions but further research in this aspect is warranted.

4.6 References

1. Storey, K. B., and Storey, J. M. (2017) Molecular physiology of freeze tolerance in vertebrates. Physiol. Rev. 97, 623–665
2. Storey, K. B., and Storey, J. M. (2013) Molecular biology of freezing tolerance. Compr. Physiol. 3, 1283–1308
3. Storey, K. B. (1987) Organ-specific metabolism during freezing and thawing in a freeze-tolerant frog. Am. J. Physiol. 253, 292–297
4. Storey, K. B., and Storey, J. M. (1986) Freeze tolerant frogs: cryoprotectants and tissue metabolism during freeze–thaw cycles. Can. J. Zool. 64, 49–56
5. Storey, K. B. (1998) Survival under stress: molecular mechanisms of metabolic rate depression in animals. South African J. Zool. 33, 55–64
6. Storey, K. B. (2004) Molecular mechanisms of anoxia tolerance. Int. Congr. Ser. 1275, 47–54
7. Storey, J. M., Wu, S., and Storey, K. B. (2021) Mitochondria and the Frozen Frog. Antioxidants. 10, 543
8. Hermes-Lima, M., Moreira, D. C., Rivera-Ingraham, G. A., Giraud-Billoud, M., Genaro-Mattos, T. C., and Campos, É. G. (2015) Preparation for oxidative stress under hypoxia and metabolic depression: Revisiting the proposal two decades later. Free Radic. Biol. Med. 89, 1122–1143
9. Shao, D., Zhai, P., Del Re, D. P., Sciarretta, S., Yabuta, N., Nojima, H., Lim, D.-S., Pan, D., and Sadoshima, J. (2014) A functional interaction between Hippo-YAP signalling and FoxO1 mediates the oxidative stress response. Nat. Commun. 5, 3315
10. Mao, B., Gao, Y., Bai, Y., and Yuan, Z. (2015) Hippo signaling in stress response and homeostasis maintenance. Acta Biochim. Biophys. Sin. (Shanghai). 47, 2–9
11. Meng, Z., Moroishi, T., and Guan, K.-L. (2016) Mechanisms of Hippo pathway regulation. Genes Dev. 30, 1–17
12. Piccolo, S., Dupont, S., and Cordenonsi, M. (2014) The biology of YAP/TAZ: Hippo signaling and beyond. Physiol. Rev. 10.1152/physrev.00005.2014
13. Cai, W. F., Wang, L., Liu, G. S., Zhu, P., Paul, C., and Wang, Y. (2016) Manipulating the hippo-yap signal cascade in stem cells for heart regeneration. Ann. Palliat. Med. 10.21037/apm.2016.03.03
14. Basta, J., and Rauchman, M. (2015) The nucleosome remodeling and deacetylase complex in development and disease. Transl. Res. 165, 36–47
15. Tantin, D. (2013) OCT transcription factors in development and stem cells: insights and mechanisms. Development. 140, 2857–2866
16. Gupta, A., and Storey, K. B. (2020) Regulation of antioxidant systems in response to anoxia and reoxygenation in *Rana sylvatica*. Comp. Biochem. Physiol. Part B Biochem. Mol. Biol. 243–244, 110436
17. Beyer, T. A., Weiss, A., Khomchuk, Y., Huang, K., Ogunjimi, A. A., Varelas, X., and Wrana, J. L. (2013) Switch Enhancers Interpret TGF-β and Hippo Signaling to Control Cell Fate in Human Embryonic Stem Cells. Cell Rep. 5, 1611–1624
18. Kim, W., Cho, Y. S., Wang, X., Park, O., Ma, X., Kim, H., Gan, W., Jho, E., Cha, B., Jeung, Y., Zhang, L., Gao, B., Wei, W., Jiang, J., Chung, K.-S., and Yang, Y. (2019) Hippo signaling is intrinsically regulated during cell cycle progression by APC/C Cdh1. Proc. Natl. Acad. Sci. 116, 9423–9432
19. Zhou, D., Conrad, C., Xia, F., Park, J.-S., Payer, B., Yin, Y., Lauwers, G. Y., Thasler, W., Lee, J. T., Avruch, J., and Bardeesy, N. (2009) Mst1 and Mst2 Maintain Hepatocyte Quiescence and Suppress Hepatocellular Carcinoma Development through Inactivation of the Yap1 Oncogene. Cancer Cell. 16, 425–438
20. Zhou, D., Zhang, Y., Wu, H., Barry, E., Yin, Y., Lawrence, E., Dawson, D., Willis, J. E., Markowitz, S. D., Camargo, F. D., and Avruch, J. (2011) Mst1 and Mst2 protein kinases restrain intestinal stem cell proliferation and colonic tumorigenesis by inhibition of Yes-associated protein (Yap) overabundance. Proc. Natl. Acad. Sci. 108, E1312–E1320

21. Xin, M., Kim, Y., Sutherland, L. B., Murakami, M., Qi, X., McAnally, J., Porrello, E. R., Mahmoud, A. I., Tan, W., Shelton, J. M., Richardson, J. A., Sadek, H. A., Bassel-Duby, R., and Olson, E. N. (2013) Hippo pathway effector Yap promotes cardiac regeneration. Proc. Natl. Acad. Sci. 110, 13839–13844
22. Fallahi, E., O'Driscoll, N. A., and Matallanas, D. (2016) The MST/Hippo pathway and cell death: A non-canonical affair. Genes (Basel). 10.3390/genes7060028
23. Gerber, V. E. M., Wijenayake, S., and Storey, K. B. (2016) Anti-apoptotic response during anoxia and recovery in a freeze-tolerant wood frog (*Rana sylvatica*). PeerJ. 4, e1834
24. Gupta, A., and Storey, K. B. (2021) Coordinated expression of Jumonji and AHCY under OCT transcription factor control to regulate gene methylation in wood frogs during anoxia. Gene. 788, 145671
25. Zhang, J., and Storey, K. B. (2013) Akt signaling and freezing survival in the wood frog, *Rana sylvatica*. Biochim. Biophys. Acta - Gen. Subj. 1830, 4828–4837
26. Pellissier, F., Glogowski, C. M., Heinemann, S. F., Ballivet, M., and Ossipow, V. (2006) Lab assembly of a low-cost, robust SYBR green buffer system for quantitative real-time polymerase chain reaction. Anal. Biochem. 350, 310–312
27. Bustin, S. A., Benes, V., Garson, J. A., Hellemans, J., Huggett, J., Kubista, M., Mueller, R., Nolan, T., Pfaffl, M. W., Shipley, G. L., Vandesompele, J., and Wittwer, C. T. (2009) The MIQE Guidelines: Minimum Information for Publication of Quantitative Real-Time PCR Experiments. Clin. Chem. 55, 611–622
28. Schmittgen, T. D., and Zakrajsek, B. A. (2000) Effect of experimental treatment on housekeeping gene expression: validation by real-time, quantitative RT-PCR. J. Biochem. Biophys. Methods. 46, 69–81
29. Eaton, S. L., Roche, S. L., Llavero Hurtado, M., Oldknow, K. J., Farquharson, C., Gillingwater, T. H., and Wishart, T. M. (2013) Total protein analysis as a reliable loading control for quantitative fluorescent western blotting. PLoS One. 8, e72457
30. Taylor, S. C., Nadeau, K., Abbasi, M., Lachance, C., Nguyen, M., and Fenrich, J. (2019) The Ultimate qPCR Experiment: Producing Publication Quality, Reproducible Data the First Time. Trends Biotechnol. 37, 761–774
31. Zhang, J., and Storey, K. B. (2016) RBioplot: an easy-to-use R pipeline for automated statistical analysis and data visualization in molecular biology and biochemistry. PeerJ. 4, e2436
32. Kenneth, N. S., and Rocha, S. (2008) Regulation of gene expression by hypoxia. Biochem. J. 414, 19–29
33. Lehtinen, M. K., Yuan, Z., Boag, P. R., Yang, Y., Villén, J., Becker, E. B. E., DiBacco, S., de la Iglesia, N., Gygi, S., Blackwell, T. K., and Bonni, A. (2006) A Conserved MST-FOXO Signaling Pathway Mediates Oxidative-Stress Responses and Extends Life Span. Cell. 125, 987–1001
34. Goldstein, D. S., and Kopin, I. J. (2007) Evolution of concepts of stress. Stress. 10, 109–120
35. Del Re, D. P., Yang, Y., Nakano, N., Cho, J., Zhai, P., Yamamoto, T., Zhang, N., Yabuta, N., Nojima, H., Pan, D., and Sadoshima, J. (2013) Yes-associated Protein Isoform 1 (Yap1) Promotes Cardiomyocyte Survival and Growth to Protect against Myocardial Ischemic Injury. J. Biol. Chem. 288, 3977–3988
36. Bae, S. J., and Luo, X. (2018) Activation mechanisms of the Hippo kinase signaling cascade. Biosci. Rep. 10.1042/BSR20171469
37. Zhao, B., Li, L., Tumaneng, K., Wang, C.-Y., and Guan, K.-L. (2010) A coordinated phosphorylation by Lats and CK1 regulates YAP stability through SCF -TRCP. Genes Dev. 24, 72–85
38. Zhao, B., Wei, X., Li, W., Udan, R. S., Yang, Q., Kim, J., Xie, J., Ikenoue, T., Yu, J., Li, L., Zheng, P., Ye, K., Chinnaiyan, A., Halder, G., Lai, Z.-C., and Guan, K.-L. (2007) Inactivation of YAP oncoprotein by the Hippo pathway is involved in cell contact inhibition and tissue growth control. Genes Dev. 21, 2747–2761
39. Song, H., Mak, K. K., Topol, L., Yun, K., Hu, J., Garrett, L., Chen, Y., Park, O., Chang, J., Simpson, R. M., Wang, C.-Y., Gao, B., Jiang, J., and Yang, Y. (2010) Mammalian Mst1 and Mst2 kinases play essential roles in organ size control and tumor suppression. Proc. Natl. Acad. Sci. 107, 1431–1436

40. Nakatani, K., Maehama, T., Nishio, M., Goto, H., Kato, W., Omori, H., Miyachi, Y., Togashi, H., Shimono, Y., and Suzuki, A. (2016) Targeting the Hippo signalling pathway for cancer treatment. J. Biochem. 10.1093/jb/mvw074
41. Wang, W., Xiao, Z.-D., Li, X., Aziz, K. E., Gan, B., Johnson, R. L., and Chen, J. (2015) AMPK modulates Hippo pathway activity to regulate energy homeostasis. Nat. Cell Biol. 17, 490–499
42. Rider, M. H., Hussain, N., Horman, S., Dilworth, S. M., and Storey, K. B. (2006) Stress-induced activation of the AMP-activated protein kinase in the freeze-tolerant frog *Rana sylvatica*. Cryobiology. 53, 297–309
43. Bartrons, M., Ortega, E., Obach, M., Calvo, M. N., Navarro-Sabaté, À., and Bartrons, R. (2004) Activation of AMP-dependent protein kinase by hypoxia and hypothermia in the liver of frog *Rana perezi*. Cryobiology. 49, 190–194
44. Carling, D. (2004) The AMP-activated protein kinase cascade – a unifying system for energy control. Trends Biochem. Sci. 29, 18–24
45. Horman, S., Hussain, N., Dilworth, S. M., Storey, K. B., and Rider, M. H. (2005) Evaluation of the role of AMP-activated protein kinase and its downstream targets in mammalian hibernation. Comp. Biochem. Physiol. Part B Biochem. Mol. Biol. 142, 374–382
46. Hong, M., Li, N., Li, J., Li, W., Liang, L., Li, Q., Wang, R., Shi, H., Storey, K. B., and Ding, L. (2019) Adenosine Monophosphate-Activated Protein Kinase Signaling Regulates Lipid Metabolism in Response to Salinity Stress in the Red-Eared Slider Turtle *Trachemys scripta elegans*. Front. Physiol. 10.3389/fphys.2019.00962
47. Malik, A. I., and Storey, K. B. (2009) Activation of extracellular signal-regulated kinases during dehydration in the African clawed frog, *Xenopus laevis*. J. Exp. Biol. 212, 2595–2603
48. Rider, M. H., Hussain, N., Dilworth, S. M., Storey, J. M., and Storey, K. B. (2011) AMP-activated protein kinase and metabolic regulation in cold-hardy insects. J. Insect Physiol. 57, 1453–1462
49. Rider, M. H. (2016) Role of AMP-activated protein kinase in metabolic depression in animals. J. Comp. Physiol. B. 186, 1–16
50. Vassilev, A. (2001) TEAD/TEF transcription factors utilize the activation domain of YAP65, a Src/Yes-associated protein localized in the cytoplasm. Genes Dev. 15, 1229–1241
51. Zheng, Y., and Pan, D. (2019) The Hippo Signaling Pathway in Development and Disease. Dev. Cell. 50, 264–282
52. Moris, D., Spartalis, M., Spartalis, E., Karachaliou, G.-S., Karaolanis, G. I., Tsourouflis, G., Tsilimigras, D. I., Tzatzaki, E., and Theocharis, S. (2017) The role of reactive oxygen species in the pathophysiology of cardiovascular diseases and the clinical significance of myocardial redox. Ann. Transl. Med. 5, 326–326
53. Ray, P. D., Huang, B.-W., and Tsuji, Y. (2012) Reactive oxygen species (ROS) homeostasis and redox regulation in cellular signaling. Cell. Signal. 24, 981–990
54. Korge, P., Ping, P., and Weiss, J. N. (2008) Reactive Oxygen Species Production in Energized Cardiac Mitochondria During Hypoxia/Reoxygenation. Circ. Res. 103, 873–880
55. Covello, K. L. (2006) HIF-2 regulates Oct-4: effects of hypoxia on stem cell function, embryonic development, and tumor growth. Genes Dev. 20, 557–570
56. Lee, J., Cho, Y. S., Jung, H., and Choi, I. (2018) Pharmacological regulation of oxidative stress in stem cells. Oxid. Med. Cell. Longev. 2018, 1–13
57. Chang, Y. K., Hwang, J. S., Chung, T.-Y., and Shin, Y. J. (2018) SOX2 Activation Using CRISPR/dCas9 Promotes Wound Healing in Corneal Endothelial Cells. Stem Cells. 36, 1851–1862
58. Bani-Yaghoub, M., Tremblay, R. G., Lei, J. X., Zhang, D., Zurakowski, B., Sandhu, J. K., Smith, B., Ribecco-Lutkiewicz, M., Kennedy, J., Walker, P. R., and Sikorska, M. (2006) Role of Sox2 in the development of the mouse neocortex. Dev. Biol. 295, 52–66
59. Cui, C. Bin, Cooper, L. F., Yang, X., Karsenty, G., and Aukhil, I. (2003) Transcriptional Coactivation of Bone-Specific Transcription Factor Cbfa1 by TAZ. Mol. Cell. Biol. 23, 1004–1013

60. Hong, J.-H. (2005) TAZ, a Transcriptional Modulator of Mesenchymal Stem Cell Differentiation. Science (80). 309, 1074–1078
61. Murakami, M., Nakagawa, M., Olson, E. N., and Nakagawa, O. (2005) A WW domain protein TAZ is a critical coactivator for TBX5, a transcription factor implicated in Holt-Oram syndrome. Proc. Natl. Acad. Sci. 102, 18034–18039
62. Varelas, X., Sakuma, R., Samavarchi-Tehrani, P., Peerani, R., Rao, B. M., Dembowy, J., Yaffe, M. B., Zandstra, P. W., and Wrana, J. L. (2008) TAZ controls Smad nucleocytoplasmic shuttling and regulates human embryonic stem-cell self-renewal. Nat. Cell Biol. 10, 837–848
63. Jeong, H., Bae, S., An, S. Y., Byun, M. R., Hwang, J., Yaffe, M. B., Hong, J., and Hwang, E. S. (2010) TAZ as a novel enhancer of MyoD-mediated myogenic differentiation. FASEB J. 24, 3310–3320
64. Le Grand, F., and Rudnicki, M. A. (2007) Skeletal muscle satellite cells and adult myogenesis. Curr. Opin. Cell Biol. 19, 628–633
65. Hernández-Hernández, J. M., García-González, E. G., Brun, C. E., and Rudnicki, M. A. (2017) The myogenic regulatory factors, determinants of muscle development, cell identity and regeneration. Semin. Cell Dev. Biol. 72, 10–18
66. Lemley, J. M., and Meneely, G. R. (1952) Effects of Anoxia on Metabolism of Myocardial Tissue. Am. J. Physiol. Content. 169, 66–73
67. Allen, D. G., and Orchard, C. H. (1987) Myocardial contractile function during ischemia and hypoxia. Circ. Res. 60, 153–168
68. Chaillou, T., Koulmann, N., Meunier, A., Chapot, R., Serrurier, B., Beaudry, M., and Bigard, X. (2014) Effect of hypoxia exposure on the recovery of skeletal muscle phenotype during regeneration. Mol. Cell. Biochem. 390, 31–40
69. Favier, F. B., Britto, F. A., Freyssenet, D. G., Bigard, X. A., and Benoit, H. (2015) HIF-1-driven skeletal muscle adaptations to chronic hypoxia: Molecular insights into muscle physiology. Cell. Mol. Life Sci. 10.1007/s00018-015-2025-9
70. Chaillou1, T., and Lanner, J. T. (2016) Regulation of myogenesis and skeletal muscle regeneration: effects of oxygen levels on satellite cell activity. FASEB J. 30, 3929–3941

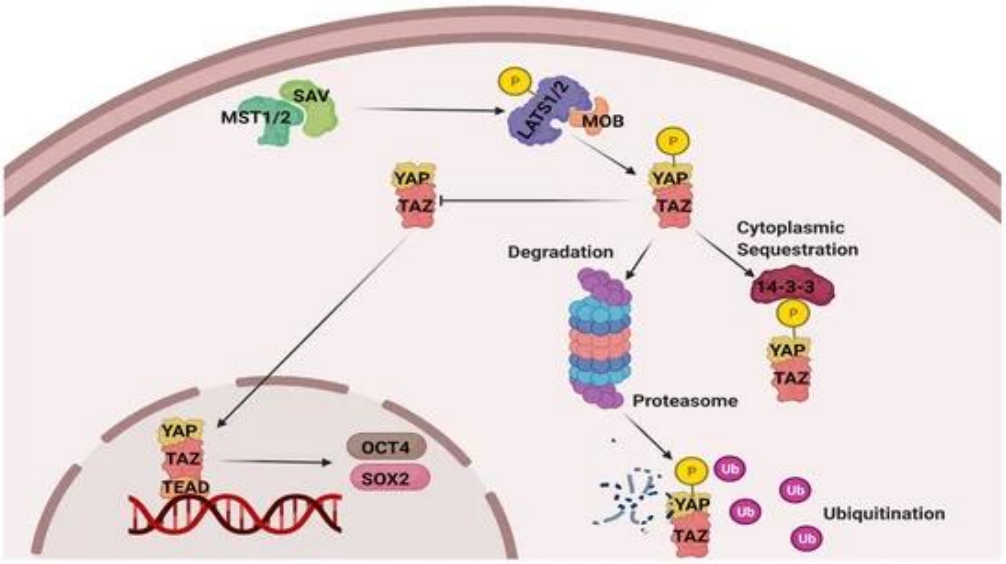

Figure 4.1. Schematic representation of the Hippo pathway. Upon encountering stress, the pathway gets activated and initiates a series of phosphorylation, where MST1/2 interacts with SAV to phosphorylate LATS1/2 that further phosphorylates YAP. Depending on the site of phosphorylation, either p-YAP interacts with 14-3-3 to sequester in cytoplasm or attach to proteosome to degrade via ubiquitination. Unphosphorylated YAP/TAZ translocates to the nucleus and forms complex with TEAD. The YAP/TAZ/TEAD complex binds to promoter region of DNA to initiate gene transcription and activation. MST: mammalian Ste20-like kinases ½, SAV: salvador 1, LATS1/2: large tumor suppressor 1 and 2 kinases, MOB: Mps one Binder, YAP: Yes-associated protein, TAZ: transcriptional coactivator with PDZ-binding motif, TEAD: TEA domain family member, OCT4: Octamer-binding transcription factor 4, and SOX2: SRY (sex determining region Y)-box 2. Credit "Created with BioRender.com" accessed on 14 October 2021.

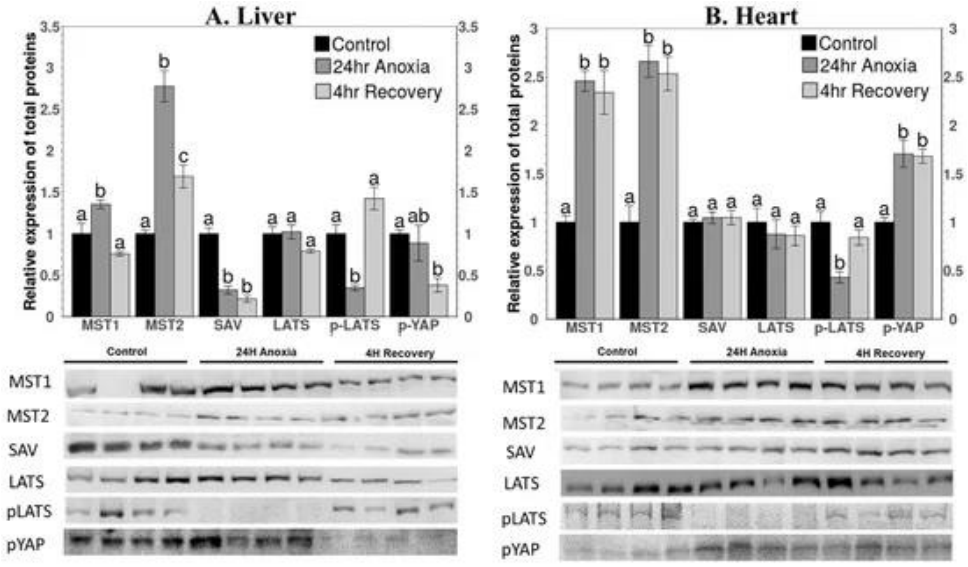

Figure 4.2. Relative expression levels of proteins involved in the Hippo pathway that are known to be cytoplasmic in (A) liver and (B) heart whole-tissue extracts of R. sylvatica under control, 24 h anoxia

exposure, or 4 h aerobic recovery from anoxia. Proteins were detected by Western immunoblotting and immunoblot bands are shown below histograms. Data are mean ± SEM, n = 3–4 independent trials on samples from different animals. Data were analyzed using analysis of variance with a post hoc Tukey test; different letters denote values that are significantly different from each other ($p < 0.05$). Other information as Figures S1–S9.

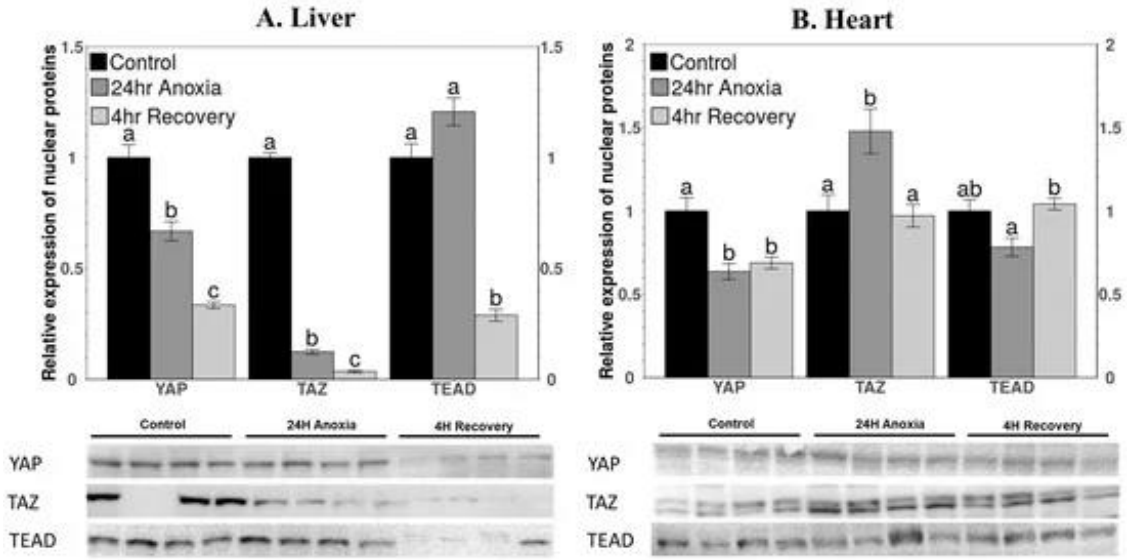

Figure 4.3. Relative expression levels of nuclear proteins (nuclear fraction) involved in the Hippo pathway in (A) liver and (B) heart of R. sylvatica under control, 24 h anoxia exposure, or 4 h aerobic recovery from anoxia conditions as determined by Western immunoblotting. Other information as in Figure 4.2.

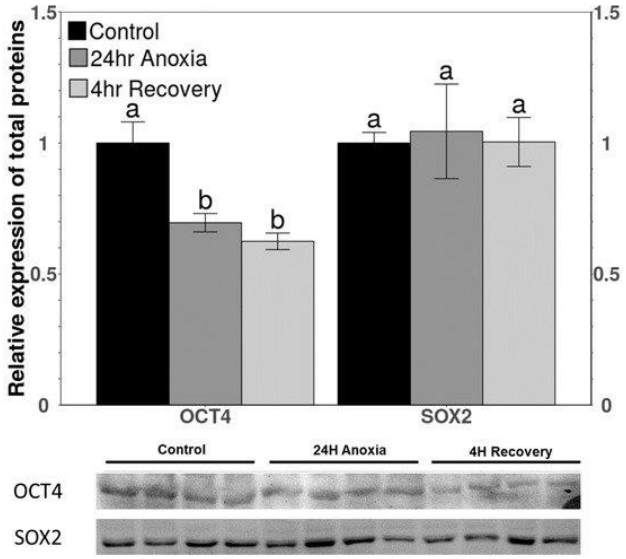

Figure 4.4. Relative expression levels of downstream targets of YAP/TEAD binding to promoter region in heart of R. sylvatica under control, 24 h anoxia exposure or 4 h aerobic recovery from anoxia conditions as determined by western immunoblotting. Other information similar to Figure 4.2.

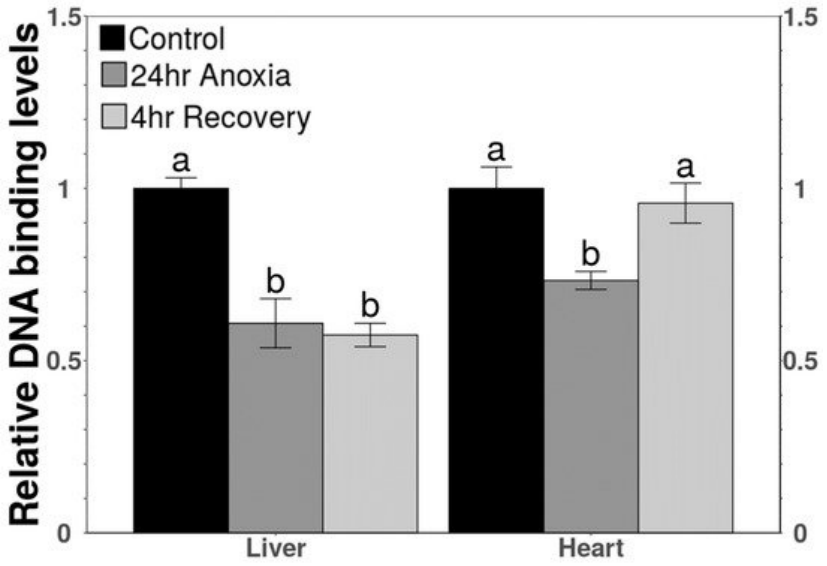

Figure 4.5. Relative DNA-binding levels of TEAD in total protein extracts in liver and heart of R. sylvatica under control, 24 h anoxia or 4 h recovery conditions as determined by TF-ELISA or DPI-ELISA. Other information similar to Figure 4.2.

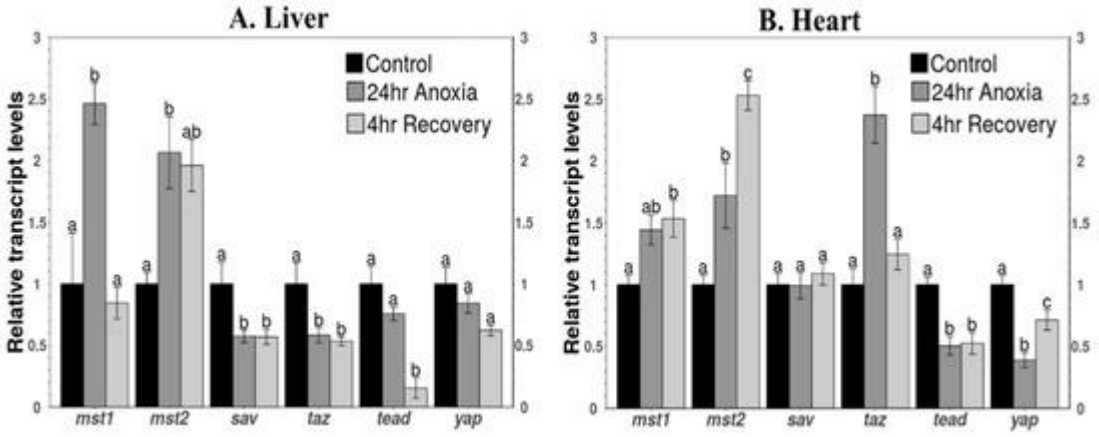

Figure 4.6. Relative expression of gene transcripts of the proteins involved in the Hippo pathway in (A) liver and (B) heart of R. sylvatica in control, 24 h anoxia, and 4 h recovery from anoxia as determined by qPCR. Other information similar to Figure 4.2.

5.Notch Signaling

A "Notch" in the cellular communication network in response to anoxia by wood frog (*Rana sylvatica*)

Aakriti Gupta and Kenneth B. Storey*

Department of Biology, Carleton University, Ottawa, Canada K1S 5B6

*Correspondence to:

Dr. Kenneth B. Storey

Department of Biology, Carleton University,

1125 Colonel by Drive, Ottawa, ON, K1S 5B6

Tel: (613) 520-2600, ext. 3678

E-mail: kenstorey@cunet.carleton.ca

5.1 Abstract

Wood frogs (*Rana sylvatica*) experience months of whole-body freezing during winter. Anoxia is one of the side stresses along with cell dehydration and hyperglycemia. Among multicellular organisms, communication and coordination is essential between neighbouring cells, particularly under stress conditions. Notch signaling is an effective communication channel between cells and regulates multiple pro-survival pathways. Signaling initiates when membrane-bound ligands Delta-like (DLL) or Jagged (JAG) interact with notch receptors. Activated receptor undergoes cleavage to release intracellular domain (NICD) in the cytoplasm. NICD translocates to the nucleus and forms a transcriptional complex with MAML and RBPJ that interacts with promoter regions and activates stress-specific genes. The role of notch signaling in enduring anoxia was assessed by studying the pathway components using immunoblots, TF-ELISA, and qPCR on treated samples of liver and heart. Bioinformatics tool Pymol was used to prepare structures based on available protein sequences for ligands, NOTCH receptor and the transcriptional complex. The results showed an increase in the levels of both ligands and receptors but decreased levels of RBPJ, suggesting an effective transmission of stress signal but suppressed gene transcription that goes in accordance with lowering energy expense required in energy crisis during anoxia. The study suggests Notch-independent activation of HES1 and HES5. Tissue-specific response of HES1, HES5, and MAML implies energy conservation and myocardial protection. The current study is the first analysis of the regulation of notch signaling in amphibians on encountering anoxic conditions that present multiple future directions.

Highlights

- Notch1 and Notch2 represent stress specific role in anoxia/recovery.
- DLL4-NOTCH1 signaling provides immune response in liver via macrophage activation.
- Decreased levels of RBPJ suggest suppressed gene transcription to lower energy expense.
- MAML and HES5 shows "functional switching" to activate MyoD for myocardial protection.
- HES1 controls glucocorticoid regulated carbohydrate metabolism to conserve energy.

Abbreviations

ROS: Reactive Oxygen Species, DLL: Delta-like, JAG: Jagged, NECD: Notch extracellular domain, ADAM: Disintegrin and Metalloproteinase domain-containing protein 10, TACE: Tumor Necrosis factor-alpha Converting Enzyme, NICD: Notch intracellular domain, MAML: Mastermind-like protein, RBPJ: Recombination Signal Binding Protein for Immunoglobulin Kappa J Region, HEY: Hairy/enhancer-of-split related with YRPW motif protein, HES: Hairy and enhancer of split-1

Keywords

Notch Signaling, metabolic rate depression, Recombination Signal Binding Protein For Immunoglobulin Kappa J Region (RBPJ), Hairy/enhancer-of-split related with YRPW motif protein (HEY) and hairy and enhancer of split-1 (HES), myocardial protection

5.2 Introduction

The wood frog (*Rana sylvatica)* has a remarkable ability to tolerate whole body freezing during the winter with 65–70% of total body water accumulating as ice in extracellular spaces. All vital functions including heartbeat, breathing, blood flow, and muscle movement are halted and this leads to anoxia and ischemia in all tissues [1], [2]. Conversion of water into extracellular ice is detected on the skin and signals are rapidly sent to the liver to trigger rapid glycogenolysis that produces high levels of glucose that are exported to all tissues to provide both cryoprotection against intracellular ice formation and elevate intracellular osmolality to limit cell volume reduction when water exits into extracellular ice masses. Tissue and plasma concentrations of glucose can rise from 5 mM (under normal conditions) to as high as 300 mM (during freezing) [3]. Hence, wood frogs must successfully endure anoxia, dehydration, and hyperglycemia as stresses during freezing [3]. The wood frog relies on anaerobic glycolysis for ATP production which limits the availability of ATP in the body since it is just a fraction of that produced from aerobic respiration [4]. In addition, during melting, the rapid reoxygenation of tissues can trigger a surge of reactive oxygen species (ROS) production [5], [6] and potentially surpass the antioxidant capacity of cells [7]. Enhanced ROS production is associated with multiple types of cellular damage that include oxidative damage to macromolecules (e.g. lipid peroxidation, protein oxidation, DNA damage) and activation of pathways such as apoptosis [8]. Therefore, to endure anoxia and make a smooth transition recovery back to aerobic metabolism, selected cellular mechanisms need to be regulated/activated to promote repair by actively initiating communication between cells.

Notch signaling is an effective communication channel between cells and regulates activities including cell differentiation, development, adhesion, proliferation, and apoptosis [9]. Notch signaling is initiated when membrane bound ligands including Delta-like (DLL) and Jagged (JAG) proteins interact with Notch receptors. The signal is transmitted by the cells expressing the ligand and is received by cells expressing the receptors [10], [11], [12], [13]. Under oxidative stress, the Notch extracellular domain (NECD) undergoes O-linked glycosylation that leads to a configuration change in the Notch receptor and facilitate binding with DLL or JAG to activate the Notch receptor (Fig. 1). By the formation of a receptor-ligand complex, activated Notch triggers a cleavage on the NECD by Disintegrin and Metalloproteinase domain-containing protein 10 (ADAM 10) or the Tumor Necrosis factor-alpha Converting Enzyme (TACE) that further facilitates S3 cleavage by γ-secretase to release the Notch intracellular domain (NICD) from the membrane. Notch signaling is a streamlined pathway where DLL and JAG are membrane bound ligands that bind to Notch, a membrane bound receptor, resulting in the cleavage of NICD that then translocates to the nucleus and induces various transcriptional targets [10], [11], [12], [13] (Fig. 1). NICD forms a DNA binding complex with Mastermind-like protein 1 (MAML) and Recombination Signal Binding Protein For Immunoglobulin Kappa J Region (RBP-Jk) [14] (**Fig. 5.1**). In the nucleus, the DNA binding complex interacts with the promoter regions of the *hes* and *hey* genes that prevent differentiation of cells [15]. Hairy/enhancer-of-split related with YRPW motif protein (HEY) and hairy and enhancer of split-1 (HES) proteins form an autoregulatory loop of negative feedback cross-repressive interactions [10]. Under hypoxia, the alpha subunit of the hypoxia-inducible factor, HIF1α, activates the Notch pathway to increase

expression of its downstream genes. This shows Notch crosstalk with HIF1α to promote the transcription of stress specific signaling mechanisms to control different aspects of response to hypoxia [11], [15].

Notch signaling is a crucial pathway in cardiogenesis. Not only does it induce angiogenesis to protect the ischemic myocardium but also initiates repair mechanisms by promoting myocardial regeneration [16]. In the liver, the pathway is known to initiate JAK/STAT3 signaling to activate the expression of manganese superoxide dismutase and protect hepatocytes from injury caused due to excessive ROS generation during ischemia and reperfusion [17]. Notch is one of the most versatile and evolutionary conserved signaling pathways that regulate cellular proliferation, differentiation, and apoptosis. In adults, it plays an important role in tissue regeneration after injuries and damage caused due to stress. The regenerative response of Notch after an injury has been extensively studied in mammalian systems [12], [18], [19], [20], [21] and this justifies the rationale behind studying this pathway in the liver and heart of wood frogs exposed to stresses that include anoxia and reoxygenation conditions associated with freeze tolerance.

5.3 Methods

5.3.1. Animal treatment

Wood frogs of approximately 5-7 g were collected from breeding ponds in the Ottawa area (Ontario, Canada) in early spring, a time when frogs are still freeze tolerant. Frogs were washed briefly in a tetracycline bath and then transferred to plastic containers containing damp sphagnum moss and acclimated for 2 weeks at 5 °C. Control frogs were sampled from this condition. The treatment described by Gerber et al., 2016 [22] was followed to expose the remaining frogs to anoxia. Briefly, animals were placed in plastic

jars (4–5 animals/jar) pre-flushed with nitrogen gas for 20 min and lined with a paper towel pre-wetted with water that had been previously bubbled with 100% nitrogen gas. The jars containing animals were again flushed with nitrogen gas through a port in the lid for 20 min before the input and output vents were sealed. The jars were returned to 5 °C for 24 h and then frogs in half of the jars were sampled as the anoxic condition whereas the remaining anoxic frogs were transferred to jars with normal air, held at 5 °C for 4 h and then sampled as the aerobic recovery condition. All animals were euthanized by pithing and tissues were dissected rapidly and immediately frozen in liquid nitrogen, followed by transfer to −80 °C for long term storage. Animal experiments followed the guidelines of the Canada Council on Animal Care and were approved by the Carleton University Animal Care committee (protocol no. 106935).

5.3.2. Total protein extractions for immunoblots

Total protein was extracted from frozen liver and heart samples as described by Gerber et al., 2016 [22]. Briefly, frozen samples were quickly weighed and mixed 1:2 w:v with homogenization buffer containing 20 mM Hepes, pH 7.4, 100 mM NaCl, 0.1 mM EDTA, 10 mM NaF, 1 mM Na_3VO_4, and 10 mM β-glycerophosphate with 1 mM phenylmethylsulfonyl fluoride and 1 µl/ml protease inhibitor cocktail (Bioshop, Burlington, ON, Canada, catalog no. PIC001.1) added immediately before homogenization using a Polytron PT10 homogenizer. Samples were stored on ice for ~15 min and then centrifuged at 12,000*g* for 15 min at 4 °C. The supernatant was transferred to a fresh tube and the pellet was discarded. Protein concentrations were determined by the Coomassie blue dye-binding method using the Bio-Rad prepared reagent (BioRad Laboratories, Hercules, CA; Cat # 500–0006). Sample concentrations were them standardized to 10 µg/µl

using small aliquots of homogenization buffer and were then mixed 1:1 v:v with 2× SDS buffer (100 mM Tris-HCl, 20% *v*/v glycerol, 4% *w*/*v* SDS, 0.2% w/v bromophenol blue, and 10% v/v 2-mercaptoethanol). The samples were then boiled for 5 min in a water bath, snap chilled on ice for 10 min, and then stored at −80 °C until use.

5.3.3. SDS PAGE and western blotting

SDS Polyacrylamide gel electrophoresis was conducted as described previously [22]. Briefly, depending on the molecular weight of the protein of interest, 10–15% resolving gels were prepared with 5% stacking gels. Aliquots of 5 µg PiNK Plus Prestained Protein Ladder (Froggabio: PM005–0500) were loaded into the first lane of each gel as a MW marker. Other lanes were loaded with 20 µg of control, 24 h anoxia or 4 h recovery samples, all $n = 4$). The gels were run at a constant volt of 180 V until the band corresponding to the closest MW of the protein of interest in the ladder lane was well resolved. The protein in the gel was transferred to the PVDF membrane (Millipore, Etobicoke, ON, catalog no. IPVH07850, 45 µm pore) using an electroblotting technique in 1× transfer buffer (25 mM Tris pH 8.5, 192 mM glycine, 20% methanol) at a constant current of 160 mA at 4 °C for 90 min (or more depending on the molecular weight of the protein). The blots were washed in TBST (20 mM Tris base, pH 7.6, 140 mM NaCl, 0.05% v:v Tween-20) and blocked using 3% milk in TBST for 30 min. The membranes were again washed three times in TBST for 5 min each wash followed by overnight incubation with primary antibody (diluted 1:1000 in TBST). The membranes were washed three times in TBST for 5 min each wash and subsequently incubated with horseradish peroxide linked secondary antibody specific for the primary antibody for 30 min. The membranes were washed again in TBST, three times for 5 min each wash. The bands were visualised using

hydrogen peroxide and luminol and quantified using a Chemi-Genius Bioimager (Syngene, Frederick, MD).

The antibodies for DLL1 (Catalog no. A14277), DLL4 (Catalog no. A12943), JAG1 (Catalog no. A12733), JAG2 (Catalog no. A14247), NOTCH1 (Catalog no. A16673), NOTCH2 (Catalog no. A0560), ADAM9 (Catalog no. A5388), RBPJ (Catalog no. A5675), MAML1 (Catalog no. A17060), HES1 (Catalog no. A11718), HES5 (Catalog no. A16237), and HEY1 (Catalog no. A16110) were purchased from Abclonal (Woburn, MA, USA). An anti-rabbit IgG conjugated with horseradish peroxidase (catalog no. APA007P.2, Bioshop, Burlington, ON, Canada) was used as a secondary antibody.

5.3.4. Total protein extractions for TF ELISA

Total protein was extracted from liver and heart frozen samples using the method described by Gupta and Storey, 2020 [23]. Briefly, the samples were homogenised in prechilled lysis buffer cocktail (Etobicoke, ON; cat. No. 43–040), with 1 mM Na3VO4, 10 mM NaF, 10 mM β-glycerophosphate and 1% protease inhibitor (Bioshop, Burlington, ON, Canada, Catalog No. PIC001) in the ratio 1:5 *w*/*v* using a dounce homogenizer. The samples were incubated on ice for 30 min and then centrifuged at 4 °C for 20 min at 14,000*g*. Supernatants were collected and protein concentrations were determined by the Coomassie blue dye-binding method, as above.

5.3.5. DNA binding activity using TF ELISA

The biotin-labeled DNA oligonucleotide sequence corresponding with the binding site of RBPJ was used to assess the binding capacity of the transcription factor under anoxia

and recovery as compared with the control conditions. The following consensus sequences were used:

RBPJ (5'Biotin- GCCCAAGCTGGGAATTGTAGTT 3′)

RBPJ complementary (5' AACTACAATTCCCAGCTTGGGC 3′)

The standard protocol was as described by Gupta and Storey [23]. The primary antibody for RBPJ (described above) was used at 1:1000 v:v dilution in phosphate buffered saline (PBST) containing 137 mM NaCl, 2.7 mM KCl, 10 mM Na_2HPO_4, 2 mM KH_2PO_4, pH 7.4) and 0.1% Tween-20.

5.3.6. RNA isolation and cDNA synthesis

RNA was isolated from frozen tissue samples of heart and liver following the method described by Gupta and Storey [24]. Briefly, samples were homogenised using a Polytron PT10 homogenizer in Trizol (BioShop, TRI118.100) at 1:20 w:v and incubated for 5 min at room temperature. Chloroform was then added at 1:4 w:v and vortexed well. Samples were again incubated for 5 min at room temperature and then centrifuged at 4 °C for 15 min at 10,000*g*. The aqueous layer was collected in a separate tube and 500 µl of isopropanol was added followed by incubation at room temperature for 15 min to precipitate RNA. Samples were then centrifuged at 4 °C for 15 min at 12,000*g*. Supernatant was discarded and the pellet was washed twice with 70% ethanol and dissolved in autoclaved distilled water. The purity of RNA was confirmed by determining the OD 260/280 ratio and integrity was checked using agarose gel electrophoresis. Synthesis of cDNA followed the protocol of Gupta and Storey [24] and cDNA was then stored at −20 °C until use.

5.3.7. Primer design and qPCR

Forward and reverse primers for *notch1, notch2* and *rbpj* were designed. Since the wood frog genome is not sequenced, a consensus sequence was identified using a sequence alignment tool and sequences from several vertebrates. Conserved regions were identified and the Primer Blast tool available on NCBI was used to design primers from selected conserved regions.

The sequences of the primers used were as follows:

notch1	Forward 5' ACGGCATCGCTACCTTCACA 3'
	Reverse 5' CTGTCCGTACACTGACCCCC 3′
notch2	Forward 5' ACGTGCATTTGTGAGCCTGG 3'
	Reverse 5' GACAAGGTCAACACAGCGGC 3′
rbpj	Forward 5' AGAAAGGGGCGATCAGACTGT 3'
	Reverse 5' CCACCCACTGCCCATGAGAT 3′
β-actin	Forward 5′ AGAAGTCGTGCCAGGCATCA-3′
	Reverse 5′ AGGAGGAAGCTATCCGTGTT-3

The qPCR reaction was performed as described in Gupta and Storey [24] using a CFX-96 Real-Time PCR detection system (Bio-Rad, Hercules, CA, USA). The PCR reaction cycles used were as follows:

notch1: 95 °C for 3 min and then 40 cycles of (95 °C 10 s, 59.5 °C 20 s and 72 °C 20 s).

notch2 and *rbpj:* 95 °C for 3 min and then 40 cycles of (95 °C 10 s, 55.8 °C 20 s and 72 °C 20 s).

β-actin: 95 °C for 3 min and then 40 cycles of (95 °C 20 s, 53.8 °C 30 s and 72 °C 20 s).

PCR reactions were followed by melt curve analysis to ensure that a single product was amplified and a final hold was applied at 4 °C. A two-fold serial dilution curve test was performed following MIQE guidelines [25] to test primers and ensure non-amplification of primer dimers. Beta-actin was used as a reference gene for standardization as its expression did not change across the experimental conditions for either of the two tissues under consideration [26].

5.3.8. Statistical analysis

Immunoblots were imaged using a Chemi-Genius Bioimager and the associated Gene Tools software was used to quantify band intensities. After imaging, blots were Coomassie stained and reimaged. The summed intensity of a group of bands well separated from the band of interest was used to account for any minor differences that occurred during sample loading [27]. The qPCR results were analysed using the ΔΔCt method [26]. For data presentation and statistical testing, the control values were set to 1 and fold changes for experimental conditions (24 h anoxia and 4 h recovery) were calculated relative to the control values. One-way ANOVA followed by a Tukey post hoc test ($n = 4$) was used to analyse the standardized values. The program RBioplot [28] was used for testing of results with $p < 0.05$ accepted as a significant difference between groups and Sigmaplot was used for graphing.

5.3.9. Bioinformatic analysis

Protein Sequences for the following components of the signaling pathway were obtained from the NCBI for the European common frog, *Rana temporaria* (a close relative of the wood frog, *R. sylvatica*). Accession numbers were as follows: DLL1 (**XP_040206986.1**), DLL4 (**XP_040189645.1**), JAG1 (**XP_040207235.1**), JAG2

(**XP_040188234.1**), receptor NOTCH1 (**XP_040180043.1**) and components of the transcriptional complex RBPJ (**XP_040191093.1**) and MAML (**XP_040200915.1**). Frog protein sequences were aligned with the corresponding human sequences using the Clustal Omega multiple sequence alignment tool [29]. Accession numbers for the human sequences used were: DLL1 (**AAQ89251.1**), DLL4 (**AAQ89253.1**), JAG1 (**AAC51731.1**), JAG2 (**AAB84215.1**), receptor NOTCH1 (**AAG33848.1**), RBPJ (**Q06330**) and MAML (**Q92585**).

The .pdb format files for the protein sequences for *R. temporaria* were obtained from SWISS-MODEL protein structure modelling tool and the sequences with a match of about 90% or above file was downloaded and used to prepare figures using PyMOL (Schrodinger; https://pymol.org/2/). The figure for transcriptional complex was based on the "structure of human Notch1 transcription complex including CSL, RAM, ANK, and MAML-1 on HES-1 promoter DNA sequence" (PDB ID: 3V79).

5.4. Results

5.4.1. Bioinformatic analysis

The Notch pathway is known to be a highly conserved pathway in animals and, indeed, the current results show a high percentage of sequence conservation in alignments between frog (*R. temporaria* being the closest genetic match to *R. sylvatica*) and human protein sequences. The protein sequence alignment analyses of the Notch pathway components (ligands, receptors, transcriptional complexes) showed about 90% conservation comparing human and frog sequences. The structural models for the NOTCH receptor, ligands, and the Notch transcription complex were generated using PyMol software based on the protein sequences obtained for *R. temporaria* from NCBI. The two major domains of the Notch

receptor, the extracellular region (NECD) and intracellular region (NICD), are illustrated in **Fig. 5.2** in blue and grey colours respectively. The structure of the Notch receptor also shows the ADAM binding site (red) (**Fig. 5.2**), where ADAM binds, and the receptor undergoes the second cleavage. The extracellular domain of the NOTCH receptor (blue) interacts with the ligands to transmit the signal. **Fig. 5.3** represents the binding of ligands (DLL and JAG) to the receptor. **Fig. 5.3A** shows the binding of DLL1 (aqua) and DLL4 (red) to NICD and **Fig. 5.3B** illustrates the binding of JAG ligands that are JAG1 (green) and JAG2 (pink). The binding of all four ligands to the receptor is represented in **Fig. 5.3c**. Previous studies have suggested that NICD (grey) on entering the nucleus binds to RBPJ (cyan) to induce a conformational change in RBPJ to facilitate the formation of the ternary structure. Following the formation of the NICD-RBPJ complex, MAML (salmon) binds to the complex [30]. The structure (**Fig. 5.4**) reveals the cooperative binding of MAML to the complexation of NICD and RBPJ. Altogether the Notch transcriptional complex is formed that binds to the promoter region of DNA to activate gene expression (**Fig. 5.4**).

5.4.2. Protein levels of ligands in Notch signaling

The relative levels of ligands associated with Notch signaling in total protein extracts of liver and heart tissue of wood frogs were assessed using SDS-PAGE and immunoblotting. No significant change in DLL1 levels occurred between aerobic control, 24 h anoxia exposure or 4 h aerobic recovery conditions in liver (**Fig. 5.5A**). Similarly, there was no significant change in DLL1 levels between control and anoxic conditions in the heart (**Fig. 5.5B**). However, in heart, DLL1 levels after 4 h aerobic recovery (0.79 ± 0.096 compared with controls) were significantly lower than those under

anoxia (1.30 ± 0.09 fold over control). A strong significant increase was observed in DLL4 levels after 24 h anoxia exposure in liver, an increase of 1.73 ± 0.09 fold, and levels remained unchanged after 4 h recovery (1.74 ± 0.08 fold compared to control) (**Fig. 5.5A**). However, in heart, an increasing trend was seen over anoxia/recovery but there was no significant change between the three conditions (**Fig. 5.5B**).

JAG1 protein levels showed no significant change in liver under either anoxia or aerobic recovery. However, in heart, a strong significant decrease in JAG1 was recorded with levels falling to 61.5 ± 8.2% of controls after after 24 h anoxia and decreasing further to just 21.5 ± 2.6% of controls after 4 h aerobic recovery (**Fig. 5.5B**). Levels of JAG2 did not change significantly during 24H anoxia in liver but increased significantly by 2.23 ± 0.08 fold over controls after 4 h aerobic recovery (**Fig. 5.5A**). A decreasing trend for JAG2 was observed during anoxia and recovery in brain but no significant difference was found (**Fig. 5.5B**).

5.4.3. Protein levels of other components of Notch signaling

The total protein levels of NOTCH1 in liver showed a very strong significant increase of 9.92 ± 1.45 fold during 24 h anoxia exposure. Levels decreased during 4 h aerobic recovery but were still significantly elevated (6.86 ± 0.12 fold) over controls (**Fig. 5.6A**). A similar trend was observed in heart with a significant increase of 2.37 ± 0.03 fold over control values after 24 h anoxia and a strong decrease to just 42.3 ± 7.8% of control levels during recovery (**Fig. 5.6A**). No significant change in the levels of NOTCH2 was observed during 24 h anoxia in either liver and heart but during aerobic recovery significant increases of 1.81 ± 0.07 fold and 2.06 ± 0.12 fold over controls were seen in liver and heart, respectively (**Fig. 5.6**).

A significant increase in the protein levels of ADAM in liver was observed during 24 h anoxia with a fold change of 1.41 ± 0.12 compared to control values and levels further increased to 1.82 ± 0.07 fold over controls during recovery (**Fig. 5.6a**). The total protein levels of ADAM increased significantly to 1.77 ± 0.09 fold over control in anoxic heart but the levels returned to the normal upon recovery (**Fig. 5.6b**). The levels of RBPJ in liver decreased significantly to 63.6 ± 5% of control levels after 24 h anoxia exposure but rose to 75 ± 3% of control upon recovery (**Fig. 5.6a**) whereas in heart no significant change was observed in RBPJ levels under anoxia but levels decreased to 57 ± 2% of controls during recovery (**Fig. 5.6b**). No significant change was observed in the protein levels of MAML under any condition in liver but the MAML showed a very strong increase of 5.77 ± 0.28 fold upon recovery from anoxia in heart (**Fig. 5.6**).

5.4.4. Protein levels of downstream of notch transcriptional complex

Protein levels of HES1 showed a significant increase after 24 h anoxia in liver, levels rising by 1.55 ± 0.07 fold compared to controls and remaining high (1.51 ± 0.1 fold over controls) during recovery (**Fig. 5.7a**). A similar response was observed in heart with HES1 levels of 4.78 ± 0.09 fold and 4.83 ± 0.06 fold higher than controls after 24 h anoxia and 4 h recovery, respectively (**Fig. 5.7b**). The levels of HES5 showed a significant decrease in anoxic liver with values reduced to 49.4 ± 9% of controls and a slight rise (but not significant) to 62.2 ± 6% of control values after 4 h recovery from anoxia (**Fig. 5.7a**). In heart a strong significant increase in HES5 protein of 4.39 ± 0.18 fold occurred under anoxia but levels decreased during recovery to 1.6 ± 0.11 fold over control values (**Fig. 5.7b**). Hey 1 did not show a significant change under any condition in liver but levels decreased significantly upon recovery in heart to 75.5 ± 6% of the control values (**Fig. 5.7**).

5.4.5. DNA binding activity of RBPJ

The binding activity of RBPJ to its consensus DNA sequence was examined using a transcription factor ELISA. A significant decrease was observed in DNA binding levels by RBPJ under anoxic conditions in both liver and heart. Binding capacity was reduced to 69.7 ± 5% in anoxic liver and to 73.7 ± 4% in anoxic heart, as compared with controls. Binding capacity remained unchanged after 4 h aerobic recovery in liver but rose again to control levels during aerobic recovery in heart (**Fig. 5.8**).

5.4.6. Transcript levels of *notch* receptors and *rbpj*

The effects of anoxia and recovery on transcript levels of *notch1* and *notch2* receptors were assessed in liver and heart (**Fig. 5.9**). Levels of *notch1* transcripts showed no significant change over anoxia and recovery in liver but transcript levels increased significantly in heart after 24 h anoxia by 2.62 ± 0.12 fold above control levels and remained high after 4 h aerobic recovery. Transcript levels of *notch2* were unchanged in both tissues during anoxia but levels increased significantly during aerobic recovery in liver (by 3.1 ± 0.9 fold). However, *notch2* transcripts in heart did not change during anoxia or recovery (**Fig. 5.9b**). Transcript levels of *rbpj* in liver decreased significantly after 24 h anoxia exposure to just 28.7 ± 5% of control values but increased again to 62.3 ± 13% of controls after aerobic recovery (**Fig. 5.9a**). No significant changes in *rbpj* transcripts occurred in heart over anoxia/recovery (**Fig. 5.9b**).

5.5. Discussion

Cellular responses to stress can range from initiation/activation of pro-survival pathways to the elimination of damaged cells by cell death pathways depending on the nature and duration of the stress. Protective responses can include antioxidant defences

against oxidative injury and shock responses to deal with unfolded proteins or enhance chaperone protein actions [31]. On the other hand, if destructive activities are not resolved, cells might activate death signals that could include apoptosis, autophagy, necrosis, etc. [32], [33]. Thus, the adaptive capacity of cells determines cellular fate. An important aspect of cell survival is the ability to communicate and transfer stress-dependent messages to other neighbouring cells. Depending on the signal received, cells can escalate protective or destructive responses to decide the fate of stressed cells. DLL1 and DLL4, when attached to Notch receptors, deliver different signals for communications that decode different patterns of HEY and HES for different cell fates and target gene expression. The duration of NICD pulses affects gene activation patterns showing that the amplitude of NICD responses plays an important role [11]. Therefore, a comparative analysis of various proteins involved in Notch pathways under anoxic conditions could provide insights to lay a foundation for future research on the role of this pathway in maintaining cellular homeostasis and regulating survival techniques under environmental stress.

The total protein levels of membrane bound ligands (DLL and JAG) and receptors (NOTCH1–2) were analysed for wood frog liver and heart under control, 24 h anoxia, and 4 h aerobic recovery conditions (**Fig. 5.5 and 5.6**). A tissue specific response was observed for all ligands. In the liver, the total protein levels of DLL1 and JAG1 showed no significant changes over the three conditions. However, total protein levels of DLL4 increased significantly in anoxic liver and remained high during aerobic recovery whereas the levels of JAG2 increased significantly only during aerobic recovery from anoxia (**Fig. 5.5a**). By contrast, total protein levels in DLL4 and JAG2 were unchanged in heart over anoxia/recovery but the levels of DLL1 showed an upward trend during anoxia but returned

to control levels after reoxygenation. The results show increased total protein levels of two notch ligands (DLL4 and JAG2) in response to anoxia/reoxygenation in liver and of DLL1 in the anoxic heart (**Fig. 5.5b**). Together with strong increases in total protein levels of receptors, NOTCH1 during anoxia and NOTCH2 during reoxygenation in both the liver and heart, this study indicates that the Notch signaling pathway could be activated in response to anoxia/reoxygenation in wood frogs. Analysis of the responses at gene transcript levels of *notch1* and *notch2* further supports the observed protein results. Levels of *notch1* transcripts showed a significant increase in anoxic heart and remained elevated during reoxygenation (**Fig. 5.9b**) and levels of *notch2* increased significantly upon reoxygenation in the liver (**Fig. 5.9a**). Since a significant increase in the levels of NOTCH1 under 24 h anoxia and dropping back substantially in recovery and by contrast NOTCH 2 levels remained low in anoxia but goes up significantly in recovery in both tissues suggests a stress specific role of the receptors, further study in this respect is required. In addition to that, surface expression versus ligand expression could be studied using immunohistochemistry to more specifically understand the nature of cell to cell communication.

Studies have shown that in adult tissue, the Notch components are differentially regulated in a stress specific manner [17], [34], [35]. For example, in response to hepatic ischemia/reperfusion injury, mRNA levels of *notch1, notch2, dll4, jag2* were significantly upregulated in liver of mice [17]. NOTCH1 and NOTCH2 proteins were expressed in hepatocytes and were upregulated during injury [36], [37]. NOTCH1 activity has also been documented in adult cardiomyocytes [38]. These results are in accordance with our current studies where an increase in the levels of ligands (DLL4 and JAG2) and receptors

(NOTCH1 and NOTCH2) in liver activate the pathway in response to stress. In wood frog heart, reduced levels of JAG1 occurred under anoxia and recovery and similar findings were also associated with the induction of the pro-inflammatory response in rat heart [39].

Previous miRNA studies from our lab on wood frogs showed upregulation of miRNA-21 transcripts [40] during freezing in liver. In another study conducted on human vascular smooth muscle cells, it was reported that in response to injury, miR146a and miR-21 supressed the JAG1/NOTCH2 pathway to enhance the proliferation of vascular smooth muscle cells in heart [41]. The levels of miR199b-5p increase during heart failure and acts as a negative regulator to JAG1 [42]. This suggests a reason for the sustained reduced levels of JAG1 during anoxia in heart and a further reduction during reoxygenation in heart. In addition, miR-210 increases the expression of NOTCH1 and activates the Notch signaling pathway to enhance angiogenesis and formation of capillary like structures after hypoxia stress [43], [44] which is understandable since oxygen deprived conditions cause serious injuries that might damage blood vessels. Therefore, pro-survival and proangiogenic pathways promoting angiogenesis are required. Strong increased expression of NOTCH1 was also demonstrated in our findings for both liver and heart. NOTCH1 upregulation has been shown to indicate liver inflammation that is further associated with liver regeneration [45]. Other reports submit DLL4-NOTCH1 signaling as one of the immune responses in the liver that appear via macrophage activation and are associated with pro-survival pathways like antioxidants and interleukins [46]. Therefore, it can be predicted that regulation via miRNA also plays an important role in the responses to anoxia/recovery in wood frogs but further research in this area is warranted to provide validity.

The ADAM protein is involved in the splicing of NOTCH receptors (S2 cleavage) following a first cleavage by furin-like convertase (S1 cleavage). Increased levels of ADAM during anoxia in both organs (**Fig. 5.6**) indicates formation and liberation of NICD to the cytoplasm after its third cleavage (S3 cleavage). Our results also showed a decreased total protein level of RBPJ and no significant change in the total protein levels of MAML during anoxia in both the liver and heart (**Fig. 5.6**). RBPJ and MAML are the proteins that complex with NICD to initiate transcriptional activation of the genes that are downstream of notch signaling. Reduced levels of RBPJ and MAML suggest a decrease or low transcriptional activity indicating suppression of the Notch transcriptional complex. The reduced transcript levels of *rbpj* in liver and lower DNA binding of RBPJ to promoter regions of target genes in both tissues during anoxia/reoxygenation further explains this assumption (**Fig. 5.8 and 5.9**). Surprisingly, a very large increase of ~5.5 fold in total protein levels of MAML was observed during reoxygenation in heart (**Fig. 5.6b**). RNAi-mediated knockdown studies on MAML showed deleterious effects on muscles suggesting its NOTCH independent role [47]. In addition, MAML acts as a potent coactivator of the MEF2C transcription factor that regulates myogenesis by inducing myogenin and MyoD in heart [47]. Therefore, the findings of Shen et al. [47] that concluded the 'functional switching' of MAML from its role as a transcriptional coactivator for NOTCH-CSL to MEF2 in response to stress signals, can be related to the current scenario, and it can be proposed that MAML could act as an activator to protect heart from damage by oxidative stress caused during reoxygenation. This supports the over-expression of MAML in reoxygenated heart irrespective of other molecules of the Notch transcriptional complex being supressed.

In addition, increased levels of NOTCH1 and reduced levels of transcriptional complex components show that Notch also mediates complex independent regulation. Studies have shown that NICD and NF-kβ show some common featured that include activation by tumor necrosis factor and hypoxia and regulation of target genes like Hes1 and Ik-βα [48], [49]. Increased levels of Hes1 (**Fig. 5.7**) in both tissues further justify this assumption. Recent studies have shown that NICD also contributes towards the transcription and/or binding activity of NF-kβ [48]. Independent of the transcriptional complex, NICD activates R-Ras and inhibits H-Ras to activate integrins [50] in order to control vascular smooth muscle cell expression. OCT4 is one of the downstream targets of Notch signaling pathway. Previous studies in our lab showed decreased levels of total proteins in OCT4 during 24 h anoxia in both liver and heart. This also supports the non formation of the Notch transcriptional complex [51], [52].

A large significant increase was observed in the levels of HES1 and HES5 in both the tissues during anoxia (**Fig. 5.7**). HES1 and HES5 are downstream targets of the Notch transcriptional complex. Previous studies showed that HES1 and HES5 could also be activated in a Notch independent manner that includes pathways like JNK signaling, HIF, BMP/ TGFβ, RAS/MAPK [53], [54], [55]. DLL and JAG induced Notch signaling results in the activation of HES1 in relation to liver inflammation and immune response [46], [56]. The current study showed a very significant increase in total protein levels of HES1 during anoxia that remained elevated during reoxygenation in both liver and heart (**Fig. 5.7**). HES1 is considered to be the master regulator of glucocorticoids [57]. Glucocorticoids are the primary stress hormones that are released in response to environmental stress and promote liver gluconeogenesis to increase blood glucose levels [58]. A HES1 knockout

study on mouse liver showed abnormal glucocorticoid-related signaling that affected downstream target genes involved in carbohydrate and lipid metabolism and energy production [59]. Furthermore, in the same study, it was established that over-expression of HES1 reduced gene expression mediated via glucocorticoids. Therefore, the high levels of HES1 seen in both organs in the current study suggests its regulation of glucocorticoid-mediated gene expression in a transcriptional repression manner in order to conserve energy and endure long periods of metabolic rate depression.

The total protein levels of HES5 showed an opposite trend in liver and heart. In liver the level of HES5 decreased during anoxia and levels remained low during recovery whereas a significant increase of about 4-fold was observed in anoxic heart and the levels decreased to about 1.5-fold over controls upon reoxygenation (**Fig. 5.7**). HES5 is an under-studied protein and its role still needs to be explored. Pathway analysis of HES5 target genes demonstrated its involvement in many enriched pathways that included stem cell pluripotency, cancer related, and PI3K-Akt signaling pathway. Further analysis showed that various HES5 targets are known MYC targets, among which *odc1* and *ldha* showed the highest downregulation at both protein and transcript levels [60]. MYC is the family of oncoproteins whose expression causes tumor initiation, progression and maintenance [61]. Therefore, transcriptional pause of MYC by HES5 in myocardium would prevent hypertrophic growth and heart failure.

Summing up the results, we can draw some notable inferences. The present work reflects towards the “functional switching” of MAML and Notch-independent activation of HES1 and HES5. Increased protein levels of HES1 in the liver and heart during anoxia controls glucocorticoid dependent stress response to regulate the pathways involved in

carbohydrate and lipid metabolism. This prevents dysregulation of metabolic pathways by glucocorticoids and works in accordance with energy saving mode under anoxic conditions. The results also reflect the myocardial protection by overexpression of MAML that activates MyoD and HES5 preventing activation of MYC family proteins (oncogene) in an anoxic heart. The current study presents a first analysis of the regulation of the Notch signaling pathway in response to anoxia in amphibians and sets forth some future directions. The increased protein levels of ligands and receptors suggest activation of the Notch signaling pathway but decreased levels of RBPJ reflect towards repression of the formation of the transcriptional complex. Therefore further analysis of the Notch signaling pathway with respect to its activation could present a potential answer to the regulation of multiple components involved in cellular communication network in a stress/ organ specific manner during anoxia in wood frogs.

5.6 References

1. K.B. Storey, J.M. Storey, Signal transduction and gene expression in the regulation of natural freezing survival, in: J.M. Storey, K.B. and Storey (Ed.), Cell Mol. Response to Stress, Vol. 2: Pr, Elsevier Press, Amsterdam, 2001: pp. 1–19. https://doi.org/10.1016/S1568-1254(01)80003-6.
2. K.B. Storey, Strategies for exploration of freeze responsive gene expression: advances in vertebrate freeze tolerance, Cryobiology. 48 (2004) 134–145. https://doi.org/10.1016/j.cryobiol.2003.10.008.
3. K.B. Storey, J.M. Storey, Molecular physiology of freeze tolerance in vertebrates, Physiol. Rev. 97 (2017) 623–665. https://doi.org/10.1152/physrev.00016.2016.
4. K.B. Storey, Molecular mechanisms of anoxia tolerance, Int. Congr. Ser. 1275 (2004) 47–54. https://doi.org/10.1016/j.ics.2004.08.072.
5. R.S. Balaban, S. Nemoto, T. Finkel, Mitochondria, Oxidants, and Aging, Cell. 120 (2005) 483–495. https://doi.org/10.1016/j.cell.2005.02.001.
6. M.P. Murphy, How mitochondria produce reactive oxygen species, Biochem. J. 417 (2009) 1–13. https://doi.org/10.1042/BJ20081386.
7. B. D'Autréaux, M.B. Toledano, ROS as signalling molecules: mechanisms that generate specificity in ROS homeostasis, Nat. Rev. Mol. Cell Biol. 8 (2007) 813–824. https://doi.org/10.1038/nrm2256.
8. C.A. Juan, J.M. Pérez de la Lastra, F.J. Plou, E. Pérez-Lebeña, The Chemistry of Reactive Oxygen Species (ROS) revisited: Outlining their role in biological macromolecules (DNA, Lipids and Proteins) and induced pathologies, Int. J. Mol. Sci. 22 (2021) 4642. https://doi.org/10.3390/ijms22094642.
9. R. Schwanbeck, S. Martini, K. Bernoth, U. Just, The Notch signaling pathway: Molecular basis of cell context dependency, Eur. J. Cell Biol. 90 (2011) 572–581. https://doi.org/10.1016/j.ejcb.2010.10.004.
10. S.G. Megason, Dynamic Encoding in the Notch Pathway, Dev. Cell. 44 (2018) 411–412. https://doi.org/10.1016/j.devcel.2018.02.006.
11. N. Nandagopal, L.A. Santat, L. LeBon, D. Sprinzak, M.E. Bronner, M.B. Elowitz, Dynamic ligand discrimination in the Notch signaling pathway, Cell. 172 (2018) 869-880.e19. https://doi.org/10.1016/j.cell.2018.01.002.
12. G. Chen, Y. Qiu, L. Sun, M. Yu, W. Wang, W. Xiao, Y. Yang, Y. Liu, S. Yang, D.H. Teitelbaum, Y. Ma, D. Lu, H. Yang, The Jagged-2/Notch-1/Hes-1 pathway is involved in intestinal epithelium regeneration after intestinal ischemia-reperfusion injury, PLoS One. 8 (2013) e76274. https://doi.org/10.1371/journal.pone.0076274.
13. K. Hori, A. Sen, S. Artavanis-Tsakonas, Notch signaling at a glance, J. Cell Sci. 126 (2013) 2135–2140. https://doi.org/10.1242/jcs.127308.
14. B. Keith, M.C. Simon, Hypoxia-Inducible Factors, stem cells, and cancer, Cell. 129 (2007) 465–472. https://doi.org/10.1016/j.cell.2007.04.019.
15. M. V. Gustafsson, X. Zheng, T. Pereira, K. Gradin, S. Jin, J. Lundkvist, J.L. Ruas, L. Poellinger, U. Lendahl, M. Bondesson, Hypoxia requires Notch signaling to maintain the undifferentiated cell state, Dev. Cell. 9 (2005) 617–628. https://doi.org/10.1016/j.devcel.2005.09.010.
16. X.L. Zhou, J.C. Liu, Role of Notch signaling in the mammalian heart, Brazilian J. Med. Biol. Res. 47 (2013) 1–10. https://doi.org/10.1590/1414-431X20133177.
17. H.-C. Yu, H.-Y. Qin, F. He, L. Wang, W. Fu, D. Liu, F.-C. Guo, L. Liang, K.-F. Dou, H. Han, Canonical notch pathway protects hepatocytes from ischemia/reperfusion injury in mice by repressing reactive oxygen species production through JAK2/STAT3 signaling, Hepatology. 54 (2011) 979–988. https://doi.org/10.1002/hep.24469.
18. S. Gupta, S. Li, M.J. Abedin, L. Wang, E. Schneider, B. Najafian, M. Rosenberg, Effect of Notch activation on the regenerative response to acute renal failure, Am. J. Physiol. Physiol. 298 (2010) F209–F215. https://doi.org/10.1152/ajprenal.00451.2009.

19. V. Boopathy, K.D. Pendergrass, P.L. Che, Y.-S. Yoon, M.E. Davis, Oxidative stress-induced Notch1 signaling promotes cardiogenic gene expression in mesenchymal stem cells, Stem Cell Res. Ther. 4 (2013) 43. https://doi.org/10.1186/scrt190.
20. X. Zhou, L. Wan, Q. Xu, Y. Zhao, J. Liu, Notch signaling activation contributes to cardioprotection provided by ischemic preconditioning and postconditioning, J. Transl. Med. 11 (2013) 251. https://doi.org/10.1186/1479-5876-11-251.
21. F. Geisler, M. Strazzabosco, Emerging roles of Notch signaling in liver disease, Hepatology. 61 (2015) 382–392. https://doi.org/10.1002/hep.27268.
22. V.E.M. Gerber, S. Wijenayake, K.B. Storey, Anti-apoptotic response during anoxia and recovery in a freeze-tolerant wood frog (*Rana sylvatica*), PeerJ. 4 (2016) e1834. https://doi.org/10.7717/peerj.1834.
23. A. Gupta, K.B. Storey, Regulation of antioxidant systems in response to anoxia and reoxygenation in *Rana sylvatica*, Comp. Biochem. Physiol. Part B Biochem. Mol. Biol. 243–244 (2020) 110436. https://doi.org/10.1016/j.cbpb.2020.110436.
24. A. Gupta, K.B. Storey, Coordinated expression of Jumonji and AHCY under OCT transcription factor control to regulate gene methylation in wood frogs during anoxia, Gene. 788 (2021) 145671. https://doi.org/10.1016/j.gene.2021.145671.
25. S.A. Bustin, V. Benes, J.A. Garson, J. Hellemans, J. Huggett, M. Kubista, R. Mueller, T. Nolan, M.W. Pfaffl, G.L. Shipley, J. Vandesompele, C.T. Wittwer, The MIQE Guidelines: Minimum Information for Publication of Quantitative Real-Time PCR Experiments, Clin. Chem. 55 (2009) 611–622. https://doi.org/10.1373/clinchem.2008.112797.
26. S.C. Taylor, K. Nadeau, M. Abbasi, C. Lachance, M. Nguyen, J. Fenrich, The ultimate qPCR experiment: producing publication quality, reproducible data the first time, Trends Biotechnol. 37 (2019) 761–774. https://doi.org/10.1016/j.tibtech.2018.12.002.
27. S.L. Eaton, S.L. Roche, M. Llavero Hurtado, K.J. Oldknow, C. Farquharson, T.H. Gillingwater, T.M. Wishart, Total protein analysis as a reliable loading control for quantitative fluorescent western blotting, PLoS One. 8 (2013) e72457. https://doi.org/10.1371/journal.pone.0072457.
28. J. Zhang, K.B. Storey, RBioplot: an easy-to-use R pipeline for automated statistical analysis and data visualization in molecular biology and biochemistry., PeerJ. 4 (2016) e2436. https://doi.org/10.7717/peerj.2436.
29. F. Sievers, A. Wilm, D. Dineen, T.J. Gibson, K. Karplus, W. Li, R. Lopez, H. McWilliam, M. Remmert, J. Söding, J.D. Thompson, D.G. Higgins, Fast, scalable generation of high-quality protein multiple sequence alignments using Clustal Omega, Mol. Syst. Biol. 7 (2011) 539. https://doi.org/10.1038/msb.2011.75.
30. I. Greenwald, K. Rhett, Notch signaling: genetics and structure, WormBook. (2013) 1–28. https://doi.org/10.1895/wormbook.1.10.2.
31. S. Fulda, A.M. Gorman, O. Hori, A. Samali, Cellular stress responses: cell Survival and cell death, Int. J. Cell Biol. 2010 (2010) 1–23. https://doi.org/10.1155/2010/214074.
32. Z. Zakeri, W. Bursch, M. Tenniswood, R.A. Lockshin, Cell death: Programmed, apoptosis, necrosis, or other?, Cell Death Differ. 2 (1995) 87–96.
33. J.F.R. Kerr, A.H. Wyllie, A.R. Currie, Apoptosis: A basic biological phenomenon with wideranging implications in tissue kinetics, Br. J. Cancer. 26 (1972) 239–257. https://doi.org/10.1038/bjc.1972.33.
34. S. Nistri, C. Sassoli, D. Bani, Notch signaling in ischemic damage and fibrosis: Evidence and clues from the heart, Front. Pharmacol. 8 (2017). https://doi.org/10.3389/fphar.2017.00187.
35. A. Croquelois, A.A. Domenighetti, M. Nemir, M. Lepore, N. Rosenblatt-Velin, F. Radtke, T. Pedrazzini, Control of the adaptive response of the heart to stress via the Notch1 receptor pathway, J. Exp. Med. 205 (2008) 3173–3185. https://doi.org/10.1084/jem.20081427.

36. L. Boulter, O. Govaere, T.G. Bird, S. Radulescu, P. Ramachandran, A. Pellicoro, R.A. Ridgway, S.S. Seo, B. Spee, N. Van Rooijen, O.J. Sansom, J.P. Iredale, S. Lowell, T. Roskams, S.J. Forbes, Macrophage-derived Wnt opposes Notch signaling to specify hepatic progenitor cell fate in chronic liver disease, Nat. Med. 18 (2012) 572–579. https://doi.org/10.1038/nm.2667.
37. R. Fiorotto, A. Raizner, C.M. Morell, B. Torsello, R. Scirpo, L. Fabris, C. Spirli, M. Strazzabosco, Notch signaling regulates tubular morphogenesis during repair from biliary damage in mice, J. Hepatol. 59 (2013) 124–130. https://doi.org/10.1016/j.jhep.2013.02.025.
38. P. Kratsios, C. Catela, E. Salimova, M. Huth, V. Berno, N. Rosenthal, F. Mourkioti, Distinct roles for cell-autonomous Notch signaling in cardiomyocytes of the embryonic and adult heart, Circ. Res. 106 (2010) 559–572. https://doi.org/10.1161/CIRCRESAHA.109.203034.
39. G. Aquila, C. Fortini, A. Pannuti, S. Delbue, M. Pannella, M.B. Morelli, C. Caliceti, F. Castriota, M. de Mattei, A. Ongaro, A. Pellati, P. Ferrante, L. Miele, L. Tavazzi, R. Ferrari, P. Rizzo, A. Cremonesi, Distinct gene expression profiles associated with Notch ligands Delta-like 4 and Jagged1 in plaque material from peripheral artery disease patients: a pilot study, J. Transl. Med. 15 (2017) 98. https://doi.org/10.1186/s12967-017-1199-3.
40. K.K. Biggar, A. Dubuc, K. Storey, MicroRNA regulation below zero: Differential expression of miRNA-21 and miRNA-16 during freezing in wood frogs, Cryobiology. 59 (2009) 317–321. https://doi.org/10.1016/j.cryobiol.2009.08.009.
41. L. Marracino, F. Fortini, E. Bouhamida, F. Camponogara, P. Severi, E. Mazzoni, S. Patergnani, E. D'Aniello, R. Campana, P. Pinton, F. Martini, M. Tognon, G. Campo, R. Ferrari, F. Vieceli Dalla Sega, P. Rizzo, Adding a "Notch" to cardiovascular disease therapeutics: A microRNA-based approach, Front. Cell Dev. Biol. 9 (2021). https://doi.org/10.3389/fcell.2021.695114.
42. B. Duygu, E.M. Poels, R. Juni, N. Bitsch, L. Ottaviani, S. Olieslagers, L.J. de Windt, P.A. da Costa Martins, miR-199b-5p is a regulator of left ventricular remodeling following myocardial infarction, Non-Coding RNA Res. 2 (2017) 18–26. https://doi.org/10.1016/j.ncrna.2016.12.002.
43. S. Hu, M. Huang, Z. Li, F. Jia, Z. Ghosh, M.A. Lijkwan, P. Fasanaro, N. Sun, X. Wang, F. Martelli, R.C. Robbins, J.C. Wu, MicroRNA-210 as a novel therapy for treatment of ischemic heart disease, Circulation. 122 (2010). https://doi.org/10.1161/CIRCULATIONAHA.109.928424.
44. M. Arif, R. Pandey, P. Alam, S. Jiang, S. Sadayappan, A. Paul, R.P.H. Ahmed, MicroRNA-210-mediated proliferation, survival, and angiogenesis promote cardiac repair post myocardial infarction in rodents, J. Mol. Med. 95 (2017) 1369–1385. https://doi.org/10.1007/s00109-017-1591-8.
45. K. Neumann, C. Rudolph, C. Neumann, M. Janke, D. Amsen, A. Scheffold, Liver sinusoidal endothelial cells induce immunosuppressive IL-10-producing Th1 cells via the Notch pathway, Eur. J. Immunol. 45 (2015) 2008–2016. https://doi.org/10.1002/eji.201445346.
46. D. Fukuda, E. Aikawa, F.K. Swirski, T.I. Novobrantseva, V. Kotelianski, C.Z. Gorgun, A. Chudnovskiy, H. Yamazaki, K. Croce, R. Weissleder, J.C. Aster, G.S. Hotamisligil, H. Yagita, M. Aikawa, Notch ligand Delta-like 4 blockade attenuates atherosclerosis and metabolic disorders, Proc. Natl. Acad. Sci. 109 (2012) E1868–E1877. https://doi.org/10.1073/pnas.1116889109.
47. H. Shen, A.S. McElhinny, Y. Cao, P. Gao, J. Liu, R. Bronson, J.D. Griffin, L. Wu, The Notch coactivator, MAML1, functions as a novel coactivator for MEF2C-mediated transcription and is required for normal myogenesis, Genes Dev. 20 (2006) 675–688. https://doi.org/10.1101/gad.1383706.
48. H.M. Shin, L.M. Minter, O.H. Cho, S. Gottipati, A.H. Fauq, T.E. Golde, G.E. Sonenshein, B.A. Osborne, Notch1 augments NF-κB activity by facilitating its nuclear retention, EMBO J. 25 (2006) 129–138. https://doi.org/10.1038/sj.emboj.7600902.
49. J. Wang, L. Shelly, L. Miele, R. Boykins, M.A. Norcross, E. Guan, Human Notch-1 inhibits NF-κB activity in the nucleus through a direct interaction involving a novel domain, J. Immunol. 167 (2001) 289–295. https://doi.org/10.4049/jimmunol.167.1.289.

50. P.S. Hodkinson, P.A. Elliott, Y. Lad, B.J. McHugh, A.C. MacKinnon, C. Haslett, T. Sethi, Mammalian NOTCH-1 activates β1 integrins via the small GTPase R-Ras, J. Biol. Chem. 282 (2007) 28991–29001. https://doi.org/10.1074/jbc.M703601200.
51. A. Gupta, K.B. Storey, Activation of the Hippo Pathway in *Rana sylvatica*: Yapping Stops in Response to Anoxia, Life. 11 (2021) 1422. https://doi.org/10.3390/life11121422.
52. A. Gupta, K.B. Storey, Regulation of antioxidant systems in response to anoxia and reoxygenation in *Rana sylvatica* , Comp. Biochem. Physiol. Part B Biochem. Mol. Biol. 243–244 (2020) 110436. https://doi.org/10.1016/j.cbpb.2020.110436.
53. C.L. Curry, L.L. Reed, B.J. Nickoloff, L. Miele, K.E. Foreman, Notch-independent regulation of Hes-1 expression by c-Jun N-terminal kinase signaling in human endothelial cells, Lab. Investig. 86 (2006) 842–852. https://doi.org/10.1038/labinvest.3700442.
54. M.-T. Stockhausen, J. Sjölund, H. Axelson, Regulation of the Notch target gene Hes-1 by TGFα induced Ras/MAPK signaling in human neuroblastoma cells, Exp. Cell Res. 310 (2005) 218–228. https://doi.org/10.1016/j.yexcr.2005.07.011.
55. S. Kamakura, K. Oishi, T. Yoshimatsu, M. Nakafuku, N. Masuyama, Y. Gotoh, Hes binding to STAT3 mediates crosstalk between Notch and JAK–STAT signalling, Nat. Cell Biol. 6 (2004) 547–554. https://doi.org/10.1038/ncb1138.
56. S. Burghardt, A. Erhardt, B. Claass, S. Huber, G. Adler, T. Jacobs, A. Chalaris, D. Schmidt-Arras, S. Rose-John, K. Karimi, G. Tiegs, Hepatocytes contribute to immune regulation in the liver by activation of the Notch signaling pathway in T Cells, J. Immunol. 191 (2013) 5574–5582. https://doi.org/10.4049/jimmunol.1300826.
57. R.H. Oakley, J.A. Cidlowski, Cellular processing of the glucocorticoid receptor gene and protein: New mechanisms for generating tissue-specific actions of glucocorticoids, J. Biol. Chem. 286 (2011) 3177–3184. https://doi.org/10.1074/jbc.R110.179325.
58. T. Rhen, J.A. Cidlowski, Antiinflammatory action of glucocorticoids — New mechanisms for old drugs, N. Engl. J. Med. 353 (2005) 1711–1723. https://doi.org/10.1056/NEJMra050541.
59. J.R. Revollo, R.H. Oakley, N.Z. Lu, M. Kadmiel, M. Gandhavadi, J.A. Cidlowski, HES1 is a master regulator of glucocorticoid receptor–Dependent gene expression, Sci. Signal. 6 (2013). https://doi.org/10.1126/scisignal.2004389.
60. S. Luiken, A. Fraas, M. Bieg, R. Sugiyanto, B. Goeppert, S. Singer, C. Ploeger, G. Warsow, J.U. Marquardt, C. Sticht, C. De La Torre, S. Pusch, A. Mehrabi, N. Gretz, M. Schlesner, R. Eils, P. Schirmacher, T. Longerich, S. Roessler, NOTCH target gene HES5 mediates oncogenic and tumor suppressive functions in hepatocarcinogenesis, Oncogene. 39 (2020) 3128–3144. https://doi.org/10.1038/s41388-020-1198-3.
61. M. Gabay, Y. Li, D.W. Felsher, MYC activation is a hallmark of cancer initiation and maintenance, Cold Spring Harb. Perspect. Med. 4 (2014) a014241–a014241. https://doi.org/10.1101/cshperspect.a014241.

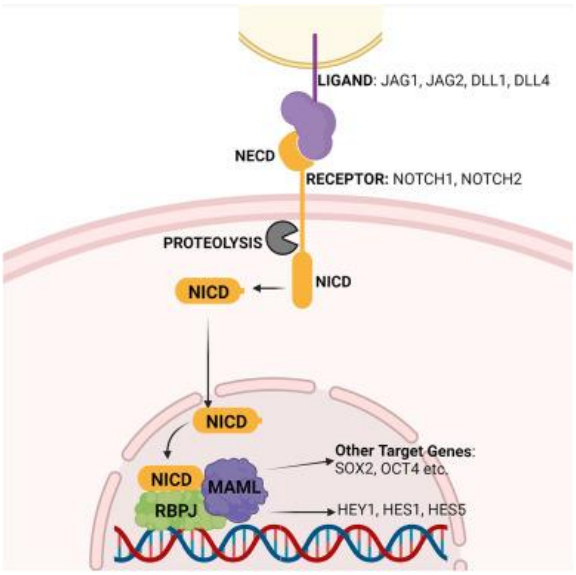

Fig. 5.1. Schematic representation of the Notch signaling pathway. Upon encountering stress, the pathway gets activated and ligands from one cell send signals to the receptors of the adjoining cells to initiate the series of proteolysis that releases NECD from the notch receptor. The NECD translocate to the nucleus and binds to the notch transcription complex and activate it. JAG: Jagged, DLL: Delta like, NECD: notch extracellular domain, MAML: Mastermind-like protein 1, RBPJ: Recombination Signal Binding Protein for Immunoglobulin Kappa J Region.

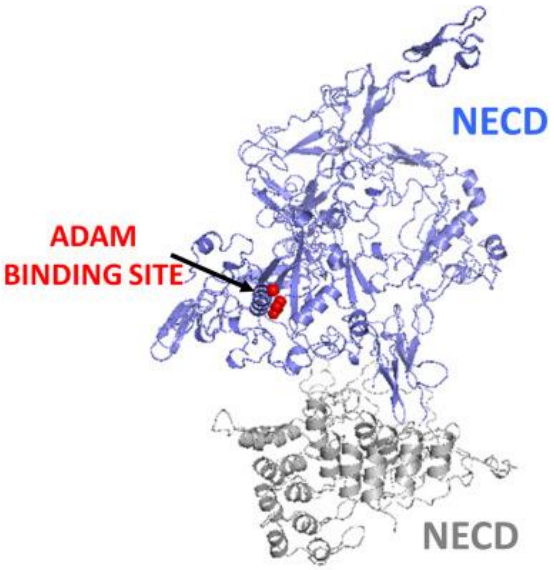

Fig. 5.2. Structure of Notch receptor: The model shows the predicted structure of Notch1 receptor using the protein sequence of *Rana temporaria*. The model represents the two major domains: the extracellular domain NECD (Blue) that consist of binding sites for ligands and the intracellular domain NICD (Grey) consist of RBPJ binding site. The ADAM binding site is represented as red colour (ball structure). Protein modelling .pdb files were generated from Protein Data Base and the model was generated using PyMOL software (https://pymol.org/2/).

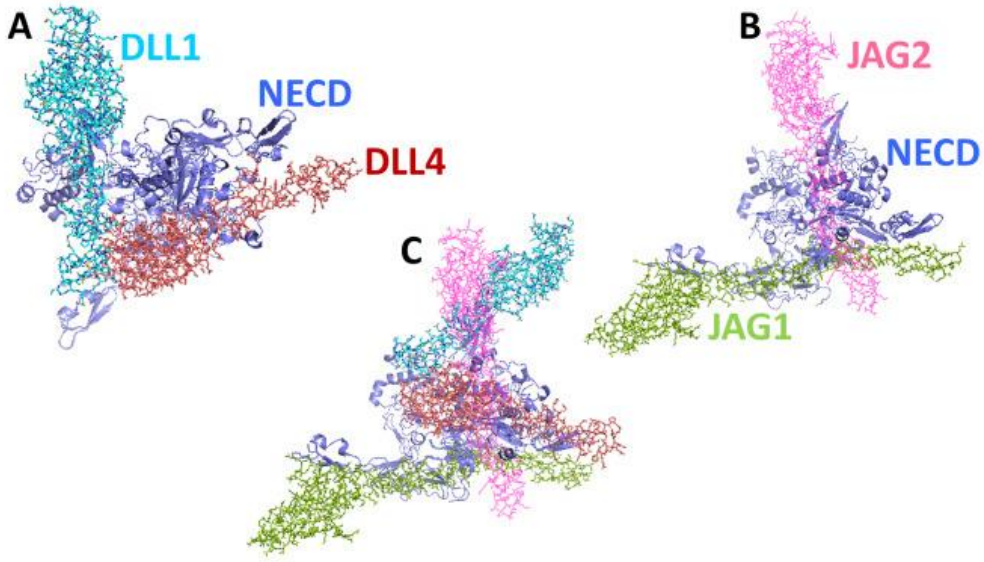

Fig. 5.3. Structure of Notch receptor and ligand complex. The structure represents Notch1 extracellular domain (NECD) (blue) in (ribbon representation) binding to the ligands (in sticks and lines) (A) binding of DLL ligands: DLL1 (aqua) and DLL4 (red) (B) binding of JAG ligands: JAG1 (green) and JAG2 (pink) (C) Binding of all four ligands (DLL1, DLL4, JAG1 and JAG2). The Notch- ligand structure represented here is illustrates the binding in cellular context. Other information similar to Fig. 5.2.

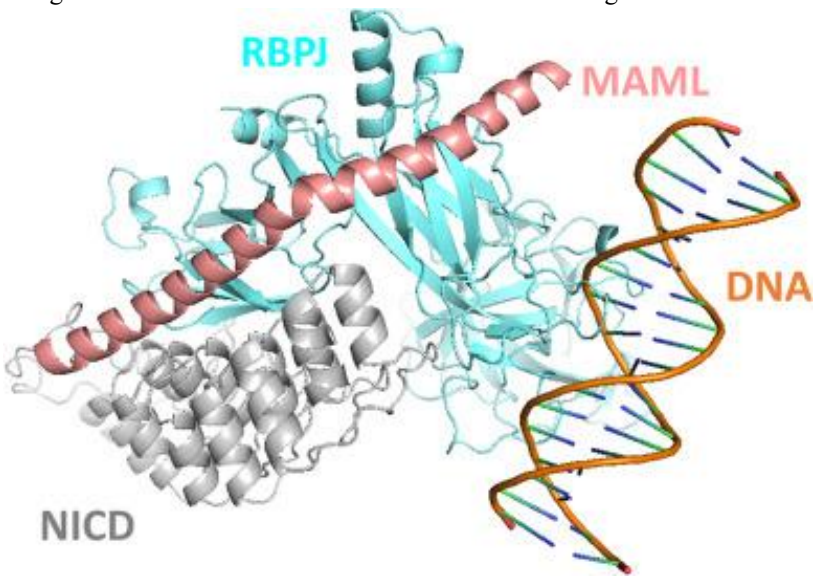

Fig. 5.4. Structure of Notch transcriptional complex bound to DNA. Ribbon diagram Notch transcriptional factor (ternary structure) complex from *Rana temporaria*. The NICD, MAML, and RBPJ are colored grey, salmon, and cyan respectively. RBPJ bound to the promoter region of the DNA where the strands are colored as orange and bases colored as blue and green. (For interpretation of the references to colour in this figure legend, the reader is referred to the web version of this article.)

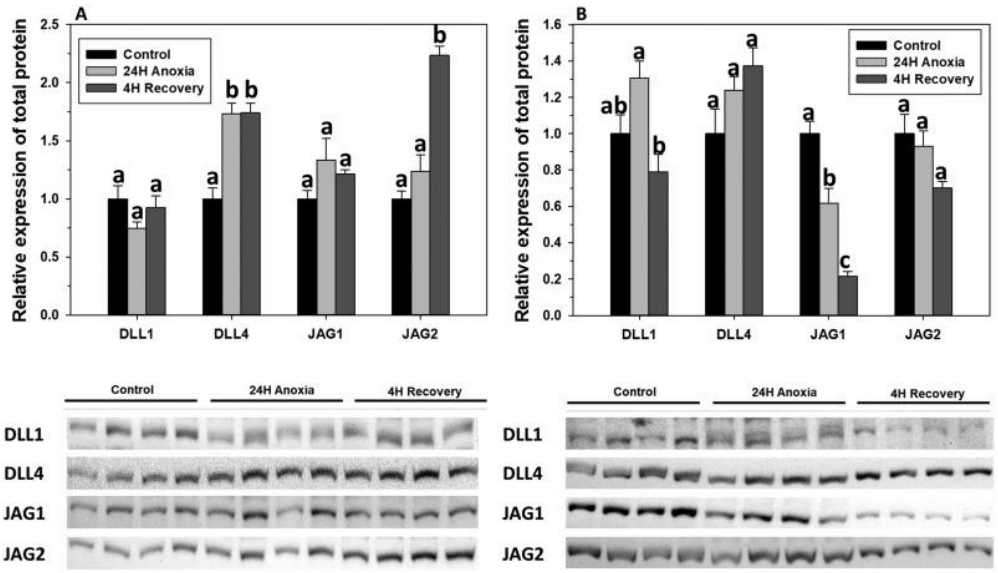

Fig. 5.5. Relative expression levels of total proteins (ligands) involved in the Notch Signaling in (A) liver and (B) heart of *R. sylvatica* under control, 24 h anoxia exposure or 4 h aerobic recovery from anoxia conditions as determined by western immunoblotting. Corresponding Western immunoblot bands are shown below histograms. Data are mean ± SEM, n = 3–4 independent trials on samples from different animals. Data were analysed using analysis of variance with a post hoc Tukey test; different letters denote values that are significantly different from each other ($p < 0.05$).

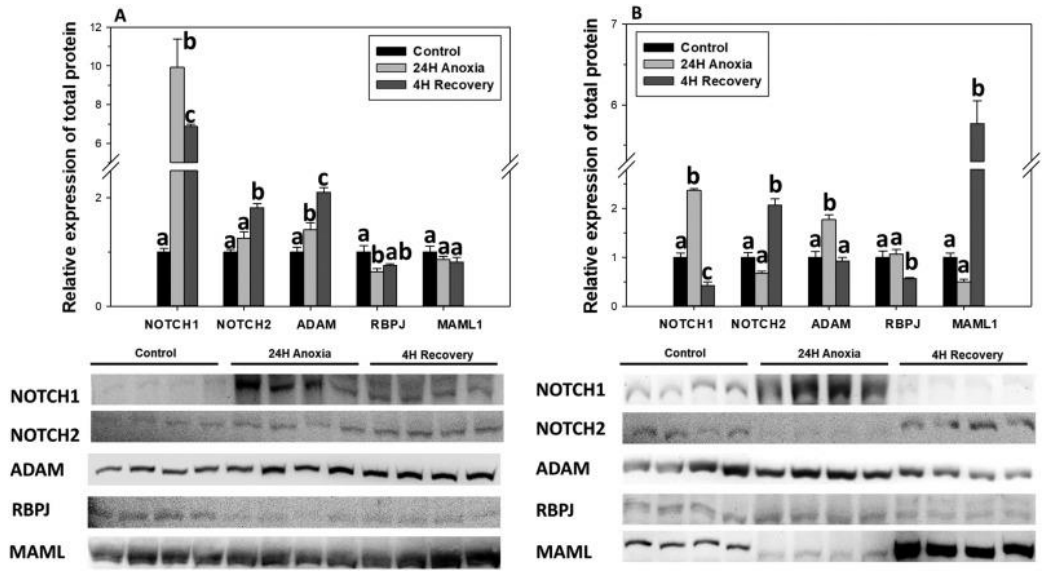

Fig. 5.6. Relative expression levels of total proteins involved in the Notch Signaling in (A) liver and (B) heart of *R. sylvatica* under control, 24 h anoxia exposure or 4 h aerobic recovery from anoxia conditions as determined by western immunoblotting. Other information similar to Fig. 5.5.

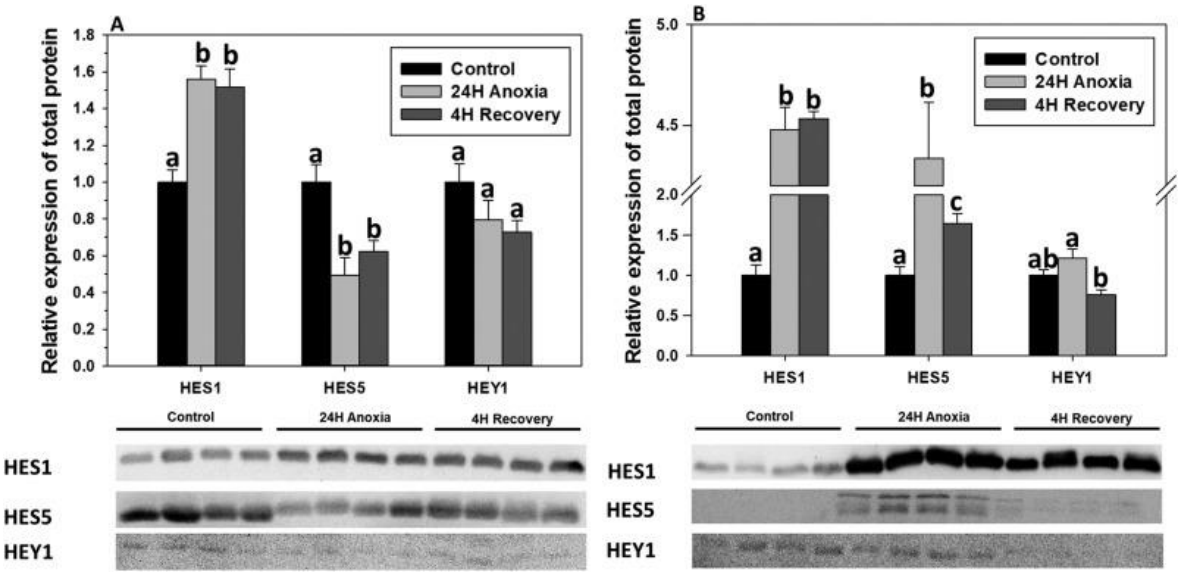

Fig. 5.7. Relative expression levels of downstream proteins of Notch Signaling in (A) liver and (B) heart of *R. sylvatica* under control, 24 h anoxia exposure or 4 h aerobic recovery from anoxia conditions as determined by western immunoblotting. Other information similar to Fig. 5.5.

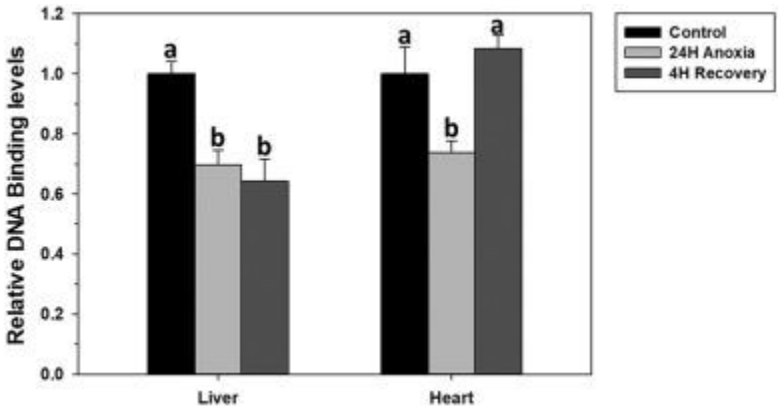

Fig. 5.8. Relative DNA binding levels of RBPJ in total protein extracts in liver and heart of *R. sylvatica* under control, 24 h anoxia or 4 h recovery conditions as determined by TF-ELISA or DPI-ELISA. Other information similar to Fig. 5.5.

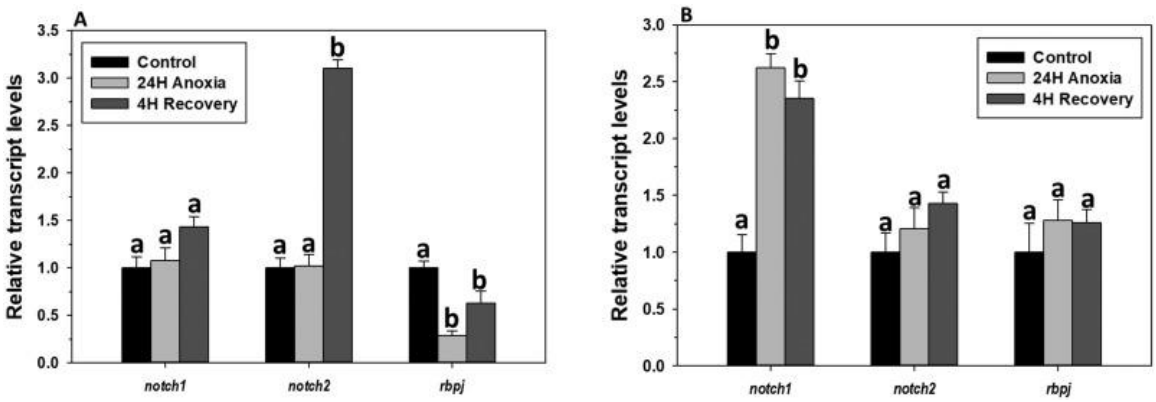

Fig. 5.9. Relative expression of gene transcripts of the proteins involved in the Notch Signaling in (A) liver and (B) heart of *R. sylvatica* in control, 24 h anoxia, and 4 h recovery from anoxia as determined by qPCR. Other information similar to Fig. 5.5.

6.Discussion

6.1 Anoxia tolerance in wood frogs

Extreme environmental conditions can be fatal and present multiple challenges to most organisms. To survive such conditions, animals adapt using a variety of survival strategies that can involve movement/migration to more favourable habitats or alteration of physiological or biochemical processes. *Rana sylvatica*, the wood frog, is a well-studied model of a freeze tolerant animal that can endure several months of extreme winter low temperatures with 65-70% of body water withdrawn from cells and into extracellular and extra organ spaces in the form of ice crystals [1]. The outflow of water causes cell shrinkage and membranes come under compression stress. To help stabilise and maintain a critical minimum cell volume, wood frogs rapidly increase cellular glucose levels from 1-5 mM under normal conditions to as high as 200-300 mM while frozen creating a state of hyperglycemia in the body [2]. These extreme levels of glucose inside cells act a cryoprotectant to limit the amount of water lost from cells into extracellular ice masses. A major consequence of freezing is a halt to blood circulation. Heartbeat and breathing are also arrested leading to a state of anoxia and ischemia. Thus, the cells of wood frogs must develop tolerance and adaptation to not just freezing but to three component stresses of freezing: cell water loss (dehydration), hyperglycemia, and anoxia.

Wood frogs have adapted to endure anoxia as one of the major components of freeze tolerance and can also survive anoxia as an independent stress [3]. The difference between the oxygen-deprived condition during freezing and anoxia in the unfrozen state is that freezing has more severe consequences, halting blood circulation and thereby causing ischemia and disrupting the delivery of oxygen and all other blood-borne metabolites to organs. Recovery from anoxia or freezing also has negative consequences. Reoxygenation of tissues leads to increased production reactive oxygen species (ROS) that can exceed the normal antioxidant capacity of cells, thus creating a

condition of oxidative stress [4]. As a result, animals need to activate transcription factors and signaling pathways that enhance the synthesis of antioxidants to minimize oxidative stress. In addition, anoxic conditions compel a switch to anaerobic metabolism that reduces ATP production from 36 ATP per glucose molecule catabolized in the presence of oxygen to only 2 ATP per glucose when converted to lactate [5]. Even though glucose is readily available during anoxia, the amount of energy produced is 18 times lower than that from respiration, suggesting high glucose levels would not be enough to sustain normal cellular metabolism by the ATP energy generated anaerobically. Therefore, survival under low energy availability is only possible by lowering cellular energy demands. Hence, animals suppress their metabolism and remain in the state of metabolic rate depression (MRD) until normal conditions return.

A major interest in this thesis was to develop an understanding of the coordinated working of various transcription factors that are regulated via stress specific signaling pathways to ensure tolerance to complete anoxia in wood frogs. A thorough understanding of molecular mechanisms involved in anoxia tolerance could provide some novel insights towards finding cures for medical problems occurring as a consequence of oxygen lack, for example ischemic stroke, oxidative stress, tissue damage, etc.

6.2 Transcriptional and translational repression during metabolic rate depression

Anoxia tolerant vertebrates can typically suppress their metabolic rate by ~90% under oxygen deprived conditions in order to match the reduction in ATP availability from anaerobic metabolism, as compared to aerobic conditions [6,7]. Available energy is directed towards the pathways that are essential for survival through prolonged anoxia exposures. In **Chapter 2**, regulation of two transcription factors, NRF2 and OCT4, was studied with respect to their role in antioxidant

defense mechanisms and assessing their responses to 24 H anoxia and 4 H reoxygenation (recovery) in wood frog liver and skeletal muscle. Surprisingly, the experiments conducted in **Chapter 2** showed no change in the total protein levels of OCT4 and NRF2 in the liver over anoxia/reoxygenation (**Chapter 2, Fig. 2.2a and 2.3a**) but the levels of both transcription factors decreased upon reoxygenation in skeletal muscle (**Chapter 2, Fig. 2.2b and 2.3b**). DNA binding levels also decreased during anoxia for both NRF2 and OCT4 in liver and skeletal muscle (**Chapter 2, Fig. 2.7 and 2.8**). The reduced DNA binding levels suggest decreased transcription of target genes leading to reduced translation of transcripts and reduced protein products. As discussed in **Chapter 1**, transcription and translation are two highly energy expensive processes that are suppressed when a cell undergoes MRD. Therefore, reduced DNA binding levels of both NRF2 and OCT4 are consistent with anoxia-induced MRD. A knockdown study by Escoll *et al.* on glioblastomas showed that knockdown of NRF2 drastically reduced the expression of TAZ at transcriptional levels [8]. In a similar study, knockdown of TAZ decreased the protein levels of NRF2 but did not produce any change at transcript levels, further indicating that transcript and protein levels of TAZ are governed by NRF2. These results propose TAZ as a downstream target of NRF2. A decrease of 88% and 97% in the total protein levels of TAZ compared to controls was observed during 24 H anoxia and 4 H reoxygenation, respectively, in frog liver (**Chapter 4, Fig. 4.3a**) and a 42% decrease in transcript levels of *taz* in anoxic liver (**Chapter 4, Fig. 4.6a**) matched well with the above inference. In addition, NRF2 and Notch signaling share a co-regulatory relationship where RBPJ, acting via the Notch transcriptional complex, regulates the expression of NRF2 [9] and NRF2 positively regulates Notch signaling [10]. The in-silico analysis of *rbpj* suggested the presence of RBPJ binding sites on the regulatory region of *nrf2* [9]. A study by Wakabayashi *et al.,* concluded that "Notch to Nrf2" signaling plays an important role in the stress response in liver and promotes cytoprotective signaling

responses [9]. No change was observed in the total protein levels of NRF2 in liver (**Chapter 2, Fig. 2.2a**) under any of the three conditions (aerobic, anoxic, recovery) and this could be due to decreased total protein and DNA binding levels of RBPJ in anoxic liver (**Chapter 5, Fig. 5.6a and 5.8**). However, levels remained unchanged during recovery compared to anoxic conditions (**Chapter 5, Fig. 5.6a and 5.8**).

OCTs are another group of transcription factors that respond to cellular stresses. Among these, OCT1 and OCT4 are the best studied for their roles in stress resistance and metabolic control by providing transcriptional regulation [11–13]. OCTs are direct downstream targets of two major signaling pathways discussed in the current thesis, the hippo pathway (**Chapter 4**) and the Notch signaling pathway (**Chapter 5**) [14–16]. No change or a decrease in the total protein levels of OCT4 was observed under 24 H anoxia and 4 H recovery as compared to control levels in liver, skeletal muscle and heart (**Chapter 2, Fig. 2.3a and 2.3b, Chapter 4, Fig. 4.4**). These results fit well with the decreased DNA-protein binding levels of TEAD (**Chapter 4, Fig. 4.5**) and RBPJ (**Chapter 5, Fig. 5.8**), both being upstream of OCT4. This makes sense since cells, upon encountering oxygen limitation, tend to reduce their metabolic requirements by reprioritization and/or activation of only pro-survival pathways and implementing "functional switching" of select proteins.

OCTs are a group of transcription factors that can switch between active and repressive states in a signal/stress specific manner [17,18], although details related to the regulators and cofactors involved in switching state/function are not well studied. Hence, it can be proposed that even though the levels of OCT4 (**Chapter 2, Fig. 2.3 a and b, Chapter 4, Fig. 4.4**) and OCT1 (**Chapter 3, Fig. 3.2**) did not show any significant change in liver, skeletal muscle or heart during anoxia, the available amount of OCTs in cells could function in a signal specific manner without spending extra energy on transcription/translation of another set of proteins. One possible reason for "functional switching"

could be a varied number of interactions due to availability of multiple posttranslational modifications (PTMs). Some of the known PTMs on OCTs are methylation, acetylation, phosphorylation, and O-GlcNAcylation (the addition of O-linked β-N-acetylglucosamine) to selected residues. These play essential roles in the regulation of a wide range of cellular processes [19]. This network is now often termed a "PTM switchboard". The combination of different PTMs is stress-dependent and demonstrates the functional variability of a single transcription factor and enhances their efficiency under suppressed metabolism.

Such "functional switching" was also observed in the expression of MAML (**Chapter 5**). Irrespective of a decrease in the levels of total protein for all the components of the Notch transcriptional complex (**Chapter 5, Fig. 5.6b**) and decreased binding levels of RBPJ to the promoter sequence (**Chapter 5, Fig. 5.8**), a strong increase was observed in the total protein levels of MAML (**Chapter 5, Fig. 5.6b**) upon reoxygenation in heart. This suggested an additional role for MAML other than being just a coregulator in the Notch transcriptional complex. Shen et al. presented the idea of function switching in MAML based on knockdown studies conducted on multiple adult tissues in mice [20]. Their results coincide with the study presented in **Chapter 5** since a MAML response to stress could work in a Notch-independent manner to act as a coregulator in MEF2 mediated transcription.

Chapter 3 discusses the regulation of demethylases and JMJDs by OCT1. JMJDs are oxygen sensitive enzymes that are involved in gene activation under hypoxic/anoxic conditions. The downstream targets of JMJDs include proteins associated with the methylation cycle that regulate epigenetic control of histones. A significant decrease in transcript levels of OCT1 was observed under all conditions in liver, compared to controls (**Chapter 3, Fig. 3.5a**), follows the transcriptional repression pattern seen in **Chapter 4** and **Chapter 5**. Moreover, the low binding levels of OCT1,

even with increased total protein levels upon reoxygenation in the liver (**Chapter 3, Fig. 3.2a**), could be due to the presence of PTMs. PTMs could play either of two functions: 1. prevent the movement of OCT1 to the nucleus or 2. hinder its binding to the promoter region of the DNA segment. Further study of the individual roles of PTMs on the structure/function of OCTs could provide clarity. The chapter further discussed the transcript and protein levels of demethylases. The study showed that total protein levels of JMJD1A decreased significantly in both liver and muscle during anoxia and later during reoxygenation (**Chapter 3, Fig. 3.2**). Reduced demethylation suggests global gene suppression and is in accordance with metabolic suppression induced during anoxia. Another important observation from the results discussed in **Chapter 3** is increased total protein levels of H3K9Me2 and JMJD2C in anoxic muscle that further increased during reoxygenation (**Chapter 3, Fig. 3.2b and 3.3b**). H3K9Me2 is known as a repressive epigenetic modification that is most abundant among heterochromatin modifications [21]. Further studies also speculated that these modifications would poise genes for their rapid induction [22–25]. Hence, it can be proposed that H3K9Me2 is the intermediate stage of histone methylation between mono and trimethylation and its elevated levels suggest that genes present in a poised state under the "preparation towards predictive stress" could be immediately activated in response to stress and, thereby, could prevent or limit damage that would otherwise be caused by a time delay.

As mentioned in **Chapter 4**, activation of the Hippo pathway led to phosphorylation and sequestration of YAP/TAZ to the cytoplasm, inhibiting their import to the nucleus. Recent knockout studies performed on mouse liver [26] and heart [27] presented the role of MST1 and MST2 in tumor suppression by controlling the levels of YAP/TAZ. The Notch pathway (**Chapter 5**) is activated by cell-to-cell communication that induces proteasomal cleavage and releases NICD into the cytoplasm to form a ternary complex and regulate target genes at transcriptional levels [28]. Both pathways show

interplay to regulate cellular activities that include cell division and tissue repair. A study conducted by Kim et al. concluded that loss of MST1 led to activation of the Notch signaling pathway that formed a positive autoregulatory loop with YAP/TAZ resulting in severe liver enlargement and tumorigenesis [29]. Many studies further conclude that YAP/TAZ acts upstream of Notch signaling by targeting NOTCH2 and JAG1 in both the liver and heart under oxidative stress [30–33]. The results presented in **Chapter 4** and **Chapter 5** parallel the above-mentioned findings from previous studies. Decreased levels of YAP at both protein and transcript levels (**Chapter 4, Fig. 4.3 and 4.6**) along with reduced DNA binding levels of TEAD (**Chapter 4, Fig. 4.5**) during anoxia and recovery suggests reduced expression of genes regulated by the YAP/TAZ/TEAD transcriptional complex. Considering that NOTCH2 and JAG1 are regulated by the Hippo transcriptional complex, their protein levels must either be decreased or unchanged during anoxia. Expected results were obtained for the total protein levels of JAG1 during 24 H anoxia and later 4 h recovery in both liver and heart (**Chapter 5, Fig. 5.5**). Surprisingly, the total protein levels of NOTCH2 increased significantly during 4 H recovery, suggesting two possibilities. Firstly, increased levels of NOTCH2 during reoxygenation indicate a role specific to recovery, and secondly, presents the possibility of being regulated by signaling pathways other than the YAP/TAZ/TEAD transcriptional complex.

MRD is an essential technique that suppresses energy expensive pathways and regulates signaling pathways that enable cell survival under stress conditions. Overall, the results presented in this thesis uncovered transcriptional repression by presenting a molecular network of stress responsive signaling pathways that describes the interplay of major transcriptional factors to regulate cellular processes in response to anoxia. The repressive histone modifications decreased binding of transcription factors to gene promoter regions, and holding stress responsive genes in a poised state

support a model whereby animals could endure long term anoxia exposure by minimizing energy requirements.

6.3 Protection from oxidative damage

Surviving anoxia requires organisms to endure a variety of consequences and, similarly, recovery from anoxia also requires adaptive responses. When oxygen is reintroduced, cells encounter a burst of oxygen free radical production, in addition to depleted energy reserves (glucose) and, together, these may limit the immediate availability of ATP. Consequently, select antioxidants could be synthesized to work efficiently to combat elevated ROS production during the crucial recovery period. **Chapter 2** examined the total protein levels of major NRF2 regulated antioxidants. NRF2 is well known for its ability to bind to the promoter region of antioxidant genes and stimulate transcription [34]. Although OCT4 has not been intensively studied for its regulation of antioxidants, its role in managing oxidative stress is well known [13,35,36], for example, inhibiting the expression of BMP4 [37]. In addition, NRF2 is also known to regulate OCT4 levels via a protein called proteasomal maturation protein (POMP) that is involved in proteasomal ubiquitination/degradation [38]. In total, a complex network of antioxidants that combat elevated levels of ROS and suppression of ROS-producing transcription factors was identified and studied.

Glutathione S-transferases (GSTs) showed similar trends in both liver and muscle during anoxia and later during reoxygenation. Of the five GSTs examined, GSTT1 showed a significant increase during anoxia and GSTP1 increased significantly during reoxygenation (**Chapter 2, Fig. 2.5**). Another set of antioxidants, aldo-keto reductases (AKRs) had a tissue specific response (**Chapter 2, Fig. 2.6**). AKR1A3 showed a significant response in anoxic liver whereas the levels of AFAR1 increased significantly during recovery compared to anoxic muscle. Elevated levels of AKR1A3 play an important role in liver detoxification, especially in response to increased lipid

peroxidation that generates malondialdehyde (MDA) and 4-hydroxynonenal (4-HNE) [39]. Another study stated that the role of AKR in liver was to detoxify reactive aldehydes and AKR levels showed an increase in response to oxidative, electrophilic and osmotic stress [40]. Previous studies from our lab showed increased levels of GSTs and AKRs in a stress/organ specific manner. For example, total GST activity increased significantly during the freeze/thaw process (that can also be considered as an anoxia/reoxygenation event) in wood frog organs [41]. Significantly higher levels of manganese superoxide dismutase were also observed in heart and muscle during anoxia in the freshwater red-eared slider turtle, *Trachemys scripta elegans* [42]. In a similar study on turtles by Breedon et al., elevated levels of GSTs were observed under anoxia in a tissue specific manner during anoxia/recovery [42]. Total protein levels of GSTs and AKRs also showed an organ specific increase in *Xenopus laevis* upon encountering dehydration [43]. These examples confirm a consistent activation of antioxidants in response to stress among several animal species.

The increased total protein levels of OCT1 (**Chapter 3, Fig. 3.2a**) in the liver during recovery from anoxia emphasizes the role of this "stress sensor" and responds to the predicted oxidative stress that could occur with a rapid increase in oxygen levels in liver during recovery from anoxia. DNA binding levels of OCT1 also increased during reoxygenation after anoxia in skeletal muscle (**Chapter 3, Fig. 3.4**). Increased binding suggested a potential activation of proteins/pathways downstream of OCT1 (e.g. Bcl-2, Cyclin D1, iNOS) to prevent or minimize damage that could result due to a high rate of ROS production [11]. A Chip assay showed the global association of OCT1 in regulating stress responsive pathways [11]. Another notable result observed in Chapter 3 was a significant increase in the total protein levels of AHCY in anoxic liver that remained unchanged during reoxygenation (**Chapter 3, Fig. 3.3a**). AHCY not only acts to maintain the SAM/SAH ratio to determine the methylation capacity of cells but is also involved in cellular redox control [44]. Studies

showed that AHCY deficient animals had increased oxidative stress due to a reduction in the levels of homocysteine for glutathione production via the transsulfuration pathway [45–47]. Therefore, increased levels of OCT1 and AHCY could be a response of animals towards anticipated stress upon reoxygenation.

6.4 Tissue repair

Oxygen plays an important role in the regulation of many intracellular functions that include differentiation and cell survival. Oxygen deprivation has multiple deleterious effects leading to cell necrosis, activation of apoptosis, tissue injuries, membrane damage, and many more [48]. Declining oxygen or full oxygen deprivation in the environment affects tissues gradually by creating hypoxic conditions initially and often rising to complete anoxia conditions. The transition time through hypoxia to full anoxia can allow cells/tissues to enhance anaerobic pathways, initiation MRD and make other adjustments to pathways and processes that support survival.

Even though the total protein levels of most of the proteins assessed in **Chapter 3** did not show any significant change, surprisingly, a 3-fold increase in total protein levels was observed for JMJD2C during anoxia in skeletal muscle and levels increased by 3.7-fold during reoxygenation (**Chapter 3, Fig. 3.2b**). Furthermore, increased transcript levels of *jmjd2c* in anoxic muscles (**Chapter 3, Fig. 3.5b**) confirmed the protective role of JMJD2C in skeletal muscle in response to anoxia. Previous studies showed that JMJD2C increased the transcript activity of MyoD [49,50]. A tissue protective action in response to anoxia was also observed in anoxic heart with levels of TAZ increasing by 1.5-fold compared to controls (**Chapter 4, Fig. 4.3b**). In response to injury, TAZ acts as an enhancer of MyoD to accelerate its DNA binding activity [51]. MyoD is a transcriptional activator involved in myogenesis and its levels increase during the cell cycle, DNA repair, and apoptosis [52]. MyoD is also necessary for muscle regeneration in adults [53]. Therefore, it can be

said that a potential increase in levels of MyoD due to increased protein levels of JMJD2C and TAZ in both skeletal and cardiac muscles, respectively, would initiate myogenesis for tissue repair after oxygen deprivation.

Notch signaling not only promotes cell division but also contributes to regeneration during/after tissue injury associated with hypoxia or anoxia. A strong increase in the total protein levels of NOTCH1 during anoxia in wood frog liver and heart (**Chapter 5, Fig. 5.6**) presents a protective role that goes well with the previous studies that suggested a role for the Notch pathway in wound healing, tissue repair, and regulating angiogenesis by activation of interleukin 6 (IL6) to induce the release of vascular endothelial growth factor [54,55]. Furthermore, a study by Liu et al. demonstrated that upregulation of Hes1 suppresses miR1 and miR206 to initiate tissue repair mechanisms [56]. Results obtained in **Chapter 5** fit with the studies demonstrating increased total protein levels of HES1 in both liver and muscle during anoxia and levels remaining high during reoxygenation (**Chapter 5, Fig. 5.7**). In addition to that, upon recovery in heart, total protein levels of MAML increased by 5.7-fold (**Chapter 5, Fig. 5.6b**). MAML acts as a coregulator of MEF2 to regulate/induce the activation of MyoD in response to stress [20]. This is understandable since cardiac muscles are highly sensitive to oxidative stress and damage could be irreversible. Therefore, increased total protein levels of MAML could potentially activate MyoD allowing a cascade of reactions to overcome the effects of increasing levels of ROS upon reoxygenation.

6.5 Conclusion

This thesis focussed on three major problems associated with anoxia that need to be addressed for cell, tissue and animal survival. These are (1) decreased availability of ATP that triggers a survival strategy of metabolic rate depression, (2) increased oxidative stress, or (3) tissue damage due to lack of oxygen (anoxia) and elevated levels of ROS (reoxygenation). During MRD, cells

undergo epigenetic changes by activation of genes/proteins involved in the methylation cycle. The transcriptional complexes formed in stress responsive pathways (e.g. Hippo pathway, Notch signaling) showed decreased binding to their respective promoter regions on genes suggesting a suppression of the transcription of their downstream targets. The functional switching of proteins like OCTs and MAML reflects an efficient use of available resources (proteins) presenting stress specific functions. A tissue specific increase in antioxidants was observed during anoxia and reoxygenation in both liver and skeletal muscle. The increased levels of AHCY was evidence of redox control in anoxic liver. An increase in the total protein levels of JMJD2C, TAZ, and MAML in skeletal and cardiac muscle suggested a potential increase in the expression of MyoD to initiate muscle regeneration in response to tissue damage caused due to oxidative stress. Hence, it can be deduced that the current thesis provides new insights into the role of regulatory pathways involved in amphibian anoxia tolerance and metabolic rate depression with specific implications for freezing survival by wood frogs. These studies can lead to multiple future directions and explore new opportunities to understand the processes that maintain cellular homeostasis under conditions of prolonged anoxia and metabolic rate depression.

6.6 References

[1] K.B. Storey, J.M. Storey, Metabolic rate depression in animals: transcriptional and translational controls, Biol. Rev. 79 (2004) 207–233. https://doi.org/10.1017/S1464793103006195.

[2] K.B. Storey, J.M. Storey, Molecular physiology of freeze tolerance in vertebrates, Physiol. Rev. 97 (2017) 623–665. https://doi.org/10.1152/physrev.00016.2016.

[3] C.P. Holden, K.B. Storey, Second messenger and cAMP-dependent protein kinase responses to dehydration and anoxia stresses in frogs, J. Comp. Physiol. - B Biochem. Syst. Environ. Physiol. 167 (1997) 305–312. https://doi.org/10.1007/s003600050078.

[4] K.B. Storey, Metabolic adaptations supporting anoxia tolerance in reptiles: Recent advances, Comp. Biochem. Physiol. Part B Biochem. Mol. Biol. 113 (1996) 23–35. https://doi.org/10.1016/0305-0491(95)02043-8.

[5] K.B. Storey, J.M. Storey, Oxygen Limitation and Metabolic Rate Depression, in: K.B. Storey (Ed.), Funct. Metab., John Wiley & Sons, Inc., Hoboken, NJ, USA, 2005: pp. 415–442. https://doi.org/10.1002/047167558X.ch15.

[6] K.B. Storey, Molecular mechanisms of anoxia tolerance, Int. Congr. Ser. 1275 (2004) 47–54. https://doi.org/10.1016/j.ics.2004.08.072.

[7] K.B. Storey, Regulation of hypometabolism: insights into epigenetic controls, J. Exp. Biol. 218 (2015) 150–159. https://doi.org/10.1242/jeb.106369.

[8] M. Escoll, D. Lastra, M. Pajares, N. Robledinos-Antón, A.I. Rojo, R. Fernández-Ginés, M. Mendiola, V. Martínez-Marín, I. Esteban, P. López-Larrubia, R. Gargini, A. Cuadrado, Transcription factor NRF2 uses the Hippo pathway effector TAZ to induce tumorigenesis in glioblastomas, Redox Biol. 30 (2020) 101425. https://doi.org/10.1016/j.redox.2019.101425.

[9] N. Wakabayashi, D. V. Chartoumpekis, T.W. Kensler, Crosstalk between Nrf2 and Notch signaling, Free Radic. Biol. Med. 88 (2015) 158–167. https://doi.org/10.1016/j.freeradbiomed.2015.05.017.

[10] A. Sparaneo, F.P. Fabrizio, L.A. Muscarella, Nrf2 and Notch Signaling in Lung Cancer: Near the Crossroad, Oxid. Med. Cell. Longev. 2016 (2016) 1–17. https://doi.org/10.1155/2016/7316492.

[11] J. Kang, M. Gemberling, M. Nakamura, F.G. Whitby, H. Handa, W.G. Fairbrother, D. Tantin, A general mechanism for transcription regulation by Oct1 and Oct4 in response to genotoxic and oxidative stress, Genes Dev. 23 (2009) 208–222. https://doi.org/10.1101/gad.1750709.

[12] D. Tantin, OCT transcription factors in development and stem cells: insights and mechanisms, Development. 140 (2013) 2857–2866. https://doi.org/10.1242/dev.095927.

[13] J. Kang, A. Shakya, D. Tantin, Stem cells, stress, metabolism and cancer: a drama in two Octs, Trends Biochem. Sci. 34 (2009) 491–499. https://doi.org/10.1016/j.tibs.2009.06.003.

[14] N. Bora-Singhal, J. Nguyen, C. Schaal, D. Perumal, S. Singh, D. Coppola, S. Chellappan, YAP1 Regulates OCT4 Activity and SOX2 Expression to Facilitate Self-Renewal and Vascular Mimicry of Stem-Like Cells, Stem Cells. 33 (2015) 1705–1718. https://doi.org/10.1002/stem.1993.

[15] T. Kiyota, A. Kato, C.R. Altmann, Y. Kato, The POU homeobox protein Oct-1 regulates radial glia formation downstream of Notch signaling, Dev. Biol. 315 (2008) 579–592. https://doi.org/10.1016/j.ydbio.2007.12.013.

[16] D.L.C. van den Berg, T. Snoek, N.P. Mullin, A. Yates, K. Bezstarosti, J. Demmers, I. Chambers, R.A. Poot, An Oct4-Centered Protein Interaction Network in Embryonic Stem Cells, Cell Stem Cell. 6 (2010) 369–381. https://doi.org/10.1016/j.stem.2010.02.014.

[17] I. Aksoy, R. Jauch, J. Chen, M. Dyla, U. Divakar, G.K. Bogu, R. Teo, C.K. Leng Ng, W. Herath, S. Lili, A.P. Hutchins, P. Robson, P.R. Kolatkar, L.W. Stanton, Oct4 switches partnering from Sox2 to Sox17 to reinterpret the enhancer code and specify endoderm, EMBO J. 32 (2013) 938–953. https://doi.org/10.1038/emboj.2013.31.

[18] A. Shakya, J. Kang, J. Chumley, M.A. Williams, D. Tantin, Oct1 Is a Switchable, Bipotential Stabilizer of Repressed and Inducible Transcriptional States, J. Biol. Chem. 286 (2011) 450–459. https://doi.org/10.1074/jbc.M110.174045.

[19] A.R. Shakoori, D.C. Hoessli, Nasir-ud-Din, Post-translational modifications in activation and inhibition of oct-1-DNA binding complex in H2B and other diverse gene regulation: Prediction of interplay sites, J. Cell. Biochem. 114 (2013) 266–274. https://doi.org/10.1002/jcb.24382.

[20] H. Shen, A.S. McElhinny, Y. Cao, P. Gao, J. Liu, R. Bronson, J.D. Griffin, L. Wu, The Notch coactivator, MAML1, functions as a novel coactivator for MEF2C-mediated transcription and is required for normal myogenesis, Genes Dev. 20 (2006) 675–688. https://doi.org/10.1101/gad.1383706.

[21] B. Wen, H. Wu, Y. Shinkai, R.A. Irizarry, A.P. Feinberg, Large histone H3 lysine 9 dimethylated chromatin blocks distinguish differentiated from embryonic stem cells, Nat. Genet. 41 (2009) 246–250. https://doi.org/10.1038/ng.297.

[22] H. Niwa, Open conformation chromatin and pluripotency: Figure 1., Genes Dev. 21 (2007) 2671–2676. https://doi.org/10.1101/gad.1615707.

[23] E. Meshorer, T. Misteli, Chromatin in pluripotent embryonic stem cells and differentiation, Nat. Rev. Mol. Cell Biol. 7 (2006) 540–546. https://doi.org/10.1038/nrm1938.

[24] Y.-H. Loh, W. Zhang, X. Chen, J. George, H.-H. Ng, Jmjd1a and Jmjd2c histone H3 Lys 9 demethylases regulate self-renewal in embryonic stem cells, Genes Dev. 21 (2007) 2545–2557. https://doi.org/10.1101/gad.1588207.

[25] S. Efroni, R. Duttagupta, J. Cheng, H. Dehghani, D.J. Hoeppner, C. Dash, D.P. Bazett-Jones, S. Le Grice, R.D.G. McKay, K.H. Buetow, T.R. Gingeras, T. Misteli, E. Meshorer, Global Transcription in Pluripotent Embryonic Stem Cells, Cell Stem Cell. 2 (2008) 437–447. https://doi.org/10.1016/j.stem.2008.03.021.

[26] D. Zhou, C. Conrad, F. Xia, J.-S. Park, B. Payer, Y. Yin, G.Y. Lauwers, W. Thasler, J.T. Lee, J. Avruch, N. Bardeesy, Mst1 and Mst2 Maintain Hepatocyte Quiescence and Suppress Hepatocellular Carcinoma Development through Inactivation of the Yap1 Oncogene, Cancer Cell. 16 (2009) 425–438. https://doi.org/10.1016/j.ccr.2009.09.026.

[27] K.A. Moses, F. DeMayo, R.M. Braun, J.L. Reecy, R.J. Schwartz, Embryonic expression of anNkx2-5/Cre gene usingROSA26 reporter mice, Genesis. 31 (2001) 176–180. https://doi.org/10.1002/gene.10022.

[28] K. Hori, A. Sen, S. Artavanis-Tsakonas, Notch signaling at a glance, J. Cell Sci. 126 (2013) 2135–2140. https://doi.org/10.1242/jcs.127308.

[29] W. Kim, S.K. Khan, J. Gvozdenovic-Jeremic, Y. Kim, J. Dahlman, H. Kim, O. Park, T. Ishitani, E. Jho, B. Gao, Y. Yang, Hippo signaling interactions with Wnt/β-catenin and Notch signaling repress liver tumorigenesis, J. Clin. Invest. 127 (2016) 137–152. https://doi.org/10.1172/JCI88486.

[30] P. Jeliazkova, S. Jörs, M. Lee, U. Zimber-Strobl, J. Ferrer, R.M. Schmid, J.T. Siveke, F. Geisler, Canonical Notch2 signaling determines biliary cell fates of embryonic hepatoblasts and adult hepatocytes independent of Hes1, Hepatology. 57 (2013) 2469–2479. https://doi.org/10.1002/hep.26254.

[31] D.F. Tschaharganeh, X. Chen, P. Latzko, M. Malz, M.M. Gaida, K. Felix, S. Ladu, S. Singer, F. Pinna, N. Gretz, C. Sticht, M.L. Tomasi, S. Delogu, M. Evert, B. Fan, S. Ribback, L. Jiang, S. Brozzetti, F. Bergmann, F. Dombrowski, P. Schirmacher, D.F. Calvisi, K. Breuhahn, Yes-Associated Protein Up-regulates Jagged-1 and Activates the NOTCH Pathway in Human Hepatocellular Carcinoma, Gastroenterology. 144 (2013) 1530-1542.e12. https://doi.org/10.1053/j.gastro.2013.02.009.

[32] S. Zhang, J. Wang, H. Wang, L. Fan, B. Fan, B. Zeng, J. Tao, X. Li, L. Che, A. Cigliano, S. Ribback, F. Dombrowski, B. Chen, W. Cong, L. Wei, D.F. Calvisi, X. Chen, Hippo Cascade Controls Lineage Commitment of Liver Tumors in Mice and Humans, Am. J. Pathol. 188 (2018) 995–1006. https://doi.org/10.1016/j.ajpath.2017.12.017.

[33] T. Heallen, M. Zhang, J. Wang, M. Bonilla-Claudio, E. Klysik, R.L. Johnson, J.F. Martin, Hippo Pathway Inhibits Wnt Signaling to Restrain Cardiomyocyte Proliferation and Heart Size, Science (80). 332 (2011) 458–461. https://doi.org/10.1126/science.1199010.

[34] Q.M. Chen, A.J. Maltagliati, Nrf2 at the heart of oxidative stress and cardiac protection., Physiol. Genomics. 50 (2018) 77–97. https://doi.org/10.1152/physiolgenomics.00041.2017.

[35] F.-Q. Zhao, Octamer-binding transcription factors: genomics and functions, Front. Biosci. 18 (2013) 1051. https://doi.org/10.2741/4162.

[36] I.R. Lemischka, Hooking Up with Oct4, Cell Stem Cell. 6 (2010) 291–292. https://doi.org/10.1016/j.stem.2010.03.011.

[37] A.K.K. Teo, Y. Ali, K.Y. Wong, H. Chipperfield, A. Sadasivam, Y. Poobalan, E.K. Tan, S.T. Wang, S. Abraham, N. Tsuneyoshi, L.W. Stanton, N.R. Dunn, Activin and BMP4 Synergistically Promote Formation of Definitive Endoderm in Human Embryonic Stem Cells, Stem Cells. 30 (2012) 631–642. https://doi.org/10.1002/stem.1022.

[38] X. Dai, X. Yan, K.A. Wintergerst, L. Cai, B.B. Keller, Y. Tan, Nrf2: Redox and Metabolic Regulator of Stem Cell State and Function, Trends Mol. Med. 26 (2020) 185–200. https://doi.org/10.1016/j.molmed.2019.09.007.

[39] Y.H. Koh, Y.S. Park, M. Takahashi, K. Suzuki, N. Taniguchi, Aldehyde reductase gene expression by lipid peroxidation end products, MDA and HNE, Free Radic. Res. 33 (2000) 739–746. https://doi.org/10.1080/10715760000301261.

[40] Y. Jin, T.M. Penning, Aldo-Keto Reductases and Bioactivation/Detoxication, Annu. Rev. Pharmacol. Toxicol. 47 (2007) 263–292. https://doi.org/10.1146/annurev.pharmtox.47.120505.105337.

[41] D.R. Joanisse, K.B. Storey, Oxidative damage and antioxidants in *Rana sylvatica*, the freeze-tolerant wood frog., Am. J. Physiol. 271 (1996) R545-53. https://doi.org/10.1152/ajpregu.1996.271.3.R545.

[42] S.A. Breedon, H. Hadj-Moussa, K.B. Storey, Nrf2 activates antioxidant enzymes in the anoxia-tolerant red-eared slider turtle, *Trachemys scripta elegans*, J. Exp. Zool. Part A Ecol. Integr. Physiol. 335 (2021) 426–435. https://doi.org/10.1002/jez.2458.

[43] A.I. Malik, K.B. Storey, Activation of antioxidant defense during dehydration stress in the African clawed frog, Gene. 442 (2009) 99–107. https://doi.org/10.1016/j.gene.2009.04.007.

[44] G.S. Ducker, J.D. Rabinowitz, One-Carbon Metabolism in Health and Disease, Cell Metab. 25 (2017) 27–42. https://doi.org/10.1016/j.cmet.2016.08.009.

[45] N.S. Yee, K. Lorent, M. Pack, Exocrine pancreas development in zebrafish, Dev. Biol. 284 (2005) 84–101. https://doi.org/10.1016/j.ydbio.2005.04.035.

[46] R.P. Matthews, K. Lorent, R. Mañoral-Mobias, Y. Huang, W. Gong, I.V.J. Murray, I.A. Blair, M. Pack, TNFα-dependent hepatic steatosis and liver degeneration caused by mutation of zebrafish s-adenosylhomocysteine hydrolase, Development. 136 (2009) 865–875. https://doi.org/10.1242/dev.027565.

[47] L. Belužić, I. Grbeša, R. Belužić, J.H. Park, H.K. Kong, N. Kopjar, G. Espadas, E. Sabidó, A. Lepur, F. Rokić, I. Jerić, L. Brkljačić, O. Vugrek, Knock-down of AHCY and depletion of adenosine induces DNA damage and cell cycle arrest, Sci. Rep. 8 (2018) 14012. https://doi.org/10.1038/s41598-018-32356-8.

[48] G.K. Cox, T.E. Gillis, Surviving anoxia: the maintenance of energy production and tissue integrity during anoxia and reoxygenation, J. Exp. Biol. 223 (2020). https://doi.org/10.1242/jeb.207613.

[49] W. Jin, J. Peng, S. Jiang, The epigenetic regulation of embryonic myogenesis and adult muscle regeneration by histone methylation modification, Biochem. Biophys. Reports. 6 (2016) 209–219. https://doi.org/10.1016/j.bbrep.2016.04.009.

[50] E.-S. Jung, Y.-J. Sim, H.-S. Jeong, S.-J. Kim, Y.-J. Yun, J.-H. Song, S.-H. Jeon, C. Choe, K.-T. Park, C.-H. Kim, K.-S. Kim, Jmjd2C increases MyoD transcriptional activity through inhibiting G9a-dependent MyoD degradation, Biochim. Biophys. Acta - Gene Regul. Mech. 1849 (2015) 1081–1094. https://doi.org/10.1016/j.bbagrm.2015.07.001.

[51] H. Jeong, S. Bae, S.Y. An, M.R. Byun, J. Hwang, M.B. Yaffe, J. Hong, E.S. Hwang, TAZ as a novel enhancer of MyoD-mediated myogenic differentiation, FASEB J. 24 (2010) 3310–3320. https://doi.org/10.1096/fj.09-151324.

[52] M. Simonatto, F. Marullo, F. Chiacchiera, A. Musaró, J.Y.J. Wang, L. Latella, P.L. Puri, DNA damage-activated ABL-MyoD signaling contributes to DNA repair in skeletal myoblasts, Cell Death Differ. 20 (2013) 1664–1674. https://doi.org/10.1038/cdd.2013.118.

[53] H. Weintraub, V.J. Dwarki, I. Verma, R. Davis, S. Hollenberg, L. Snider, A. Lassar, S.J. Tapscott, Muscle-specific transcriptional activation by MyoD., Genes Dev. 5 (1991) 1377–1386. https://doi.org/10.1101/gad.5.8.1377.

[54] X. Zheng, S. Narayanan, V.G. Sunkari, S. Eliasson, I.R. Botusan, J. Grünler, A.I. Catrina, F. Radtke, C. Xu, A. Zhao, N.R. Ekberg, U. Lendahl, S.-B. Catrina, Triggering of a Dll4–Notch1 loop impairs wound healing in diabetes, Proc. Natl. Acad. Sci. 116 (2019) 6985–6994. https://doi.org/10.1073/pnas.1900351116.

[55] S. Chigurupati, T. V. Arumugam, T.G. Son, J.D. Lathia, S. Jameel, M.R. Mughal, S.-C. Tang, D.-G. Jo, S. Camandola, M. Giunta, I. Rakova, N. McDonnell, L. Miele, M.P. Mattson, S. Poosala, Involvement of Notch Signaling in Wound Healing, PLoS One. 2 (2007) e1167. https://doi.org/10.1371/journal.pone.0001167.

[56] W. Liu, Y. Wen, P. Bi, X. Lai, X.S. Liu, X. Liu, S. Kuang, Hypoxia promotes satellite cell self-renewal and enhances the efficiency of myoblast transplantation, Development. 139 (2012) 2857–2865. https://doi.org/10.1242/dev.079665.

Appendices

Appendix A: List of publications

Published Manuscripts

1. **Gupta, A.**, Brooks, C., Storey, K.B., 2020. Regulation of NF-κB, FHC and SOD2 in response to oxidative stress in the freeze tolerant wood frog, *Rana sylvatica*. Cryobiology 97, 28–36. https://doi.org/10.1016/j.cryobiol.2020.10.012
2. **Gupta, A.**, Storey, K.B., 2020. Regulation of antioxidant systems in response to anoxia and reoxygenation in *Rana sylvatica* . Comp. Biochem. Physiol. Part B Biochem. Mol. Biol. 243–244, 110436. https://doi.org/10.1016/j.cbpb.2020.110436
3. Zhang, J., **Gupta, A.**, Storey, K.B., 2021. Freezing stress adaptations: Critical elements to activate Nrf2 related antioxidant defense in liver and skeletal muscle of the freeze tolerant wood frogs. Comp. Biochem. Physiol. Part B Biochem. Mol. Biol. 254, 110573. https://doi.org/10.1016/j.cbpb.2021.110573
4. **Gupta, A.**, Storey, K.B., 2021. Coordinated expression of Jumonji and AHCY under OCT transcription factor control to regulate gene methylation in wood frogs during anoxia. Gene 788, 145671. https://doi.org/10.1016/j.gene.2021.145671
5. **Gupta, A.**, Hadj-Moussa, H., Al-attar, R., Seibel, B.A., Storey, K.B., 2021. Hypoxic Jumbo Squid Activate Neuronal Apoptosis but Not MAPK or Antioxidant Enzymes during Oxidative Stress. Physiol. Biochem. Zool. https://doi.org/10.1086/714097
6. Logan, S.M., **Gupta, A.**, Wang, A., Levy, R.J., Storey, K.B., 2021. Isoflurane and low-level carbon monoxide exposures increase expression of pro-survival miRNA in neonatal mouse heart. Cell Stress Chaperones. https://doi.org/10.1007/s12192-021-01199-0
7. **Gupta, A.**, Varma, A., Storey, K.B., 2021. New Insights to Regulation of Fructose-1,6-bisphosphatase during Anoxia in Red-Eared Slider, *Trachemys scripta elegans*. Biomolecules 11, 1548. https://doi.org/10.3390/biom11101548
8. **Gupta, A.**, Storey, K.B., 2021. Activation of the Hippo Pathway in *Rana sylvatica*: Yapping Stops in Response to Anoxia. Life 11, 1422. https://doi.org/10.3390/life11121422

9. **Gupta, A.**, Storey, K.B., 2022. A “notch” in the cellular communication network in response to anoxia by wood frog (*Rana sylvatica*). Cell. Signal. 93, 110305. https://doi.org/10.1016/j.cellsig.2022.110305

Manuscripts under review

1. **Gupta, A.**, Breedon, S., Storey, K.B., Activation of p53 in anoxic freshwater crayfish, *Faxonius virilis.* Submitted to Journal of Experimental Biology (Submission ID: JEXBIO/2022/244145)
2. Breedon, S., **Gupta, A.**, Storey, K.B., Regulation of apoptosis and autophagy during anoxia in the freshwater crayfish, *Faxonius virilis.* Submitted to Marine Biotechnology (Submission ID: 256e736358950390)
3. Rehman, S., Varma, A., **Gupta, A.**, Storey, K.B., The regulation of m6A related proteins during whole-body freezing of the wood frog, *Rana sylvatica*. Submitted to Journal of Experimental Zoology, Part A (Submission ID: JEZ-A-2022-04-0058)

Appendix B: Communications at scientific meetings

1. **Gupta, A.**, Storey, K.B. Activation of the Hippo Pathway in *Rana sylvatica*: Yapping Stops in Response to Anoxia. 24th Annual conference, Concordia University, Montreal, Canada, November 11, 2021. (Oral presentation)
2. **Gupta, A**., Storey, K.B. NRF2-transcriptional network in anoxia-tolerant vertebrates. 22nd Annual Conference, Concordia University, Montreal, Canada, Nov. 15, 2019 (Oral presentation)
3. **Gupta, A**., Storey, K.B. Holding back jumonji: OCT-1 induced epigenetic changes combat oxidative stress. 22nd Annual Conference, Concordia University, Montreal, Canada, Nov. 15, 2019 (Poster presentation)
4. **Gupta, A**., Storey, K.B. NRF2-transcriptional network in anoxia-tolerant vertebrates. 10th International Congress of Comparative Physiology and Biochemistry, Ottawa, Ontario, Canada, August 8, 2019. (Oral presentation)
5. **Gupta, A**., Storey, K.B. Holding back jumonji: OCT-1 induced epigenetic changes combat oxidative stress. 10th International Congress of Comparative Physiology and Biochemistry, Ottawa, Ontario, Canada, August 6, 2019. (Poster presentation)
6. **Gupta, A**., Storey, K.B. OCT4 triggers a NRF2-mediated antioxidant response in anoxia-tolerant frogs. 16th Annual Ottawa-Carleton Institute of Biology Symposium, Carleton University, Ottawa, Ontario, Canada, May 2, 2019. (Oral presentation)
7. **Gupta, A**., Storey, K.B. OCT induced transcriptional network in the freeze tolerant wood frog. 21st Annual Conference, Concordia University, Montreal, Canada, Nov. 9, 2018 (Poster presentation)

Appendix C: Representative images

1. Representative immunoblots

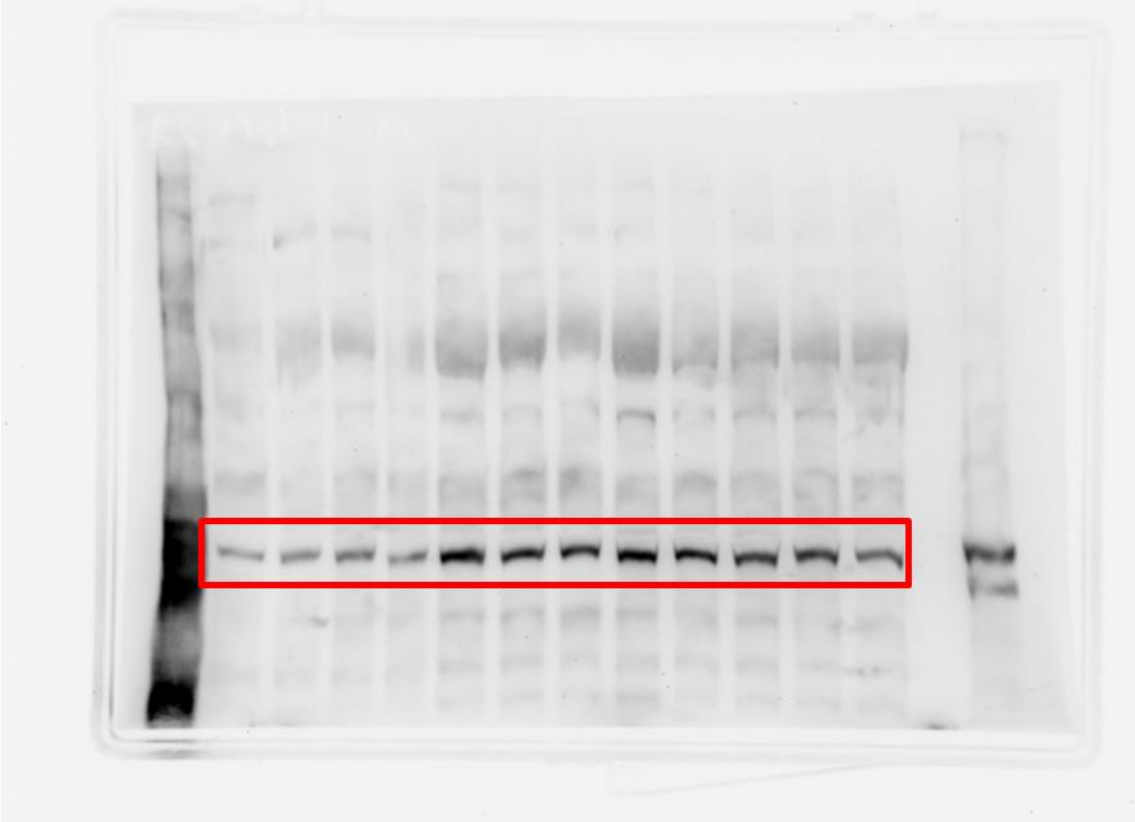

The ECL showing total protein levels of MST1 in extracts of heart of R. sylvatica. Lane 1 representing a protein mol. wt. ladder, lane2 to 5 represents control samples, lane 6 to 9 represents 24 h anoxia exposure and lane 10-13 represent 4 h aerobic recovery from anoxia, lane 15 represents the control sample from mammalian tissue. The protein quantified is highlighted in red box.

2. Bioinformatic check for antibody compatibility

The epitope sequence of the commercial antibody was aligned to the different vertebrates to identify the conserved regions throughout the vertebrates (humans, *gallus gallus, Xenopus tropicalis, turtle*) using NCBI-derived amino acid sequences and Clustal Omega. The following is an example of what was done to determine if an antibody has conserved epitope region.

```
CLUSTAL O(1.2.4) multiple sequence alignment


tropicalisXP_031751216.1      ---------------------------------------------MAPVVTGKFGERPQPK      16
laevisXP_018084494.1          ---------------------------------------------MAPVVTGKFGERPQPK      16
RBPJ-abclonal                 -----------------------------------------------MGGCRKFGERPPPK      14
gallusXP_025005620.1          ------------------------------------------------------------      0
turtleXP_023959303.1          MQERHILVFVFHRFLQLFLLLSGTRQCVRHAARSWEFLHSIPVIDSLCGLGKFGERPQPK      60


tropicalisXP_031751216.1      RLTREAMRNYLKERGDQTVLILHAKVAQKSYGNEKRFFCPPPCVYLMGSGWKKKKEQMER      76
laevisXP_018084494.1          RLTREAMRNYLKERGDQTVLILHAKVAQKSYGNEKRFFCPPPCVYLMGSGWKKKKEQMER      76
RBPJ-abclonal                 RLTREAMRNYLKERGDQTVLILHAKVAQKSYGNEKRFFCPPPCVYLMGSGWKKKKEQMER      74
gallusXP_025005620.1          ------MRNYLKERGDQTVLILHAKVAQKSYGNEKRFFCPPPCVYLMGSGWKKKKEQMER      54
turtleXP_023959303.1          RLTREAMRNYLKERGDQTVLILHAKVAQKSYGNEKRFFCPPPCVYLMGSGWKKKKEQMER      120
                                    ********************************************************


tropicalisXP_031751216.1      DGCSEQESQPCAFIGIGNSDQEMQQLNLEGKNYCTAKTLYISDSDKRKHFMLSVKMFYGN      136
laevisXP_018084494.1          DGCSEQESQPCAFIGIGNSDQEMQQLNLEGKNYCTAKTLYISDSDKRKHFMLSVKMFYGN      136
RBPJ-abclonal                 DGCSEQESQPCAFIGIGNSDQEMQQLNLEGKNYCTAKTLYISDSDKRKHFMLSVKMFYGN      134
gallusXP_025005620.1          DGCTEQESQPCAFIGIGNSDQEMQQLNLEGKNYCTAKTLYISDSDKRKHFMLSVKMFYGN      114
turtleXP_023959303.1          DGCSEQESQPCAFIGIGNSDQEMQQLNLEGKNYCTAKTLYISDSDKRKHFMLSVKMFYGN      180
                              ***:********************************************************


tropicalisXP_031751216.1      SDDIGVFLSKRIKVISKPSKKKQSLKNADLCIASGTKVALFNRLRSQTVSTRYLHVEGGN      196
laevisXP_018084494.1          SDDIGVFLSKRIKVISKPSKKKQSLKNADLCIASGTKVALFNRLRSQTVSTRYLHVEGGN      196
RBPJ-abclonal                 SDDIGVFLSKRIKVISKPSKKKQSLKNADLCIASGTKVALFNRLRSQTVSTRYLHVEGGN      194
gallusXP_025005620.1          SDDIGVFLSKRIKVISKPSKKKQSLKNADLCIASGTKVALFNRLRSQTVSTRYLHVEGGN      174
turtleXP_023959303.1          SDDIGVFLSKRIKVISKPSKKKQSLKNADLCIASGTKVALFNRLRSQTVSTRYLHVEGGN      240
                              ************************************************************


tropicalisXP_031751216.1      FHASSQQWGAFYIHLLDDEESEGEEFTVRDGYIHYGQTVKLVCSVTGMALPRLIIRKVDK      256
laevisXP_018084494.1          FHASSQQWGAFYIHLLDDEESEGEEFTVRDGYIHYGQTVKLVCSVTGMALPRLIIRKVDK      256
RBPJ-abclonal                 FHASSQQWGAFFIHLLDDDESEGEEFTVRDGYIHYGQTVKLVCSVTGMALPRLIIRKVDK      254
gallusXP_025005620.1          FHASSQQWGAFYIHLLDDDESEGEEFTVRDGYIHYGQTVKLVCSVTGMALPRLIIRKVDK      234
turtleXP_023959303.1          FHASSQQWGAFYIHLLDDDESEGEEFTVRDGYIHYGQTVKLVCSVTGMALPRLIIRKVDK      300
                              ***********:******:******************************************


tropicalisXP_031751216.1      QTALLDADDPVSQLHKCAFYLKDTERMYLCLSQERIIQFQATPCPKEPNKEMINDGASWT      316
laevisXP_018084494.1          QTALLDADDPVSQLHKCAFYLKDTERMYLCLSQERIIQFQATPCPKEPNKEMINDGASWT      316
RBPJ-abclonal                 QTALLD------------------------------------------------------      260
gallusXP_025005620.1          QTALLDADDPVSQLHKCAFYLKDTERMYLCLSQERIIQFQATPCPKEPNKEMINDGASWT      294
turtleXP_023959303.1          QTALLDADDPVSQLHKCAFYLKDTERMYLCLSQERIIQFQATPCPKEPNKEMINDGASWT      360
                              ******


tropicalisXP_031751216.1      IISTDKAEYTFYEGMGPVNAPVTPVPVVESLQLNGGGDVAMLELTGQNFTPNLRVWFGDV      376
laevisXP_018084494.1          IISTDKAEYTFYEGMGPVNAPVTPVPVVESLQLNGGGDVAMLELTGQNFTPNLRVWFGDV      376
RBPJ-abclonal                 ------------------------------------------------------------      260
gallusXP_025005620.1          IISTDKAEYTFYEGMGPVHAPVTPVPVVESLQLNGGGDVAMLELTGQNFTPNLRVWFGDV      354
turtleXP_023959303.1          IISTDKAEYTFYEGMGPVHAPVTPVPVVESLQLNGGGDVAMLELTGQNFTPNLRVWFGDV      420
```

Figure: Protein sequence alignment of RBPJ to the epitope region provided by Abclonal

3. Bioinformatic check for primer designing

All the primers were designed using sequence of *Xenopus tropicalis* or *Rana temporaria* (the closest sequenced amphibian to wood frog). Before primer designing a sequence alignment was performed using the CDS sequence from different vertebrates to identify the conserved regions throughout the vertebrates (humans, *gallus gallus, Xenopus tropicalis, Anolis carolinensis*). Later, the conserved regions were used to design the primers.

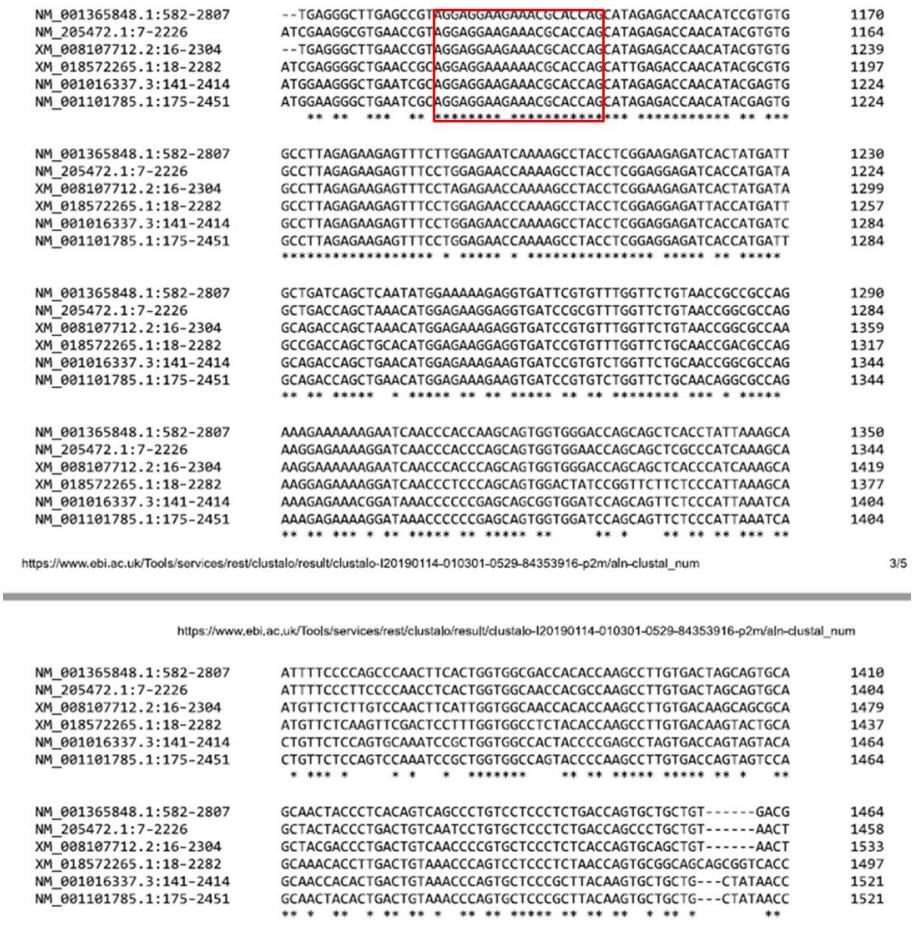

Figure: Nucleotide sequence alignment of *oct1* in the CDS region of different vertebrate. NM_001016337.3 is the sequence of *Xenopus tropicalis*.